UNIVERSITY OF SOUTHAMPTON

FACULTY OF MEDICINE, HEALTH AND LIFE SCIENCES
SCHOOL OF BIOLOGICAL SCIENCES

Submitted for
Doctor of Philosophy

MODIFIED IMMUNOGLOBULIN-BINDING DOMAINS OF PROTEIN L FROM *PEPTOSTREPTOCOCCUS MAGNUS.*

2006

Robert Andrew Phillips, B.Sc. M.Sc.

UNIVERSITY OF SOUTHAMPTON

ABSTRACT

FACULTY OF MEDICINE, HEALTH AND LIFE SCIENCES
SCHOOL OF BIOLOGICAL SCIENCES

Doctor of Philosophy

MODIFIED IMMUNOGLOBULIN-BINDING DOMAINS OF PROTEIN L FROM PEPTOSTREPTOCOCCUS MAGNUS.

Robert Andrew Phillips B.Sc. M.Sc.

Protein L is a multi domain Ig-binding protein from the cell wall of the Gram positive bacterium *Peptostreptococcus magnus* that is able to bind to immunoglobulins (Ig) without affecting their antigenic binding ability. Unlike other Ig-binding proteins, Protein L binds to the V_L domain of κ-chains enabling it to bind to all sub-classes of antibodies that contain κ-chains.

The complex formed between a single domain of wild-type Protein L and κ-chain is described by a dissociation constant (K_d) of approximately 150nM. Such domains, used as affinity ligands for the purification of κ-chains, or Igs bearing κ-chains, require harsh elution conditions to dissociate the complexes. This leads to degradation of the affinity column and the Ig or Ig fragment being isolated. The aim of the work described in this thesis was to develop variants of a single domain of Protein L that can offer more favourable binding characteristics improving their usefulness in some commercial applications. Thus mutants have been developed that have lower affinities for κ-chain (and Ig bearing κ-chain) but retain satisfactory conformational stabilities.

A number of mutated domains have been purified and their binding properties to κ-chain characterised by ELISA, competitive ELISA, affinity chromatography and equilibrium and pre-equilibrium fluorescence spectroscopy. These studies have shown that whereas the F39W, the N26,76D, the N26,76D,F39W, and the K33W mutants all have low dissociation constants for their complexes with κ-chain of Ig, two mutants Y53H,F39W and F39H,Y64W have substantially higher K_d values. Both of these proteins were immobilised onto Sepharose 4B gel and used in affinity chromatography experiments. These showed that human Ig was released from these two proteins at pH 3.9 and 3.8 respectively and thus make useful affinity ligands.

Pre-equilibrium binding studies have also provided a further insight into the possible mechanism by which κ-chains bind Protein L giving rise to the possibility that there are in fact two binding sites for κ-chain on a single domain of Protein L.

This research has therefore led to the development of new proteins able to be used in the affinity chromatographic purification if Ig, or fragments of Ig bearing the V_L domain of κ-chains.

Acknowledgements

I would like to thank the BBSRC for the studentship that funded the project and Dr Mike Gore for his help during this study. I would also like to thank Dr Sian Roberts for help and advice with the mutagenesis work and Nicki Muir for general technical support.

I would like to thank friends and colleagues within the lab and department who proved to be an important source of encouragement for this study and finally I would like to thank my wife and family for their support.

ABBREVIATIONS

Amp	Ampicillin
ATP	Adenosine triphosphate
APS	Ammonium persulphate
BCA	Bicinchoninic acid
BSA	Bovine serum albumin
CD	Circular dichroism
C_H	Heavy chain constant region of Ig
DH_2O	Distilled water
DNA	Deoxyribonucleic acid
DnaseI	Deoxyribonuclease I
DTT	Dithiothreitol
Dut	dUTP transferase
EDTA	Ethylenediaminetetraacetic acid
EGTA	Ethylene glycol-bis(β-aminoethyl ether)
ELISA	Enzyme linked immunosorbent assay
Fab	Antigen binding fragment of Ig
Fc	Crystalisable fragment of Ig
Fv	Ig fragment of heavy and light chain variable domains
GdnHCl	Guanidine hydrochloride
HRP	Horse radish peroxidase
Ig	Immunoglobulin
IPTG	Isopropyl-β-D-thiogalactoside
κ-chain	Kappa light chain of Ig
k	Rate constant
k_1	Rate of association
k_{1obs}	Observed rate of reaction
k_{-1}	Rate of dissociation
k_2	Forward rate of proposed conformational change
k_{2obs}	Observed rate of proposed conformational change
k_{-2}	Rate of reversal of proposed conformational change
K_d	Dissociation constant
$K_{d\ app}$	Apparent dissociation constant

LB	Luria broth
NMR	Nuclear magnetic resonance
NTP	Nuclear triphosphate
OD	Optical density
PAGE	Polyacrylamide gel electrophoresis
PBS	Phosphate buffered saline
PEG	Polyethylene glycol
PMSF	Phenylmethylsulphonylfluoride
PpL	A single Ig-binding domain from Protein L from *Peptostreptococcus magnus*
RF DNA	Replicative form of phage DNA
S_cFv	Single chain Fv
ssDNA	Single stranded DNA
SDS	Sodium dodecyl sulphate
SpA	A single Ig-binding domain of Protein A from *Staphylococcus aureus*
SpG	A single Ig-binding domain of Protein G from *Streptococcus* groups C and G
TBE	Tris borate EDTA
TE	Tris EDTA
TEMED	N,N,N',N'-tetraethylmethylenediamine
Tris	Tris(Hydroxymethyl)diamine
Tween	Polyoxyethylenesorbitan monolaurate
Ung	Uracil DNA glycosidase
UV	Ultra violet
V_L	Light chain variable domain
V_H	Heavy chain variable domain
WT	Wild type

CONTENTS

Chapter 2 Materials and Methods

FIGURES AND TABLES

Chapter 1 Introduction

Chapter 3 Site directed mutagenesis

Chapter 4 Conformational stability of PpL

Chapter 5 Binding studies at equilibrium

Chapter 6 Stopped Flow analysis of the binding reaction between PpL and κ-chain

Chapter 1

Introduction.

CHAPTER 1

INTRODUCTION

1.1 General introduction

Several Gram positive bacteria produce cell-wall proteins, often released into the media, that can bind to immunoglobulins non-antigenically and / or to other common blood proteins such as human serum albumin (Langone, 1982). This binding activity is thought to be a mechanism by which these infectious bacteria can increase their virulence (Goward *et al.*, 1993, Kastern *et al.*, 1992). Some of the more widely characterised bacterial Ig-binding proteins discovered so far are summarised in Table 1.1 including Protein A from *Staphylococcus aureus*, Protein G from groups C and G *Streptococci* and Protein L from *Peptostreptococcus magnus.*

Although these proteins carry out a similar function in general, they have been found to contain very little homology at the gene and protein sequence levels. However, at the structural level they all contain; a secretion signal sequence (cleaved during processing), a cell wall spanning region, a cell membrane anchor and a series of internally repeated domains where Ig, or other protein binding activity is located.

The differences in structure between the proteins reflect to some extent the differing structures of the cell walls of the bacteria in which they are found.

1.2 The structure of immunoglobulins

Immunoglobulins (Igs) are composed of four polypeptide chains; two light chains comprised of 220 amino acid residues (approx 23kDa) and two heavy chains comprised of 440 amino acid residues (approx 50-60kDa). These chains can be separated by reduction of the disulphide bonds e.g. using β-mercaptoethanol.

Table 1.1 : Summary of the most common Ig-binding proteins

Protein	Organism	Binds to
Protein A	*Staphylococcus aureus*	All Ig weakly via Fab IgG (except IgG_3) via Fc Human serum albumin α_2-macroglobulin Kininogen
Protein G	Group C&G *Streptococci*	IgG via Fc region Human serum albumin α_2- macroglobulin Kininogen
Protein L	*Peptostreptococcus magnus*	IgA,D,G,M,E via κ chain α_2-macroglobulin Kininogen Human serum albumin
Protein H	Group A *Streptococci*	IgG of human and rabbit Human serum albumin α_2-macroglobulin Kininogen
Protein D	*Haemophilus influenza*	IgD via Fc or Fab

In general, Igs fold into domains, each of approximately 110 residues forming two domains in the light chain and four domains in the heavy chain (see Fig.1.1). However, IgM has an extra constant domain formed in its heavy chains. This basic domain (termed the Ig fold) consists of two β-sheets, one of 4 and the other of 3 β-strands joined by a disulphide bond. Two extra β-strands are present in the variable domains. There are two antigen-binding fragments (Fab) of 25kDa formed by the interaction of the amino terminal variable regions of the light and heavy chains, V_L and V_H, respectively. The Fab fragments are joined to a highly conserved 'crystallisable fragment' (Fc) of 50kDa formed by the interaction of the two heavy chains. The C_H domains of Fc are responsible for effector functions such as the binding to receptors, secretion and membrane spanning. The antibody domains are all organised into a central hydrophobic region, a core and a peripheral region. The central hydrophobic section contains the group of residues between the two β-sheets including Cys 23 and 88 that hold the 2 β-sheets together via a disulphide bridge (shown in Fig.1.1).

The core contains the residues in the β-sheets that are common to all domains while the peripheral region contains the remaining residues, including, in the case of V_L and V_H domains, the hypervariable regions or Complimentary Determining Regions (CDRs) (Lesk and Chothia, 1982). The light chains have a Cys residue at the C-terminus to allow the formation of a disulphide bond between it and a Cys residue located in the heavy chain. There is little sequence homology (15%) between the constant and variable domains, the similarities involving some Trp and Cys residues only. However, there is more significant homology between constant chains of different classes (30%).
It is estimated that there are approximately $10^8 - 10^{10}$ different antibody allotypes in serum. This enormous diversity is generated by a number of processes. Firstly, there are multiple germ line genes that code for antibodies (V,D and J), parts of which can be combined to make a complete antibody polypeptide chain.

Figure 1.1 The structure of an IgG molecule.

IgG can be cleaved at the hinge region using papain to release two Fab and one Fc fragment. The binding site for PpL is on the κ-light chain on the Fab fragment while the main binding site for SpA and SpG is at the C_H2-C_H3 interface in the Fc region. However, both can also bind to the Fab region, at the V_HIII and C_H1 domains respectively.
(Adapted from Voet and Voet, 2nd edition)

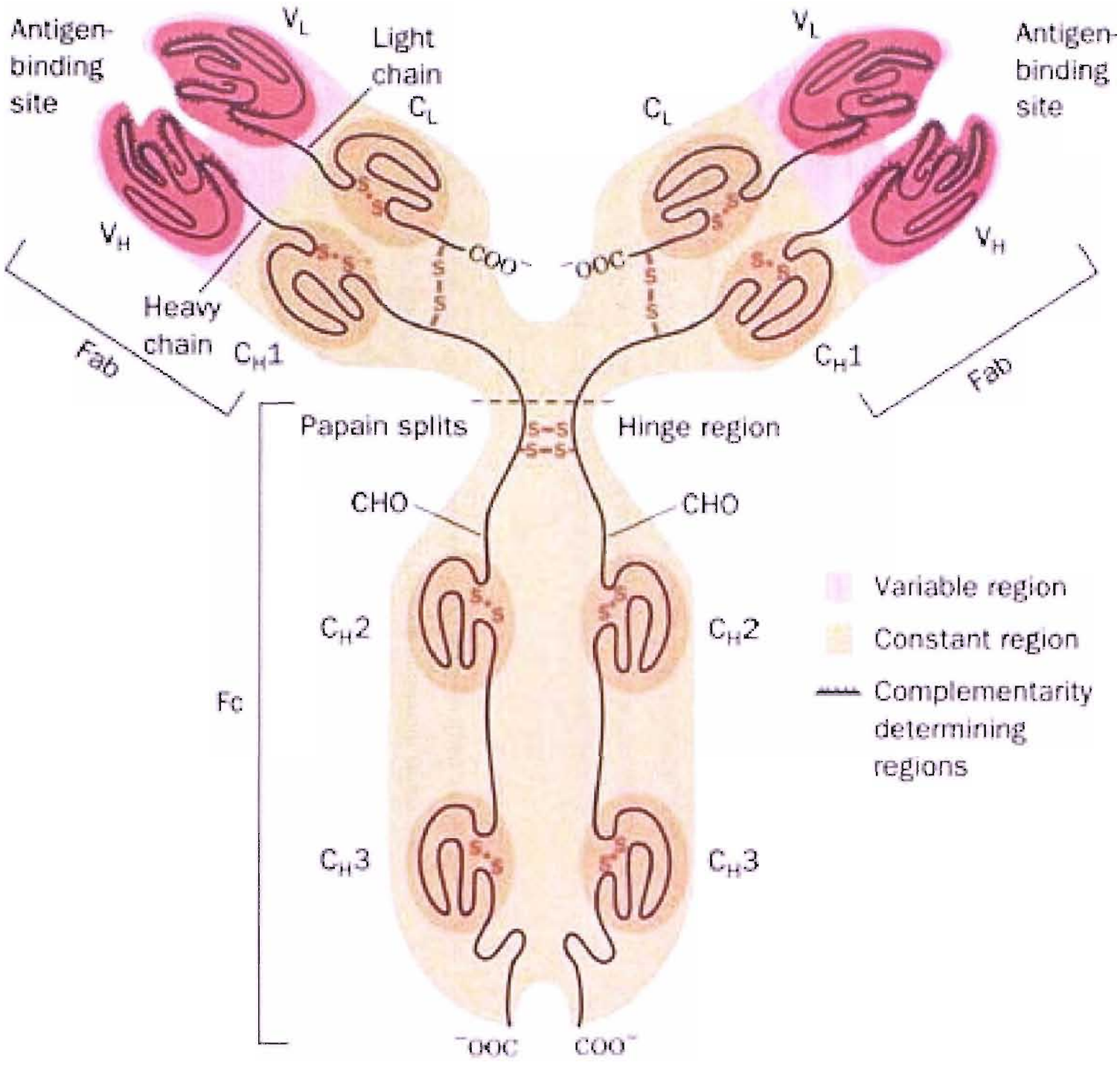
Antigen-binding site
V_L
Light chain
C_L
V_H
Heavy chain
C_H1
Fab
Papain splits
Hinge region
CHO
CHO
C_H2
C_H2
Fc
C_H3
C_H3
^-OOC
COO^-
Variable region
Constant region
Complementarity determining regions

There are two types of light chain in human antibodies termed κ or λ chains which are encoded by separate genes. There are relatively few variants of the genes that encode λ-chains and therefore sequence differences in λ-chains do not contribute much to antibody diversity. However, rearrangement of genes that code for κ-chains gives rise to about 600 different light chains and therefore 600 different antibodies. Similar recombination events in the genes coding for the heavy chains give rise to about 8000 different variations and thus the total variation in antibody sequences due to the combined effects of the above is about 5×10^6. Before these segments of genes are ligated and transcribed, nucleotides can be inserted or deleted between the gene segments, considerably increasing diversity and this is further increased by somatic mutations, particularly in the CDRs giving rise to up to 10^{10} structures (Berg *et al.*, 2002).

The carbohydrate moieties that are linked to Igs are generally linked via asparagine residues to the cleft formed between the C_H2 and C_H3 regions and are thought to provide some protection for the hinge from proteolytic degradation and increase the ability of Igs to bind to receptors and antigen.

1.3 Classes of Igs

There are five different isotypes of Igs which are defined by their Fc regions, each having a specific role in the immune response. Each will also contain either 2 κ or 2 λ light chains for antigen binding. They generally work by forming polymers with antigens which in turn causes the chemotactic attraction of phagocytic cells via the classical complement pathway (IgG and IgA), the alternative complement pathway (IgA) or by the activation of other receptors by cross linking. The Y shape of the molecule is particularly good for polymerisation. It is important to note that monomeric Igs have a low affinity for receptors, it is immune complexes consisting of more than one Ig molecule and antigen which are responsible for receptor binding (Berg *et al.*, 2002).

1.3.1 IgG (γ heavy chain)

IgG is the most commonly occuring and least specialised of Igs involved in the immune response. It has a wide range of properties and can easily diffuse into extracellular spaces. Its primary role is to neutralise bacterial toxins and to bind to harmful micro-organisms to aid phagocytosis. In addition, the binding of IgG to its antigen activates the classical complement pathway. The classical complement pathway is a cascade of 20 proteins which ultimately forms a membrane attack complex which punctures cell membranes causing lysis of the target cell. It is the only class of Ig able to cross the placenta and so protect the unborn child. The molecule is flexible in order to bind antigen and as a result the proline rich hinge region by which this flexibility is generated is vunerable to proteolytic attack. IgG is further divided into four subclasses comprising IgG_1 (65%), IgG_2 (23%), IgG_3 (8%) and IgG_4 (4%) and each of these has a specific role. They vary slightly in amino acid composition and the nature of the interchain disulphide bridges although there is 90% homology between them. IgG has the longest half life of all Igs of approximately 23 days (Berg *et al.*, 2002).

1.3.2 IgA (α heavy chain)

IgA appears in mucosal secretions such as saliva, tears and sweat as well as serum and the gut. Its main role is to protect external surfaces from micro-organisms and polymeric antigens. It does this by preventing them from adhering to the cell surface making them unable to gain entry to the body. A fragment of receptor known as a 'secretory component' of 558 amino acids remains bound to IgA, which greatly reduces its adhesive properties. It is often dimeric in secretions and can activate the alternative complement pathway via its carbohydrate groups. The alternative complement pathway arises when one of the early cascade products, C3b, binds at the microbial surface rather than continuing the cascade to release membrane attack complex. Phagocytes are

able to bind to C3b, so eosinophils which are recruited to remove microorganisms are attracted to the site. IgA is divided into 2 subclasses, IgA_1 (approx 80-90%) and IgA_2 which lacks interchain disulphide bridges between heavy and light chains. IgA and IgM (below) both contain J chains of 137 amino acids which are thought to aid polymerisation. IgA has a half life of 5-6 days.

1.3.3 IgM (μ heavy chain)

IgM is usually found as an oligomer (a monomer in lymphocytes) consisting of five, four-peptide subunits. The latter are IgG-like but contain an extra C_H domain. Although it has a theoretical valency of ten for small antigens it usually has a practical valency of five because of steric clashes. Because of this, IgM is a good agglutinating agent for antigens with multiple epitopes, in particular bacteria, to allow easier disposal by phagocytic cells. Most natural antibodies to microorganisms are IgM e.g. to typhoid endotoxin. IgM is produced early in response to infection and monomeric IgM is used by B lymphocytes to recognise antigens which are anchored to the cell membrane by means of a hydrophobic sequence at the C-terminal end of the molecule. IgM has a half life of 5 days.

1.3.4 IgD (δ heavy chain)

IgD is thought to have a role in the control of lymphocyte activation and suppression as most IgD is found on the surface of some lymphocytes where they operate in conjunction with IgM forming mutually interacting receptors. It has a short half-life (approx 3 days) due to an extended hinge region (four times as long as that in IgG) although additional carbohydrate is present in IgD which affords some protection from degradation.

1.3.5 IgE (ε heavy chain)

IgE is found on mast cell surfaces and, when in contact with antigen, releases a series of inflammatory mediators derived from arachidonic acid, cytokines and amines such as histamine, prostaglandins and leukotrienes which attract large numbers of IgG molecules, granulocytes and eosinophils. It is responsible for inflamatory reactions e.g. asthma and hay fever. Its function is to protect sites that are prone to pathogen entry. It has a half life of 2.5 days.

Table 1.2 The composition of total Ig in blood (Roitt,1997)

Ig class	G	A	M	D	E
Heavy chain type	γ	α	μ	δ	ε
Valency	2	2,4	5(10)	2	2
No. Basic units	1	1,2	5	1	1
% Carbohydrate	3	8	12	13	12
% of total serum Ig	80	13	6	0.1	0.002
Conc. In serum (mg/ml)	8-16	1.4-4	0.5-2	0-0.4	0.017-0.45

1.3.6 Ig light chains; kappa and lambda

Kappa or λ light chains provide half of the antigen recognition site of the Ig molecule. They consist of framework regions that are conserved in sub classes dispersed among the CDRs that form the antigen-binding site and are unique for each antigen. CDRs regions are formed by β-loop turns at the ends of the variable domains and are glycine rich which allow the peptide chains to fold back on themselves to form β-sheet structures. These enable the three CDRs,

Figure 1.2 Comparison of the four human κ-light chain subgroups.

The differences between κ_{II} and $\kappa_{I\text{-}III}$ and $_{IV}$ are shown in bold. Framework regions are denoted by hypervariable regions HVR. PpL is able to bind to the framework regions of $\kappa_{I, III}$ and $_{IV}$ but not to $_{II}$. Types $_{I}$, $_{III}$ and $_{IV}$ comprise 60%, 28% and 2% of total κ-chains respectively, allowing PpL to bind to approx 90% of all κ-chain. PpL is unable to bind to type II because of the replacement of Ser19 by Thr. PpL is unable to bind to λ-chains due to the distorted nature of the framework regions which are needed to give the λ-chains their slightly helical shape.

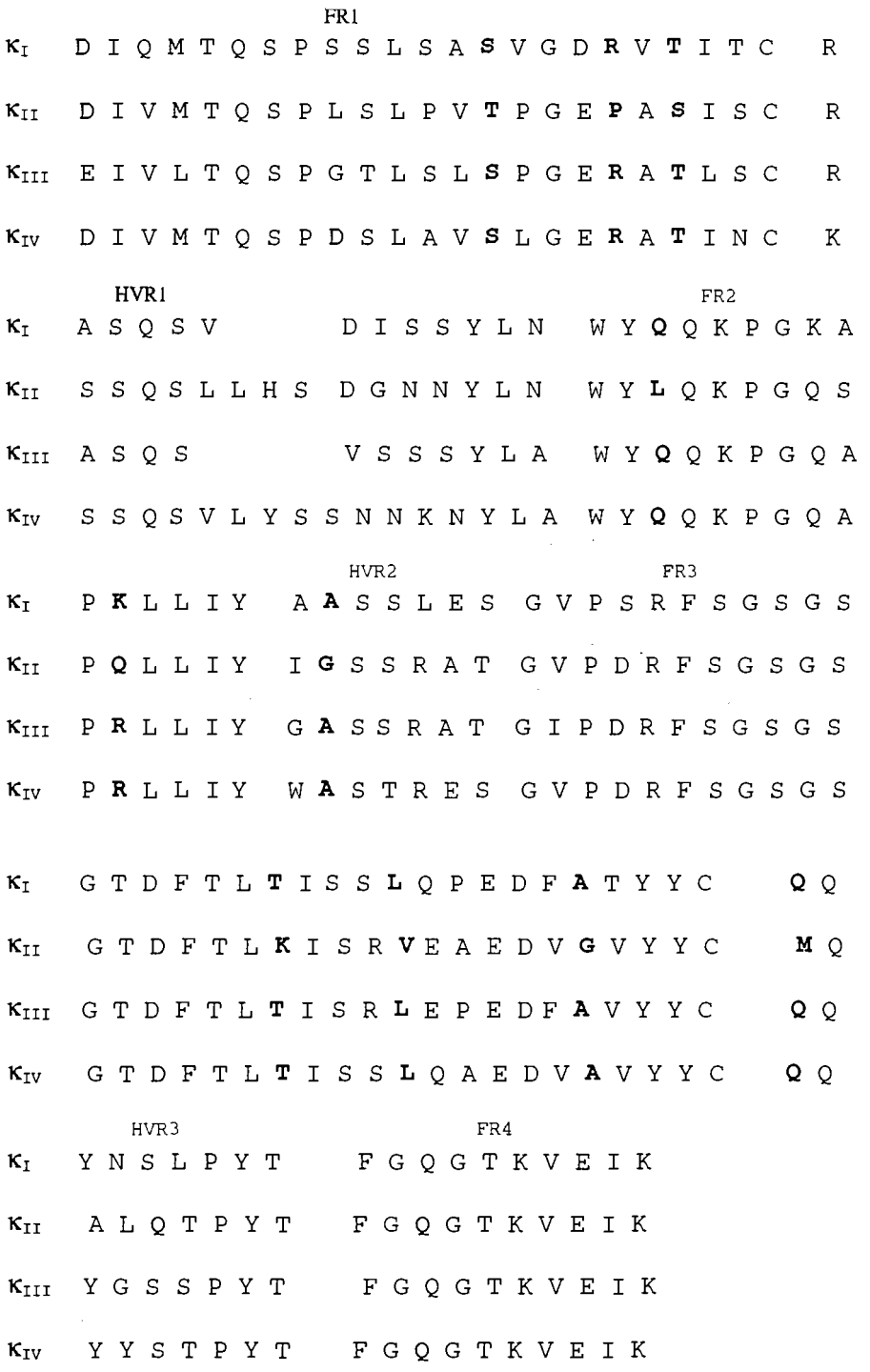
FR1
κI D I Q M T Q S P S S L S A S V G D R V T I T C R
κII D I V M T Q S P L S L P V T P G E P A S I S C R
κIII E I V L T Q S P G T L S L S P G E R A T L S C R
κIV D I V M T Q S P D S L A V S L G E R A T I N C K
HVR1
FR2
κI A S Q S V D I S S Y L N W Y Q Q K P G K A
κII S S Q S L L H S D G N N Y L N W Y L Q K P G Q S
κIII A S Q S V S S S Y L A W Y Q Q K P G Q A
κIV S S Q S V L Y S S N N K N Y L A W Y Q Q K P G Q A
HVR2
FR3
κI P K L L I Y A A S S L E S G V P S R F S G S G S
κII P Q L L I Y I G S S R A T G V P D R F S G S G S
κIII P R L L I Y G A S S R A T G I P D R F S G S G S
κIV P R L L I Y W A S T R E S G V P D R F S G S G S
κI G T D F T L T I S S L Q P E D F A T Y Y C Q Q
κII G T D F T L K I S R V E A E D V G V Y Y C M Q
κIII G T D F T L T I S R L E P E D F A V Y Y C Q Q
κIV G T D F T L T I S S L Q A E D V A V Y Y C Q Q
HVR3
FR4
κI Y N S L P Y T F G Q G T K V E I K
κII A L Q T P Y T F G Q G T K V E I K
κIII Y G S S P Y T F G Q G T K V E I K
κIV Y Y S T P Y T F G Q G T K V E I K

each consisting of about 10 residues, to be spacially close together. Small antigens usually bind in a cleft and may only require the involvement of 15 residues of the Ig molecule, however, larger proteins may need to bind to all of the six CDRs of the Ig. They are held by a combination of hydrophobic interactions, hydrogen bonds, electrostatic interactions and Van der Waals forces.

λ- chains are divided into four subclasses – Meg, Ke $^{-}$Oz $^{-}$, Ke $^{-}$Oz $^{+}$ and Ke $^{+}$ Oz $^{-}$. Oz^{-} has a Lys at position 188 while Oz $^{+}$ has Arg188. Ke^{+} has Gly at position 157 while Ke $^{-}$ has Ser at 157. κ-chains are also divided into several subclasses depending on species and the sequences of human κ-chains are shown in Fig 1.2. These subclasses are thought to have arisen through gene shuffling during evolution and are not thought to have individual functions.

1.4 Immunoglobulin binding proteins

1.4.1 Protein A

Protein A was the first Ig-binding protein to be widely studied and has been commercially available as an affinity ligand for the isolation of Ig for a number of years (Langone, 1982, Jendeberg *et al.,* 1996, Braisted and Wells, 1996). It has a molecular weight of 58kDa and can be extracted from 95% of *Staphylococcus aureus* strains found in human isolates (Langone, 1982). It consists of 5 consecutive Ig-binding domains, each of approximately 58 residues (named A, B, C, D and E). However, Protein A can only bind to two IgG molecules simultaneously, steric restrictions prevent more than two of the five binding domains being occupied at any one time (Ljungquist *et al.,* 1989).

It binds weakly ($K_d = 10^{-7}$M, Sasso *et al.,* 1991) to all classes of Igs from the V_HIII gene family via interactions with the V_H domain in the Fab (Sasso *et al.,* 1991). However, it has a much higher affinity interaction with the Fc region of IgG from a variety of species, in particular to human, rabbit and pig IgG, (K_d of 15nM, Kronvall, 1973). It binds to the Fc region at the C_H2-C_H3 interface of IgG_1, IgG_2 and IgG_4 but not to IgG_3. This is due to His 435 in IgG subclasses 1,

2 and 4 being replaced by the bulkier Arg residue in IgG_3 (Deisenhofer, 1981) which sterically restricts the approach of Protein A.

X-ray crystallography studies of the B domain of Protein A in a complex with human IgG_1 have suggested that the binding domain consists of two anti-parallel α helices (1 and 2) with an unstructured C-terminal region (Deisenhofer, 1981). However, NMR studies (Torigoe *et al.,* 1990) have suggested that the unstructured C-terminal region found by crystallographic studies is in fact a third helix when the protein is in free solution and that contacts only found in the crystal disrupt folding of this part of the domain (Fig.1.3). The studies of Bottomley *et al.,* (1994) suggest that the presence of the third helical motif contributes to the overall stability of the binding site for IgG. Crystallographic studies have now shown that helices 1 and 2 are involved in Fc binding while Fab binding is mediated by helices 2 and 3 (Graille *et al.*, 2000).

The binding of Protein A to IgG-Fc is stabilised by side chains that are found on the lower halves of helices 1 and 2. These participate in four hydrogen bonds and several hydrophobic interactions with residues and peptide backbone contacts in Fc (Deisenhofer, 1981).

A number of biological responses have been noted that are induced by Protein A and Protein A-IgG complexes. These have been found to activate the serum complement system in a way analogous to that of antigen-antibody complexes (Stahlenheim *et al.,* 1973). They have also been found to stimulate lymphocytes and induce interferon production, this has been studied as a possible cancer therapy (Smith *et al.,* 1983). Protein A has also been found to interfere with phagocytosis and chemotaxis of human polymorphonuclear lymphocytes (Musher *et al.,* 1981).

Figure 1.3 The X-ray crystallographic structure of the complex formed between Protein A and Fc region of IgG.

Protein A is at the top of the diagram in yellow with a view looking down the two antiparallel α-helices. Below, protein A is the β-sheet structure of the C_H2 and C_H3 domains of the Fc region of IgG. Protein A binds to the C_H2-C_H3 interface via hydrophobic interactions and four hydrogen bonds.

The four hydrogen bonds are formed between the following residues ;

Protein A		**Fc**	
Gln 13	Donor	Ser 254	Acceptor
Asn 15	Donor	Asn 434	Acceptor
Tyr 18	Donor	Leu 432	Acceptor
Asn 32	Acceptor	Gln 311	Donor

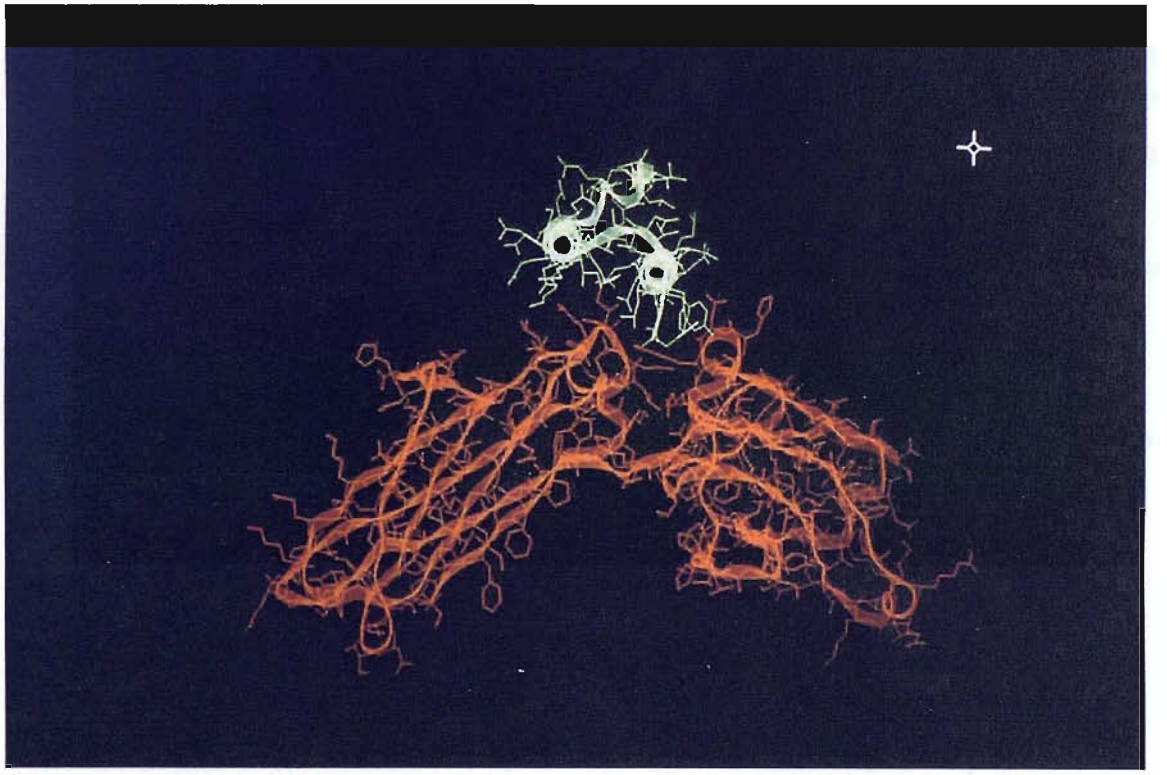

1.4.2 Protein G

Protein G from *Streptococcus*, groups C and G was shown to have Ig-binding properties by Kronvall, (1973) and can be extracted from the cell surface of *Streptococci* by digestion with papain (Björck and Kronvall, 1984, Reis *et al.*, 1984). There are usually three Ig-binding domains in Protein G that have been designated C1, C2 and C3 (Guss *et al.*, 1986) although this is dependent upon the strain of *Streptococci* from which the protein is isolated, more domains may occur. The structure of a single domain has been determined by NMR (Lian *et al.*, 1992) and X-ray crystallography (Achari *et al.*, 1992) and shows that it consists of a four-stranded β sheet made up of two antiparallel β hairpins connected by an α-helix (Fig.1.4). The two internal hairpins β1 and β4 are parallel and the outer strands, β2 and β3 are linked by the α-helix which lies at an angle of 40° to the β-strands (Gronenborn *et al.*, 1991). The binding site for the Fc region of IgG is formed by the third β-strand and the loop region connecting the third β-strand to the α-helix. The structure shows that 95% of the amino acid residues are involved in forming the secondary structure, giving rise to large numbers of hydrogen bonds. The secondary structure is folded in such a way as to give a hydrophobic core with polar residues at the solvent surface. The domain has been shown to be exceptionally stable to denaturants and elevated temperatures (Alexander *et al.*, 1992).

Unlike Protein A, it binds to all subclasses of IgG showing that although it also binds to Fc at the same site as Protein A, its interactions are subtly different (see Table 1.1). It also possesses domains which are able to bind to the most common human serum protein, albumin and to α_2-macroglobulin (Kronvall, 1973). It binds to Ig from a wider range of species than Protein A, perhaps suggesting that there are fewer interactions with Fc than formed by Protein A (Sjöbring *et al.*, 1991). In contrast to the interactions between Protein A and IgG (four H bonds and hydrophobic contacts) Protein G binds to the Fc region of IgG via salt bridges and hydrogen bonds (Sauer-Eriksson *et al.*, 1995). Binding studies have shown that a complex formed between domain C1 and

Figure 1.4 The structure of a single domain of Protein G.

The domain consists of two pairs of antiparallel β-strands linked by an α-helix. An extra residue (cf. PpL) is present in the loop joining the helix to the 3rd β-strand causing the helix to lie at an angle of 40° to the two pairs of β-strands. It is the loop region between the carboxyl end of the α-helix and β-strand 3 that allows binding to the Fc region of IgG.

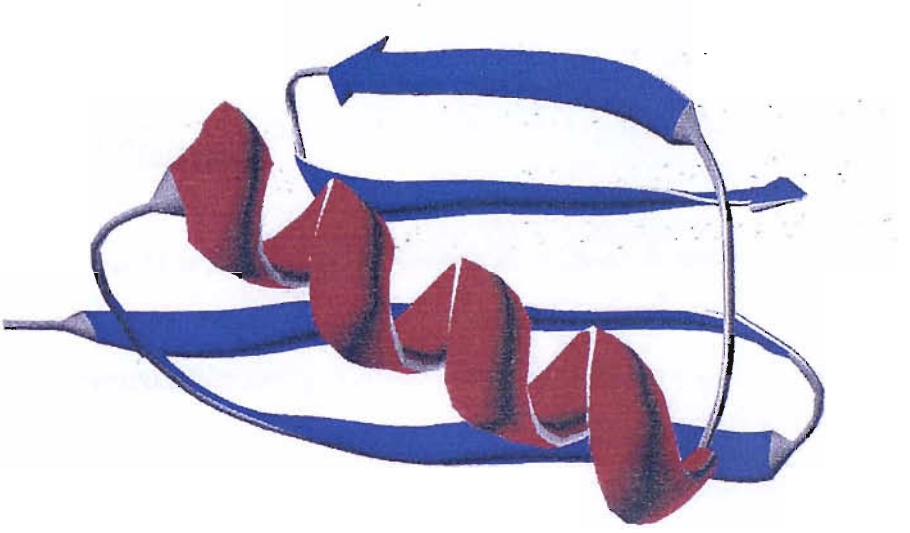

IgG-Fc has a K_d of 2.5 x 10^{-8}M while that formed between C3 and IgG-Fc has a K_d of 5 x 10^{-9}M (Åkerström and Björck, 1986).

Protein G can bind to the Fab region of IgG weakly by aligning the second β-strand of Protein G with the last β-strand in the C_H1 domain of Fab (Fig. 1.5) forming an extended β- sheet (Derrick and Wigley, 1994). The loop region between the helix and third β-strand is also involved, stabilised by hydrogen bonds (Lian *et al.,* 1994).

Both Proteins A and G are superantigens. Together with HIV-1, gp120 and CD4 they stimulate a large number of B-cells to produce antibodies (Eliasson *et al.,* 1989).

1.4.3 Protein H

Protein H is isolated from *Streptococci* group A, and only binds to human and rabbit IgG at the C_H2-C_H3 interface (Akesson *et al.,* 1990). This might be expected since group A *Streptococci* infect a far narrower range of organisms than groups C and G *Streptococci* which possess Protein G and bind to a much greater species range. The Ig- binding domains of Protein H consist of a three α-helical bundle and show no homology with binding domains of Proteins A or G, but do show some homology with a cell surface protein from group A *Streptococci* known as M6.

Protein H has been found to interact with components of the complement pathway. The interaction of Protein H with IgG on bacterial cell surfaces inhibits complement function by blocking C_{1q} binding to IgG. Protein H-IgG complexes can be released from the bacterial cell surface by an extracellular cysteine proteinase. This released complex is thought to cause toxic shock and rheumatic fever (Berge *et al.,* 1997).

Figure 1.5 The complex formed between a single domain of Protein G and Fab.

Binding occurs at the C_H1 domain of the IgG molecule by edge contacts that extend the β-sheet. There is an antiparallel alignment of the 2^{nd} β-strand of Protein G and the last β-strand in the C_H1 domain of Fab forming an extended β-sheet. The complex is stabilized by H-bonds between side chains of Protein G and the backbone of the C_H1 domain. Protein G is in the top left of the picture.

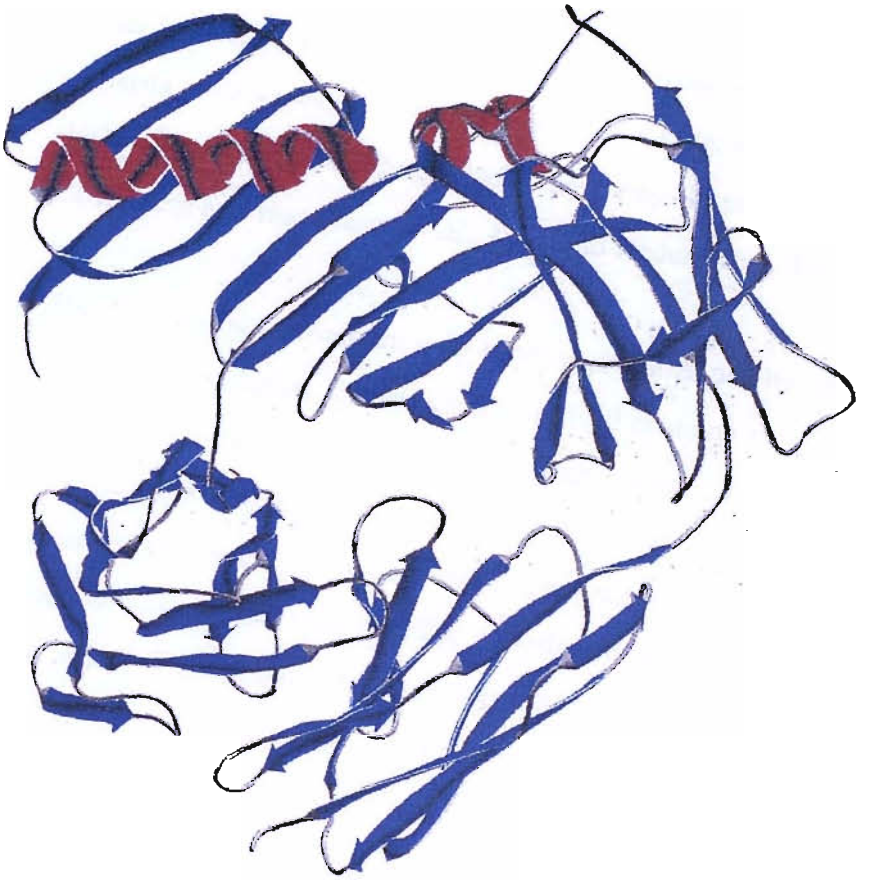

1.4.4 Protein D

Protein D is isolated from *Haemophilus influenzae*, which usually causes infections of the respiratory tract. It is not therefore surprising that Protein D binds only to IgD, the main Ig of the respiratory tract. Protein D is the only known Ig-binding protein from a Gram negative bacterium (Forsgren and Grubb, 1979).

Other Ig-binding proteins include M6 from group A *Streptococci* which consists of two α-helices wound around each other (Pancholi and Fischetti, 1988), also two IgA binding proteins have been found in group B *Streptococci* called Arp and Bac (Sasso *et al.*, 1991 and Heden *et al.*, 1991).

The differences between these Ig-binding proteins may be due to rapid convergent evolution; independently evolved proteins able to bind common blood proteins to offer the bacterium an advantage. The evolution of common structural features such as a signal peptide, cell membrane anchor and cell spanning region may have been due to gene duplication and swapping of gene fragments known as cassettes. The presence of Ig-binding proteins in such a variety of Gram positive bacteria suggests that they are important. The differences in the number of binding domains and differing sequences reflect the variety of host species for the different bacteria in which the proteins are found (Frick *et al.*, 1992).

1.5 Protein L

Protein L was first isolated from *Peptostreptococcus magnus* by Myhre and Erntell (1985) and was named due to its interaction with the light chains of Ig (Björck, 1988) . *Peptostreptococcus magnus* is a rod shaped Gram positive bacterium, which is widely found on most body surfaces, especially in the urogenitary and gastrointestinal tracts and often exists in long chains. It can also congregate at the site of wounds. These bacteria are part of the indigenous flora but can sometimes cause infections, often in conjunction with other

micro-organisms or when the body's defences are low; it is an opportunist pathogen. Studies using a DNA probe encoding the B1 binding domain from Protein L have shown that between 10-20% of *Peptostreptococcus magnus* strains possess Protein L. However, from strains isolated from patients with clinical infections, occurrence of Protein L is greater than 20% implicating Protein L as a virulence factor (Kastern *et al.,* 1990). Protein L binding to immunoglobulins has been detected in the serum of 12 out of 23 mammalian species tested (De Château *et al.,* 1993).

There are several possible mechanisms by which Protein L could increase the virulence of the bacterium in which it is found (Goward *et al.,* 1993). The coating of the bacterial cells with common blood proteins from the host may act as a 'disguise' for the cell, preventing recognition by the host immune system. A covering of host proteins may also help the bacteria to colonise sites of wounds where blood plasma protein levels are increased, as this coating makes them "sticky". However, an accumulation of Ig molecules makes the bacterial cell more susceptible to attack by host basophils. This is clearly a disadvantage but is thought to be outweighed by the virulence-enhancing effects of Protein L. This illustrates that the host parasite relationship is a delicate balance (Kastern *et al.,* 1990).

1.5.1 Protein L *in vivo*

Protein L has been found to cause histamine release in humans at an optimum temperature of 37°C and in the presence of 1mM Ca^{2+} (Patella *et al.,* 1990). Protein L also activates human basophils and mast cells by interacting with κ-chains of IgE. It acts as a complete 'secretagogue' i.e. makes a cell release all of its secretory chemicals. It also makes basophils release the chemical mediators sulphidopeptide leukotriene C4 and PGD2 (Patella *et al.,* 1990). The characteristics of this release by Protein L are similar to that caused by rabbit IgG or anti-Fc fragment of human IgE (anti-IgE) that binds to the Fc region of the IgE molecule on the basophil membrane. Protein A and G have also been found to activate basophils, but to a much lesser extent than Protein L. Protein

A has been shown to induce increased production of antibodies with rheumatoid factor activity by V_HIII expressing lymphocytes to which Protein A is able to bind (Kristiansen *et al.*, 1994).

Many of these Ig-binding proteins can also bind to proteinase inhibitors. This activity could have two possible effects. It takes away proteinase inhibitors from the close environment of the bacterium which may affect the bacterium's own proteolysis. In addition, it may also prevent attack by host proteinases e.g. from the complement pathway.

1.5.2 The structure of Protein L

Protein L has been isolated and structurally characterised from two different strains of *Peptostreptococcus magnus*. The Protein L gene from *Peptostreptococcus magnus* strain 312 shows a polypeptide chain of 719 amino acid residues and is an elongated fibrous protein of 77kDa (Åkerström and Björck, 1989). It is heat stable and resistant to trypsin digestion. Protein L has been isolated from the cell wall by solubilising the cell wall with mutalysin or isolated from the culture medium by a single affinity chromatography step on human IgG-sepharose. Each bacterial cell can contain up to 80,000 molecules of Protein L (Kastern *et al.*, 1992) and 1ml of packed *Peptostreptococcus magnus* cells produces approximately 0.92g of Protein L.

Protein L from *Peptostreptococcus magnus* 312 has been shown by NMR studies (Wikström *et al.*, 1995) to consist of the following structural features ;

- An initial sequence of 18 residues (cleaved during processing).
- NH_2 terminal region 'A' of 79 residues.
- Five homologous 'B' repeats each of 72-76 residues.
- Two homologous 'C' repeats each of 52 residues.
- A proline rich membrane spanning region 'W'
- A hydrophobic membrane anchor 'M' at the C-terminal end which has four negatively charged residues which protrude into the cytoplasm.

Figure 1.6 Comparison of the sequence organization of the most characterized Ig-binding proteins A, G and L.

All the proteins have a membrane spanning region and a membrane anchor typical of a gram positive bacterial protein. The Ig binding properties in L have been shown to be due to the B repeats, analogous to repeats in A and G where binding activity has been located. There is no homology between these domains, however, as they all bind to different parts of the Ig. The C repeats in Protein L are thought to bind to other common blood proteins e.g. Human serum albumin and proteinase inhibitors. The N and C terminals are at opposite ends of each domain to allow domains to be connected linearly in a chain to reduce steric hindrance when binding to Igs. S is the signal peptide, M is a membrane anchor domain and W is a cell wall spanning region.

Protein A (*Staphylococcus aureus*)

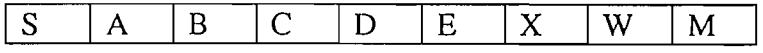

Protein G (Group C and G *Streptococci*)

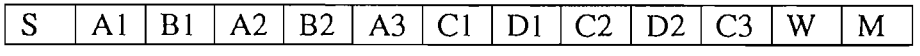

Protein L (Strain 3316 of *Peptostreptococcus magnus*)

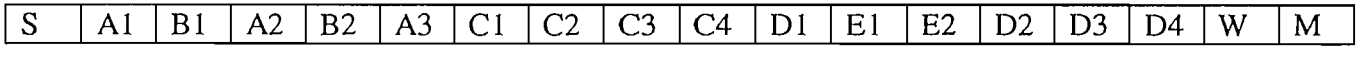

Protein L (Strain 312 of *Peptostreptococcus magnus*)

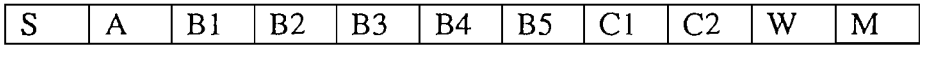

The membrane spanning region consists of 17 tripeptide units X1-pro-X2, a proline surrounded by one hydrophobic residue and one hydrophilic residue on its amino and carboxyl side, respectively. X1 is threonine six times and valine three times. X2 is serine ten times, asparagine three times or glutamine twice. This is typical of a Gram positive cell wall protein (Murphy *et al.*, 1994).

The 'C' repeats are highly homologous to each other but have no homology with other parts of the protein. It is thought their function may be to bind other common blood proteins other than Igs e.g. proteinase inhibitors and human serum albumin. The domain organisation of Protein L is shown in Fig 1.6.

The Ig-binding properties of Protein L have been shown to be due to the 'B' repeats, analogous to repeats in Protein A and G where binding activity has also been located. There is no homology between the Ig-binding domains of Protein L and the binding domains of other Ig-binding proteins. This is not too surprising since Protein L binds to the κ-light chains of all classes of Igs (Myhre and Erntell, 1985) while the others generally bind to the Fc region of a single class of Ig. The N and C terminals are at opposite ends of the folded domains enabling the domains to be connected in a linear arrangement in the native protein to reduce steric hindrance during binding to Igs.

1.5.3 Protein L from *P. magnus* strain 3316

Protein L has also been isolated and studied from *Peptostreptococcus magnus* strain 3316 (Murphy *et al.*, 1994) which differs slightly from that found in strain 312. It has 992 amino acid residues and a molecular weight of 106kDa. It has the following structure in addition to the membrane anchor and cell spanning region common to all Ig-binding proteins ;

- Three 'A' units of 28 residues (function unknown)
- Two 'B' units of 33 residues (function unknown)
- Four 'C' units of 72-75 residues (Ig-binding domains)

- Four 'D' units of 62 residues (albumin binding domains)
- Two 'E' units of 50 residues (function unknown)

1.5.4. The structure of a single Ig-binding domain from Protein L

A single Ig-binding domain from Protein L (PpL) consists of two pairs of antiparallel β-strands, which are joined by an α-helix. The helix lies at an angle of 10^{o} (almost parallel) to the pairs of β-strands (Fig.1.7) . The flexible N terminal region is not thought to be involved in binding interactions and NMR studies have not detected a conformational change on binding to κ-chains (Wikström *et al.,* 1995, Wikström *et al.,* 1996). Residues implicated by the NMR studies to be involved in the binding interaction are found mainly in the second β-strand, the C-terminal end of the α-helix and the loop region connecting the α-helix with the third β-strand. The binding residues are conserved in both strains of *P.magnus* from which Protein L has been isolated (Fig.1.8). The residues for strain 312 are numbered by the method of Wikström (1993) and those of strain 3316 are numbered as described in Bottomley *et al.,* (1995). Overall, there is a 60% homology between binding domains from 312 and 3316 with the main differences occurring at the N-terminal end of the domain. Interestingly, Proteins A and G both bind at a similar site on the Ig-Fc but have different tertiary structures whilst Proteins G and L have similar tertiary structures but bind at different sites on Ig (Fig.1.9). The difference in angle of the α-helix relative to the β-strands of SpG and PpL is caused by the presence of an extra residue in SpG in the loop between the α-helix and strand 3, and this could account for the difference in binding specificity of the two proteins since the α-helix has an important role in SpG binding to Fc. The loss of a residue in this region may well account for the inability of Protein L to bind Fc (Fig.1.10).

Figure 1.7 The structure of a single domain of Protein L.

The domain consists of two pairs of antiparallel β-strands linked by an α-helix which is at an angle of 10^{o} to the pairs of β-strands. This gives a compact structure with a well defined hydrophobic core and a simple convex binding surface. The binding residues are mainly located in the 2^{nd} β-strand, the loop region joining the 2^{nd} strand to the α-helix and on the C-terminal end of the α-helix.

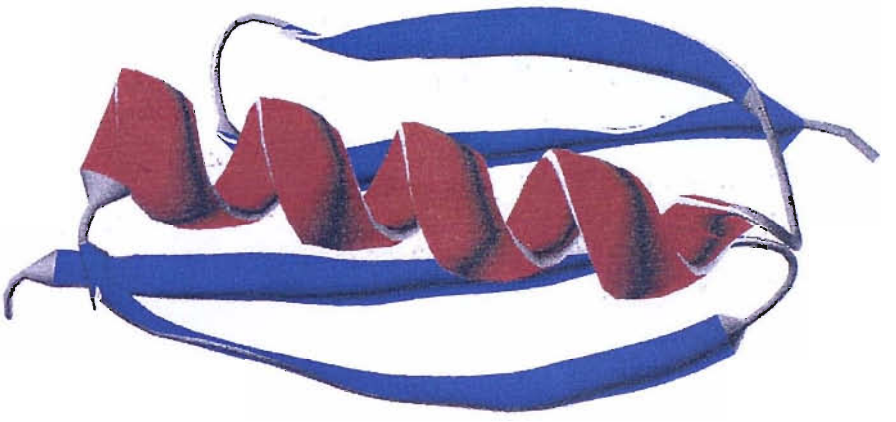

Figure 1.8 The comparison of the sequences of the Ig-binding domains of PpL_{312} and PpL_{3316}.

The figure shows the amino acid sequences of Ig-binding domains from strains 312 and 3316 of *Peptostreptococcus magnus*. Highlighted in bold are residues implicated in binding by the NMR studies of Wikström *et al.*, (1996).

The residues for strain 312 are numbered by the method of Wikeström *et al.*, (1993) and those of strain 3316 are numbered as described by Bottomley *et al.*, (1995).

Overall there is a 60% homology between binding domains from 312 and 3316, with the main differences occurring at the N-terminal end of the domain.

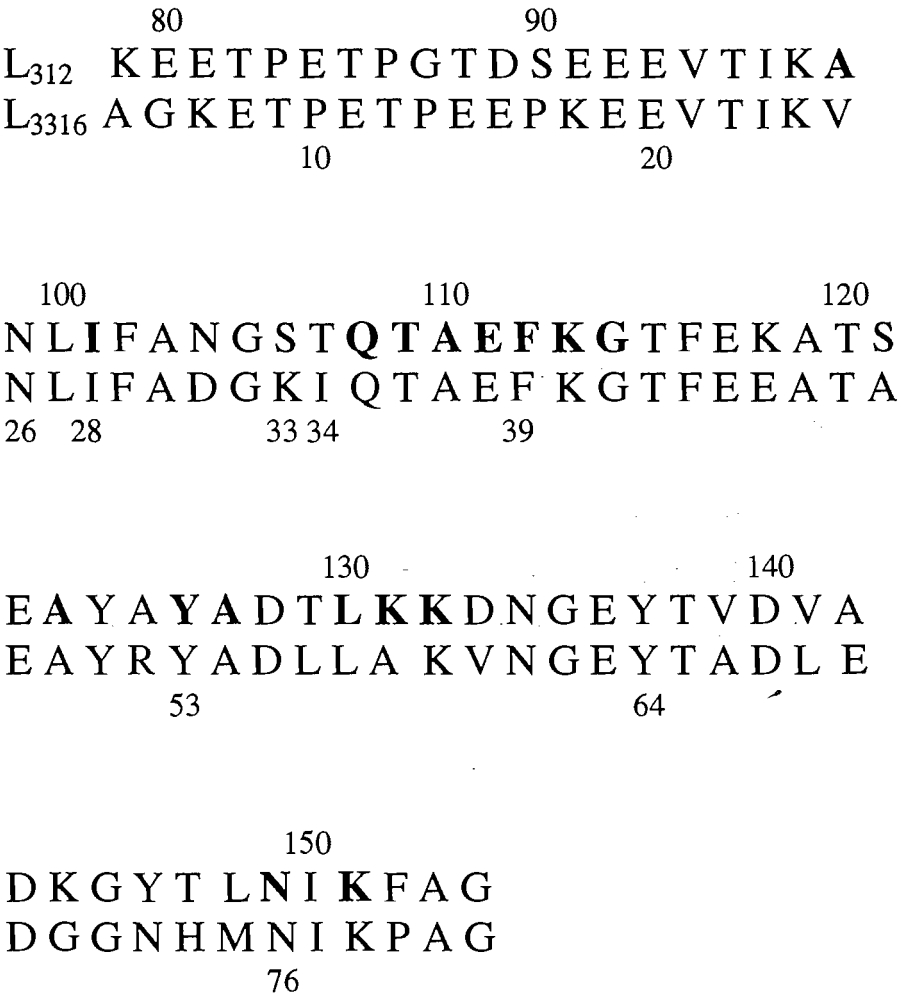
80
90
L312 K E E T P E T P G T D S E E E V T I K A
L3316 A G K E T P E T P E E P K E E V T I K V
10
20
100
110
120
N L I F A N G S T Q T A E F K G T F E K A T S
N L I F A D G K I Q T A E F K G T F E E A T A
26 28
33 34
39
130
140
E A Y A Y A D T L K K D N G E Y T V D V A
E A Y R Y A D L L A K V N G E Y T A D L E
53
64
150
D K G Y T L N I K F A G
D G G N H M N I K P A G
76

Figure 1.9 Comparison of the binding of PpL and SpG to light chains.

PpL and SpG have similar tertiary structures but bind at different sites on the Fab molecule. The loop region between the α helix and strand 3 of SpG has an extra residue which could account for the difference in binding specificity compared with PpL.

The left hand diagram shows the binding of PpL to light chain (at site 1). PpL binds to the framework between the hypervariable loops of the κ light chains. The Fab is joined to the β2 strand of PpL in a β-zipper interaction via 6 H-bonds.

The right hand diagram shows the binding of SpG to the C_H1 domain of Fab. SpG binds to the Fab region by aligning the second β-strand with the last β-strand in the C_H1 domain of Fab forming an extended β-sheet.

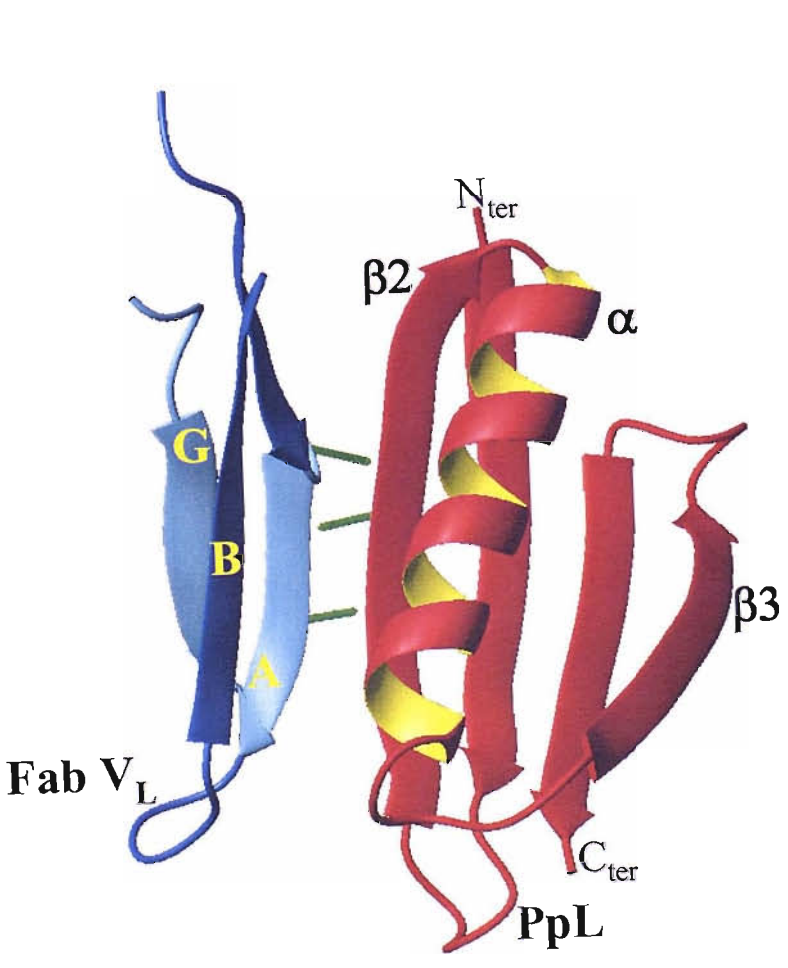
N ter
β2
α
G
B
β3
A
Fab V L
C ter
PpL

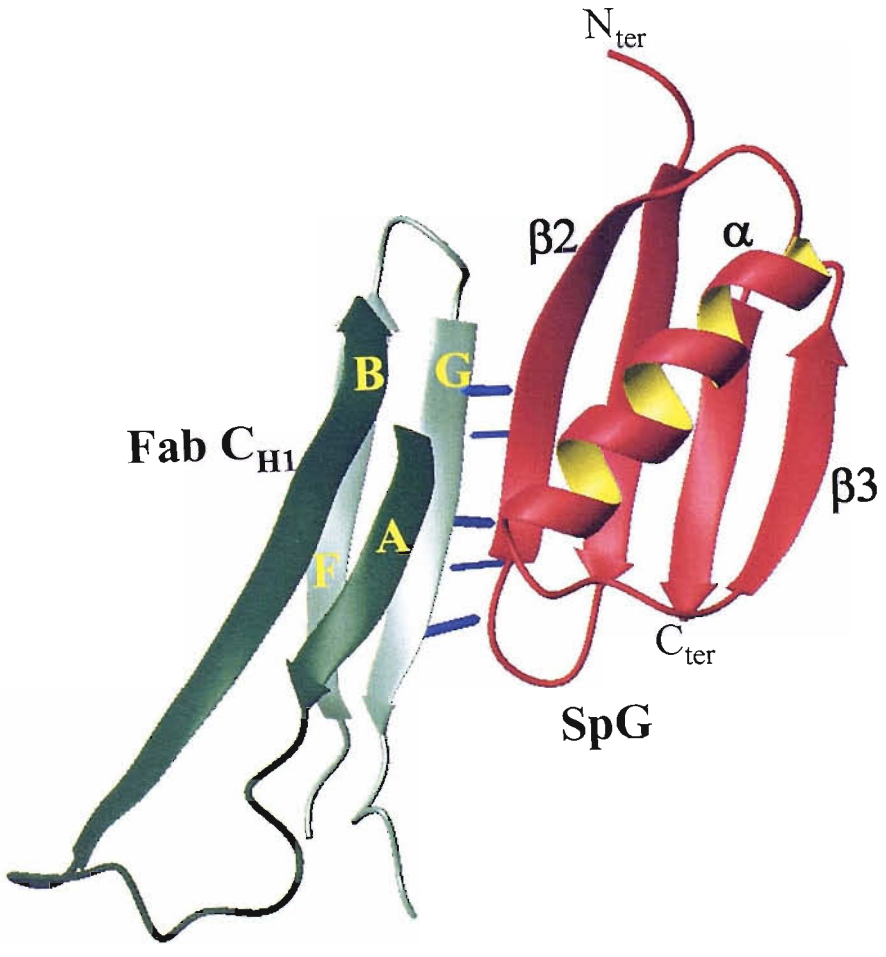
N ter
β2
α
B
G
Fab C H1
β3
F
A
C ter
SpG

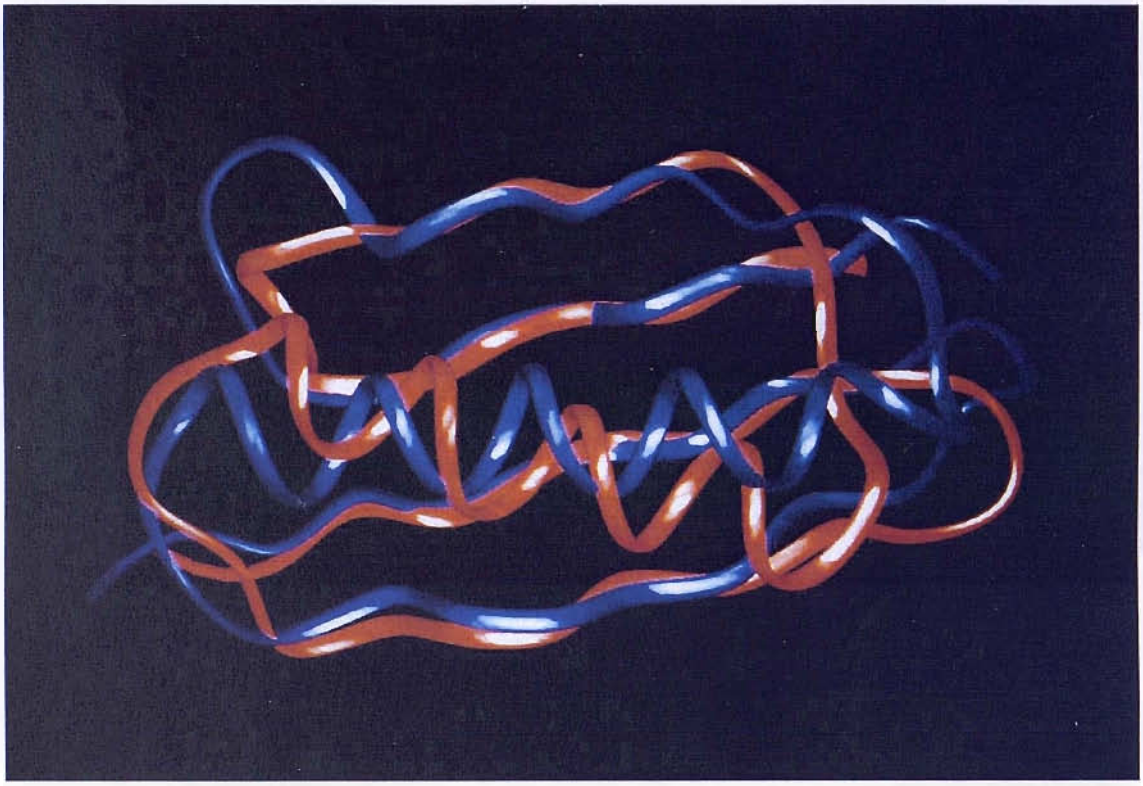

Figure 1.10 Comparison of the secondary structure of Protein G (red) and Protein L (blue).

Protein G has an additional residue in the loop region joining the α-helix to the 3rd β-strand causing the α-helix to lie at an angle of 40°. This extra residue in the loop region and lack of sequence homology between Proteins G and L explains why Protein G an L bind to different regions of the antibody molecule despite having similar tertiary structures.

1.5.5. Mechanism of binding

Protein L binds to the framework regions between the hypervariable loops of the variable domain of κ-light chains without affecting the binding of the Ig to its antigen. It has been shown that Protein L binds to κ-chains type 1, 3 and 4 (Nilson *et al.*, 1992) which comprise 60%, 28% and 2% of total human κ-chains, respectively (Solomon, 1976). Protein L is unable to bind to κ-chain type 2 because of the replacement of Ser 19 by Thr. No λ-chain binding has been detected for Protein L which is thought to be due the distortion of the framework region needed to give the hypervariable regions of λ-chains their slightly helical shape (Foote and Winter, 1992). It is thought that the complete V_L domain is required for Protein L binding indicating that more than one region on the domain is involved.

1.5.6 Thermal stability

Protein L has a high thermal stability that is achieved without any disulphide bridges. Differential scanning calorimetry shows a simple two-state model (folded and unfolded states in equilibrium) for the unfolding of a single domain of Protein L from *P. magnus* strain 312 (Alexander *et al.*, 1992). It also has a high thermal stability that is a consequence of the small size of a domain giving a favourable surface area to volume ratio. There are a large number of hydrogen bonds within the molecule, adding to its stability, which is typical of a larger globular protein. However, high thermal stability does not necessarily mean high stability at physiological temperature to other denaturants (Privalov and Gill, 1988). The simplicity of the PpL domain and the lack of disulphide bonds and proline residues has allowed it to be used as a model for unfolding studies both using computer modelling (Sorenson and Head-Gordon, 2002) and by mutagenesis studies (Scalley *et al.*, 1999) which show that the rate limiting step in the folding of the domain is the formation of the first β-hairpin.

1.5.7 Crystal Structure

A single domain of Protein L from *P. magnus* 3316 has been crystallised and its structure elucidated (Brian Sutton, private communication) (Fig.1.11). The unit cell was found to be square bipyramidal in shape and the crystal diffracted to 2.2Å resolution. It contains two molecules of the domain related by a non-crystallographic 2 fold axis (Sohi *et al.,* 1995).

The Protein L dimer found in the crystals is stabilised by two hydrogen bonds between Asn 26 and Gly 32 and between Asn 73 and Phe 29 and by hydrophobic interactions between the side chains of Ile 28 and Ile 34 of each domain. Ultracentrifugation studies, however, indicate that PpL does not exist as a dimer in free solution at concentrations up to 3mg / ml (Sutton, private communication). Recently, computer modelling has been used to predict an obligate dimer for PpL_{312} containing three mutated residues (Kuhlman *et al.*, 2001).

1.6 Uses of Ig-binding proteins.

Protein A has been commercially available for many years and has many uses in both purification and diagnostic applications. However, in principle and practice Protein A may be substituted by other Ig-binding proteins such as Protein G or the much more recently discovered Protein L. Perhaps Ig-binding proteins main uses are as affinity ligands, e.g. Protein A has been immobilised onto Sepharose or controlled glass beads to purify antibodies (Hjelm *et al.,* 1972).

Protein A has also been used in 'extra-corporeal shunt therapy' in the removal of antibodies from blood, eg. removal of the anti-HLA antibodies (human histocompatability antigen) prior to organ transplants (Palmer *et al.*, 1989). After organ transplants, between 20-30% of patients produce anti-HLA antibodies that cause the transplant to fail. If the plasma is passed down a Protein A affinity column, most of the anti-HLA antibodies are removed since

the majority of them are IgG. This technique has been used successfully in kidney transplants without side effects and is more effective than the traditional plasma exchange method (Barocci and Nocera, 1993).

It has been used to enhance the sensitivity of ELISAs and radio-immunoassays. (Engvall, 1980).

Protein A is also useful as a fusion protein e.g. the gene encoding IGF1 (insulin growth factor) can be fused to the gene encoding one Ig-binding domain of Protein A and the expressed fusion protein purified using an IgG affinity column. The purified fusion protein can be chemically cleaved to release IGF1 and the liberated Protein A removed by a second passage down a column of immobilised IgG (Moks *et al.,* 1987).

Fusion proteins can be created which increase the effectiveness of Ig-binding proteins e.g. the fusion protein Protein A-Protein G that displays the binding characteristics of both proteins (Eliasson *et al.,* 1989). Fusion proteins have been created for use in ELISAs e.g. Protein A fused with alkaline phosphatase (Uhlen *et al.,* 1983), with luciferase (Lindbladh *et al.,* 1991, Lindbladh *et al.,* 1993), with aequorin (Zenno and Innouye, 1990) and with β-lactamase (Baneyx *et al.,* 1990).

Immobilised Protein A has been used to remove various potentially harmful antibodies e.g. anti-factor 8 from the serum of some haemophiliacs, anti glomerular basement membrane antibodies in Goodpastures Syndrome and anti-double stranded DNA antibodies in systemic lupus erythematosis (Palmer *et al.,* 1989).

Protein G has similar potential uses to Protein A, however, Protein G has been found to be more stable than Protein A, with a higher affinity for IgG than Protein A and a broader species range for the binding of IgG. It has been explored as a possible anti-cancer agent since it may be possible to use Protein

Figure 1.11 The structure of PpL as shown in the crystal asymmetric unit (Wan, T. and Sutton B.J. unpublished X-ray crystallographic data).

Residues at the dimer interface are shown as follows : Ile residues 28 and 34 from each domain form hydrophobic interactions and Asn residues 26 and 76 act as donors in four hydrogen bonds to main chain carbonyl groups at positions 29 and 32.

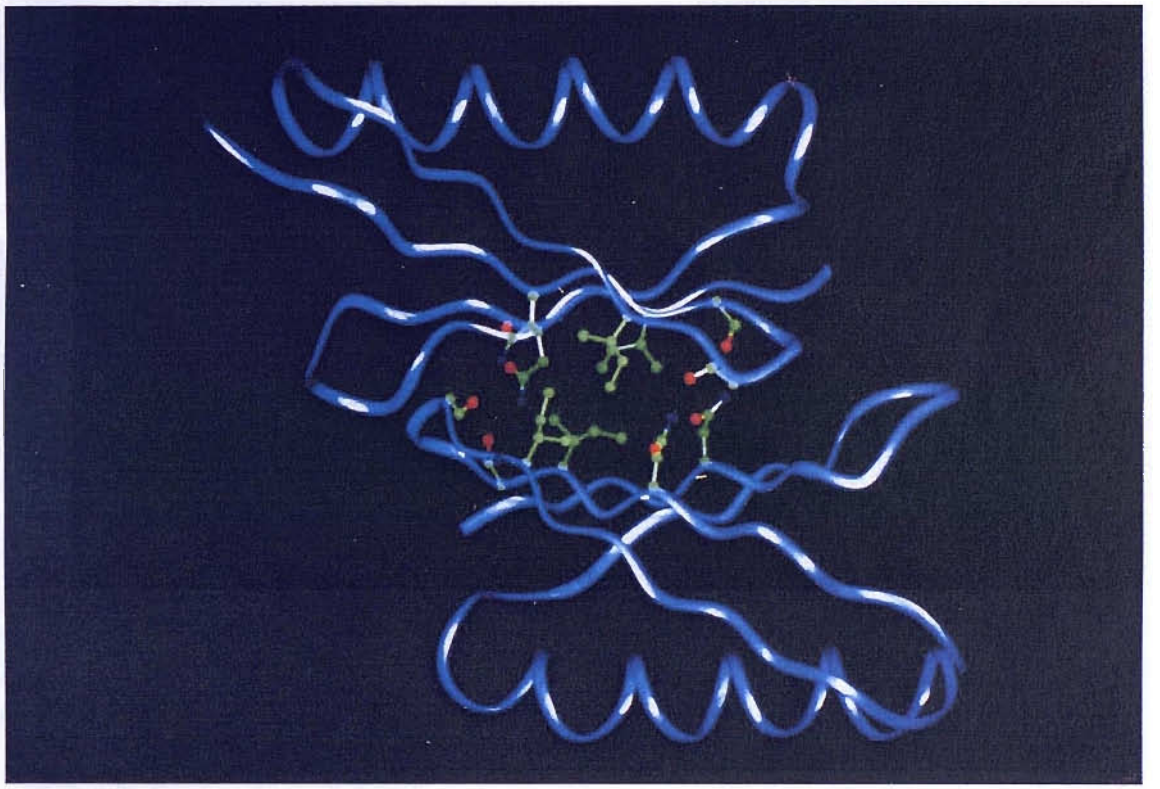

G to cause antibodies to congregate at cancer sites (Terman *et al.,* 1980) and induce the complement cascade.

Protein L has already been used to purify engineered antibodies (Nilson *et al.,* 1993) and can also be used to purify S_cFv fragments due to its κ light chain-binding ability. S_cFv fragments are dimers formed from the V_H and V_L domains of an Ig linked by a hydrophilic spacer (Huston *et al.,* 1988). The advantage of using Protein L is that it can bind to all classes of immunoglobulins. Using a Protein L affinity column it is possible to isolate about 50% of total immunoglobulins from human serum (the percentage found with κ light chains of types 1,3 and 4) and about 40% of mouse immunoglobulin. Compared with intact Igs, Fab fragments are more readily expressed in recombinant systems and do not have the side effects associated with Fc, such as complement activation and receptor binding. Therefore, Protein L offers a clear advantage over Protein A and Protein G for their purification (Nilson *et al.*, 1993). Furthermore, many monoclonal antibodies and fragments of antibodies expressed by bacteria do not bind to Protein A or Protein G (only 28% of human polyclonal Fab interact with Protein G, (Sasso *et al.,* 1991)).

It may be possible to generate proteins consisting of domains from different Ig-binding proteins with very specific binding abilities. For example, a hybrid protein has been constructed which contains four binding domains from Protein L and two binding domains from Protein G. This hybrid is able to bind to all subclasses of IgG and any other Ig molecules containing κ-chains (Kihlberg *et al.,* 1996). Protein LA has also been engineered consisting of 4 domains from Protein A and 4 domains from Protein L also binds to a wider variety of Ig molecules (Svensson *et al.*, 1998).

1.7 Previous work in these laboratories

The gene encoding the single domain of Protein L has been cloned into plasmid vector pKK223-3 which is under the control of an IPTG inducible

promoter. This vector, when used to transform *E. coli,* leads to the over-expression of a single domain of Protein L which has been used in a number of chemical and spectroscopic studies.

The role of all of the Tyr residues (residues 51, 53 and 64) in a single domain has been investigated by previous workers in these laboratories (Beckingham *et al.*, 1999; Beckingham *et al.*, 2001). Chemical modification of PpL by tetranitromethane showed that two residues were modified, Tyr 51 and 53, however, although modification of Tyr 53 considerably weakens binding, modification of Tyr 51 has little apparent effect on the binding detected by ELISA. This confirms initial NMR studies of Wikström *et al.,* (1995) which suggested Tyr 53 was an important residue in binding.

A series of mutants had previously been constructed including two mutants bearing unique Trp residues (Beckingham, 1997). These versions of Protein L give improved fluorescence characteristics since the WT does not contain Trp. The mutants, F39W and Y64W, have the Trp residues on the 2^{nd} strand and 3^{rd} strand respectively. The improved fluorescent characteristics of these proteins allowed both equilibrium and pre-equilibrium binding studies to be carried out. Pre-equilibrium studies using stopped flow fluorescence spectroscopy show a two phase signal change on binding – an initial fast phase, which is protein concentration dependent and a second, slow, uni-molecular step which increases the stability of the complex approximately 30 – 50 fold depending upon conditions. These results suggest that binding takes place with the formation of an initial encounter complex followed by a structural transition that leads to an increase in affinity at equilibrium. This is discussed in more detail in Chapter 6.

The mutant double mutantY53F,Y64W was made to enable stopped-flow fluorescence spectroscopy to determine the effect of the Y53F mutation on the rates of binding / dissociation of its complex with κ-light chains and the K_d for the complex. The results showed that the second, slow change in fluorescence, noted in the mutant Y64W, no longer takes place suggesting that Y53 may be

important for the conformational rearrangement after formation of an encounter complex. This is supported by the observation of a H-bond between Y53 and Fab in the X-ray structure determined by Graille *et al.*, (2001). The K_d for Y53F,Y64W and κ-chains is approximately 3μM which is approximately 30 – 50 fold higher than for the WT.κ-chain complex, clearly indicating that Y53 is implicated in binding (Fig. 1.12).

These kinetic and spectroscopic methods (Beckingham *et al.,* 1999) suggested that a small structural rearrangement may take place after the initial binding between PpL and κ-chain. The crystal structure, however, suggests that no large conformational change occurs in either protein although side-chain rotations occur (Graille *et al.*, 2001). The structural rearrangement observed by fluorescence techniques may simply be a movement of the PpL domain to make better contact with the κ-chain after initial docking of the two proteins.

Recent work carried out after the work described in this thesis has revealed the possibility of a second, much lower affinity binding site for Fab domain on the PpL single domain (Graille *et al.*, 2001). A crystal structure has been obtained showing PpL sandwiched between two Fab domains (Figs.1.13 and 1.14). The reason for this second weak binding site is as yet unclear, it may simply increase the overall avidity of the binding interaction or bind antibodies that cannot bind to site 1.

The first binding interface is consistent with previous crystallographic and NMR data (Wikström *et al.*, 1995). Twelve residues from β2 strand and the α-helix form 6 H-bonds with 13 residues of the Fab domain, 10 of which are located in the framework region of the Fab joining the β2 strand of PpL to the β-sheet of the Fab domain in what is known as a β-zipper interaction. The second binding interface involves 14 residues from the β3 strand and α-helix from the PpL domain and 15 residues from the Fab domain, 10 of these Fab residues are common to the first binding interface. These form 6 H-bonds and two salt bridges. H-bonds and salt bridges involved in the two interfaces are

Figure 1.12 The residues on the κ-chain and PpL that interact at site 1 (Classical Interface).

H-bond between Y53 of PpL and T20 of κ-chain shown in red which has been the subject of several experiments in this thesis and other work.
Other H-bonds formed are shown below ;

Ser L9 to Glu38
Ser L9 to Lys40
Ser L10 to Glu38
Ser L10 to Glu38
Ser L12 to Thr36

(See also Table 1.3)

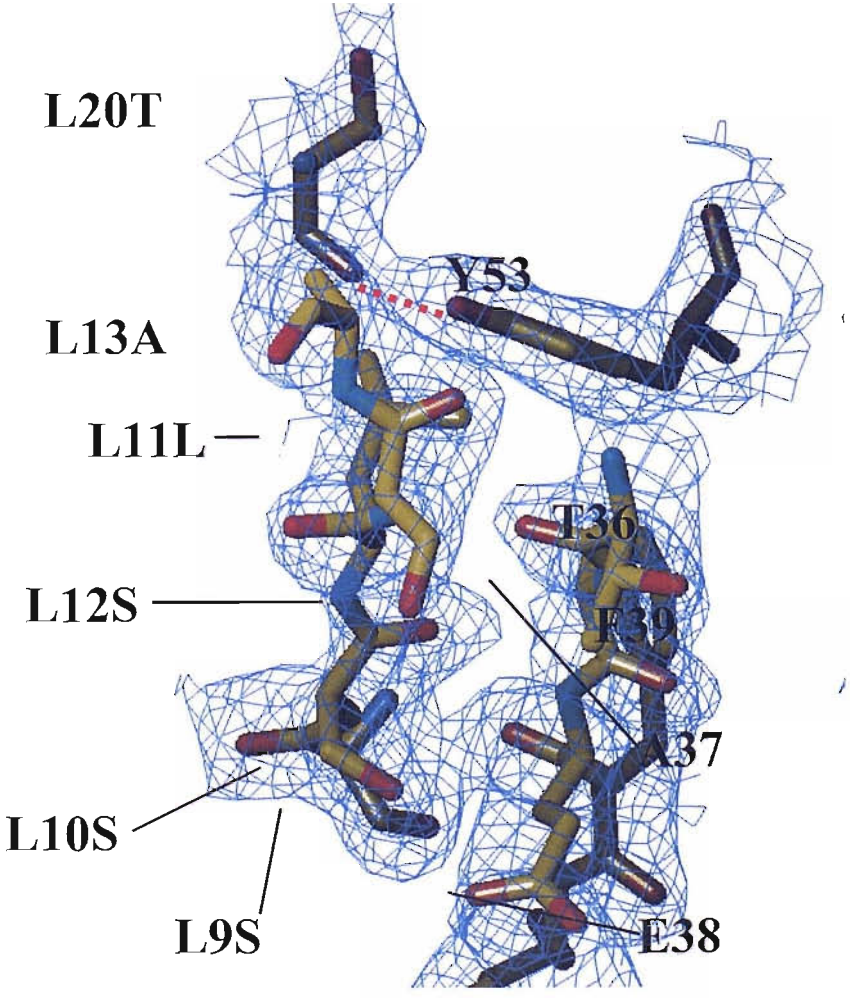
L20T
Y53
L13A
L11L
T36
L12S
E39
A37
L10S
L9S
E38

Figure 1.13 Showing the interaction between PpL and Fab fragments (1).

The figure shows the interaction between PpL shown end-on (centre, red) and variable domains from two Fab fragments. Most of the residues implicated in binding to site 1 (The "classical" interface) are located in strand 2 and the N terminal end of the helix while those of the newly observed alternative interface at site 2 are located in strand 3 and the C terminal end of the helix. The diagram clearly shows that the antigen binding sites (Ag) are not affected by PpL binding.

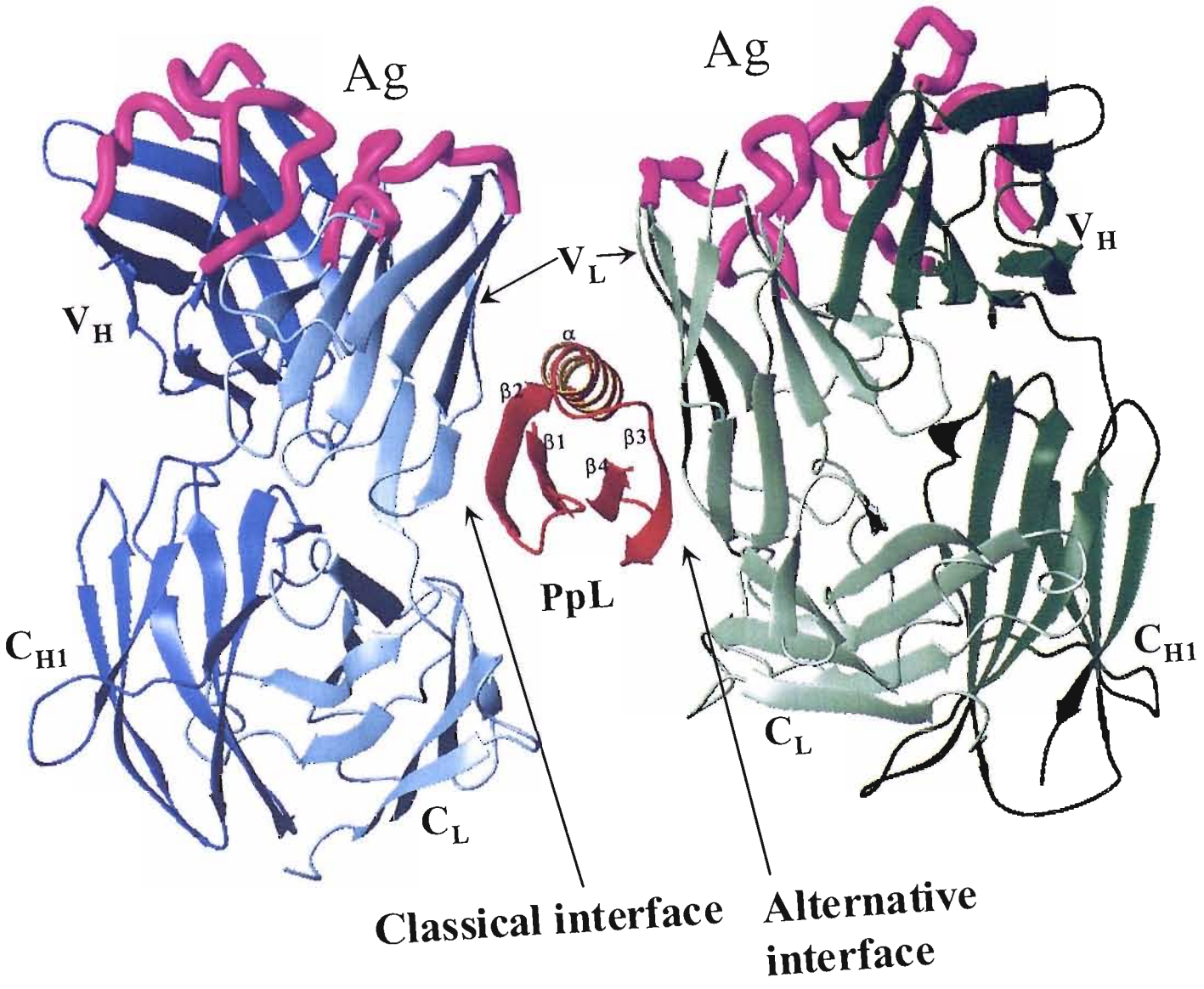
Ag
Ag
V_H
V_L
V_H
α
β2
β1
β3
β4
PpL
C_{H1}
C_L
C_L
C_{H1}
Classical interface
Alternative interface

Figure 1.14 Showing the interaction between PpL and Fab fragments (2).

The figure shows the interaction between PpL shown side-on (centre, purple) showing site 1 and site 2 bound to two Fab fragments. Most of the residues implicated in binding to site 1 (The "classical" interface) are located in strand 2 and the N terminal end of the helix while those of the newly observed alternative interface at site 2 are located in strand 3 and the C terminal end of the helix.

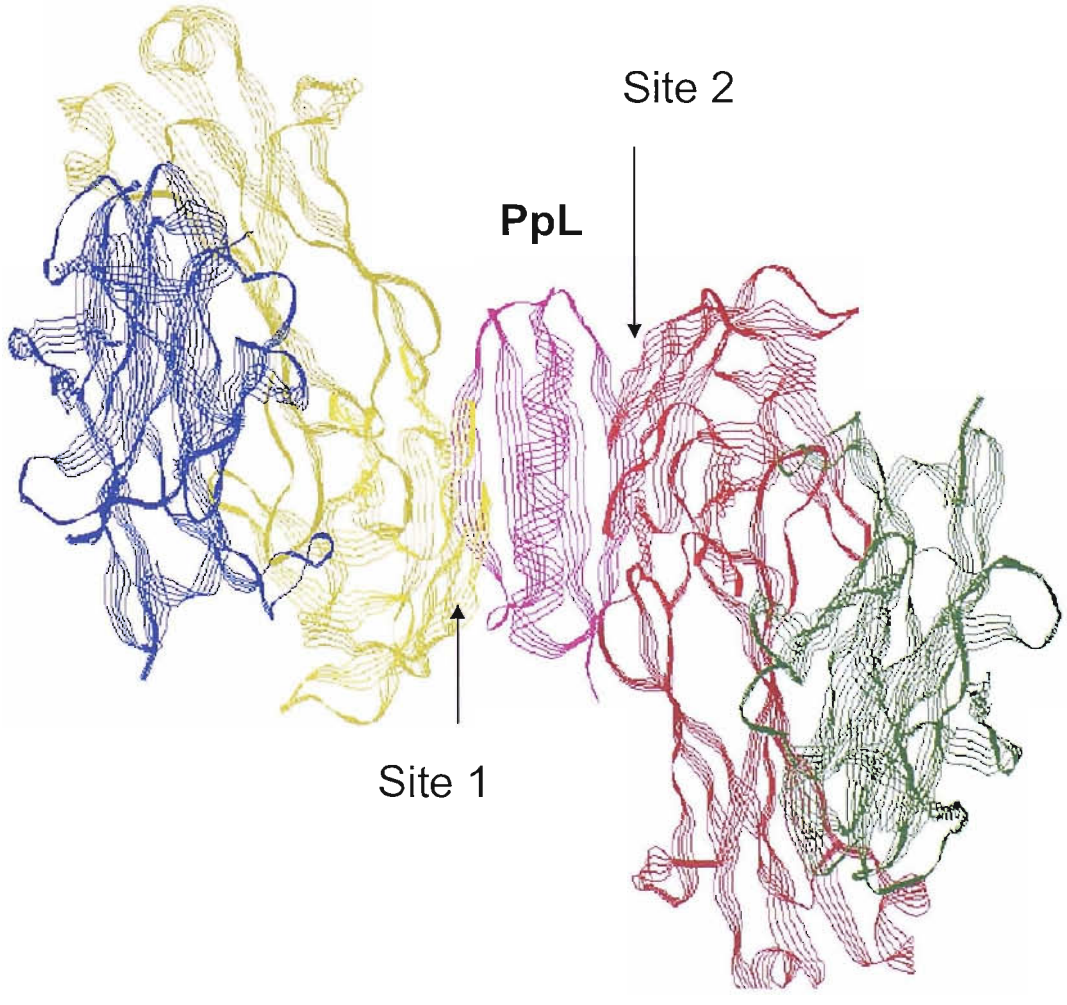
Site 2
PpL
Site 1

detailed in Table 1.3 and 1.4 (Graille *et al.*, 2001). See Fig.1.15 for residues on κ-chain that interact with PpL.

Table 1.3. H-bonds involved in the site 1 interface

V_L residue	Atom	PpL residue	Atom	Bond length (Å)
Ser L9	N	Glu38	O	2.8
Ser L9	Oγ	Lys40	N	3.1
Ser L10	Oγ	Glu38	O	2.9
Ser L10	O	Glu38	N	3.1
Ser L12	N	Thr36	O	2.7
Thr L20	O	Tyr53	Oη	2.6

Table 1.4. H-bonds and salt bridges involved in the site 2 interface

V_L residue	Atom	PpL residue	Atom	Bond length (Å)
Ser L7	Oγ	Asp55	Oδ	2.9
Ser L10	Oγ	Thr65	Oγ	3.2
Ser L12	N	Ala66	O	2.9
Ser L12	O	Leu68	N	2.6
Arg L18	N	Gly71	O	3.1
Arg L24	Nη	Asp55	Oδ	2.7
Lys L107	Nξ	Asp67	Oδ	2.6
Lys L107	Nξ	Leu68	O	2.9

Superimposing the two sites on each other (Fig.1.16 and 1.17) shows a striking similarity between the two, with corresponding residues of similar chemical character (see Table 1.5) involved in addition to similarities at secondary structure level.

Figure 1.15 The residues on κ-chain that interact with PpL.

The residues which interact are well away from the antigen combining site (purple) allowing an Ig bound to PpL to still bind its antigen.

The residues on κ-chain which form bonds with PpL are as follows;

Site 1 (Also see Table 1.3)

Ser- L9

Ser-L10

Ser-L12

Thr-L20

Site 2 (Also see Table 1.4)

Ser-L7

Ser-L10

Ser-L12

Arg-L18

Arg-L24

Lys-L107

L1-3 (purple) are the hypervariable loop regions.

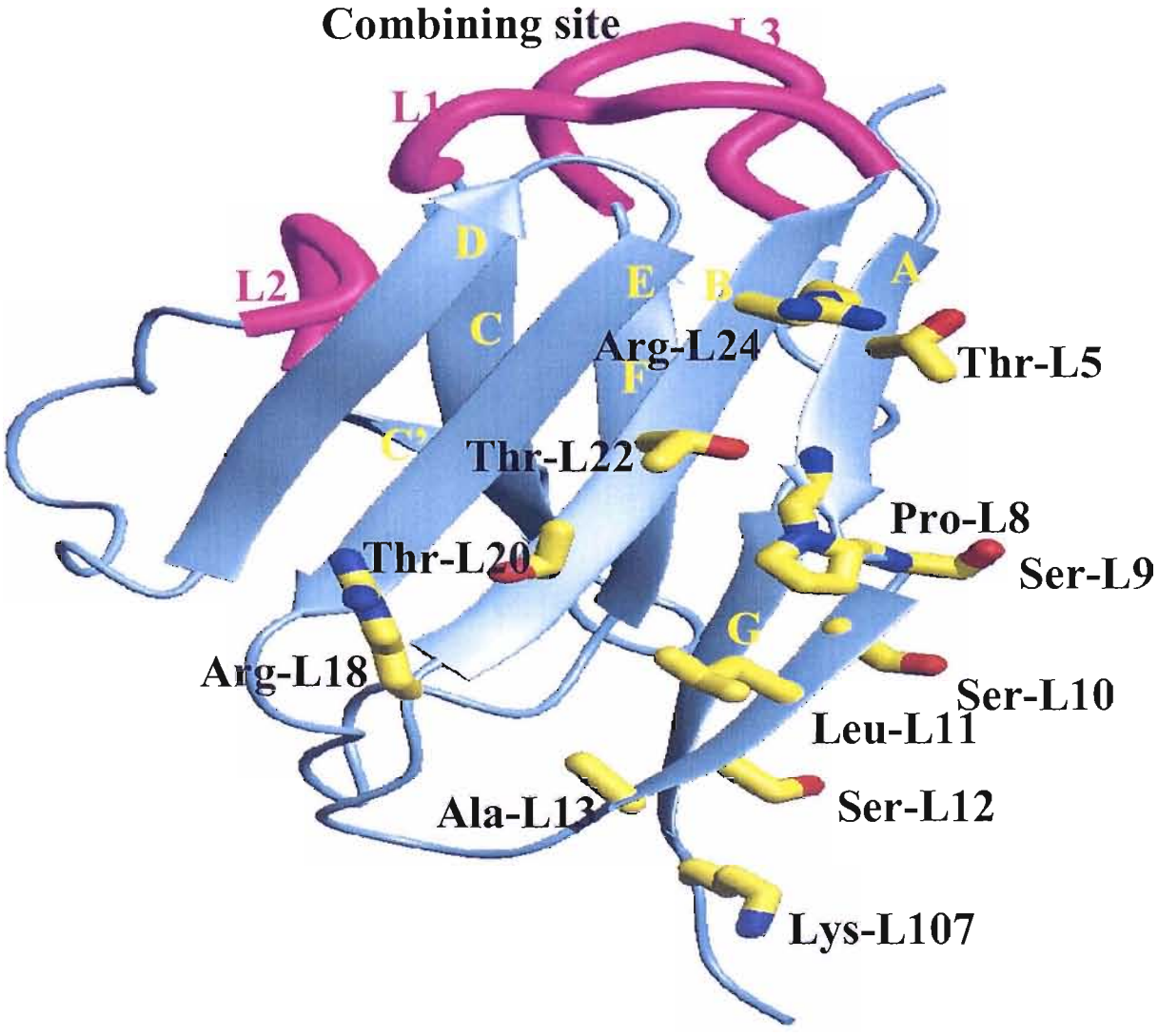
Combining site
L3
L1
L2
D
E
B
A
C
Arg-L24
F
Thr-L5
C'
Thr-L22
Pro-L8
Thr-L20
Ser-L9
G
Arg-L18
Ser-L10
Leu-L11
Ala-L13
Ser-L12
Lys-L107

Figure 1.16 Comparison of the residues implicated in κ-chain binding for sites 1 and 2 for PpL.

The residues marked in red are in those involved in binding κ-chain at site 1 (Classical) and the residues marked in black are in the newly identified alternative site 2. R52 (marked in green) is common to both.

The sites have clear similarities in terms of secondary structure and also similarity in terms of chemical character of the residues involved.

PpL_{3316} Residues Implicated In kappa chain binding

L
3316 A G K E T P E T P E E P K E E V T

I K V N L I F A D G K I Q T A E F K G T

39

F E E A T A E A Y R Y A D L L A K V N G

51 53

E Y T A D L E D G G N H M N I K F A G

64

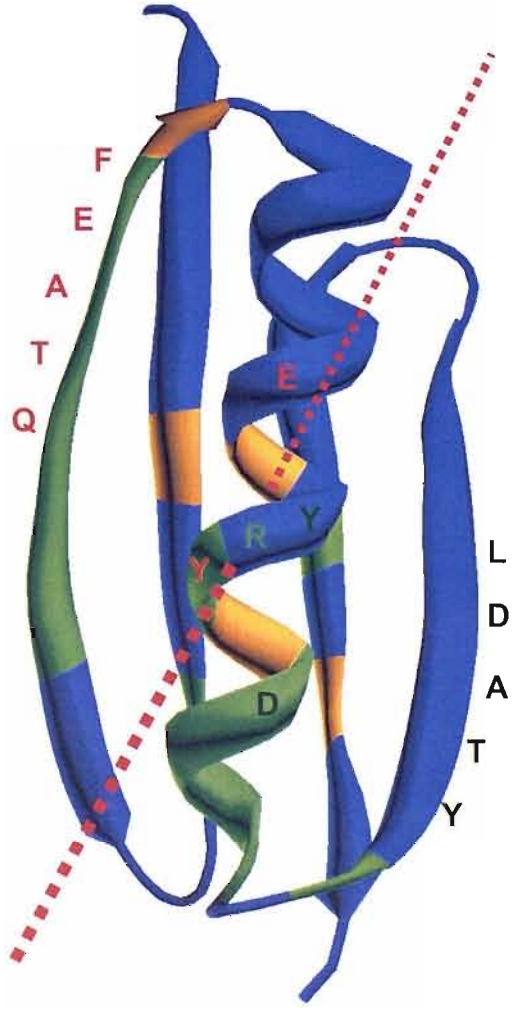

Figure 1.17 Superimposing the two κ-chain binding sites on PpL.

The figure shows the striking similarities observed in terms of tertiary structure and chemical character of the residues involved when sites 1 and 2 are superimposed.
The residues involved in site 1 (classical) binding are numbered in red, with the residues coloured in yellow, and the residues involved in site 2 (alternative) binding are numbered in blue, with residues coloured pale blue.

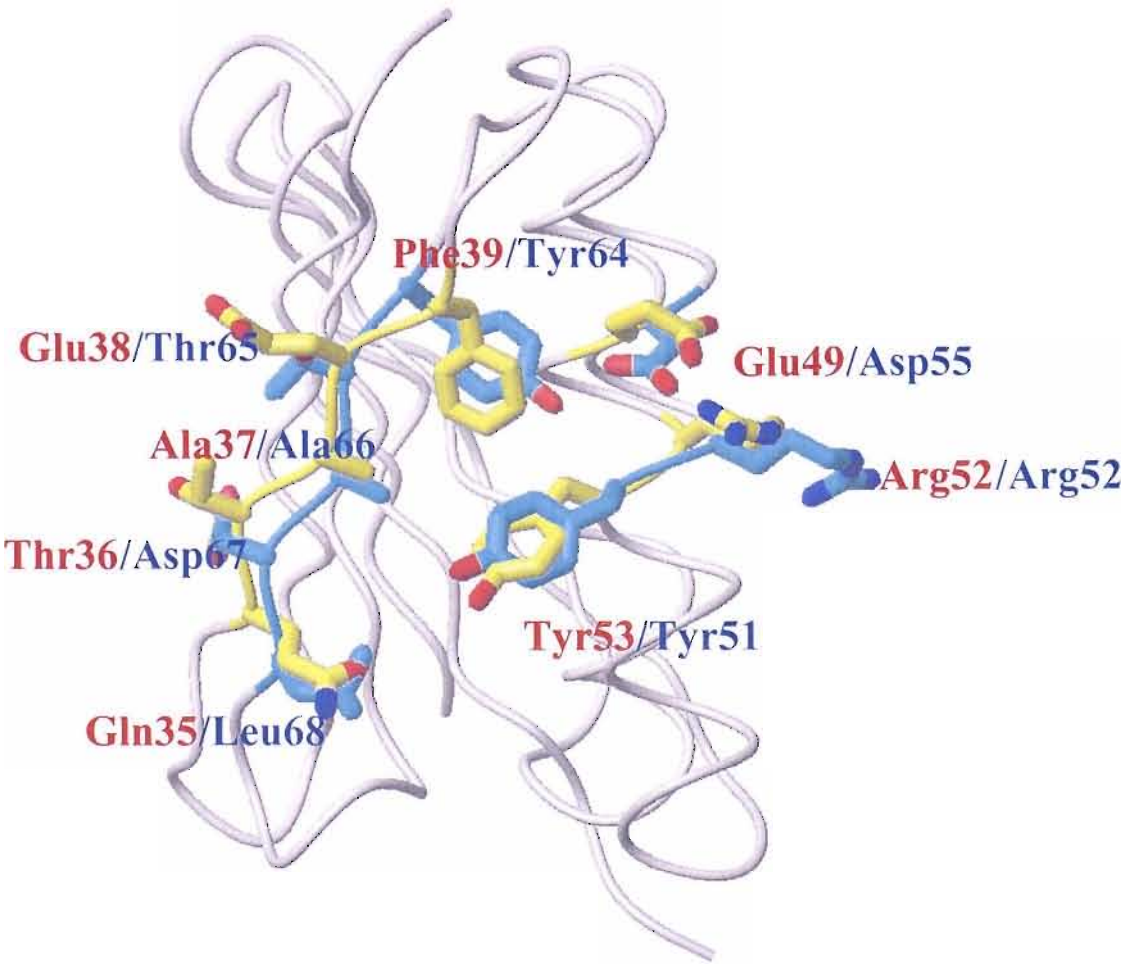
Phe39/Tyr64
Glu38/Thr65
Glu49/Asp55
Ala37/Ala66
Arg52/Arg52
Thr36/Asp67
Tyr53/Tyr51
Gln35/Leu68

Table 1.5. Overlapping residues in site 1 and site 2

Site 1	Site 2
Thr 36	Asp 67
Ala 37	Ala 66
Glu 38	Thr 65
Phe 39	Tyr 64
Glu 49	Asp 55
Arg 52	Arg 52
Tyr 53	Tyr 51

The presence of two non-identical binding sites is similar to that found in human growth hormone and erythropoietin and are likely to have arisen by structural convergence rather than simply by gene duplication (de Vos *et al.*, 1992; Cunningham *et al.*, 1991)..

As stated above, evidence suggests that the second binding interaction is considerably weaker than the first; it has yet to be detected by spectroscopic binding studies in the presence of a functional site 1. Recent analytical ultracentrifugation studies have also suggested that the affinities for Fab for the two interfaces are likely to differ by approximately two orders of magnitude (Graille *et al.*, 2001). The observation that chemical modification of Tyr 51 (which appears to lie in the same position in site 2 as Tyr 53 is in site 1) by tetranitromethane (see above) does not appear to decrease the affinity of the PpL domain for κ-chain is further evidence that site 2 binds considerably weaker than site 1 and is unlikely to be seen in binding assays (Beckingham *et al.*, 2001).

Significantly, a D55A mutant which removes an H-bond and a salt bridge from the second binding interface shows no apparent change in K_d for the interaction between PpL and κ-chain (Graille *et al.*, 2001), suggesting that the second binding site contributes little to overall binding. However, a mutant (Y53F) that eliminates a H-bond in the first binding interface, causes an approximately 30 – 50 fold reduction in affinity (depending upon conditions), indicating that binding at the first interface is dominant and that the binding affinity at site 2 must be at least 30 - 50 fold weaker than at site 1.

PpL mutant D55A,has been used to compare the binding of PpL domains to a different family of κ-chains, κ_{IV} as compared to previously used κ_I, which have 50% sequence homology. Comparing WT PpL and D55A PpL complexes with Fab containing κ_I and κ_{IV} chains respectively, 6 of the 12 residues involved from Fab domain are different during κ_{IV} complex formation although chemical character of differing residues is conserved. In the β-zipper interaction, only 20 residues (11 from Fab, 9 from PpL are involved during D55A κIV complex formation compared to 25 (13 from Fab, 12 from PpL) during WT κI binding. Four hydrogen bonds including that formed by the Tyr 53 residue are common to both while the others are formed by the most flexible parts of the Fab and PpL domains. Because PpL contacts mainly backbone atoms in V_L domains, it allows binding to a wide range of V_L domains regardless of sequence providing the sequence changes do not alter backbone conformation.

The biological significance of this second site of interaction is not clear, however, this mechanism resembles that of the ability of human growth hormone to bind to two receptors (de Vos *et al.*, 1992). This function may allow PpL to bridge two IgE molecules anchored at the membrane of mast cells inducing histamine release, indeed, Protein L has been shown to activate basophils to a much greater extent than either Protein A or G (Patella *et al.*, 1990). The dual binding sites may, as with SpA and SpG, prevent host antibodies from attacking PpL or the bacterial cell on which it is located.

1.8 Aims of the project

The current annual world market for therapeutic and diagnostic antibodies is currently about $10Billion and this is increasing by about 15% per annum. These represent approximately one third of all protein products in the medically related industry (van den Beuken *et al.*, 2003) and thus antibodies are very valuable commercial products and there is a requirement for methods that permit their rapid and efficient production and purification (http://www.bioportfolio.com/reports/Datamonitor_DMHC1956.htm). At present about 85% of the recombinant antibodies produced are purified by use of affinity columns based upon Protein A or its derivatives and this represents an annual market worth approximately $120Million (Chadd and Chamow, 2001) However, despite its current prominence there are several problems associated with the use of Protein A. These include its failure to bind some classes or fragments of antibodies and its extremely high affinity for some antibodies that makes it difficult to elute off bound IgG from an affinity column (very low pH conditions are required). Since Protein L is able to bind to all classes of antibodies and to the new generation of therapeutics based upon recombinant Fab and S_cFvs, it has a great potential as a substitute for Protein A in this very valuable market. However, it too presents some problems to its general use as an affinity ligand. The binding interaction of Protein L to Ig bearing κ-chains is very strong and also requires extremes of pH or salt to separate the complex and release Ig from an affinity column made from PpL. A pH of 1.75 is required to elute Ig from a column consisting of immobilised, single domain PpL (K_d = 100nM). This is damaging to Ig, to possible Ig-fusion proteins and to the affinity matrix. It would be useful to engineer a protein that is able to bind κ-chains but will release them at a milder pH. A binding affinity of 2-3μM would be ideal for this purpose (S. Pearson, Affinity Chromatography Ltd, Cambridge). Any such mutant protein must also have a high stability to temperature and to other denaturants that may be used in protein preparation or affinity column regeneration if it is to be of significant use as an affinity ligand.

Previously, it would have been a priority to engineer PpL to bind λ-chains as these are present in about 40% of human Igs. However, the advent of recombinant technology in the production of antibodies for therapy or other uses means that the producer is able to select, or engineer, the type of light chain made to facilitate its purification. Therefore this is no longer a major goal in studies such as these.

Chapter 2

Materials and Methods.

CHAPTER 2

MATERIALS AND METHODS

2.1 Chemicals

General laboratory reagents, buffers, salts etc. were obtained from **Merck Limited, Poole, Dorset, U.K.** All chemicals, apart from those used for bacterial growth, were of AnaLaR grade or equivalent.

Other reagents were obtained from the following companies.

Amersham Life Sciences, Amersham, U.K.
Thermo sequenase fluorescent labelled primer cycle sequencing kit with 7-deaza-dGTP'.

Boehringer Mannheim U.K. Ltd., Lewes, East Sussex, U.K.
Restriction enzymes, DNA modification enzymes.

FMC Bioproducts, Rockland, ME. U.S.A.
Agarose for DNA gels.

Lab M, Bury, Lancs, U.K.
Tryptone, yeast extract and Agar No.1.

Melford Laboratories Ltd., Chelsworth, Suffolk, U.K.
High-grade guanidine hydrochloride for spectroscopy, EDTA, ampicillin and isopropyl-β-D-thiogalactoside (IPTG).

MWG Biotech, Milton Keynes, U.K.
IRD-700 fluorescently tagged oligonucleotide primers for automated DNA sequencing on a LiCor 4000 sequencer.

National Diagnostics, Hessle, Hull, U.K.

Protogel.

Northumbria Biosciences Ltd, Cramlington, Northumberland, U.K.

Ampicillin and chloroamphenicol.

Oswel Ltd., Southampton, U.K.

All oligonucleotides for mutagenesis.

Pharmacia AB, Uppsala, Sweden.

Plasmid Flexiprep kits, Agarose (NA grade) and cyanogen bromide-activated Sepharose.

Molecular Probes, U.S.A.

Eosin-5-maleimide and pyrene-5-maleimide.

Qiagen Ltd. Crawley, U.K.

Gel extraction kit, Qiaspin mini kit for plasmid preparation, M13 purification kit.

Sigma Chemical Company, Poole, Dorset, U.K.

Specific chemical reagents such as PMSF, bicinchoninic acid, deoxyribonuclease 1, IgG-HRP conjugate and other immunoassay reagents and Q-Sepharose.

Immunoglobulins, and immunoglobulin fragments, IgG and Bence-Jones κ-light chain were generous gifts from Professor Martin Glennie of The Tenovus Laboratories, Southampton General Hospital.

2.2 Microbiological techniques

2.2.1 Sterilisation

Media, pipette tips, stock solutions and microfuge tubes were sterilised by autoclaving at 120°C for 20 min and subsequently dried in an oven at 65°C. Antibiotics and IPTG were filter-sterilised by passage through 0.45μm Millipore filters.

2.2.2 Media

Bacterial cultures were grown in Luria Broth and when necessary ampicillin added to a final concentration of 50μg/ml for JM103 cells or chloroamphenicol to 35μg/ml for CJ236 cells.

Luria Broth (grams per 4 litres)

Tryptone	40g
Yeast extract	20g
NaCl	20g

Luria Broth plates

These were made using LB as described above with the addition of 1.5% w/v of agar no.1.

Agar for H-bottom plates (1 litre)

Tryptone	10g
NaCl	8g
Agar no.1	12g

Agar for H-top plates (1 litre)

Tryptone	10g
NaCl	8g
Agar no.1	12g

2.2.3 Bacterial strains

Strain	Genotype
E.coli JM103	Δlac-proAB, supE, thi, rpsL, endA, SbcB15, [F', traD36, proAB, lacI^q, ZΔM15] Messing *et al.*, (1981)
E.coli CJ236	dut-1, ung-1, thi-1, relA1/pCJ105 (cam^r F') Kunkel *et al.*, (1987)

2.2.4 Cloning vectors

M13 mp18 (Yanisch-Perron *et al.*, 1985)
Phage DNA used to produce single stranded DNA for mutagenesis. It contains a multiple cloning site.

pKK223-3 (Brosius and Holy, 1984)
Expression vector with a *tac* promoter that is IPTG inducible. It contains a multiple cloning site and confers ampicillin resistance to the host.

2.2.5 Preparation of competent cells for electroporation

Competent cells for electroporation were prepared by allowing JM103 cells, obtained from an overnight culture, to grow to an OD of 0.4 at 600nm in 500ml of LB. The cells were then centrifuged for 10 min at 3000rpm and the cell pellet washed with ice cold sterile distilled water three times. After washing, 1ml of ice cold distilled sterile water was added to the cells, glycerol added to 10% v/v and cells aliquoted out into 160μl fractions.

2.2.6 Transformation of competent cells with plasmid DNA

Plasmid DNA (approx 20-200ng) was added to 60µl of cold competent cells and electroporation carried out using an Easyject Basic electroporator (Flowgen). The cells were then added immediately to 1ml of LB and grown for 60 min at 37° C before plating out onto LB plates containing the required antibiotic. Plates were inverted and grown overnight at 37° C. Controls to test for competence and sterility were also included.

2.2.7 Transfection of competent cells with M13 phage DNA

After electroporation as above, transfected cells were added to 3-4ml of molten H-top agar at 42° C and poured onto pre-warmed H-bottom plates. These were allowed to set before being inverted and placed overnight at 37°C to allow phage plaques to develop. Positive and negative controls to test for the competence of the cells and for sterility were included as described for transformations.

2.3 DNA Techniques

2.3.1 Agarose gel electrophoresis

Agarose was dissolved in 1x TBE buffer by boiling and then cooling to 50°C. At this temperature ethidium bromide was added to a final concentration of 0.1µg/ml. The percentage of agarose used ranged from 0.8-2.0% depending on the size of fragments to be identified / separated. Molten agarose was poured onto a glass plate containing a well-former and after setting was placed in an electrophoresis tank containing 1xTBE buffer and the well-former was removed. Loading buffer (5x) was added to each DNA sample and 2-10µl of each sample was loaded into the wells. The gel was run at 100V until fragments were sufficiently separated and viewed using a UV trans-illuminator.

Buffers used

10 x TBE	108g Tris, 55g boric acid, 9.3g EDTA / litre H_2O
6 x loading buffer	0.25% w/v bromophenol blue, 30% v/v glycerol

2.3.2 Restriction digestion of DNA

All of the restriction enzymes used were purchased with the required buffers and used as recommended by the supplier.

2.3.3 Isolation of DNA fragments from agarose gels

DNA fragments of size 200-1000 base pairs were isolated from agarose gels using a Qiagen mini spin purification kit as the manufacturer's instructions.

2.3.4 Dephosphorylation

Vector DNA had the 5' phosphate group removed by calf intestinal alkaline phosphatase (CIAP) to prevent self-ligation during ligation reactions. To 50µl of vector DNA in sterile water was added 5µl of 10 x phosphatase buffer (supplied with enzyme) and 2 units of CIAP. After incubation at 37° C for 45min a second aliquot of CIAP was added and incubation continued for a further 20 min. The enzyme was then inactivated by incubation at 65° C for 20 min.

2.3.5 Plasmid DNA preparations

Plasmid DNA was prepared using either Flexiprep kit (Pharmacia) or Qiagen spin miniprep kit following the manufacturers instructions.

2.3.6 Preparation of single stranded DNA

20µl of a fresh overnight culture of JM103 was diluted into 5ml of LB and inoculated with a single plaque of M13mp18. This was incubated at 37°C with shaking for 5 hours before the cells were pelleted by centrifugation. The supernatant was removed to a clean tube and 0.1 volumes of 40% w/v PEG and 0.1 volumes of 5M sodium acetate pH 7.0 added. After mixing, this was left on ice for 30 min then centrifuged for 10 min to obtain the phage pellet. The pellet was then resuspended in 100µl of TE buffer and phenol extractions (3) and a chloroform extraction performed to purify the DNA. The DNA was then concentrated by ethanol precipitation and resuspended in an appropriate volume of TE buffer.

The TE buffer was stored as a 10 x working concentration solution containing; (108g Tris, 55g Boric acid, 9.3g Na_2 EDTA.$2H_2O$ per litre of water)

2.3.7 Phenol extraction of DNA

To remove contaminating proteins from DNA, phenol extraction was used. An equal volume of phenol / chloroform solution (Sigma) was added to the DNA solution and the mixture vortexed for 1 min to form an emulsion before being centrifuged for 4 min. Samples were centrifuged for approximately 5min in a microfuge to separate out the two layers. The upper aqueous layer containing the DNA was removed and placed in a clean tube. This procedure was repeated if necessary.

2.3.8 Chloroform extraction

A further purification step involved a chloroform extraction to remove any traces of phenol from DNA solutions after phenol extraction. An equal volume of chloroform was added to the DNA solution, vortexed for 1 min and centrifuged for 4 min in a microfuge. The upper layer containing the DNA was transferred to a clean tube.

2.3.9 Ethanol precipitation of DNA

DNA solutions were concentrated by adding 0.1 volumes of 3M sodium acetate pH 5.0 and 2.5 volumes of absolute ethanol (stored at -20°C). The mixture was vortexed for 1 min and tubes placed at -70 °C for 30 min. DNA was pelleted by centrifugation in a microfuge for 10 min. After washing the pellet in 70% ice cold ethanol to remove any remaining salts the pellet was allowed to dry in air for 10 min and the DNA was then resuspended in an appropriate volume (10 - 20μl) of sterile water.

2.3.10 Preparation of uracil rich single stranded DNA for mutagenesis

10μl of an overnight culture of CJ236 cells were added to 10ml of LB containing 30μg/ml chloroamphenicol for 6 hours at 37° C. Phage was then added and the cells grown overnight. The next morning the cells were pelleted and single stranded DNA prepared as previously described.

2.3.11 Phosphorylation of the mutagenic primer

Primers were phosphorylated by mixing 200pmol primer with 4.5 units of T4 DNA kinase, 4μl kinase buffer, 1.3μl 10mM ATP and made up to 40μl with sterile water then incubating at 37°C for 45min followed by 10min at 65°C then the mixture was frozen until required.

2.3.12 Annealing of mutagenic primer to uracil rich DNA template

To approximately 200ng of template single stranded DNA in 1μl of sterile water was added 2 - 10pM of phosphorylated mutagenic primer. In addition, 1μl of annealing buffer and further sterile H_2O was added to a final volume of 10μl. The mixture was heated to 70°C for 10 min then allowed to cool to 30° C over 40 min. The remainder of the mutagenic strand was synthesised by adding

1µl of T4 DNA ligase, 2.5µl of T4 DNA polymerase and 1µl of 10x synthesis buffer (4mM each dNTP, 75mMATP, 175mM Tris-HCl buffer pH 7.4, 37.5mM $MgCl_2$, 15mM DTT). This mixture was put on ice for 5 min followed by 5 min at room temperature and then incubated at 37° C for 90 min. 20µl of TE buffer was then added to stop the reaction and the DNA frozen until required. The DNA could then be used to transfect JM103 cells.

2.3.13 Selection of mutants

Double stranded M13 DNA was transfected into JM103 cells and the plaques obtained used to transfect an overnight culture (10ml) of JM103 cells. The cells were incubated with shaking for 5 hours after which a double stranded DNA prep was performed.

2.3.14 DNA sequencing

Originally, DNA sequencing reactions were carried out by the dideoxy chain termination method of Sanger *et al.*, (1997) using a Sequenase 2.2 sequencing kit. The sequencing reactions were performed following the manufacturer's instructions using α-^{35}S-dATP as the radiolabel. However, the sequencing reactions were later changed to make use of an automated DNA sequencer. DNA sequencing was then performed using the Amersham Life Science Thermo sequenase fluorescent labelled primer cycle sequencing kit with 7-deaza-dGTP and the reactions run on a Li-Cor 4000 DNA sequencer.

2.3.15 Ligation of DNA

The ligation mixture was incubated in a 2 litre beaker containing water at 25° C, which was then placed at 4°C and allowed to cool overnight. A ligation control, containing no insert, was also prepared in this manner. The next day, 5µl of each ligation mix were transformed into JM103 cells as previously described.

2.4 Protein techniques

2.4.1 Protein preparation

A single colony of JM103 cells containing the protein L gene in the expression vector pKK223-3 was placed in 10ml of LB with a final ampicillin concentration of 50μg/ml and grown overnight at 37 °C with shaking at approximately 160 rpm. This culture was then used to inoculate 8 x 500ml volumes of LB containing 50μg / ml ampicillin by adding 1ml of inoculum to each flask. The flasks were shaken at 160 rpm at 37° C until an optical density of 0.6 - 0.8 at 600nm was reached. At this point filter-sterilised IPTG was added to a final concentration of 0.4mM and the cells incubated overnight in the same conditions as before.

Cells were pelleted in a Sorvall RC-3B centrifuge at 5000rpm for 25 min using a 4 x 1 litre rotor at 4° C. The cell pellets were then resuspended in 30ml of sonication buffer (20mM Tris.HCl pH 8.0, 0.1 mM EGTA, 0.1mM EDTA, 0.1% Triton X -100) and the suspension placed in a sonication vessel in ice and PMSF (to inhibit serine proteases) and DNase I (to digest the released DNA) were added. The mixture was sonicated using a MSE Soniprep 150 for 10 cycles of 30 seconds on, 30 seconds off at 15 amplitude microns. Cell debris was removed by centrifugation for 25 min at 12000 rpm in a Beckman J2-21 centrifuge using an 8 x 50ml rotor. The pellet was discarded and the supernatant heat-treated by placing it at 70° C for 40 min. Less stable mutants (those containing the mutation F39W) were heated to 65° C for the same time period. Denatured protein was removed by centrifugation at 15000rpm for 20min using an 8 x 50ml rotor in a Beckman J2-21 centrifuge. The supernatant was diluted to 100ml and loaded onto a Q-Sepharose anion exchange column equilibrated with buffer A (20mM Tris.HCl pH 8.0 at 4°C). The protein was eluted by running a linear gradient of 0 - 30% buffer B (20mM Tris-HCl pH 8.0, 1M NaCl, 4°C) using a Biorad Econo system. 5ml fractions were collected and the protein concentration monitored by measuring the absorbance at 280nm. Peaks were investigated for their protein content by running a 15% SDS-PAGE and fractions containing pure PpL were pooled,

concentrated by an 80% ammonium sulphate precipitation and stored at 4°C until required. For long term storage a trace of sodium azide was added to prevent microbial growth.

2.4.2 Polyacrylamide gel electrophoresis

The discontinuous Tris-glycine buffer system of Laemmli (1970) was used to separate proteins on SDS-PAGE. The gel was prepared from stock solutions supplied under the name Protogel.

15% Running gel

Protogel	3.00ml
3.7M Tris-HCl buffer pH 8.8	0.6ml
10% SDS	60µl
TEMED	5µl
APS	20µl
Distilled H_2O	2.34ml

Stacking gel

Distlilled H_2O	2.48ml
Protogel	0.60ml
0.625M Tris-HCl buffer pH 6.8	0.80ml
10% SDS	40µl
TEMED	4µl
APS	20µl

5x Running buffer

Tris	12g
Glycine	57.6g
10% SDS w/v	5g
H_2O	To one litre

2x sample buffer

0.625M Tris-HCl pH6.8	2ml
Distilled H_2O	1ml
2-mercaptoethanol	1ml
10% SDS	4ml
Glycerol	2ml
Bromophenol blue	trace

Stain solution

Methanol	454ml
Acetic acid	92ml
Distilled H_2O	454ml
Coomassie blue	2.5g

Destain solution

Methanol	250ml
Acetic acid	375ml
Distilled H_2O	4375ml

2.4.3 Estimation of protein concentration

This was carried out using the Bicinchoninic acid assay using BSA as the protein standard (Smith *et al.*, 1985).

2.4.4 Dialysis

Protein was dialysed against 4 litres of 10mM phosphate pH 8.0 buffer for a minimum of 5 hours at 4°C using appropriate sized dialysis tubing.

2.5 Binding and stability studies

2.5.1 Circular Dichroism spectroscopy

Experiments were carried out in 20mM phosphate buffer, pH 8.0 which was filtered and degassed prior to use. Near UV experiments were performed in the wavelength range 250-300nm and far UV studies performed in the range 180-250nm using a Jasco J720 CD spectrometer. For near UV spectra the protein concentration used was 1mg / ml in a cell of path length 1cm. For far UV spectra, 0.1-0.2mg / ml protein was used in a cell of path length 0.1cm. The scan-rate used was typically 20nm / min with a response factor of 4s. The spectra were measured three times and the resultant spectra and data given are the average of these runs. The experiments were all carried out at 20°C unless otherwise stated.

2.5.2 Fluorimetry

Fluorimetry was carried out on a Hitachi F2000 spectrofluorimeter fitted with a water-jacketed cell holder. Light at 280nm was used to excite fluorescence from the protein. Spectra were scanned using 10nm slit widths for both the excitation and emission monochromators at a scan speed of 60nm per min. For experiments that involved prolonged periods between readings, the excitation light was cut off until a reading was about to be taken.

2.5.3 Fluorescence measurements

Experiments were carried out in 20mM phosphate buffer pH 8.0 which had been prepared using deionised water and subsequently filtered through a 0.45μm Millipore filter to reduce light scattering from particulate matter. Fluorescence emission intensities were read three times and the average value used in all calculations or plots. The fluorescence readings were corrected for dilution and for the inner filter effect where necessary using the following equation:

$$F_{corr} = F_{obs} \exp^{0.5A_{280}}$$

Where A is the absorbance of the excitation light, F_{obs} is the measured fluorescence intensity and F_{corr} is the corrected fluorescence intensity. In practice this is only necessary when the total absorbance of the excitation light exceeds 0.05 / cm. In extreme cases a similar correction should be made for the self-absorption of the emitted light as well.

2.5.4 Fluorescence titrations

Titrations were carried out at 25°C by serial additions of small volumes of 150μM PpL into 1.5ml of 1.5μM κ-chain in 20mM phosphate buffer pH 8.0. The excitation wavelength was 280nm and emission intensities measured at 335nm (for mutants containing tryptophan residues) and 302nm (or for unfolding studies, 305nm) for the WT PpL. The addition of PpL causes the fluorescence intensity to increase since most of the mutants contain a tryptophan, present as a reporter group. Thus the experiment involved the use of titrations of PpL into buffer and PpL into κ-chain. The values of the fluorescence intensity derived from the titration of PpL into buffer (A) were subtracted from those derived from titrations of PpL into κ-chain (B) to give (C) values. Finally, the small fluorescence intensity due to κ-chain in buffer was subtracted from values of (C). Data were fitted to a Michaelis-Menten hyperbola to calculate the total change in signal intensity due to the saturation process. K_d was then determined using a plot (Stinson and Holbrook, 1973) as described by the equation;

$$\frac{1}{1-\alpha} = \frac{1}{K_d} \times \frac{P}{\alpha} + n\kappa$$

in which α is the fractional saturation of the available binding sites for the ligand (in this case PpL), P is the total concentration of the added ligand , κ is the concentration of κ-chain and n is the number of binding sites for PpL on a single κ-chain. A plot of 1 / 1-α against P /α will yield a straight line plot with a slope of 1 / K_d and an intercept of $n\kappa$ on the abscissa.

2.5.5 Stopped-flow fluorescence studies

Stopped flow measurements were made on an Applied Photophysics stopped flow SX17 ASVD spectrofluorimeter fitted with 2ml syringes. The excitation wavelength used was 280nm and the emission wavelength was determined by use of a 335nm cut off filter. Protein solutions were made up in 20mM phosphate buffer at pH 8.0 and the temperature used was 25°C unless otherwise specified. In association experiments the κ-chain concentration was kept constant (concentration after mixing 2μM) while the concentration of PpL was varied (concentration after mixing 10-30μM). The excess of one reactant allowed the reactions to be analysed as a pseudo first order reaction as only the concentration of the κ-chain changes significantly during the reaction. To measure the rate of dissociation of the complex, a preformed complex of PpL.κ chain (formed by mixing 8μM of PpL with 8μM κ-chain) was rapidly diluted 1:1 v/v with 60μM WT PpL. Measurements were made over a 2, 10 or 50second time period with 1000 data points for each. Some of the reaction curves were biphasic and were analysed either as two separate components using single exponential curve fitting equations (a) or by a double exponential equation (b) below.

(a) $$F_t = F_0 \exp^{-kt} + C$$

where F_o and F_t are the fluorescence intensities at time 0 and time t respectively, k is the first order rate constant for the reaction and C is a constant. However, the reaction progress curves were also analysed by a double exponential equation -

(b) $$F(t) = A_1\exp(-k_1t) + A_2\exp(-k_2t) + C$$

In which F(t) is the fluorescence at time t, A_1 and A_2 are the amplitudes of the different phases of the change in fluorescence, k_1 and k_2 are the rate constants for the first and second phase respectively and C is a constant.

All of the data in stopped-flow experiments were obtained using a 1:1 v/v mixing ratio and from hereon the concentrations of reactants quoted will be the final ones after the mixing has been completed.

2.5.6 Unfolding studies

These were carried out using guanidine hydrochloride (GdnHCl) solutions at pH 8.0 in 20mM phosphate buffer. Accurate measurements of the concentration of the GdnHCl solution were made by measuring the refractive index of the solution and fitting the data into the following equation (Pace *et al.*, 1986)

$$57.147(\Delta N) + 38.68\ (\Delta N)^2 - 91.6\ (\Delta N)^3 = [\text{GdnHCl}]$$

in which ΔN is the difference between the refractive index of the GdnHCl solution and the refractive index of the buffer.

1ml samples of protein (10μM) in various concentrations of GdnHCl in buffer were set up and incubated for at least 1hour in a water bath at the experimental temperature before fluorescence measurements were taken. The GdnHCl concentrations ranged from 0 - 5M in increments of 0.25M. A set of GdnHCl solutions (without protein) were made in the same way for use as blanks and their fluorescence intensities measured and subtracted from those values determined for the protein solutions at the equivalent concentrations of denaturant.

Stopped flow determinations of the rates of unfolding of Y64W and F39W domains were made by rapidly mixing 20μM protein in phosphate buffer, pH 8.0 1:1 v/v with 6M GdnHCl in the same buffer at 25°C. The changes in protein fluorescence were monitored and analysed as described above.

2.5.7 Labelling of cys mutants for fluorescence studies

A mutant containing a single cysteine mutation, H74C, was labelled with pyrene maleimide to allow unfolding and binding studies. Pyrene-5-maleimide was dissolved in 95% ethanol to give a 10mM stock to reduce the volume of ethanol added to the protein solution. An equimolar amount of pyrene-5-maleimide was then added to H74C and allowed to incubate at 4°C overnight. Excess label was then removed using a gel filtration column. Pyrene-5-maleimide was excited at 340nm and fluorescence emission measured at 380nm. A stock solution of eosin-5- maleimide was made in a similar way for cysteine labelling experiments. Eosin-5-maleimide was excited at 524nm and emission measured at 544nm.

2.5.8 Enzyme Linked Immunosorbant Assay (Standard ELISA)

A 96-well microtitre plate was coated with 200µl of coating buffer (0.8g Na_2CO_3, 1.46g $NaHCO_3$ per 500ml) pH9.0. 150µl of protein solution were added to lane 2, then serially diluted along the plate by taking 150µl and transferring to lane 3 etc. The plate was left at 37° C for 3 hours then washed 3 times with PBS containing 0.5% Tween 20 at pH 6.0. 200µl of IgG was diluted into 25ml PBS-Tween 20 and 200µl of this were added to each well of the microtitre plate and incubated at room temperature for 45 min. The plate was again washed 3 times and 200µl of goat anti IgG-HRP (20µl of stock solution diluted into 25ml of PBS-Tween added to the plate). Following a 45 min incubation at room temperature the plate was washed 3 times again and 200µl of substrate in buffer (10mg *o*-phenylenediamine, 20µl H_2O_2 , 25ml citric acid buffer (10x citrate buffer is 21g citric acid, 35.5g Na_2HPO_4 in 200ml H_2O) pH 6.0) added to each well and the colour allowed to develop for 30 min. The absorbance for each well was measured at 490nm. All ELISA data quoted is the average of at least three assays.

2.5.9 Competitive ELISA

A standard 96-well microtitre plate was used for these experiments. The wells were coated by the addition of 100µl of coating buffer to each well. To the wells of lanes 2 - 12 were added 100µl of a 0.04 mg / ml solution of WT PpL leaving lane 1 as a negative control. The plate was left to coat for 2hrs at 37°C or overnight at room temperature. It was then washed three times with PBS-Tween to remove unbound WT PpL. 100µl of PBS-Tween were then added to each well followed by 50µl of 0.2 mg / ml competing protein to lane 2. Competing protein was serially diluted across the plate by removing 50µl and transferring this to the next column and mixing the solutions. Lane 12 was left as a positive control (maximum binding, ie. no competing protein). 200µl of human IgG were added to each well as with the standard ELISA and following a 45min incubation at room temperature, the plate was washed three times with PBS-Tween to remove excess IgG and IgG competing protein complex. 200µl of goat anti-human IgG-HRP were added to each well as in a standard ELISA described above and the plate incubated for 45min. The plate was then washed three times and substrate added as in a standard ELISA and absorbance at 495nm measured.

The K_d for the complex formed between the competing protein and Ig or κ-chain was calculated using the following equation;

$$K_{d\ mutant} = K_{d\ WT} \times M1 / M2$$

Where M1 is the concentration of added mutant protein that causes a decrease of 50% in the absorbance at 495nm and M2 is the concentration of the added wild-type protein that causes a decrease of 50% in the absorbance at 495nm on the same microtitre plate. This technique can only be used to obtain an estimate of K_d since it assumes that the immobilisation process leaves wells uniformly coated with PpL and that the same percentage of the PpL is available for interaction with Ig or kappa chains. Furthermore, it assumes that the various interactions with Ig or kappa chains are freely reversible under the conditions used.

2.5.10 Preparation of the affinity chromatography matrix containing immobilised PpL

Affinity chromatography was carried out using CNBr-activated Sepharose 4B. The protein to be coupled was dialysed overnight against 4 litres of coupling buffer (0.1M $NaHCO_3$, pH 8.3 containing 1M NaCl). 0.33g of dry CNBr-activated Sepharose 4B was washed with 200ml of 1mM HCl giving a swollen gel volume of 1ml. 2ml of a 3 mg / ml protein solution was added to the gel and the mixture rotated in a stoppered column for 1hr at room temp. The supernatant was drained off and excess ligand was then removed by passing 5 vol of coupling buffer through the column and the remaining active groups blocked by adding 5ml of 0.1M Tris-HCl buffer, pH 8.0 at room temp for 2 hrs. The column was then washed with three cycles of buffers with alternating pH ie. 5vols each of 0.1M acetate buffer pH 4.0 containing 0.5M NaCl followed by 0.1M Tris-HCl buffer pH 8.0 containing 0.5M NaCl. The amount of protein bound to the column was estimated by BCA analysis of the supernatant of the protein-gel mixture at time zero and after the full incubation period. The difference in protein concentration was used to estimate the amount of protein coupled to the gel matrix.

2.5.11 Use of the affinity chromatography matrix

1ml of 5 mg / ml of human IgG in 20mM phosphate buffer, pH 8.0 at 20°C was added to a column containing 1ml of the gel matrix. The two were allowed to mix with inversion for 5 min and then the column was eluted by the same buffer until the absorbance at 280nm of the eluate returned to the buffer baseline value. Then, a gradient of pH between pH 8.0 and 1.5 was set up on a Waters HPLC system and applied at a rate of 1ml per min. The pH gradient was constructed using the following buffers; (a) 50mM sodium acetate buffer, pH 1.5, (b) 50mM sodium acetate buffer pH 5.0 and (c) 20mM phosphate buffer pH 8.0. The pH could therefore be reduced stepwise from pH 8.0 to pH 1.5.

The absorbance at 280nm was read for each fraction collected (1ml) and used to calculate the amount of protein retained and eluted from the columns.

Chapter 3

Site-directed mutagenesis and protein purification.

CHAPTER 3

SITE DIRECTED MUTAGENESIS AND PROTEIN PURIFICATION

3.1 Introduction

The use of site directed mutagenesis to study the structure and function of proteins has rapidly developed in recent years. Unlike chemical modification methods, site directed mutagenesis can be used to study the role of individual residues in the function of a protein without exposure of the protein to harsh, sometimes non-specific reagents and without the addition of large chemical groups to the target amino acid side-chain. For example, it has been used to identify essential catalytic residues in enzymes (Chen *et al.,* 1998), to corroborate the identification / function of a residue implicated by chemical modification (Greasley *et al.,* 1993), to provide fluorescent reporter groups for folding / unfolding or ligand binding studies (Matoucheck *et al.,* 1989) or to increase the stability of a protein. For example, by introducing disulphide cross links (Perry and Wetzel, 1984), replacing Gly with Ala and Ala with Pro which reduces backbone conformational entropy without affecting 3D structure (Matthews *et al.,* 1987) and more generally by eliminating cavities, introducing new interactions in rigid parts of the structure and elimination of unsatisfied H-bonding groups (Alber and Wozniak, 1985). However, amino acid substitution by mutagenesis is by no means a risk-free technique; careful consideration must be made about the choice of replacement residue. For example, the change of protein sequence may lead to the failure of the protein to fold to the same structure as the wild-type protein. This may be due to a number of different reasons e.g.
(a) a replacement of an amino acid residue with a hydrophilic side chain by one with a hydrophobic side chain.

(b) the choice of a replacement residue with a different propensity for α-helix or β-sheet secondary structures.
(c) or simply because a residue with a larger side-chain has replaced one with a small side chain with resultant steric hindrance to folding.
Nevertheless, site directed mutagenesis can be used very effectively. Previous work in this laboratory, and work described in this thesis, has been based upon the use of this technique to modify a gene encoding a single Ig-binding domain of Protein L (PpL) to achieve a number of goals.

(a) In order to modify its binding characteristics for Ig and κ-chain.
(b) In order to provide a better understanding of its structure by the inclusion of Trp reporter groups to aid fluorescence spectroscopy.

3.2 Site directed mutagenesis

Mutagenesis can be performed in a variety of ways, for example;
(a) the method of Taylor *et al.,* (1985) is based upon the use of thio-dCTP modified nucleotides. A single stranded DNA template is copied using nucleotides containing thio-dCTP. The unmodified strand is subsequently destroyed using restriction enzymes that fail to cleave the DNA containing the modified bases. The remaining modified strand is then used to transform bacteria in which it is used as a template to create double stranded mutated DNA.

(b) Cleland *et al.*, (1996) developed another method based upon the use of the polymerase chain reaction (PCR). Initial disadvantages included the relatively high cost of this method due to the requirement for more than one oligonucleotide primer and Taq polymerase and the 'copying' errors introduced by the Taq polymerase used. However, more recently, pfu polymersase (from *Pyrococcus furiosis*) has been used which gives a much lower error rate.

(c)The cassette mutagenesis technique has been used successfully to mutate synthetic genes of Protein A and other proteins (Popplewell, 1991, Ferris, 1992). Residues of importance can be flanked by unique restriction sites and a cassette containing these residues can be removed by restriction digestion. A synthetic oligonucleotide cassette containing the desired mutation or mutations can be ligated in its place. This method has the advantages of being able to mutate several residues at once. However, the gene for PpL was cloned by PCR techniques and therefore does not contain many unique restriction enzyme sites. Therefore it was decided to use the 'mismatch primer' method of mutagenesis for creating mutants and the Kunkel method for their selection (Kunkel *et al.,* 1987). This procedure has a high success rate for the selection / identification of mutants (50-70%), is simple to carry out and has been previously used with success for mutagenesis of Proteins L and G. The method requires the preparation of single stranded DNA from M13 phage containing the wild type PpL gene which is then used to infect CJ236 *E.coli* cells. This strain is deficient in dUTPase and uracil glycosylase. As a result, dUTP levels in the cells are raised competing with TTP and uracil is incorporated into the DNA. Uracil, once incorporated, cannot be removed due to the lack of uracil glycosylase. The mutagenic primer is annealed to single stranded UDNA template prepared from the infected CJ236 cells and the second strand is completed in *vitro.* When re-introduced to a dut+ ung+ host such as *E.coli* JM103, the UDNA template is destroyed and double stranded mutant DNA is produced which then replicates as normal. This method produces mutants at about 50% efficiency.

3.3 Sub-cloning

Once a mutant had been identified in M13 by automated sequencing, the gene was excised with *Sac*I and *Pst*I restriction enzymes giving a 249bp fragment which could be isolated from a 2% agarose gel (Figs 3.1-3.2). Major features of the M13mp18 and pKK223-3 are described in Figs 3.3 and 3.4.

Figure 3.1 An ethidium bromide stained 2% agarose gel showing PpL gene cut from M13.

(left to right)

1. λ*Hind*III/*Eco*R1 marker
2. 249b.p. F39H,Y64W gene cut from M13 with *Sac*I/*Pst*I
3. Uncut M13 DNA
4. 249b.p. F39H,Y64W gene cut from M13 with *Sac*I/*Pst*I
5. 100b.p. ladder marker

Figure 3.2 An ethidium bromide stained 2% agarose gel showing PpL gene cut from pKK223-3.

(left to right)

1. λ*Hind*III/*Eco*R1 marker
2. pKK223-3 cut with *Sac*I/*Pst*I
3. pKK233-3 cut with *Sac*I/*Pst*I
4. pKK233-3 cut with *Pst*I only (linearised)
5. Uncut pKK223-3
6. 100b.p. ladder

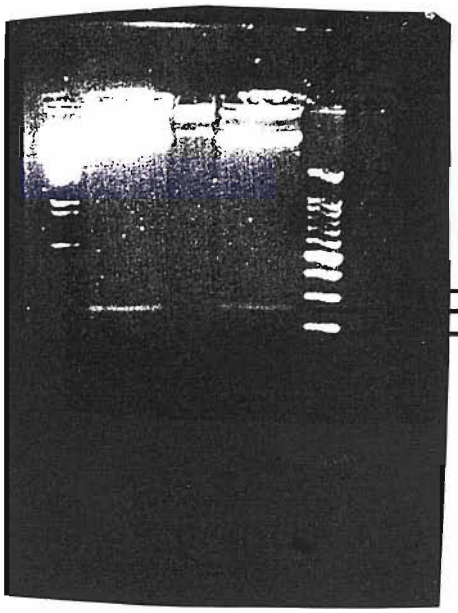
300 bp marker
249 bp Sac I, Pst I fragment
200 bp marker

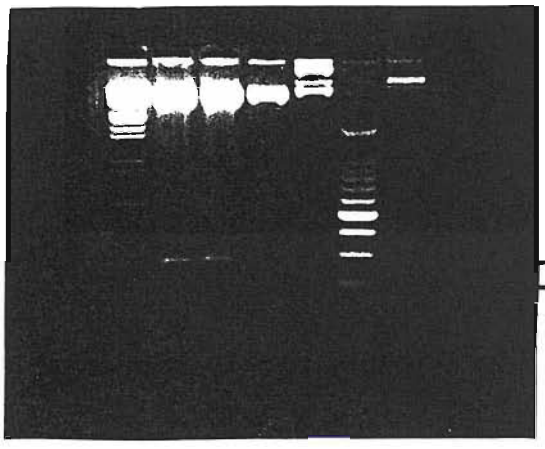
249 bp Sac I, Pst I fragment
200 bp marker

Figure 3.3 The M13mp18 vector.

The PpL gene was cloned into the *Sac*I – *Pst*I cut M13mp18 vector to produce single stranded DNA to which mutagenic primers were annealed.

Figure 3.4 The vector pKK223-3.

The double stranded mutated DNA was cut from M13mp18 using *Sac*I and *Pst*I and ligated into a derivative of pKK223-3 that was available in the laboratory. This vector contained a synthetic gene fro bovine DNaseI ligated between the *Eco*RI site and *Hind*III site of pKK223-3. The inserted gene contained a Shine-Dalgarno site, a *Sac*I site and further downstream a *Pst*I site. Therefore the gene for PpL was ligated into a *Sac*I-*Pst*I cut version of this vector. The sequence from the *Eco*RI site to the *Sac*I site was as follows:

GAATTCGATTCCT**AGGAGG**TGAGCTC

The Shine-Dalgarno site is in bold

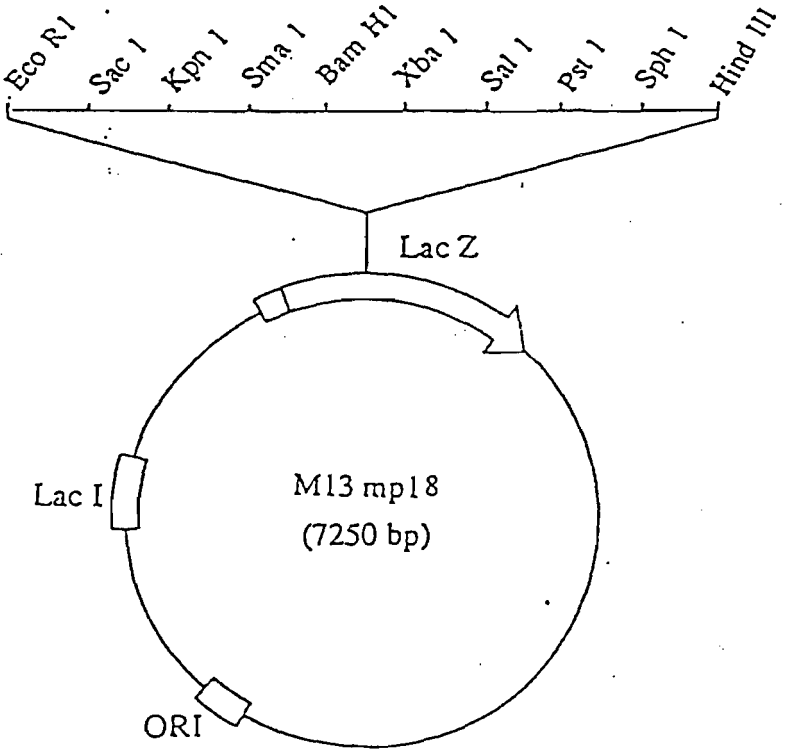
Eco R1
Sac 1
Kpn 1
Sma 1
Bam H1
Xba 1
Sal 1
Pst 1
Sph 1
Hind III
Lac Z
Lac I
M13 mp18
(7250 bp)
ORI

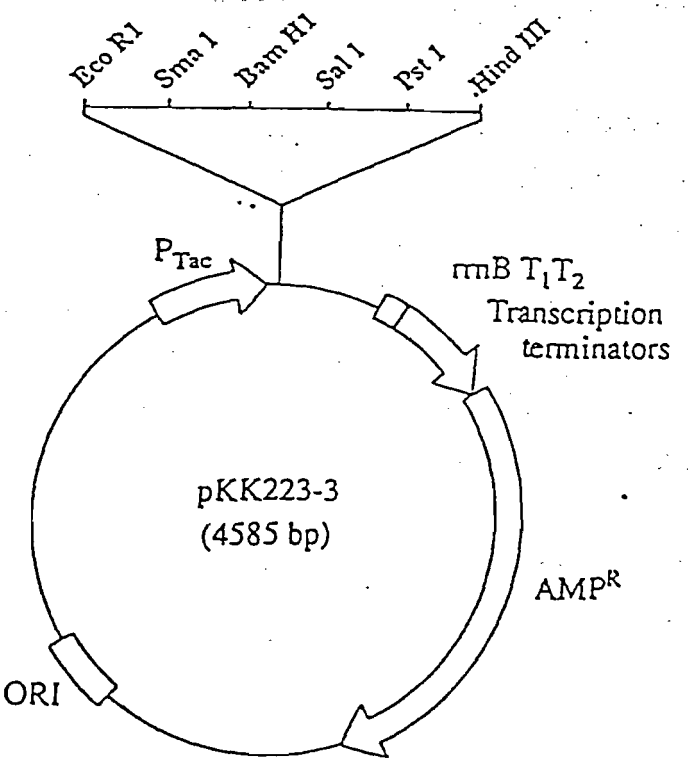
Eco R1
Sma 1
Bam H1
Sal 1
Pst 1
Hind III
P Tac
rrnB T1T2
Transcription
terminators
pKK223-3
(4585 bp)
AMP R
ORI

25µl of dsDNA from M13 was cleaved first by the addition of 2µl *Sac*I for 4 hours at 37°C then the further addition of *Pst*I with overnight incubation at 37°C. This was prolonged incubation was necessary because *Sac*I and *Pst*I require different buffers to function efficiently. The fragment was ligated into pKK223-3 that had also been treated with the same enzymes and treated with alkaline phosphatase to prevent self ligation.

pKK223-3 plasmid containing the PpL gene was then used to transform *E.coli* JM103. Although PpL is not naturally produced by *E.coli* cells it is successfully expressed in *E.coli* JM103 cells in a soluble form to a high level (40mg/4l cells).

3.4 Selection of target sites for mutagenesis.

Wild-type, multi-domain Protein L and PpL form their respective complexes with κ-chain with extremely low K_ds (1×10^{-9} M and 1×10^{-7}M respectively, (Nilson *et al.*, 1992 and Beckingham *et al.*, 1999)). Thus these proteins have the potential of acting as good affinity ligands for the isolation of κ-chain and Ig or Fab or S_cFv fragments containing κ-chain. However, an affinity ligand should have a high binding affinity under one set of conditions, but should preferably have a low affinity under a different set of conditions so that separation of the complex can be achieved for recovery of the bound target protein. If a 'switch' between high and low affinities cannot be developed then an affinity ligand should have a K_d for the complex with its target protein of about 10^{-6}M (Affinity Chromatography Ltd, personal communication). This will allow a good binding capacity with relatively easy elution.

The high binding affinity between PpL and κ-light chain necessitates extreme conditions e.g. high salt or low pH to dissociate the complex.

This could damage the Ig or Ig fragment (particularly S_cFvs which are unstable below pH 2.5) being eluted from a column. It would therefore be advantageous to produce a mutant that would dissociate from κ-chain under less extreme conditions. Since PpL has a lower affinity for κ-chain than multi-domain Protein L, PpL was chosen as the template construct upon which mutations would be made.

Amino acid substitutions are more likely to give a stable mutant protein if the amino acids are of a similar size and nature. Serious deformation of the structure caused by an inappropriate choice of amino acid substitution will prevent correct folding and the protein will then be subject to host protease degradation. Deformation can occur if a residue is substituted into secondary structure where it is not normally found e.g. a glycine into an α helix. With a small molecule such as PpL it becomes even more important that changes are as conservative as possible, particularly in terms of side chain size. If side chains are too small to allow Van der Waals contacts, water molecules may have access to the core, whereas side chains which are too large will disrupt the structure by steric clashes (Chou and Fasman, 1974).

With these considerations in mind the mutagenesis strategy developed involved changing the charges of amino acids shown to make contact with κ-chain by the NMR studies of Wikström *et al.,* (1996). For example, the residue Gln35 in β strand 2 was selected to be replaced by a His residue to investigate the effect of a positive charge (when the imidazole ring becomes protonated) on the interaction between PpL and κ-chain. It was hoped that a positive charge at pH values around 5- 6 would disrupt interactions within the complex and lead to dissociation at a milder pH. Two mutants (Y64W,Q35H and F39W,Q35H) were produced, each with a Trp reporter molecule present to allow spectroscopic characterisation of the interaction. Previously studies reported that the single mutations Y64W and F39W have no significant effect on the K_d of the complex formed with κ-chain (Beckingham, 1997). Mutants containing more than

one mutation were made by mutating the required residues sequentially. Other mutants include; E38Q, a loss of a negative charge; F39H, a possible gain of a positive charge. Both substitutions are therefore charge changes close to the binding site for κ-chain. Y53H also introduced an ionisable group in a residue previously shown to be involved in binding by NMR studies. N26,76D was created in an attempt to discover whether the complex binding reactions between PpL and κ-chain are due to a dimeric form of PpL in solution. X-ray crystallisation studies in collaboration with Dr. Brian Sutton (King's College, London) have shown that PpL associates to form dimers in its crystal form. These dimers are stabilised by hydrophobic interactions between Ile and Leu residues and by hydrogen bonding. N26 and 76 on one molecule form hydrogen bonds with corresponding positions on the second molecule in the crystal unit. It was anticipated that the removal of these hydrogen bonds would ensure that no dimeric form of PpL existed in solution and that such changes might simplify reaction progress curves.

3.5 Primers selected

Oligonucleotide primers of 21 bases were prepared, encoding for 3 amino acids either side of the mutation in order to ensure site specific binding to the template using codons preferred by *E.coli* where possible. Oligonucleotides were obtained from Oswell DNA services, Southampton. Oligonucleotides selected are shown below with the mutated amino acid shown in bold. The sequence of wild-type PpL is shown in Fig.3.5. Double mutants were made sequentially.

Q35H	5' TCC TGC TGT **GTC** TAT CTT TCC 3'
E38Q	5' TCC TTT GAA **TTG** TGC TGT TTG 3'
F39H	5' TGT TCC TTT **ATG** TTC TGC TGT 3'

Figure 3.5 The DNA and protein sequence of the gene for PpL.

The figure shows DNA sequence in bold and the protein sequence below in lower case letters. Numbered residues are those mentioned in later chapters. The asterisk denotes stop codon.

TTG AAC ATT AAA TTT GCT GGA AAA GAA ACA CCA GAA
met asn ile lys phe ala gly lys glu thr pro glu

ACA CCA GAA GAA CCA AAA GAA GAA GTT ACA ATC AAA
thr pro glu glu pro lys glu glu val thr ile lys

26 **33**
GTT AAC TTA ATC TTT GCA GAT GGA AAG ATA CAA ACA
val asn leu ile phe ala asp gly lys ile gln thr

39
GCA GAA TTC AAA GGA ACA TTT GAA GAA GCA ACA GCA
ala glu phe lys gly thr phe glu glu ala thr ala

53
GAA GCT TAC AGA TAT GCA GAC TTA TTA GCA AAA GTA
glu ala tyr arg tyr ala asp leu leu ala lys val

64
AAT GGC GAA TAT ACA GCA GAC TTA GAA GAT GGT GGA
asn gly glu tyr thr ala asp leu glu asp gly gly

74 **76**
AAC CAT ATG AAC ATT AAA TTT GCT GGA AAA TAA
asn his met asn ile lys phe ala gly lys *

Y53H 5' TAA GTC TGC **ATG** TCT GTA AGC 3'

N26D 5' AAA GAT TAA **GTC** AAC TTT GAT 3'

N76D 5' AAA TTT AAT **GTC** CAT ATG GTT 3'

The phosphorylated oligonucleotide was annealed to uracil-rich template DNA and mutagenesis reactions carried out as described in Chapter 2. The reaction mixture was used to transfect JM103 cells and template DNA was used as a negative control. Three plaques were taken and used to infect a 10ml of LB containing 20µl JM103 cells from an overnight culture. After 6 hours growth, DNA was extracted from cells as described in chapter 2 and analysed by automated sequencing. The sequences of the DNA from mutants are shown in Fig.3.6.

3.6 Expression of mutants

Both mutants containing the Q35H substitution (Q35H, F39W and Q35H, Y64W) failed to express protein from the pKK223-3 expression vector although the mutant sequence was confirmed when cloned into M13 and successfully sub-cloned into pKK223-3. The E38Q mutant was also unable to be expressed despite successful sub-cloning. The 38 position is at the loop between the 2nd β strand and the α helix of the protein and it has been shown that these 'corner' positions which join strands are important for the stability of the protein (Lars Björck, private communication). The F39H,Y64W mutant was successfully expressed to a high level as were the mutants Y64W; F39W; N26,76D, F39W; N26,76D; K33W and Y53H,F39W.

3.7 Protein expression and purification

1ml of an overnight culture of *E.coli* JM103 cells was used to inoculate 500ml of media in each of 8 x 2 l flasks, each containing ampicillin as

Figure 3.6 Sections of the sequencing gels showing the DNA sequence around the site of the mutations.

All mutated genes were submitted to DNA sequencing as described in chapter 2. In each case the 5' end is at the bottom of the ladder of the sequence shown down the side of the gel. The sequence given is that of the anticoding strand.

(a) Site N26D
(b) Site N76D
(c) Site F39H
(d) Site Y64W
(e) Site Y53H
(f) Site F39W
(g) Site E38Q
(h) Site Q35H

(a)

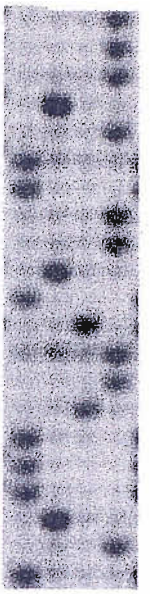

T T T C T A A T T C A G T T G A A A C T

A C G T

(b)

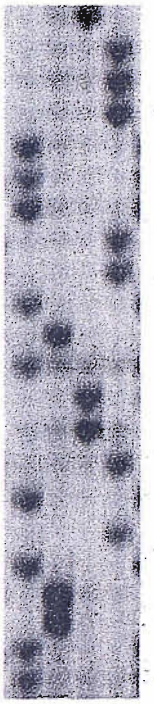

G T T T A A A T T A C A G G T A T A C C A A

A C GT

(c)

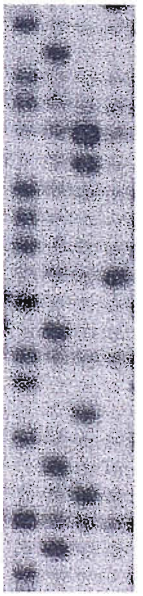

A C A A G G A A A T A C A A C A C G A C A

A C G T

(d)

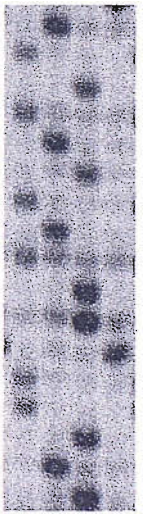

C A G A C G A C A G G T A A G C G

A C G T

(e)

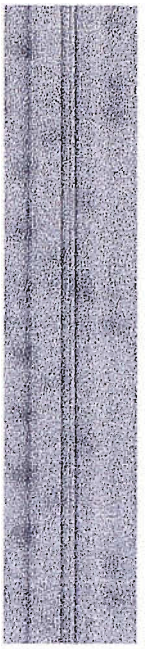

T A T T C A G A C G T A C A G A C C A T T C

A C G T

(f)

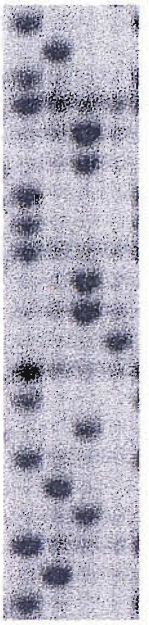

A C A A G G A A A G G T A A G A C G A C A

A C G T

(g)

A C A A G G A A A G G G A A A C T

A C G T

(h)

A C G A C A C A C A T A G A A

A C G T

described in Chapter 2. After reaching an OD_{600} of approximately 0.6 / cm, cells were induced to express the cloned gene by the addition of IPTG and the cells then grown overnight. The following morning the cells were spun down and the cell paste placed in a sonication vessel. 5 volumes of sonication buffer were added at pH 8.0 which contained 0.005% Triton-X100. In addition, PMSF to inhibit host proteinases, and DNaseI to hydrolyse cell DNA was added (See Chapter2). After cell disruption and centrifugation at 12000rpm with an 8 x 50ml rotor to remove cell debris, protein was purified in three stages from the crude extract.

The first step was a heat treatment of the crude extract at 70°C for 40mins. For mutant proteins containing the F39W substitution this was reduced to 65°C for 40mins due to its reduced thermostability caused by the F39W mutation. Other mutants (Y64W, K33W, N26,76D) were able to be treated at 70°C. Precipitated protein was removed by centrifugation.

The second step was anion exchange chromatography using a Q-Sepharose column. The supernatant was diluted to 100ml with 20mM Tris pH 8.0 buffer and loaded onto the column equilibrated in the same buffer at 1.5ml/min. After an initial wash for 150mins with 20mM Tris pH 8.0 to remove protein unable to bind to the column, a salt gradient was applied to the column over 400 mins at 1.5ml/min from 0-30% of 1M NaCl in 20mM Tris pH8.0. Protein peaks were identified by reading the absorbance of the solution at 280nm. Samples from each peak that were eluted from the column were analysed by SDS PAGE using a 15% gel to identify the location and purity of PpL. An elution profile is shown in Fig.3.7, with the peak corresponding to PpL between fractions 44-56.

The third step involved pooling fractions containing PpL and concentrating the protein by 80% ammonium sulphate precipitation. Precipitated PpL was recovered by centrifugation. Typically, 40-50mg of protein would be obtained from 2l of cell culture. PpL was stored as an ammonium sulphate precipitate at 4°C until required whereupon it was

Figure 3.7 The elution profile of PpL from a Q-Sepharose column.

The graph shows the elution profile from a Q-Sepharose column (2cm x 15cm) initially equilibrated at pH 8.0 by 20mM Tris – HCl buffer. The proteins were eluted by application of a linear salt gradient and the eluting protein was detected from its absorption at 280nm and collected in 7ml fractions. PpL and mutants of PpL were collected between fractions 44 and 56.

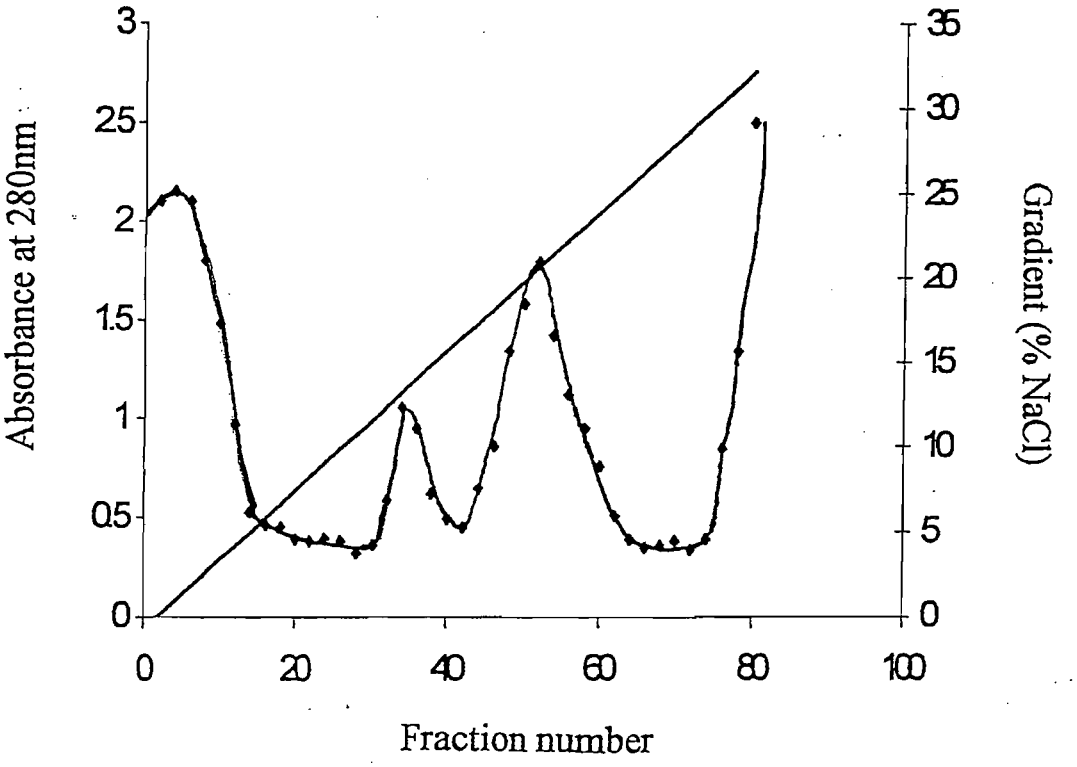
Absorbance at 280nm
3
2.5
2
1.5
1
0.5
0
0
20
40
60
80
100
Fraction number
35
30
25
20
15
10
5
0
Gradient (% NaCl)

dialysed overnight against 4l of 20mM phosphate pH8.0 buffer before use in experiments.

Figure 3.8 A 15% SDS-PAGE gel of the protein at various stages of the purification protocol.

The gel was stained with Coomassie Blue.

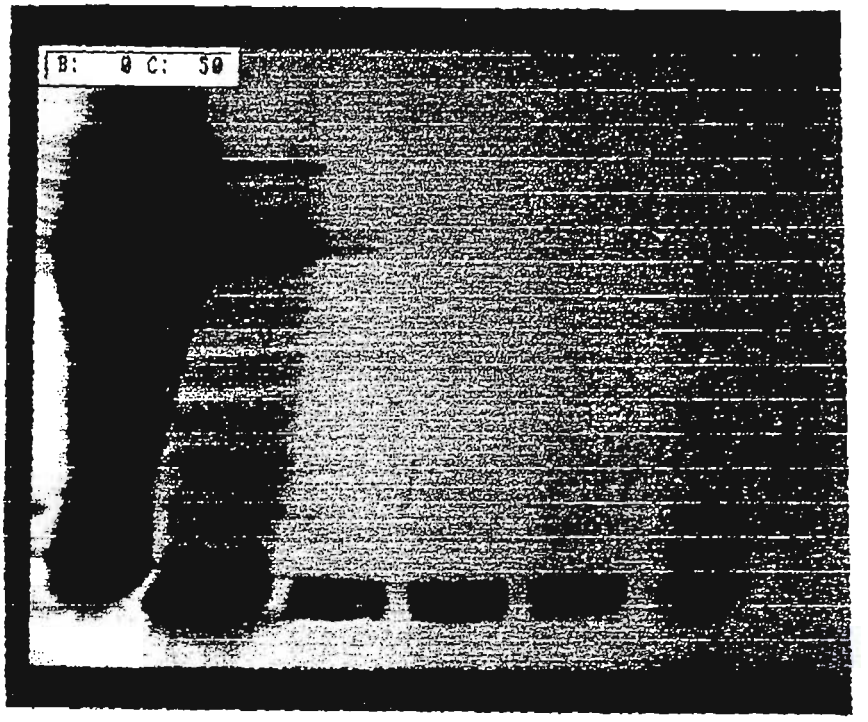

1 2 3 4 5 6

Lane 1 Supernatant after sonication and removal of cell debris

Lane 2 After 70°C heat treatment for 40mins

Lane 3 After anion exchange chromatography

Lane 4 After ammonium sulphate cut and subsequent dialysis

Lane 5 Protein L standard

Lane 6 Markers- 17.0, 14.4, 10.7, 8.13 and 6.2 kDa

Chapter 4

Conformational stability of PpL.

CHAPTER 4

CONFORMATIONAL STABILITY OF PpL

4. Introduction

In the current commercial production of native, multi-domain Protein L, the protein is expressed from a derivative of a pET vector that targets the protein to the periplasmic space of an *E. coli* host. The protein is then released from the periplasmic space by a heat treatment step (around 70°C for 20 min, Dr M. Isaken, Affitech Ltd. Personal communication). If this method of production is to be maintained for mutants of the protein developed with improved binding characteristics, it is essential that they be able to withstand or refold from exposure to high temperature. Assessing the heat stability of each mutant of PpL indicates the likelihood of its suitability for commercial production and applications. Therefore only mutant constructs able to withstand 30min at 65 - 70°C , as part of their purification protocol, have been studied in detail and their properties described in this thesis.

The ability to withstand the presence of other denaturing agents such as guanidine hydrochloride (GdnHCl), urea or low pH is also important as such agents have been used to regenerate columns of immobilised proteins e.g. a domain of protein A (Popplewell, 1991). Furthermore, the determination of the conformational stability of each construct allows any gross differences in secondary and tertiary folding to be quickly ascertained. This helps corroborate data from other techniques such as circular dichroism spectropolarimetry that can give valuable information of the secondary structural content of proteins but not necessarily how these elements interact.

The biological function of a protein is dependent on its native conformation and the stability of this conformation. Protein structure is maintained by covalent bonds such as the peptide bond that link amino acid residues creating the peptide backbone and sometimes by disulphide bridges formed between cysteine residues adjacent to each other in three dimensional space and in oxidative conditions. In addition, the 3-D conformation of the protein is held together by a combination of non-covalent forces - hydrogen bonds, salt bridges, hydrophobic interactions and Van der Waal forces which are determined by interactions between side-chains of different amino acid residues. Proteins are only marginally more stable in folded form than unfolded form (Creighton, 1992), therefore these forces which stabilise proteins are easily disrupted. This can be achieved by heating, extremes of pH or chaotropic agents such as GdnHCl and urea. This disruption is known as denaturation ; the unfolding of polypeptide chains without cleavage of the peptide bonds. After denaturation has taken place, the biological activity can often be restored by removing the denaturant and allowing the protein to refold as the information required for correct folding is held within the polypeptide chain (Anfinsen, 1972).

Although unfolding is a complex process, sometimes involving many intermediates, it is usually described as a single step, first order reaction (Creighton, 1992). In reality there are likely to be a large number of different forms of the unfolded and folded protein in rapid equilibrium with each other. The position of the equilibrium between the folded and unfolded forms of a protein depends upon the conditions. However, unless a stable intermediate in the folding / unfolding pathway can be clearly demonstrated, a simple two-state model is usually employed in which the protein is assumed to exist either in a completely folded or completely unfolded state (Pace, 1986). From experiments involving the controlled unfolding of a protein, the equilibrium constant for the folding / unfolding process and the free energy change associated with that process can be calculated to give the conformational stability of the protein.

4.1 Conformational stability of PpL

This chapter describes controlled unfolding experiments of PpL and some mutants of PpL using the chaotropic agent GdnHCl. This agent unfolds proteins by disrupting non-covalent bonds and forming intermolecular hydrogen bonds with the protein thus breaking intramolecular hydrogen bonds and loosening the packing of the side-chains leading to the solvation of buried residues. The unfolding process is driven by more denaturant molecules binding to unfolded protein than to folded protein i.e. the equilibrium between folded and unfolded protein is increasingly shifted towards the unfolded state as GdnHCl interacts with more of the protein surface of unfolded proteins (Creighton, 1992).

4.2 Detection of the unfolding process

Fluorescence from molecules is initiated when an electron is raised to a higher energy level by absorbing a photon of light at a specific wavelength. When the excited state electron returns to its ground state it emits light of a wavelength higher than that absorbed (the difference between the wavlengths of the absorbed and emitted light is known as the Stokes shift) because it has lost energy to the solvent and due to dissipation of vibrational energy. The fluorescent amino acid residues found in proteins are those containing delocalised electrons in aromatic rings ie. Tyr, Phe and Trp. These have emission maxima in water at 280 nm (Phe), 303 nm (Tyr) and most importantly 348 nm (Trp) (Lakowicz, 1983). Tryptophan is by far the most fluorescent of the amino acid residues, typically accounting for 80% of fluorescence in proteins when present. This is due not only to Forster resonance energy transfer processes (Forster, 1965) from Phe and Tyr to Trp but also because Trp has a much higher molar extinction coefficient (see Table 4.1).

Table 4.1. The spectral parameters for the aromatic amino acid residues in proteins. The data given are for solutions in water (Eftink, 1991)

Amino acid	λ max. absorbance (nm)	$\varepsilon_{\lambda max.}$ ($M^{-1}cm^{-1}$)	λ_{max} emission (nm)	Quantum Yield (in H_20)
Phenylalanine	258	200	282	0.02
Tyrosine	275	1400	304	0.14
Tryptophan	280	5600	355	0.13

The wavelength and intensity of fluorescence emission depends upon the microenvironment of these chromophores i.e. the nature of nearby residues and how exposed the chromophore is to the solvent. If the environment becomes more polar light is emitted at a longer wavelength i.e. with lower energy and its intensity usually decreases due to collisional quenching effects of ions in solution. If the environment becomes more hydrophobic i.e. the residue becomes more buried, its emission maximum is at a shorter wavelength and intensity normally increases (Lakowicz, 1983). Therefore when a protein unfolds, the environment of the aromatic residues is likely to change and therefore fluorescence emission will change with exposure to increasing denaturing conditions. The amount of structural disturbance required to perturb the fluorescence emission intensity from Trp may well be dependent upon the individual protein. This is because in some situations it is possible to imagine local relaxation of tertiary packing around a Trp residue being enough to allow water to access the indole ring with resulting fluorescence changes. This may well occur before substantial unfolding of the peptide backbone of the protein occurs as in "molten globule" unfolding intermediates (Creighton, 1992). Nevertheless fluorescence data have been shown to be accurate for measuring conformational stability of many proteins. For example, the conformational stability of barnase was determined by fluorescence studies which were in close agreement with data obtained using solvent perturbation difference spectroscopy (Pace *et al.*, 1992) and fluorescence and far-UV CD studies have also given similar values for the conformational stability of α1-antitrypsin and detected intermediates in the unfolding pathway (James *et al.*,

1999) . Recently, Kim *et al.*, (1998, 2000) have used pre-equilibrium stopped-flow fluorimetry to examine the order of folding of the secondary structures in PpL from strain 312 of *Peptostreptococcus magnus*.

4.3 Fluorescence of PpL

The single domain of WT Protein L used in these experiments contains 3 Tyr and 5 Phe residues, the latter having very low molar extinction coefficients and quantum yields (see Table 4.1). The major contributors to the fluorescence properties of PpL are therefore the three Tyr residues when light at 280nm is applied. The fluorescence intensity from these residues at 305nm was able to be measured in the presence of increasing concentrations of GdnHCl to obtain an unfolding curve, however, three unique Trp residues were substituted into domains separately creating Y64W, F39W or K33W PpL to significantly enhance the fluorescence of these domains and facilitate fluorescence studies.

The fluorescence properties of Trp residues were used to determine the conformational stabilities of WT PpL and mutants Y64W, F39W, K33W, and N26,76D,F39W. The conformational stability of N26,76D was also measured using endogenous Tyr residues as reporter groups.

4.4 Data Analysis

A plot of fluorescence intensity against GdnHCl concentration gives a sigmoidal curve with three distinct regions. Proteins in aqueous buffer are normally considered to be 'folded' although in principle there is a minute proportion of the molecules in unfolded states that are in equilibrium with the folded states. A protein is considered to be stable if the position of the equilibrium does not alter very much over a certain period of time. However, as the conditions begin to favour unfolding, eg. by the addition of a denaturant, the average structure remains unchanged but there is increased flexibility in some parts of the protein, particularly the side-chains and the local conformation may alter slightly. This part of the curve gives rise to the pre-transition region that does not usually result

in a large fluorescence change. After this follows the transition region in which the protein unfolds completely and cooperatively over a small range of conditions. This change from a predominance of folded to unfolded protein normally shows a large change in fluorescence. The change in fluorescence intensity depends upon the local environment before and after the unfolding has occurred. Usually it decreases when the protein unfolds, alternatively it may increase if the Trp lies close to quenching groups only in the folded protein e.g. thiols or charged species (for examples see Churchich *et al.*, 1996, Krauss and Gore, 1996 and Clark *et al.*, 1996). The post-transition region occurs when the protein has been completely unfolded. The pre- and post- transitional regions may still show changes in fluorescence intensity with increases in GdnHCl despite no significant unfolding occurring. These spectral changes arise from the effects of the denaturant on the fluorophores in the folded and unfolded states of the protein respectively.

Data from all three regions are used to calculate the conformational stability of the protein.

4.5 Calculations

The simplest model for protein unfolding is based upon an assumed two-state process that can be described by the following equation;

$$\text{(Folded)}\quad F \underset{k_f}{\overset{k_u}{\rightleftharpoons}} U \quad \text{(Unfolded)}$$

Protein unfolding

Protein folding

At equilibrium, $k_f(U) = k_u(F)$

and thus $k_u / k_f = U / F = K_{eq}$

in which k_f is the rate of folding and k_u is the rate of unfolding of the protein and K_{eq} is the equilibrium constant for the reaction under set conditions.
From experiments involving the controlled unfolding of a protein, the equilibrium constant and free energy change (ΔG^o) at given concentrations of denaturant can be calculated and these data used to give the conformational stability of the protein in water (ΔG^o_{H20}).

The fraction of protein unfolded (F_u) at a particular concentration of GdnHCl is given by:

$$F_u = (I_F - I) / (I_F - I_U)$$

and the fraction of the protein folded (F_F) at a particular concentration of GdnHCl is given by;

$$F_F = (I - I_U) / (I_F - I_U)$$

where I is the observed fluorescence intensity at a given wavelength and I_F and I_U are the values of the fluorescence intensity of the fully folded and fully unfolded forms of the protein at the same wavelength, respectively. The values for completely folded and unfolded forms are taken from the pre- and post-transitional regions of the unfolding curve.
Thus

$$K_{eq} = (I_F - I) / (I - I_U)$$

The difference in free energy between the folded and unfolded conformations, ΔG^o is given by :

$$\Delta G^o = - RTIn\ K_{eq}$$

or

$$\Delta G^o = - RTln\ (I_F - I) / (I - I_U)$$

where R is the molar gas constant ($8.31 kJmol^{-1}K^{-1}$) and T is the absolute temperature (K).

There is a linear dependence of ΔG^{o} upon denaturant concentration and data fit the equation:

$$\Delta G^{o} = \Delta G^{o}_{H2O} - m\,[GdnHCl] \qquad \text{(Pace, 1986)}$$

where m is the proportionality constant ($kJmol^{-1}M^{-1}$) that describes the dependence of ΔG^{o} on denaturant concentration. It is proportional to the surface area exposed to the solvent on unfolding per increase in denaturant concentration (Tanford, 1968), in other words it describes the cooperativity of the unfolding process. ΔG^{o}_{H2O} is the difference in free energy between the folded and unfolded structures of the protein in water. The value of ΔG^{o} in the absence of denaturant, ΔG^{o}_{H2O}, is calculated by plotting the ΔG^{o} of unfolding reactions within the transition region against GdnHCl concentration and extrapolating the line to the ordinate. The intercept on the ordinate gives ΔG^{o}_{H2O}, the conformational stability in the absence of denaturant at that particular temperature. However, it can be also calculated by multiplying the slope, m ($kJmol^{-1}M^{-1}$) by the concentration of denaturant necessary to cause 50% unfolding of the protein i.e. where Keq = 1. this avoids the need for long extrapolation.

4.6 Fluorescence spectra of folded and unfolded PpL

Fluorescence spectra for folded, partly unfolded and completely unfolded PpL or mutants of PpL not containing Trp residues were obtained by incubating 3 - 10μM protein with various concentrations of GdnHCl between 0 - 5M. Solutions were incubated at 25°C for 60mins (shown to be sufficient time to allow the equilibrium to be obtained, see section 4.7) and then the fluorescence emission spectra were determined using 280nm as the excitation wavelength. As can be seen from Figure 4.1a, when PpL (or N26,76D) is denatured in GdnHCl, there is a decrease in fluorescence intensity at 305nm indicating that one or more Tyr residues (initially buried / partly buried within the hydrophobic core) becomes more accessible to the solvent on unfolding of the protein. For the Y64W mutant (or mutant derivatives containing W64), only 3μM protein was used for the experiments due to the higher fluorescence intensity of the Trp residue in this mutant. On unfolding, its (and derivative mutants) fluorescence intensity

Figure 4.1 The fluorescence emission spectra of PpL and its mutants in buffer or 6M GdnHCl.

Figure (a) shows the emission spectra of 10μM PpL in 20mM phosphate buffer pH 8.0 at 25°C containing buffer (blue) and 6M GdnHCl (red). The excitation wavelength was 280nm and slit widths were 10nm. There is a decrease in fluorescence on unfolding.

Figure (b) shows the emission spectra of 3μM Y64W in 20mM phosphate buffer pH 8.0 at 25°C containing buffer (blue) or 6M GdnHCl (red). The excitation wavelength was 280nm and slit widths were 10nm. There is a decrease in fluorescence on unfolding.

Figure (c) shows the emission spectra of 5μM F39W in 20mM phosphate buffer pH 8.0 at 25°C containing buffer (blue) and 6M GdnHCl (red). The excitation wavelength was 280nm and slit widths were 10nm. There is an increase in fluorescence on unfolding.

Figure (d) shows the emission spectra of 5μM K33W in 20mM phosphate buffer pH 8.0 at 25°C containing buffer (blue) and 6M GdnHCl (red). The excitation wavelength was 280nm and slit widths were 10nm. There is a decrease in fluorescence on unfolding.

(a)

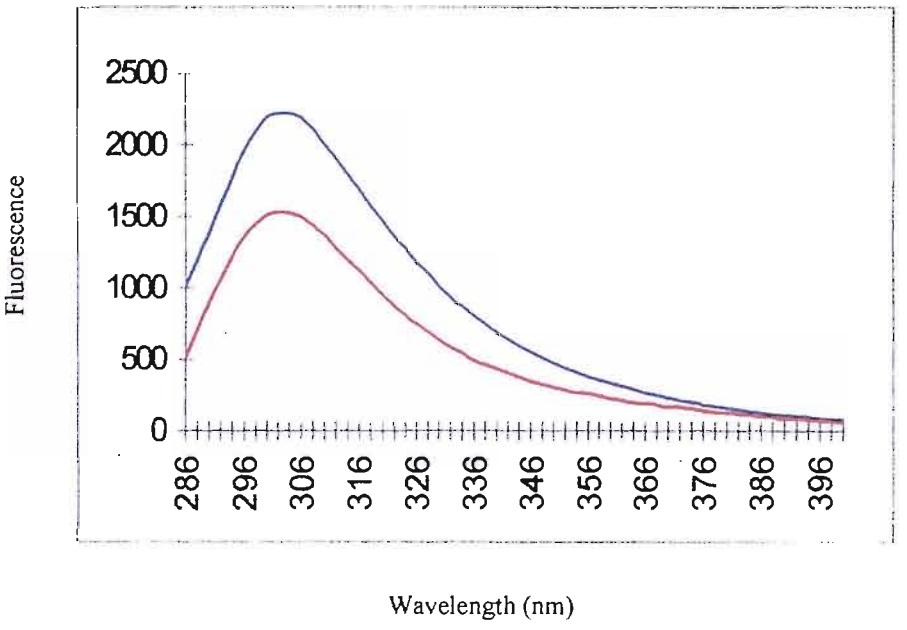
Fluorescence
2500
2000
1500
1000
500
0
286
296
306
316
326
336
346
356
366
376
386
396
Wavelength (nm)

(b)

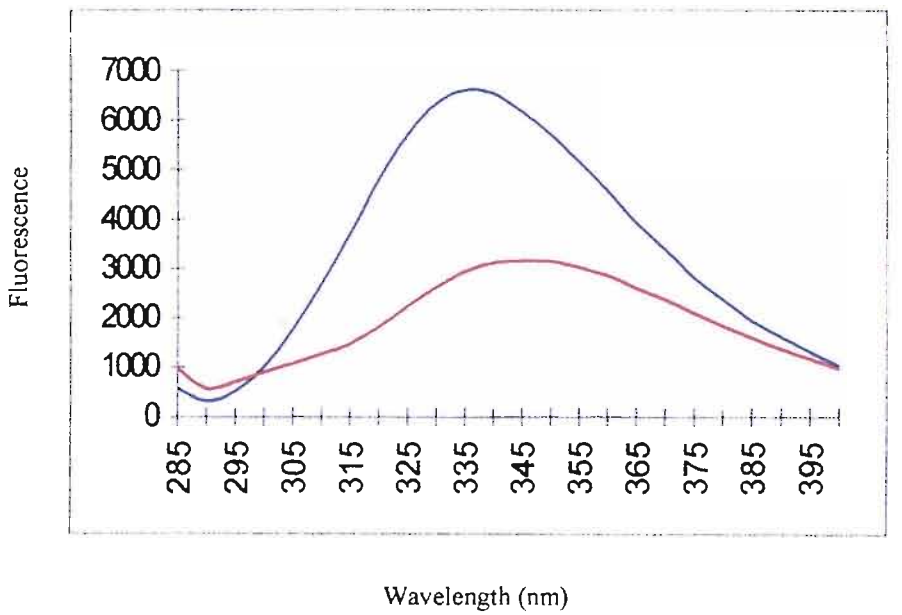
Fluorescence
7000
6000
5000
4000
3000
2000
1000
0
285
295
305
315
325
335
345
355
365
375
385
395
Wavelength (nm)

(c)

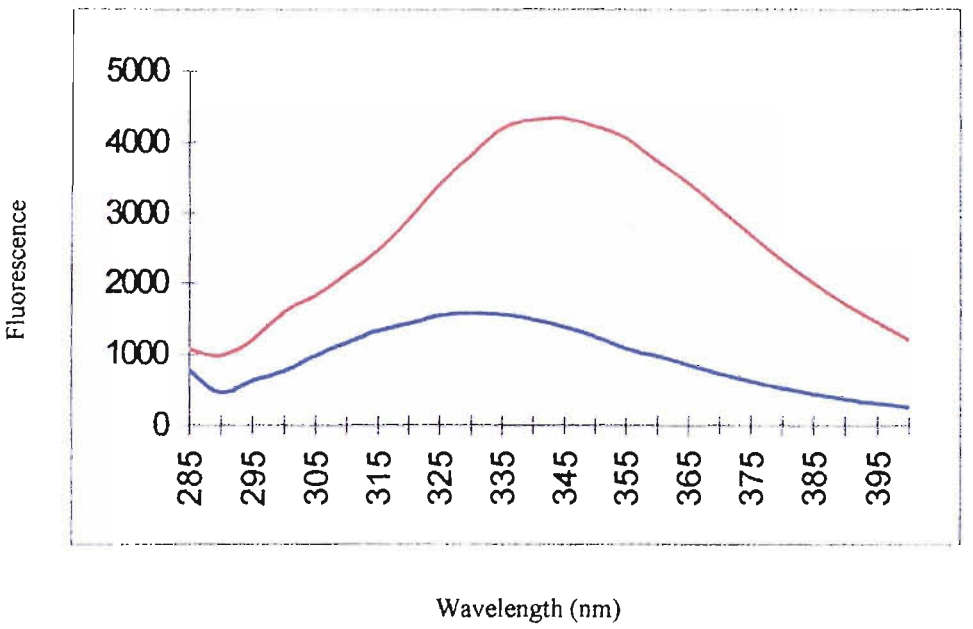
Fluorescence
5000
4000
3000
2000
1000
0
285
295
305
315
325
335
345
355
365
375
385
395
Wavelength (nm)

(d)

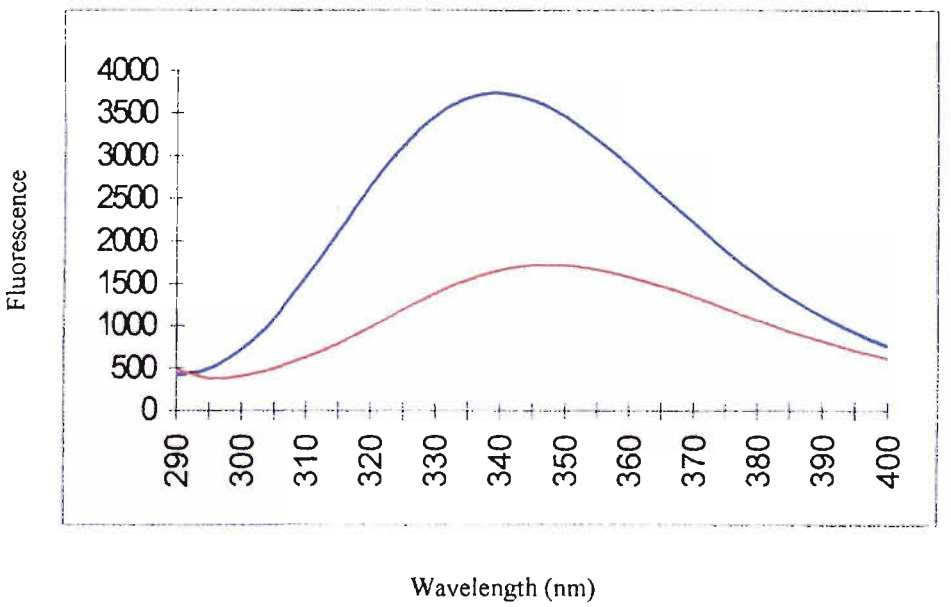
Fluorescence
4000
3500
3000
2500
2000
1500
1000
500
0
290
300
310
320
330
340
350
360
370
380
390
400
Wavelength (nm)

decreases markedly at 332 nm and the emission maximum shifts from 332 nm to 348 nm (Fig.4.1b). The F39W mutant (or mutant derivatives of this bearing W39) was studied in a similar manner using 5μM protein for the experiments. Fig.4.1c shows that the emission maximum for this mutant (or derivatives) shifts from 328 nm to 344 nm. In contrast to the observations made using the other mutants, there is a significant increase in fluorescence on unfolding of the protein suggesting that the W39 side-chain may be subject to static quenching by, e.g., neighbouring charged residues (e.g. E38 and / or K40) prior to unfolding (see Fig 4.8b).

Finally, the spectrum of folded K33W shows a red emission maximum at 342nm (see Fig. 4.1d) and the fluorescence intensity of the protein at this wavelength decreases as the concentration of denaturant is increased.

4.7 Rate of unfolding of PpL

These studies were necessary prior to the unfolding experiments to show that the correct conditions for unfolding were used in subsequent experiments.
The unfolding process was followed over time by rapidly mixing 5μM Y64W or F39W with a range of concentrations of GdnHCl and following the change in fluorescence intensity on a fluorimeter using an excitation wavelength of 280nm and measuring the fluorescence emission at 338nm. The decrease in fluorescence to the level expected for unfolded protein for Y64W and the increase in fluorescence for the F39W mutant showed that unfolding in high concentrations of GdnHCl is a very rapid process which is too fast to be followed in a conventional fluorimeter e.g. unfolding takes place in fractions of a second in the presence of 3M GdnHCl. At lower concentrations of the reagent the unfolding was shown by conventional fluorimetry to be completed in 30 min. at 25°C. Therefore in unfolding experiments the samples were incubated for 30 – 60 min before any readings were taken.

In order to ensure that the change in fluorescence intensity was due to rapid unfolding and not due to any other effects (e.g. optical effects) of the denaturant, stopped flow fluorescence spectroscopy was used to follow the reaction over the

first few seconds after the protein was added to 3M GdnHCl. The excitation wavelength used was 280nm and a filter was used to transmit emitted light above 335nm therefore limiting the observation to Trp fluorescence only. An extremely rapid, but time-dependent decrease in fluorescence intensity from the Y64W mutant and a similar, but more rapid increase in fluorescence intensity from the F39W mutant, were observed. The rates of unfolding for Y64W were $10.05s^{-1}$ (Fig.4.2a) and for F39W $53.70s^{-1}$ (Fig.4.2b).

4.8 Refolding of PpL

As the calculations shown in section 4.5 assume that the unfolding of the protein follows a simple two-state reversible process, it was necessary to confirm that PpL and mutants could be refolded once unfolding had taken place. Experiments were carried out in which two solutions were set up for each protein. One solution containing protein (3 - 10μM) in 20mM phosphate buffer pH 8.0, the other containing the same amount of protein in the same buffer containing the required amount of GdnHCl to cause 95% unfolding of that particular protein. These solutions were incubated at room temperature for 30mins and fluorescence measured. All of the the solutions were then diluted into 20mM phosphate buffer 1:4 v/v, reducing the GdnHCl concentration to that of the pre-unfolding transition region for each protein. A fluorescence measurement was taken for these diluted samples and compared to the samples that had not been unfolded. The percentage of protein refolded after 2mins and 30mins is shown in Table 4.2.

Figure 4.2 Reaction progress curves for the unfolding of Y64W and F39W by GdnHCl.

The figures show the change in fluorescence intensity with time when 20μM (a) Y64W or (b) F39W are rapidly mixed 1:1 v/v with 6M GdnHCl at pH 8.0 and 25°C. In these experiments Y64W unfolds at a rate of $10.05s^{-1}$ and F39W unfolds with a rate of $53.70s^{-1}$. The curves were analysed by a single exponential equation with any steady state rate also indicated. The residuals to the fitted curves are shown below the reaction progress curves. The buffer used was 20mM potassium phosphate, pH 8.0 and temperature 25°C.

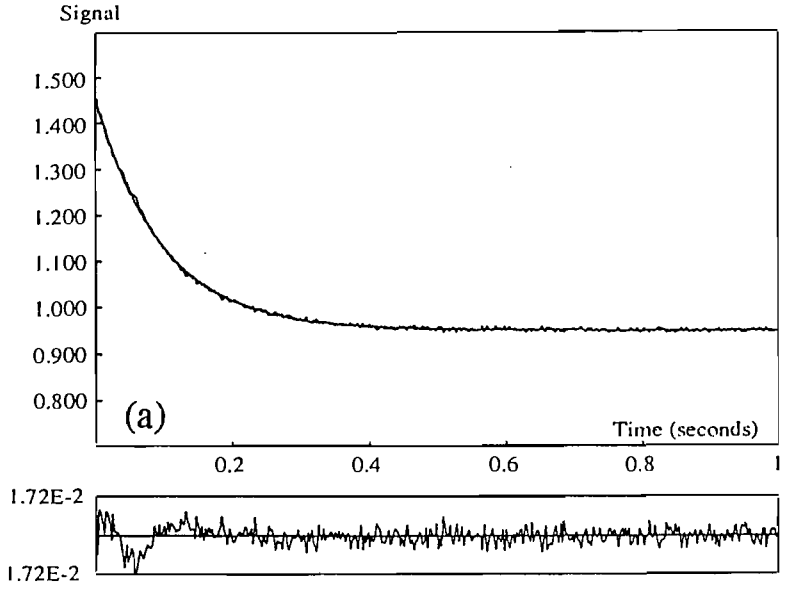

REGRESSION RESULTS:
Library: Standard Software: SX18MV v4.33
Function name: Single exponential with steady state
Formula: P(1)*EXP(-P(2)*X)+P(3)*X+P(4)

Parameter:		Value:	Std.Error:
P(1)	Amp	5.03E-1	1.43E-3
P(2)	Rate	1.05E1	6.53E-2
P(3)	Slope	-7.62E-3	1.38E-3
P(4)	Intcpt	9.56E-1	9.89E-4
Norm. Variance:		1.61E-5	Fit range: 1-400

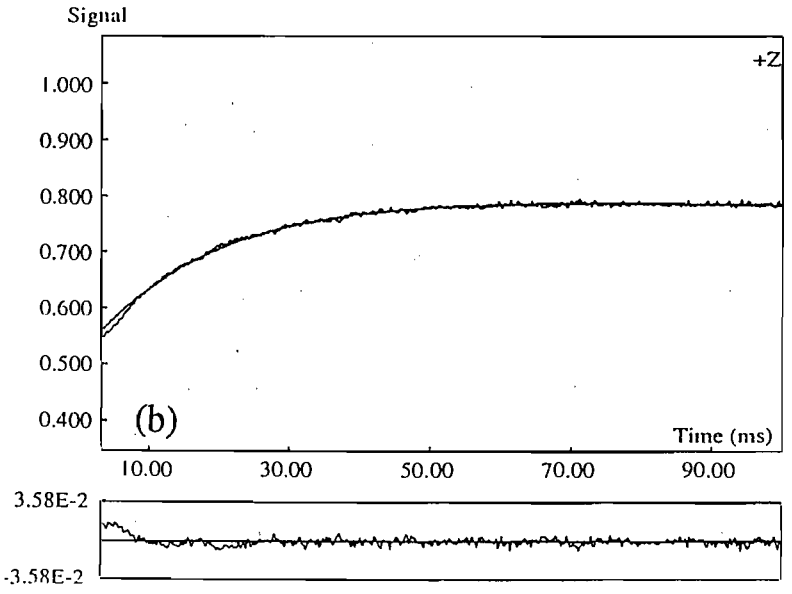

REGRESSION RESULTS:
Library: Standard Software: SX18MV v4.33
Function name: Single exponential with steady state
Formula: P(1)*EXP(-P(2)*X)+P(3)*X+P(4)

Parameter:		Value:	Std.Error:
P(1)	Amp	-3.03E-1	2.95E-3
P(2)	Rate	5.37E1	1.02E0
P(3)	Slope	-2.97E-1	3.82E-2
P(4)	Intcpt	8.15E-1	3.37E-3
Norm. Variance:		2.70E-5	Fit range: 1-400

Table 4.2. Shows the percentage of protein refolded after 2 and 30mins following the dilution of unfolded protein five fold with buffer.

Protein	% refolded after 2mins	% refolded after 30mins
WT	8.4	87.4
Y64W	12.9	85.4
F39W	2.8	87.0
K33W	4.6	88.5
N26,76D	9.6	75.2
N26,76D,F39W	4.8	77.2
F39H,Y64W	8.2	87.6
Y53H,F39W	2.2	89.1

The table shows that all of the proteins regain a fluorescence intensity to at least 75% of that of their folded form suggesting that the unfolding process is reversible. Although the effective concentration of the proteins during the refolding process was very low, between 0.6μM and 2μM, equivalent to 0.007mg / ml to 0.02 mg / ml, it is possible that the incomplete regain of fluorescence intensity is due to loss of protein from solution due to aggregation or because more than 30 minutes are required for full refolding. Recent studies by Kim *et al.*, (1998, 2000) have exploited the reversible folding / unfolding of a related PpL domain to elucidate the effect of other mutations on the stability of that protein.

4.9 Unfolding curves for WT and mutated PpL domains

A series of 1ml solutions of GdnHCl with concentrations ranging from 0 to 5M, with increments of 0.25M, were set up using a stock of filtered 6M GdnHCl solution in 20mM phosphate (adjusted to pH 8.0) and 20mM phosphate buffer pH 8.0. 10μM WT PpL and N26,76D, 3μM Y64W and F39H,Y64W domains or 5μM of F39W mutant, N26,76D,F39W mutant, Y53H,F39W mutant or K33W mutant proteins were added to samples of these solutions of GdnHCl. After incubation for 60 min at the appropriate temperature, fluorescence intensities at

302nm were recorded for WT, N26,76D and at 335nm for the remaining mutants. (for full details see Chapter 2, section 2.5.2, 2.5.5 and 2.5.6). The unfolding curve for WT PpL (Fig.4.3a) shows a midpoint of unfolding at 2.37 M GdnHCl, the ΔG^{o}_{H2O} (see Fig. 4.3b and Table 4.3) was calculated to be 17.84 ± 0.74 $kJmol^{-1}$ and m was shown to be 7.87 ± 0.43 $kJmol^{-1}M^{-1}$ at 25°C. The Y64W PpL displays a conformational stability as high as that of the WT PpL if not higher.

Recent studies in this laboratory confirm that the Y64W has a higher denaturant, temperature and alkali stability than the WT domain (Sam Fenwick, personal communication). Unfortunately, the substitution of a Trp residue at position 39 appears to decrease the overall conformational stability of the domain (12.97 kJ mol^{-1}) and this is further exacerbated by additional mutations e.g. N26,76D F39W PpL has a ΔG^{o}_{H2O} value of only 7.87 ± 1.09 $kJmol^{-1}$. It is also notable that the K33W substitution causes a significant decrease in conformational stability, possibly due to the placement of a more hydrophobic residue in what is otherwise a polar region of the protein. The unfolding curves and values of these parameters for other mutants at 25°C are shown in Figs 4.3c-4.3r and the data summarised in Table 4.3. Each set of data is from an average of three experiments (n = 3) and the data were analysed using Grafit program (Erithicus software). The H74C mutant was labelled with an extrinsic fluorophore, pyrene maleimide (see Chapter 2) which binds to the thiol group of the cysteine residue. As can be seen from Table 4.3 the effect of this mutation in this location has little effect on the stability of the protein (ΔG^{o}_{H2O} = 14.99 $kJmol^{-1}$, n = 1) with respect to denaturation using GdnHCl.

Figure 4.3 Conformational stability of PpL

Proteins were unfolded using GdnHCl at pH8.0 and 25°C (unless otherwise stated) and the extent of unfolding followed using protein fluorescence. For mutants containing tryptophan, the excitation wavelength used was 280nm and the emission was measured at 338nm. For pyrene maleimide labelled H74C, excitation was at 340nm and emission measured at 380nm. For other mutants and PpL tyrosine fluorescence was measured using excitation at 280nm and emission at 305nm.

(a) Shows unfolding curve for PpL
(b) Shows conformational stability of PpL derived from (a)

(c) Shows unfolding curve for N26,76D
(d) Shows conformational stability of N26,76D derived from (c)

(e) Shows unfolding curve for Y64W
(f) Shows conformational stability of Y64W derived from (e)

(g) Shows unfolding curve for F39W
(h) Shows conformational stability of F39W derived from (g).

(i) Shows unfolding curve for N26,76D,F39W
(j) Shows conformational stability of N26,76D,F39W derived from (i).

(k) Shows unfolding curve for K33W
(l) Shows conformational stability of K33W derived from (k).

(m) Shows unfolding curve for F39H,Y64W
(n) Shows conformational stability of F39H,Y64W derived from (m).

(o) Shows unfolding curve for Y53H,F39W

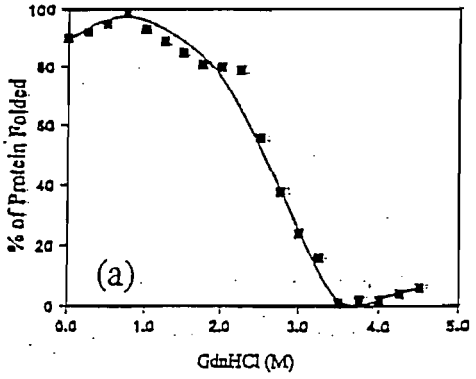
% of Protein Folded
(a)
GdnHCl (M)

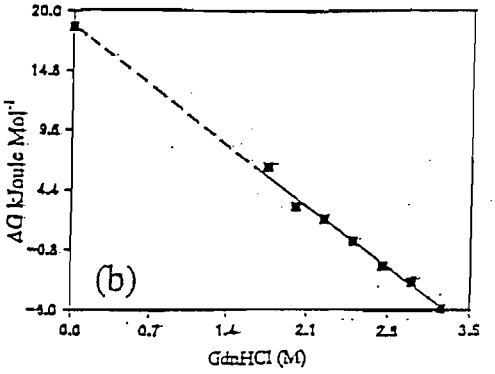
ΔG kJoule Mol⁻¹
(b)
GdnHCl (M)

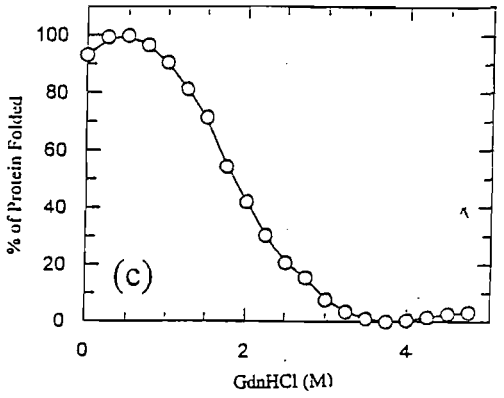
% of Protein Folded
(c)
GdnHCl (M)

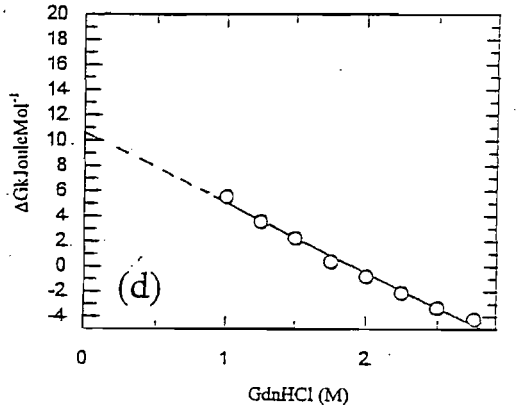
ΔGkJouleMol⁻¹
(d)
GdnHCl (M)

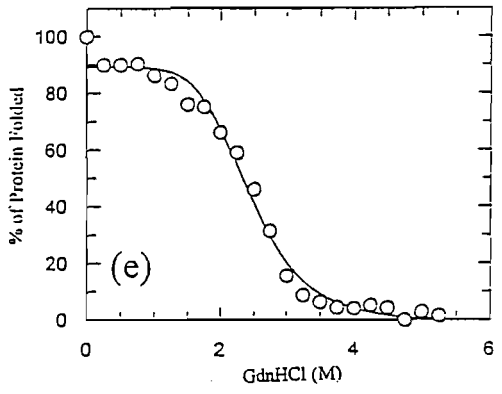
% of Protein Folded
(e)
GdnHCl (M)

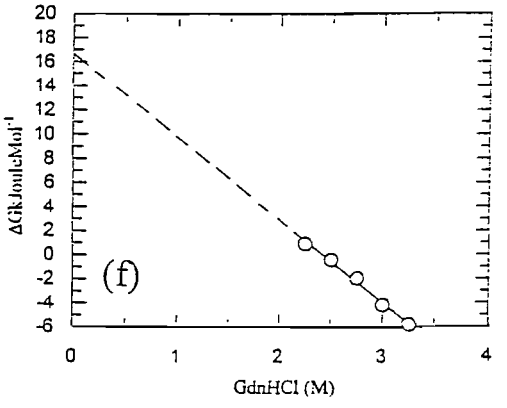
ΔGkJouleMol⁻¹
(f)
GdnHCl (M)

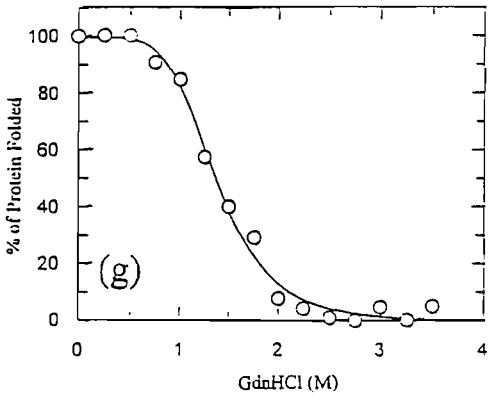
% of Protein Folded
(g)
GdnHCl (M)

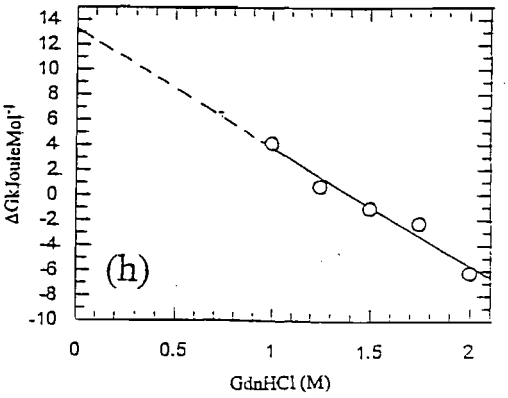
ΔGkJouleMol⁻¹
(h)
GdnHCl (M)

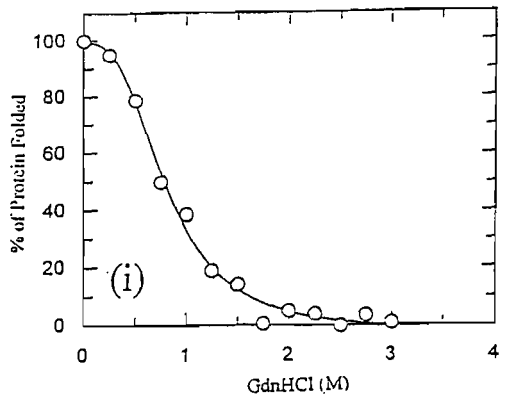
% of Protein Folded
(i)
GdnHCl (M)

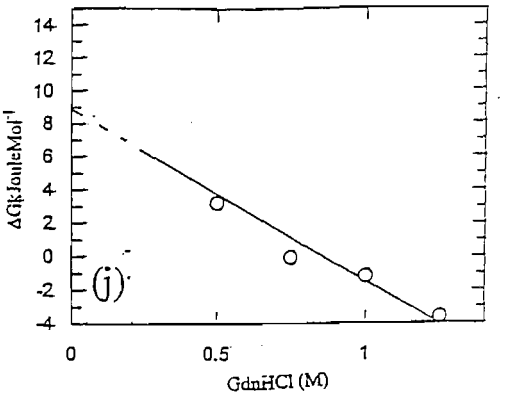
ΔGkJouleMol-1
(j)
GdnHCl (M)

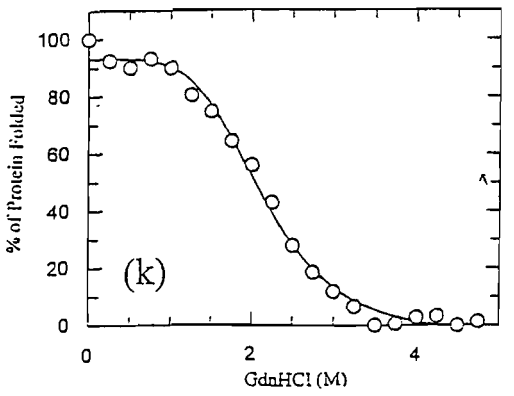
% of Protein Folded
(k)
GdnHCl (M)

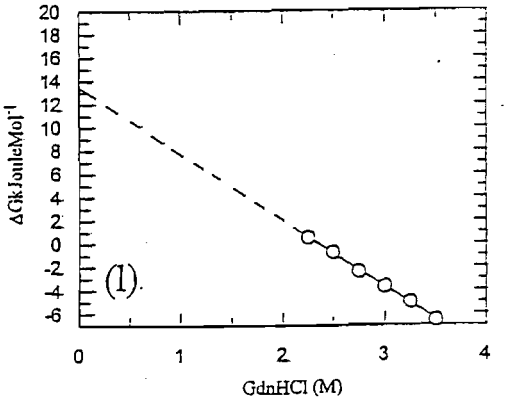
ΔGkJouleMol-1
(l)
GdnHCl (M)

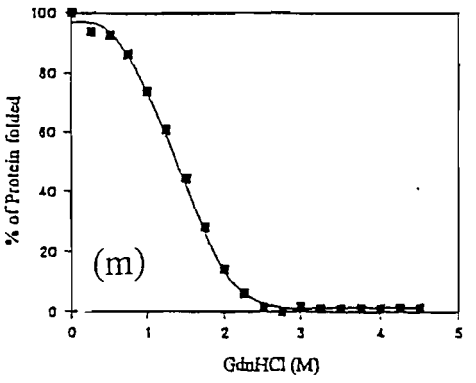
% of Protein folded
(m)
GdnHCl (M)

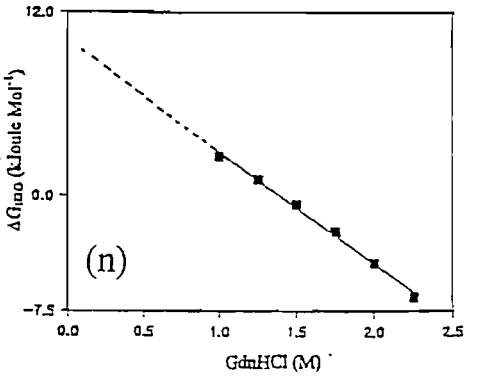
ΔGH2O (kJoule Mol-1)
(n)
GdnHCl (M)

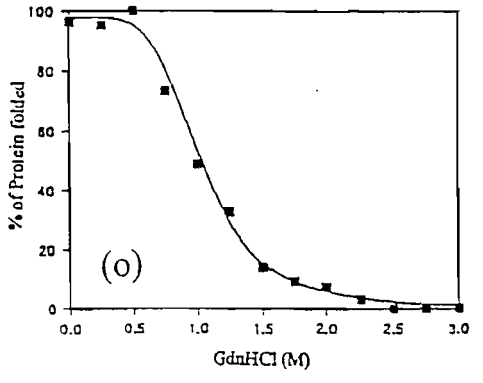
% of Protein folded
(o)
GdnHCl (M)

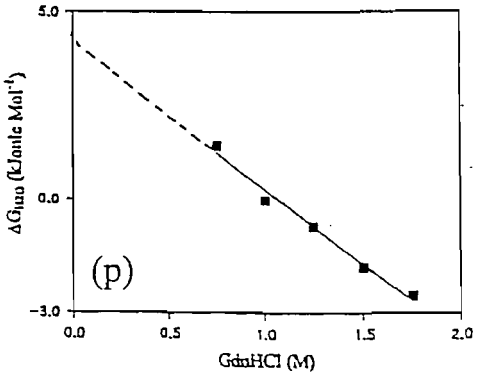
ΔGH2O (kJoule Mol-1)
(p)
GdnHCl (M)

(p) Shows conformational stability of Y53H,F39W derived from (o).

(q) Shows unfolding curve for H74C

(r) Shows conformational stability of H74C derived from (q).

(s) Shows unfolding curves for Y64W at 20 (○) 30 (●) 40 (□) and 50°C (■).

(t) Shows conformational stability of Y64W derived from curves obtained in (s). 20 (○) 30 (●) 40 (□) and 50°C (■).

(u) Shows unfolding curves for Y64W at 25 (○) 35 (●) 45 (□) and 55°C (■).

(v) Shows conformational stability of Y64W derived from curves obtained in (u). 25 (□) 35 (●) 45 (○) 55°C (■).

(w) Shows unfolding curves for F39W at 20 (□) 30 (■) 40 (○) and 50°C (●).

(x) Shows conformational stability of F39W derived from curves obtained in (w). 20 (□) 30 (○) 40 (●) and 50°C (■).

(y) Shows unfolding curves for F39W at 25 (○) 35 (●) 45 (□) and 55°C (■).

(z) Shows conformational stability of F39W derived from curves obtained in (y). 25 (○) 35 (●) 45 (□) and 55°C (■).

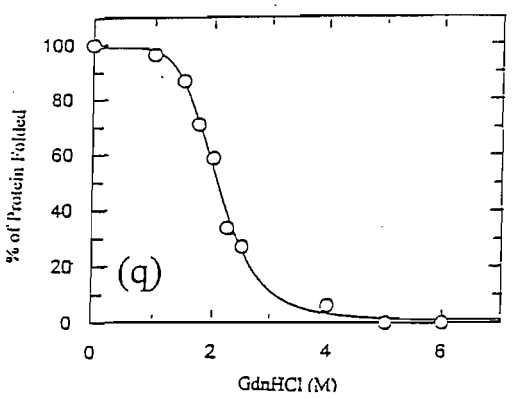
% of Protein Folded
100
80
60
40
20
0
(q)
0
2
4
6
GdnHCl (M)

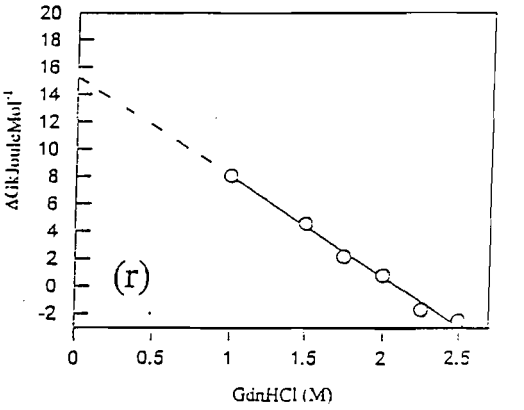
ΔGkJouleMol-1
20
18
16
14
12
10
8
6
4
2
0
-2
(r)
0
0.5
1
1.5
2
2.5
GdnHCl (M)

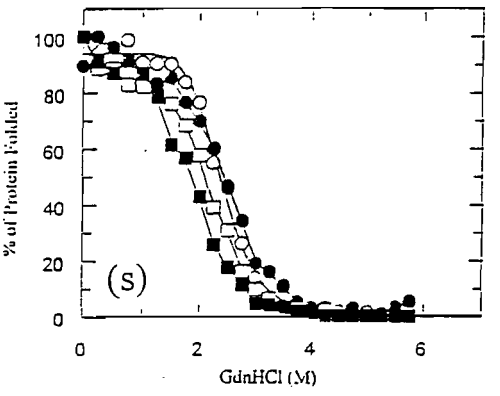
% of Protein Folded
100
80
60
40
20
0
(s)
0
2
4
6
GdnHCl (M)

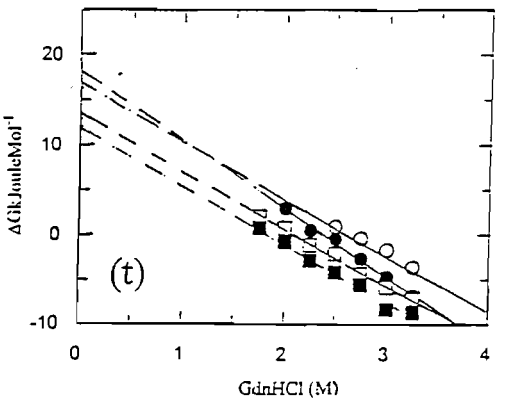
ΔGkJouleMol-1
20
10
0
-10
(t)
0
1
2
3
4
GdnHCl (M)

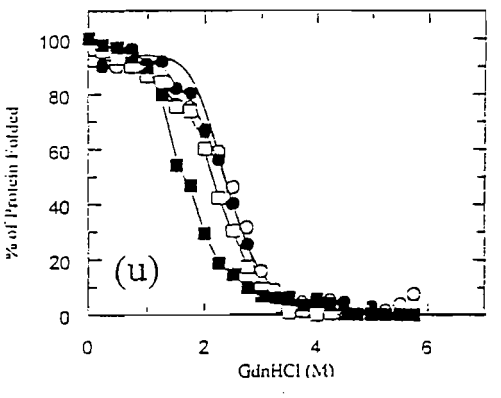
% of Protein Folded
100
80
60
40
20
0
(u)
0
2
4
6
GdnHCl (M)

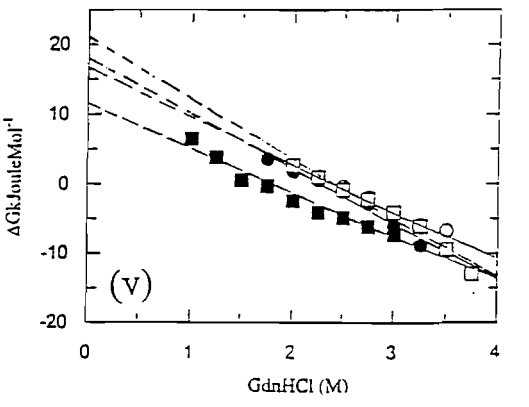
ΔGkJouleMol-1
20
10
0
-10
-20
(v)
0
1
2
3
4
GdnHCl (M)

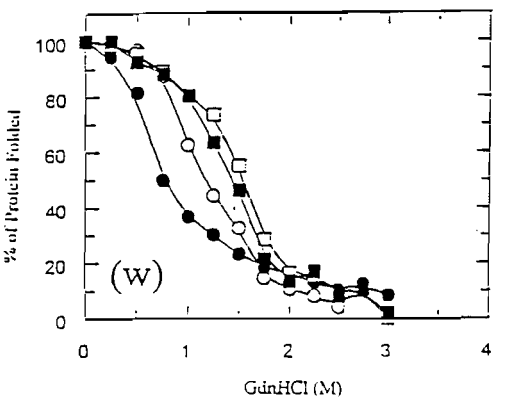
% of Protein Folded
100
80
60
40
20
0
(w)
0
1
2
3
4
GdnHCl (M)

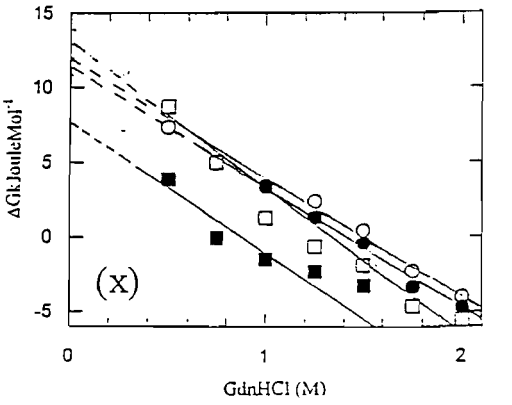
ΔGkJouleMol-1
15
10
5
0
-5
(x)
0
1
2
GdnHCl (M)

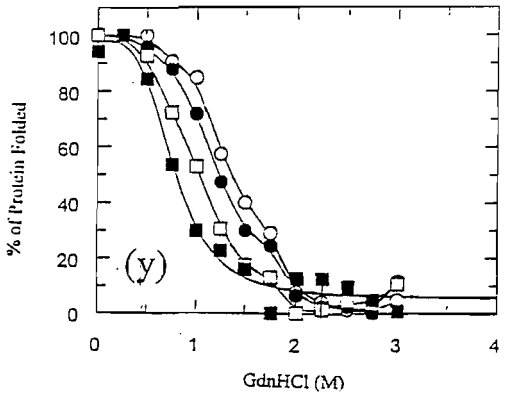
% of Protein Folded
100
80
60
40
20
0
(y)
0
1
2
3
4
GdnHCl (M)

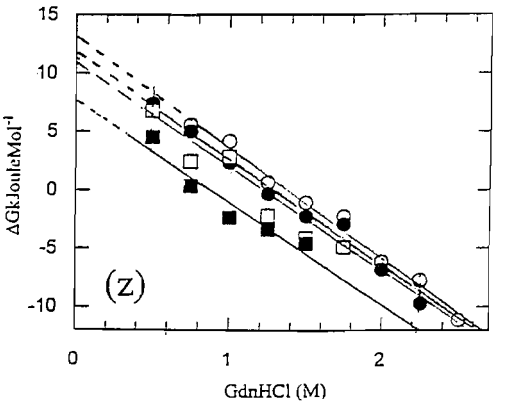
ΔGkJouleMol⁻¹
15
10
5
0
-5
-10
(z)
0
1
2
GdnHCl (M)

Table 4.3 Parameters for the unfolding of PpL and mutant PpL at 25°C . n= 3 unless otherwise stated

Protein	Midpoint conc (M)	ΔG°_{H2O} ± Std. Dev. kJ mol^{-1}. (from intercept)	ΔG°_{H2O} ± Std. Dev. kJ mol^{-1}. (calculated)	m kJ $mol^{-1}M^{-1}$ (Slope)	m kJ $mol^{-1}M^{-1}$ (calculated)
PpL	2.37 ± 0.03	18.65± 0.77	17.84± 0.74	7.53± 0.31	7.87± 0.43
Y64W	2.42 ± 0.05	16.93± 1.08	18.57± 0.67	7.67± 0.28	7.00± 0.57
F39W	1.37 ± 0.03	13.09± 0.75	12.97± 1.73	9.45± 1.05	9.57± 0.76
K33W	2.14 ± 0.15	13.29± 0.56	12.01± 2.95	5.61± 0.26	6.21± 1.08
N26,76D	1.79 ± 0.03	10.67± 0.38	9.98± 0.56	5.57± 0.22	5.97± 0.31
H74C *(n = 1)	2.06	15.27	14.99	7.28	7.41
N26,76D,F39W	0.85 ± 0.03	8.97± 0.57	7.87± 1.09	9.26± 1.26	10.55± 1.08
F39H,Y64W *(n = 2)	1.43 ± 0.04	11.15± 0.56	11.48± 0.83	8.02± 0.34	7.82± 0.63
Y53H,F39W *(n = 2)	1.02 ± 0.02	4.17± 0.49	6.02± 0.51	5.91± 0.37	4.25± 0.41

The ΔG°_{H2O} values quoted above are positive reflecting the difference in free energy in water of the unfolded state relative to the folded state due to the direction that the reaction is analysed i.e. F to U. The conformational stability (ΔG°_{H2O}) of the folded state relative to the unfolded state is the negative of the value quoted.

4.10 Unfolding curves for Y64W and F39W mutants at different temperatures

Unfolding curves for both Y64W and F39W were also produced as described above at a range of temperatures from 20-55°C in order to explore the effect of temperature on the folding / unfolding equilibrium of these two domains in the presence and absence of denaturant. The results are tabulated in Tables 4.4 - 4.5. As might be expected, the data show a marked decrease in both the concentration of denaturant at the midpoint of the transition and ΔG°_{H2O} for Y64W and F39W as temperature increases. The concentration of GdnHCl that promoted 50% unfolding decreases from 2.4M to 1.64M for Y64W as the temperature was increased from 20°C to 55°C and those for the F39W mutant from 1.49M to 0.76M for the same temperature range. It is noticeable that in both cases the value of m remains reasonably constant and therefore the decrease in ΔG°_{H2O} for each protein is largely solely due to the shift in concentration of the denaturant that causes 50% unfolding. WT was not included in this study as the small difference in fluorescence intensity between the folded and unfolded forms followed using Tyr fluorescence provided less accurate data, particularly at the higher temperatures. The data for F39W at 55°C should also be treated with caution as it is possible that some unfolding takes place even at 0M GdnHCl due to this mutant's reduced stability.

Table 4.4 Parameters for the unfolding of Y64W at 20 °C - 55°C The buffer conditions were as described in Methods (n = 1)

Temperature °C	Midpoint conc. (M)	ΔG°_{H2O} kJmol^{-1}	m kJmol^{-1}M^{-1}
20	2.40	18.10	7.54
25	2.42	20.53	8.48
30	2.50	18.02	7.21
35	2.33	15.88	6.80
40	2.20	15.93	7.22
45	2.11	13.06	6.18
50	1.88	12.16	6.44
55	1.64	11.53	7.04

Table 4.5 Parameters for the unfolding of F39W at 20 - 55°C
The buffer conditions were as described in Methods (n = 1)

Temperature °C	Midpoint conc. GdnHCl (M)	ΔG°_{H2O} kJmol^{-1}	m kJmol^{-1}M^{-1}
20	1.49	13.09	8.78
25	1.37	13.11	9.56
30	1.38	11.82	8.36
35	1.21	12.27	10.11
40	1.14	11.41	10.01
45	0.98	10.79	10.95
50	0.78	8.14	10.41
55	0.76	7.7	10.14

4.11 Van't Hoff plots using the data given in Tables 4.4 and 4.5.

The equilibrium constants for the unfolding reactions given above were plotted against 1/T K (Fig 4.4) in order to determine the contribution that changes in enthalpy (ΔH°) and entropy (ΔS°) make to the energetics of the unfolding reaction.

The fitted line has a slope which is equivalent to $-\Delta H^{\circ}/R$ and the intercept on the y axis gives $\Delta S^{\circ}/R$. From these the standard enthalpy change of the reactions (ΔH°) can be calculated as 53.51 kJmol^{-1} for F39W and 91.4 kJmol^{-1} for Y64W and the standard entropy change of the reactions (ΔS°) calculated as 0.14 kJ.mol^{-1}.deg for F39W and 0.24 kJ.mol^{-1}.deg for Y64W. The fact that the plot appears linear suggests that (ΔH°) and (ΔS°) are independent of temperature over this range. The positive value for ΔH° indicates an endothermic reaction expected for an unfolding reaction if the folded protein has the lower free energy. The free energy change at 25°C was calculated from the equation $\Delta G = \Delta H - T\Delta S$ and is in agreement with estimates derived from the equilibrium unfolding experiments above and confirms that the conformational energy of the F39W PpL is approximately only 69% of that of Y64W PpL (see Table 4.6).

Figure 4.4 Van't Hoff plots for Y64W and F39W PpL.

From $y = mx + c$

Slope (c) $= \frac{-\Delta H^{o}}{R}$

Intercept on the y-axis $= \frac{\Delta S^{o}}{R}$

For F39W (data plotted from Table 4.5)

$y = -6548.7x + 16.762$

$R^2 = 0.8685$

For Y64W (data plotted from Table 4.4)

$y = -10957x + 29.228$

$R^2 = 0.9066$

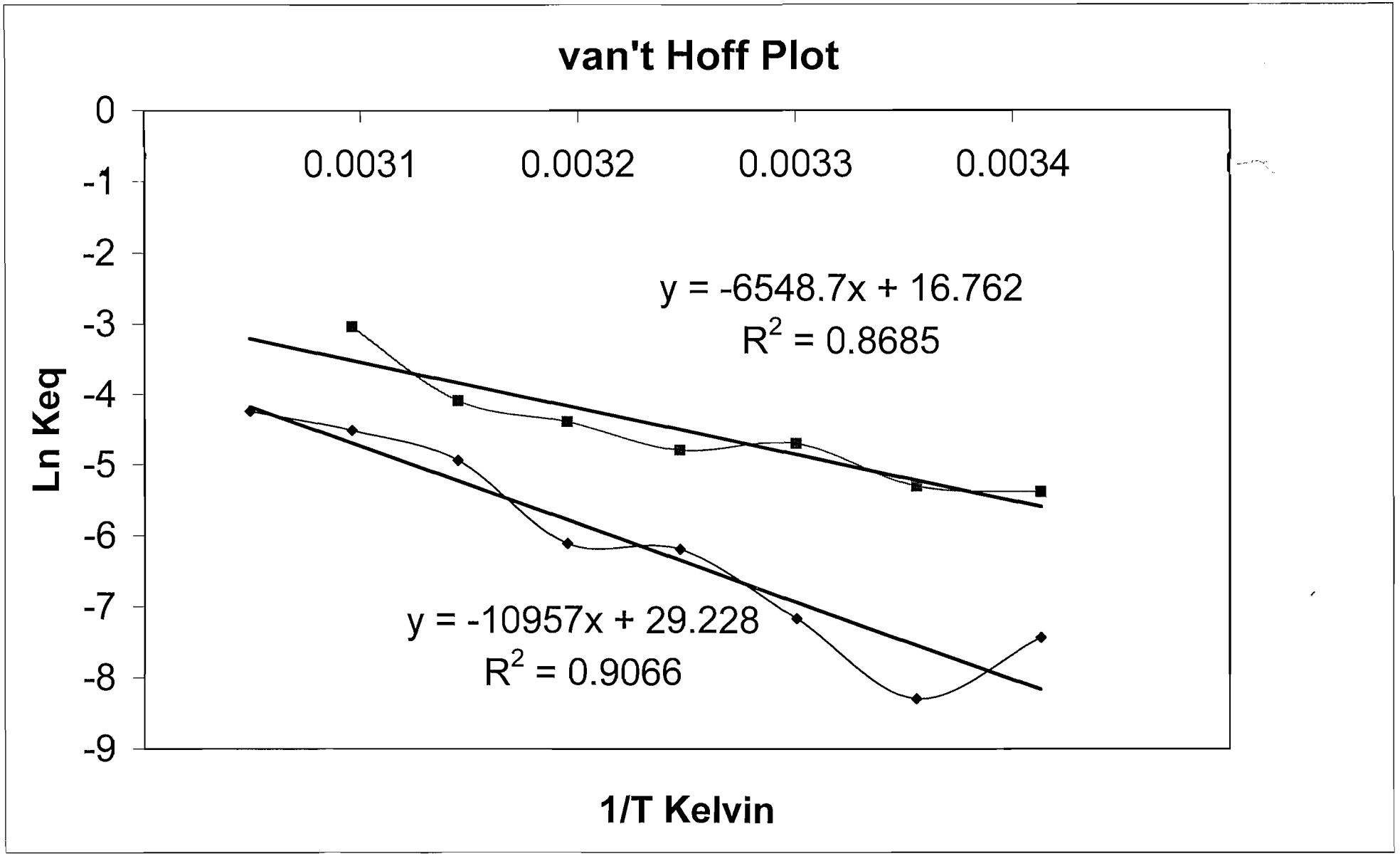
van't Hoff Plot
0
-1
-2
-3
-4
-5
-6
-7
-8
-9
0.0031
0.0032
0.0033
0.0034
Ln Keq
y = -6548.7x + 16.762
R2 = 0.8685
y = -10957x + 29.228
R2 = 0.9066
1/T Kelvin

Table 4.6 Values of ΔG^{o}, ΔH^{o} and ΔS^{o} calculated from the van't Hoff plot

Protein	ΔG^{o} kJmol^{-1}	ΔH^{o} kJmol^{-1}	ΔS^{o} kJmol^{-1}deg .
F39W PpL	12.99	54.42	0.14
Y64W PpL	19.53	91.05	0.24

4.12 Circular Dichroism spectropolarimetry

It has been reported that proteins do not always completely unfold in GdnHCl, some structures may still be present even at high GdnHCl concentrations due to clustering of hydrophobic residues (Krauss, 1996). It is possible therefore that fluorescence spectroscopy may not detect the presence of such clusters and therefore the change in fluorescence may end even when some order is present in the protein fold. Therefore, in addition to using fluorimetry to measure unfolding, it is always advisable to use a second technique such as far-UV CD to create an unfolding curve. Far-UV CD offers the advantage that it reflects the folding of the peptide backbone (secondary structures of the protein) rather than reflect the tertiary structural packing that is primarily reported by fluorimetry.

Circular dichroism occurs when a molecule has both optical activity and light absorption properties at the same wavelength. The absorption properties of a protein fall into two separate regions. In the near UV region (260-300nm) proteins absorb light due to their aromatic residues- Phe, Tyr and Trp which are normally located in the hydrophobic core of a protein and are locked at defined angles relative to each other by the packing of the neighbouring side-chains.
In the far UV at wavelengths at around 220nm, light is absorbed by the peptide bonds that occur throughout the peptide chain. All of the residues in a protein, except glycine, have a chiral α-carbon atom, and more importantly, the peptide chain folds to generate gross molecular asymmetry both of which give rise to optical activity.

Figure 4.5 Typical CD spectra showing α-helix, β-sheet and random coil structures of homopolylysine (Freifelder, 1982).

The figure shows a CD spectrum between 190 and 250nm due to 100% α-helix (solid line), 100% β-sheet (small dashes) or 100% random coil (long / short dashes).

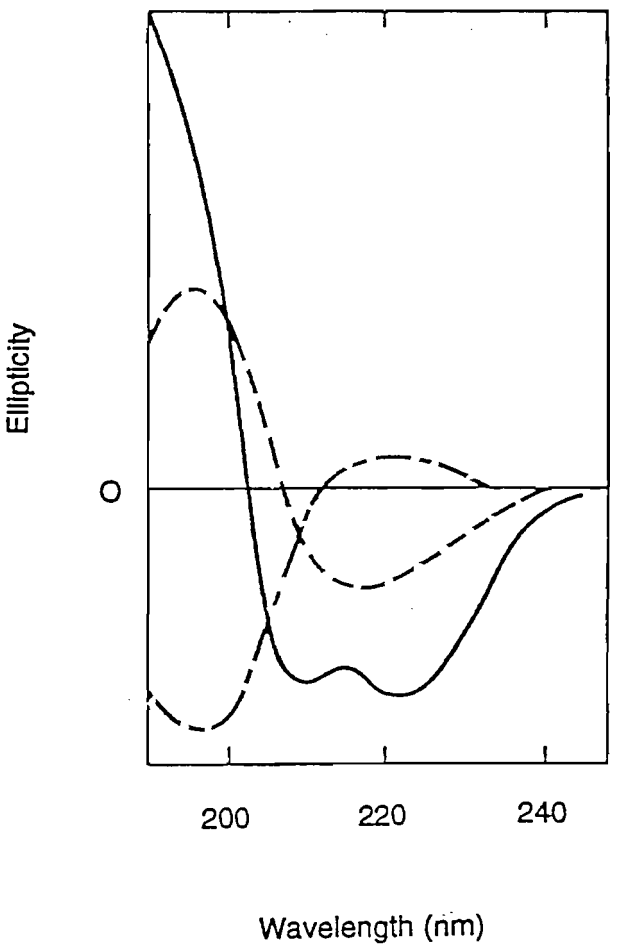
Ellipticity
0
200
220
240
Wavelength (nm)

Thus proteins have the necessary properties to generate CD spectra between 180nm and 250nm (mainly contributions from the peptide bonds) and 250nm to 340nm (exclusively due to the aromatic side-chains and due to any cysteine or disulphide bridge contributions).

The CD from peptide bonds in α-helices is much more intense at 200 – 220nm than the CD generated by β-sheets (see Fig. 4.5). This figure shows the typical spectra given by poly-L-lysine in different secondary structures (Freifelder, 1982). CD spectra of proteins with high α-helical content normally have characteristic negative ellipticities at wavelengths between approximately 205nm and 250nm with distinct minima at 208nm and 222nm. Thus, observation of the CD properties of a protein at 222nm in the presence of increasing concentrations of denaturant gives a good indication of any unfolding that occurs in a protein containing α-helical motifs. Although PpL is predominantly composed of β-sheets it does have one α-helix that contributes approximately 25% of the secondary structure of the protein. Ellipticity at 222nm was measured as the proteins were unfolded since this wavelength has contributions from the α-helix and the β-sheet and was less affected by the absorbance of the denaturant used.

Each protein was scanned in the far UV region of the spectrum in buffer or in various concentrations of denaturant as described in Methods. As the unfolding occurred the resulting increase in ellipticity at 222nm was used to produce unfolding curves for each protein at 25°C.

Figure 4.6a shows the far UV CD spectrum of 10μM WT PpL in 1mm light path cells between 195 and 240nm (the spectra are each the accumulation of 5 scans corrected for contributions from buffer). There are negative ellipicities between 205 and 250nm with a minimum at 210nm and shoulder at 222nm although no clear second minimum is evident. This is almost certainly due to the negative ellipticity of β-sheet contributions at 210nm to 220nm from the four β-strands which would `smooth out` the double peak of the α-helical contribution.

Secondary structural prediction using the method of Yang *et al.*, (1986) which bases its calculations on comparison of the test protein with a library of spectra from homo-polypeptides in 100 % α-helical, 100% β-sheet / turn or 100% random coil structures suggests that the WT PpL has approximately 30% α-helix, 36% β-sheet and β-turn and 33% random coil (no clearly defined secondary structure). Similar studies (see Figs 4.6b To 4.6e) were carried out using the same conditions as above on the Y64W mutant, the F39W mutant, the N26,76D mutant and the N26,76D,F39W mutant, all of which (except Y64W) appear to be less stable than WT on the basis of experiments already described above . The data given in Table 4.7 show that apart from the F39W domain and the N26,76D,F39W mutant which both have lower conformational stabilities , the others all have reasonably similar secondary structure predictions as the WT PpL. The higher percentage of α-helix proposed for the N26,76D,F39W mutant may arise from contributions to the ellipticity in this region from the indole side-chain or may be an accurate reflection of a change in secondary structure in this mutant. However, the spectrum of F39W does not suggest a large change in the overall folding of the domain nor does the presence of W64 change the proposed content of the α-helix . The similarity of the structure of the latter to the WT PpL has recently been confirmed by X-ray crystallographic studies (Stura *et al.*, 2002). It seems probable that the multiple mutations in N26,76D,F39W result in some conformational rearrangement. The possibility of the presence of some unfolded protein due to the low conformational stability of this mutant cannot, however, be excluded.

In the spectra of the mutants, as in that of the WT PpL, the decrease in ellipticity at 215nm due to the α-helix is smoothed out by the increase in ellipticity in the β sheet contributions at the same wavelength. This causes the characteristic double minima of the α helix at 208nm and 222nm to be obscured.

Figure 4.6 Far UV CD spectra for PpL.

The figure shows the CD spectra for PpL and mutants of PpL between 195nm - 240nm.

(a) PpL
(b) Y64W
(c) F39W
(d) N26,76D
(e) N26,76D,F39W

The spectra were all collected using 10μM protein in 20mM phosphate buffer pH 8.0 in 1mm light path cells. The wavelength was scanned at 20nm / min with a response time of 4s. The spectra shown are the accumulation of 5 separate scans.

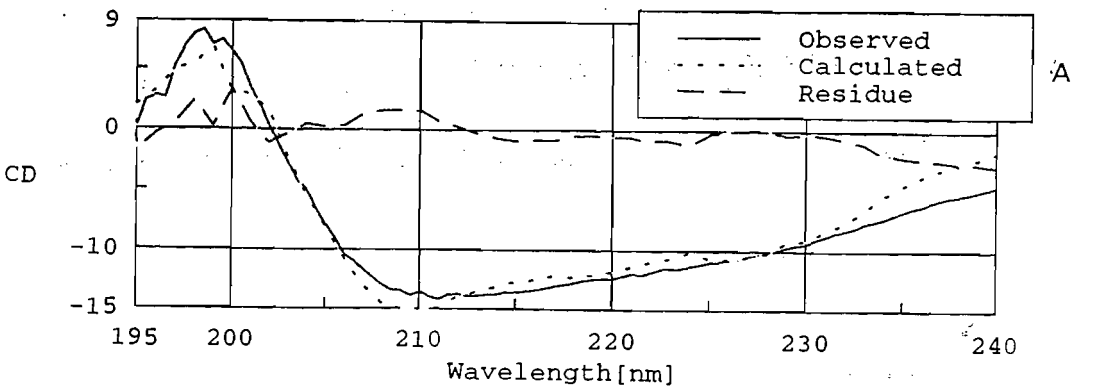
9
0
-10
-15
CD
195
200
210
220
230
240
Wavelength[nm]
Observed
Calculated
Residue
A

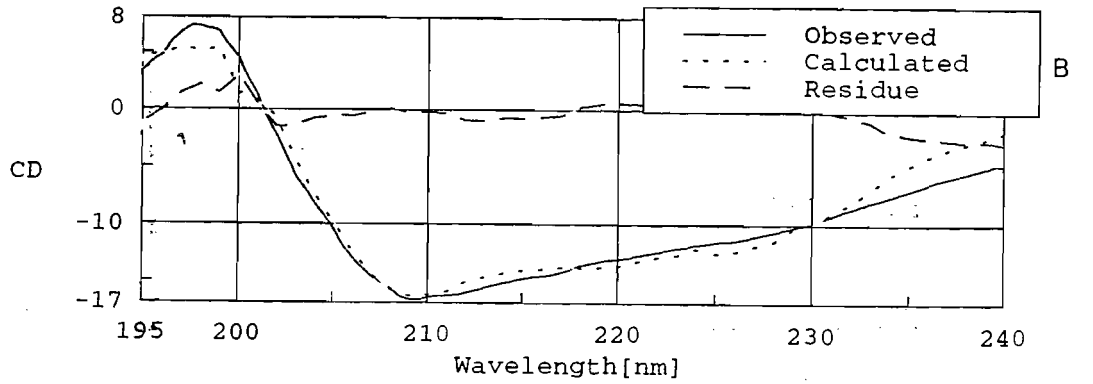
8
0
-10
-17
CD
195
200
210
220
230
240
Wavelength[nm]
Observed
Calculated
Residue
B

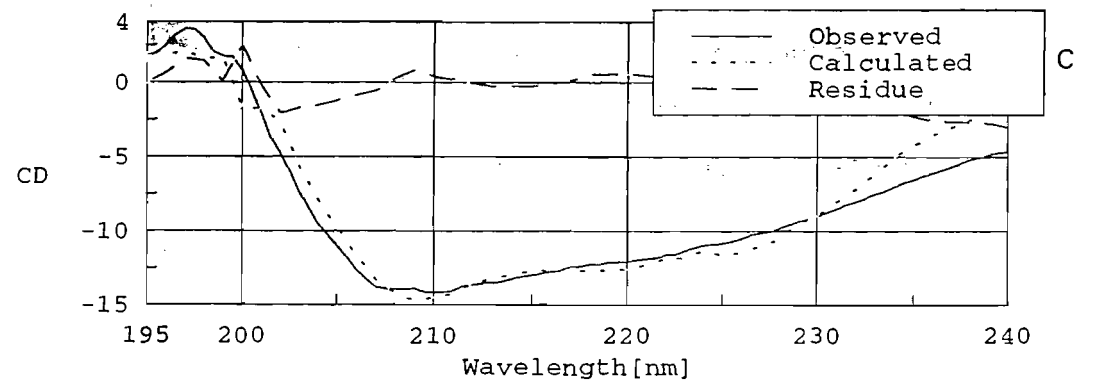
4
0
-5
-10
-15
CD
195
200
210
220
230
240
Wavelength[nm]
Observed
Calculated
Residue
C

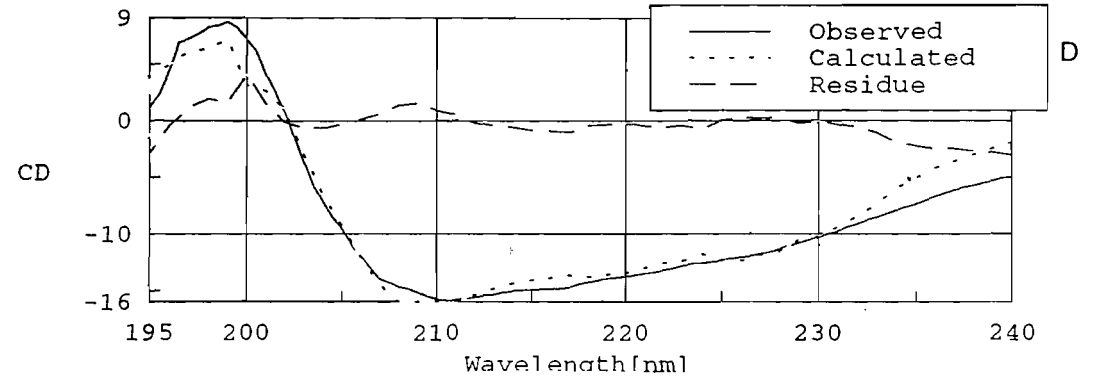
9
0
-10
-16
CD
195
200
210
220
230
240
Observed
Calculated
Residue
D

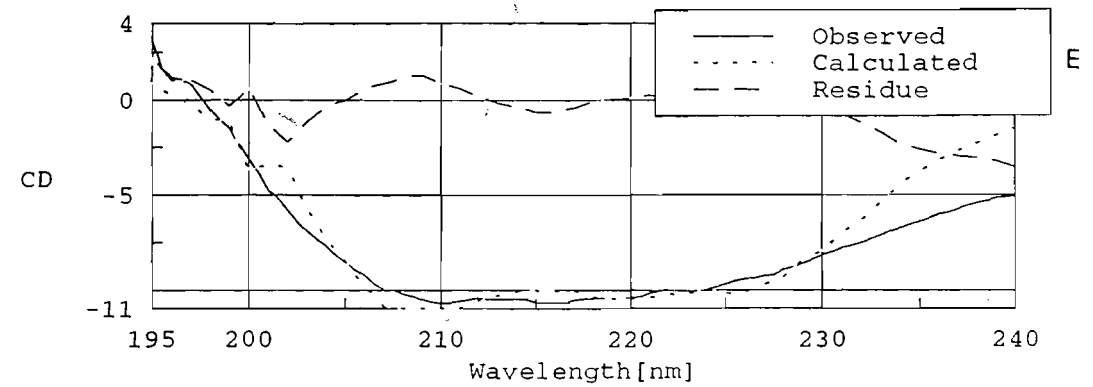
4
0
-5
-11
CD
195
200
210
220
230
240
Wavelength[nm]
Observed
Calculated
Residue
E

Figure 4.7 Unfolding of PpL determined by circular dichroism.

The unfolding curves were produced by adding 10μM protein to various concentrations of GdnHCl at pH 8.0 and 25°C and measuring the loss of secondary structure by CD spectroscopy at 222nm. Experimental conditions are described in Chapter 2.

(a) Shows the unfolding curve for WT PpL and (b) the conformational stability derived from (a).

(c) Shows the unfolding curve for Y64W and (d) the conformational stability derived from (c).

(e) Shows the unfolding curve for F39W and (d) the conformational stability derived from (f).

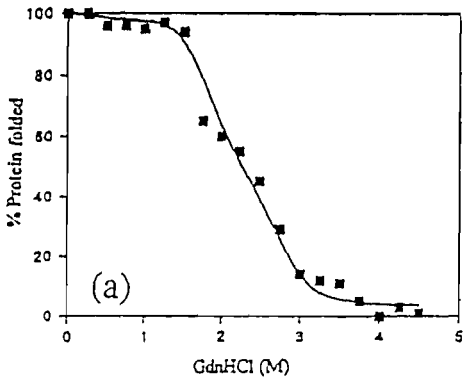
% Protein folded
100
80
60
40
20
0
(a)
0
1
2
3
4
5
GdnHCl (M)

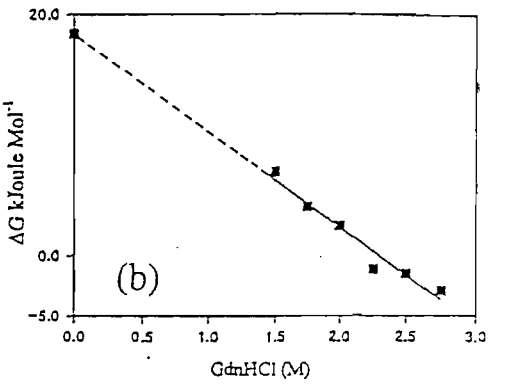
ΔG kJoule Mol-1
20.0
0.0
-5.0
(b)
0.0
0.5
1.0
1.5
2.0
2.5
3.0
GdnHCl (M)

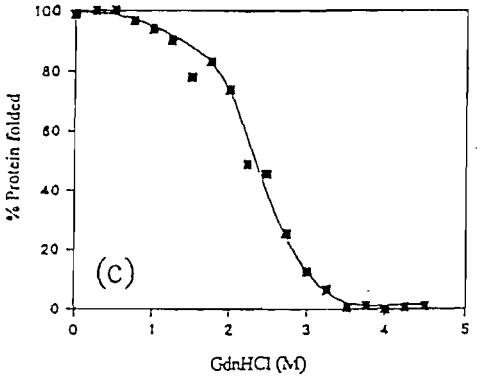
% Protein folded
100
80
60
40
20
0
(c)
0
1
2
3
4
5
GdnHCl (M)

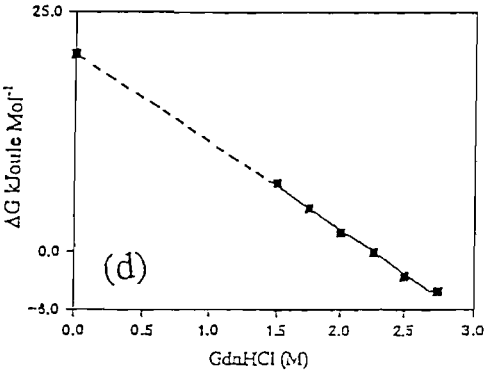
ΔG kJoule Mol-1
25.0
0.0
-5.0
(d)
0.0
0.5
1.0
1.5
2.0
2.5
3.0
GdnHCl (M)

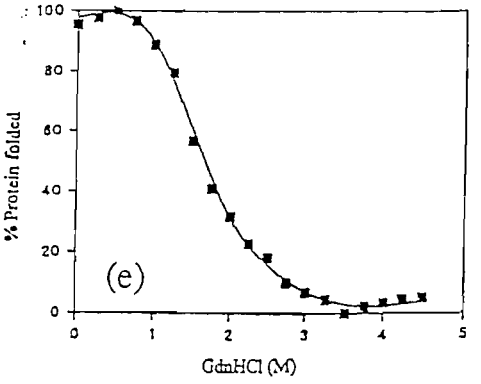
% Protein folded
100
80
60
40
20
0
(e)
0
1
2
3
4
5
GdnHCl (M)

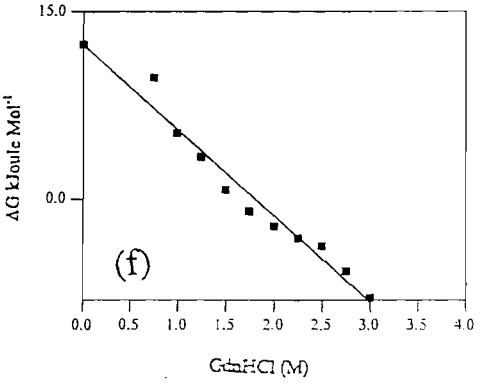
ΔG kJoule Mol-1
15.0
0.0
(f)
0.0
0.5
1.0
1.5
2.0
2.5
3.0
3.5
4.0
GdnHCl (M)

Table 4.7. The secondary structure prediction for PpL and mutants of PpL using the method of Yang *et al.*, (1986). The table also shows the molar ellipticity of each protein at 222nm

	WT PpL	F39W	Y64W	N26,76D	N26,76D, F39W
α-helix	30	26.7	29.4	31	28.1
β-sheet / β- turn	36	36.5	36.4	35.2	30.1
Random coil	33	36.7	34.3	36	41.7
θ_m 222nm deg.cm$^{2.}$ dmol^{-1}	1.27 x 10^6	1.30 x 10^6	1.50 x 10^6	1.44 x 10^6	0.98 x 10^6

The unfolding curves obtained using CD spectroscopy gave very similar values for ΔG°_{H2O} to those obtained by fluorescence spectroscopy for WT, Y64W and F39W PpL domains. For full results see Figures 4.7a-4.7f and Table 4.8.

Table 4.8 Parameters for the unfolding of PpL and PpL mutants at 25°C using CD spectropolarimetry.

Protein	Midpoint (M)	$\Delta G^{\circ}_{H2O} \pm$ Std. Dev. kJ Mol^{-1}	m kJ Mol^{-1}M^{-1}
PpL	2.30 ± 0.19	19.03 ± 0.52	8.27 ± 0.99
Y64W	2.41 ± 0.21	20.56 ± 0.58	8.53 ± 0.94
F39W	1.69 ± 0.23	12.32 ± 0.60	7.29 ± 1.56

4.13 Discussion

These studies show several interesting features about the structures and structural stability of PpL. The results suggest that the proteins studied here are all able to refold substantially and fit to a two-state model for the folding / refolding process. This is in agreement with Beckingham, (1997) and Scalley *et al.*, (1997) who showed near complete refolding for other variations of this domain.

Wild-type PpL, like the single domain from protein G (17.96 ± 0.37 $kJmol^{-1}$, S Harrison, 2003), has a very high conformational stability for a small protein that does not contain any disulphide bridges. The reason for the high stability is due to several structural features:

(a) A high degree of hydrogen bonding within the molecule, a compact structure giving a well-defined hydrophobic core which prevents water molecules from entering.

(b) A simple convex binding surface allowing a compact structure. Since only binding is required, no structural features such as mobile loops are required for enzymatic activity at the expense of stability.

(c) Finally, the structure of PpL has been shown to be fairly rigid by the NMR studies of Wikström *et al.*, 1996) making unfolding more difficult.

As can be seen from the results in Table 4.3, Y64W has a very similar, conformational stability to WT PpL. This result is supported by CD and NMR studies of Scalley *et al.*, (1997) who showed that a mutant with a Trp substitution (Y43W) in a domain from Protein L from *P. magnus* strain 312 (equivalent to Y64W in strain 3316 used in these studies) has a similar stability to the equivalent WT domain.

Modelling studies (Fig. 4.8a and 4.8b) show that the Tyr side-chain in this position can be replaced by the indole ring of Trp without any steric clash with neighbouring side-chains. Although Tyr has a low propensity for α-helices (0.61) unlike Trp (1.14) (Chou and Fasman, 1978) the presence of the latter clearly cannot disrupt the folding of PpL since both proteins have almost identical structures as determined by X-ray crystallographic studies (Graille *et al.*, 2001 and Stura *et al.*, 2002). The crystal structure of WT PpL shows that the hydroxyl hydrogen of Y64 is hydrogen bonded to the carboxyl group of D55 (Fig. 4.8a) thus stabilising the tertiary structure of the WT domain. Significantly, the indole ring of W64 cannot maintain this hydrogen bond but can instead form such a bond with the backbone carbonyl group of T65. For this to occur, however, some steric clashes occur between the Trp indole ring and residues I77 and K78 (Fig. 4.8b). It is possible that these latter residues may move slightly to accommodate the indole ring in this particular orientation. Ile77 is not a residue important for interactions with κ-chain although NMR studies show that the signal from K78 is perturbed on formation of a PpL.κ-chain complex (Wikström *et al.*, 1996) and therefore since both proteins have very similar affinities for κ-chain (see Chapter 5) it is improbable that K78 can move significantly. It is also possible, of course, that increased hydrophobic interactions between W64 and neighbouring residues may compensate for the loss of the hydrogen bond when Y64 is substituted.

The F39W mutation, however, does show markedly reduced conformational stability, although both side-chains have similar propensities for α-helices (Phe 1.12 and Trp 1.14 (Chou and Fasman, 1978), it appears that this residue (Figs. 4.8c and 4.8d) is important in maintaining the folded form of the protein. The side-chain of Trp is larger than that of Phe possibly causing a steric clash between the indole ring of the Trp with the side-chain of E49 as suggested by molecular modelling work. The mutation also causes a decrease in side-chain hydrophobicity (Kyte and Doolittle, 1982).

The increase in fluorescence of W39 on unfolding may be due to quenching of the Trp fluorescence by the proximity of the charged residues E38, E49 and K41 in

Figure 4.8 Molecular graphical representations of the regions in which substitutions have been made by site directed mutagenesis. The images were printed using the Swiss-PDB viewer, Geneva Biomedical Research Institute (http//www.exposy.ch/spdbv/mainpage/html).

(a) Y64
(b) Y64W
(c) F39
(d) F39W
(e) K33
(f) K33W
(g) Y53
(h) Y53H

Oxygen atoms are shown in red, nitrogen atoms are in blue and hydrogen bonds are shown in green. The figures illustrate the configuration around the itemised residue that has the predicted lowest free energy.

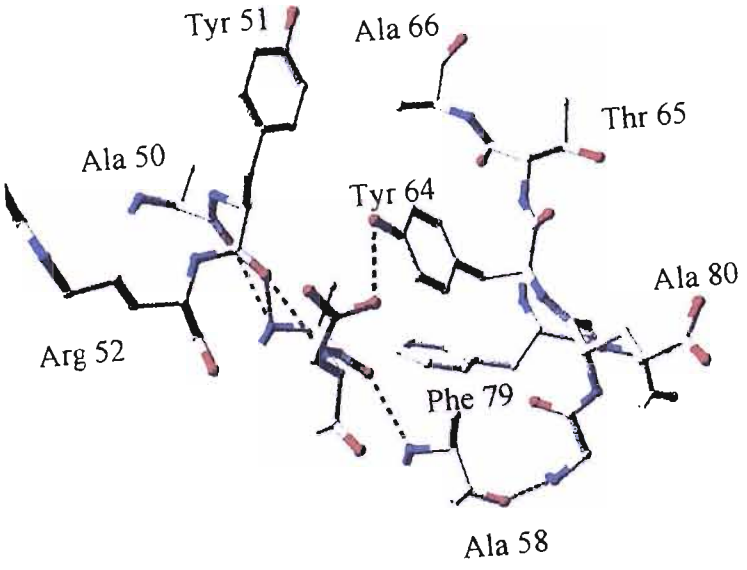
Tyr 51
Ala 66
Thr 65
Ala 50
Tyr 64
Ala 80
Arg 52
Phe 79
Ala 58

a

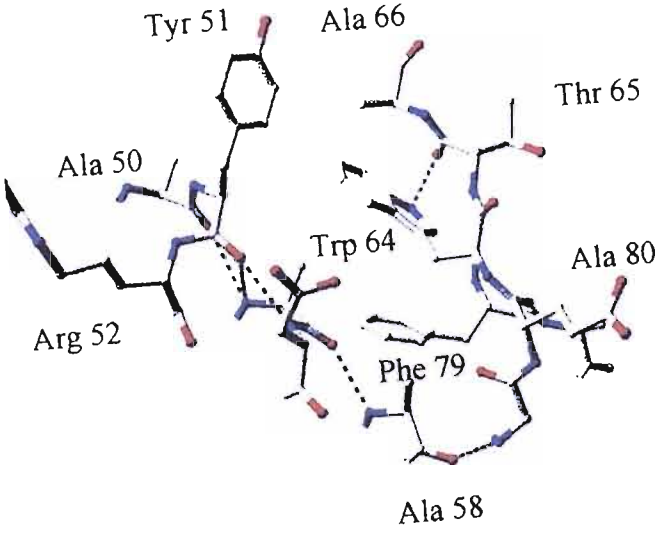
Tyr 51
Ala 66
Thr 65
Ala 50
Trp 64
Ala 80
Arg 52
Phe 79
Ala 58

b

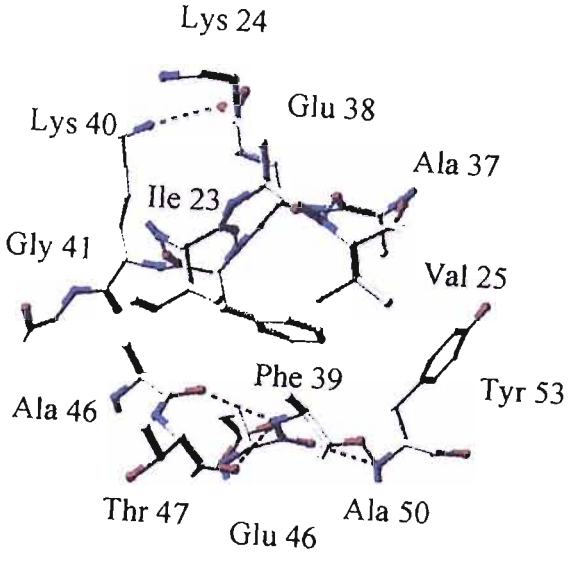
Lys 24
Lys 40
Glu 38
Ala 37
Ile 23
Gly 41
Val 25
Phe 39
Tyr 53
Ala 46
Thr 47
Glu 46
Ala 50

c

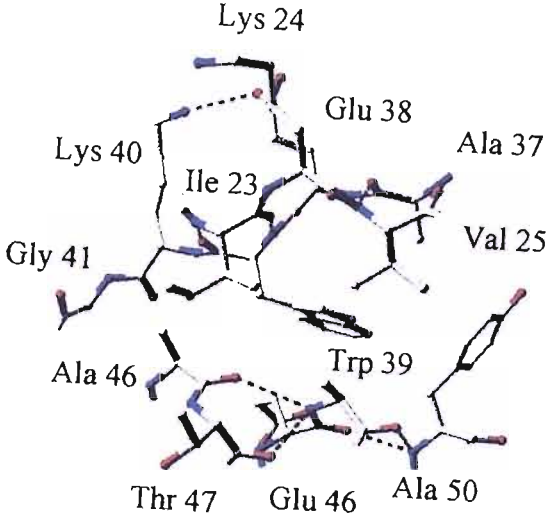
Lys 24
Glu 38
Lys 40
Ala 37
Ile 23
Val 25
Gly 41
Trp 39
Ala 46
Thr 47
Glu 46
Ala 50

d

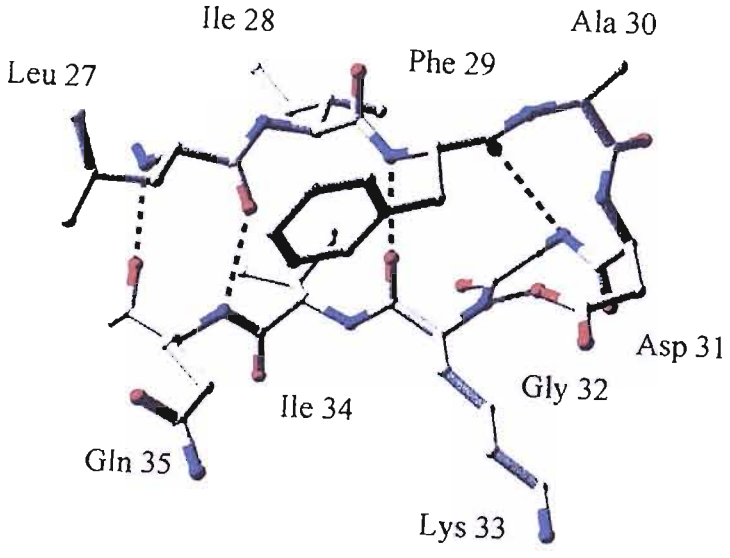
Ile 28
Ala 30
Leu 27
Phe 29
Asp 31
Gly 32
Ile 34
Gln 35
Lys 33

e

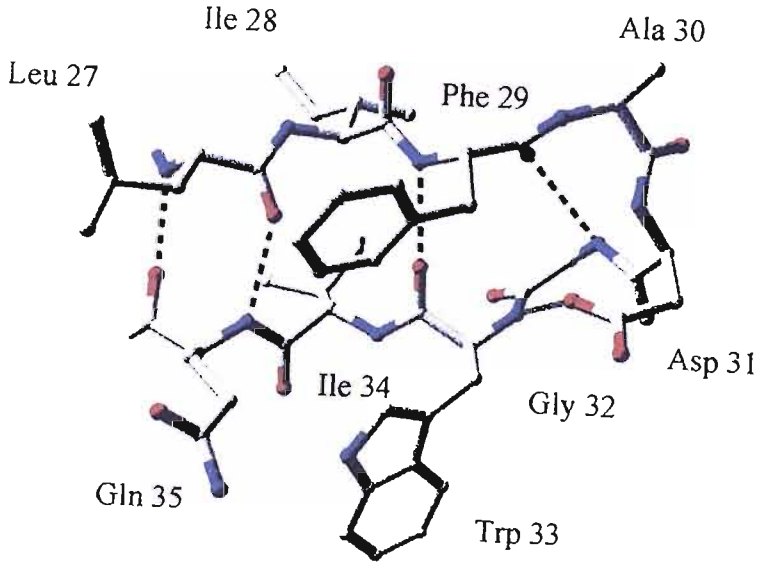
Ile 28
Ala 30
Leu 27
Phe 29
Asp 31
Ile 34
Gly 32
Gln 35
Trp 33

f

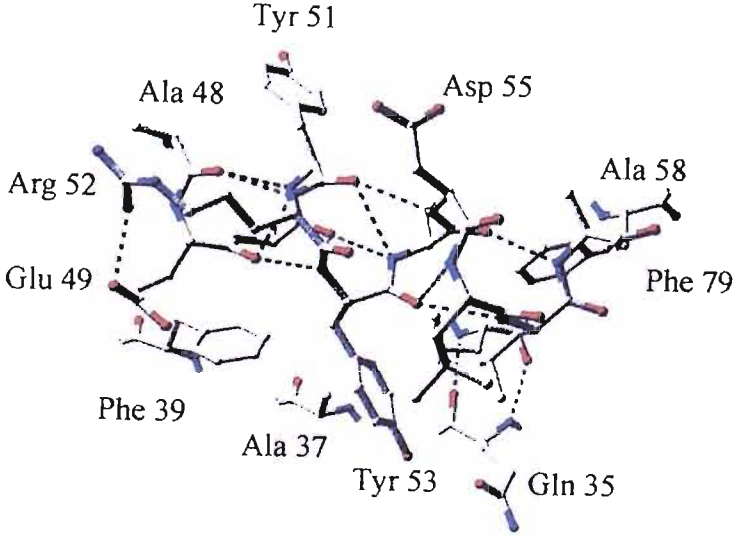
Tyr 51
Ala 48
Asp 55
Arg 52
Ala 58
Glu 49
Phe 79
Phe 39
Ala 37
Tyr 53
Gln 35

g

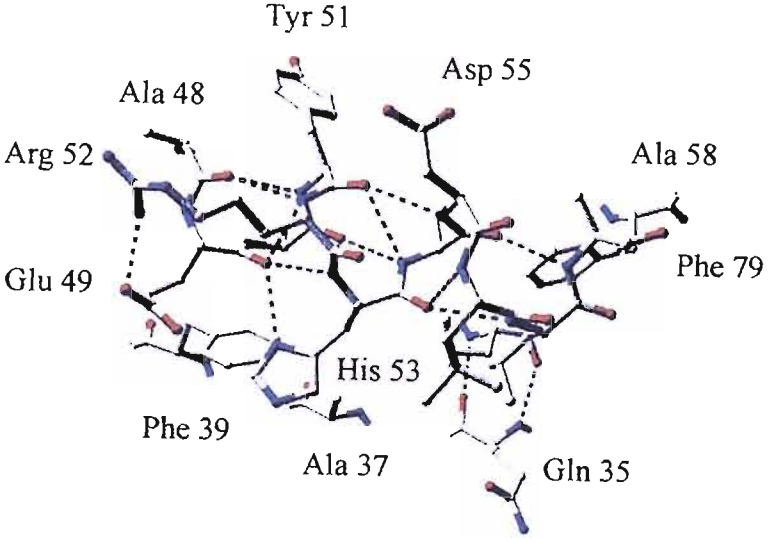
Tyr 51
Asp 55
Ala 48
Arg 52
Ala 58
Glu 49
Phe 79
His 53
Phe 39
Ala 37
Gln 35

h

the folded state of the protein. When the protein unfolds these interactions decrease, due to increased separation of the side-chains, and the resultant decrease in static quenching probably leads to an increase in fluorescence yield.

The K33W mutation involves a significant change of character from a positively charged, aliphatic side-chain to an uncharged aromatic side-chain on β-strand 2. The side-chain of K33 projects out into the solvent (see Fig. 4.8e) and is thus in a very hydrophilic environment. The change in distribution of charge and hydropathy may contribute to the reduction in conformational stability of this mutant by unfavourable interactions between the hydrophobic indole ring and the solvent. Significantly, the fluorescence emission spectrum of the folded form of this mutant shows that the Trp has a red wavelength emission maximum (around 342nm, see Fig. 4.1d) and has a low quantum yield, typical of the indole ring in an aqueous environment (see Fig.4.8f).

The double mutant N26,76D is of particular interest. The X-ray crystallographic data obtained in collaboration with Dr. Brian Sutton's group at King' College, London shows that WT PpL exists as a 'dimer' in the crystal form. The 'dimer' is stabilised by some hydrophobic interactions between I25 and I73 of each domain (see Fig. 1.11) and by four putative hydrogen bonds formed between N26 and N76 with carbonyl groups in the peptide backbone of the partner domain in the dimer. The double mutant was made in order to test whether the disruption of these putative hydrogen bonds would have any effect on the stability of the protein or on the interactions with κ-chain. (One possible reason for the biphasic reaction progress curves (see Chapter 6) is that 'dimeric' PpL forms an initial complex with κ-chain. The formation of this encounter complex may then cause the 'dimer' complex with κ-chain to dissociate and enable a higher affinity complex between a single domain of PpL and κ-chain to form. (see Chapter 1 and Chapter 6). It might be expected that the loss of stabilising, inter-subunit hydrogen bonds would be reflected by a decrease in overall conformational stability, as has been shown in previous studies on other proteins (Drewett, 1998).

The double mutant F39H,Y64W has a lower conformational stability (11.48 ± 0.8kJ mol^{-1}) than the F39W single mutant (12.97 ± 1.7 $kJmol^{-1}$) indicating that some further destabilisation has been caused by the F39H mutation. This may be due to the replacement of a hydrophobic aromatic ring by the polar imidazole ring. It is almost certainly not due to the Y64W replacement since all other studies here, and by others (Scalley *et al.*, 1997; Beckingham, 1997), have shown this mutation has no effect on protein stability.

The mutant Y53H,F39W has one of the lowest stabilities of all the mutants studied (6.02 ± 0.51 kJ mol^{-1}) despite the possibility of an extra hydrogen bond being formed between H53 and the backbone carbonyl group of R52 (see Figs. 4.8g and 4.8h). It is possible that for this bond to be made other parts of the protein may be destabilised. Beckingham, (1997) showed that the mutant Y53F had the same stability as Y53F,Y64W further indicating that F39W substitutions may make the stability of the domain more sensitive to second site mutations.

This conclusion is further supported by the results gained from experiments with the mutants N26,76D and N26,76D,F39W. The mutations N26,76D led to a net change in charge of –2 per PpL domain; two Asn residues replaced by two Asp residues per domain. The mutations do have an effect on the conformational stability of the protein, the conformational energy decreasing from 17.84 ± 0.7 $kJmol^{-1}$ (WT PpL) to 9.98 ± 0.56 $kJmol^{-1}$.

The further addition of the F39W mutation reduces stability to 7.87 ±1.09 $kJmol^{-1}$. This is similar to what would be expected for the additional mutation of F39W since the same replacement in the WT PpL leads to a decrease in conformational energy of 4.8 $kJmol^{-1}$. This infers that the three substitutions interact to disrupt the stability of this mutant with the F39W site being very significant.

The conformational stability of the H74C mutant when labelled by pyrene maleimide (14.99 $kJmol^{-1}$) is lower than that of the WT PpL (17.84 kJmol-1) but higher than those of some of the mutants examined e.g. K33W (12.01 $kJmol^{-1}$) N26,76D (9.98 $kJmol^{-1}$) or F39W (12.97 $kJmol^{-1}$). This suggests that the

hydrophobic pyrene group is tolerated as well as the smaller and more hydrophilic indole group in some positions. It is perhaps significant that the location of the thiol side-chain is on β-strand 4 pointing away from the centre of the domain into the solvent where no steric interactions take place.

The presence of a fluorimetrically-labelled cysteine is useful not only for experiments aimed at the probing of the stability of the domain, as a histological marker for cells expressing Ig on their surface or for the determination of binding parameters in the reaction with IgG but can also be used for immobilisation of PpL to an affinity matrix.

The CD spectra of these proteins suggests that they contain the same secondary structural elements with about 30% α-helical content, 36% β-sheet / β-turn and 30% unstructured contributions. The latter is higher than one would expect from the X-ray crystallography data but arises due to residues at the amino terminal end of the domain that are present to help improve expression and to provide sites for mutagenesis to improve immobilisation efficiency. This part of the protein is disordered in the crystal and is therefore not shown in the structures given in Chapter 1 (see Fig.1.11). The predicted α-helical content of WT PpL is 28.2% which is within reasonable agreement with the estimates derived from CD data. The structures of the mutant proteins are similar to that predicted for the WT PpL with the exception of the triple mutant N26,76D,F39W. This protein had a broad, shallow negative ellipticity between 195 and 240nm that suggests some changes in structure compared to the WT and other mutant domains. The lower molar ellipticity for this protein may be evidence of the presence of some unfolded protein further reflecting its lower stability.

Recent unfolding studies based on using single domain Protein L as a simple two state model have suggested that in 3M GdHCl, there is partial order to the first β hairpin (Scalley *et al.*, 1999). It appears from mutagenesis studies that this is the first part of secondary structure to form during folding which is not consistent with the idea that folding is driven by the formation of a hydrophobic core (Kuhlman *et al.*, 2002). Helix destabilising mutations were found to have little

effect on the rate of folding and in fact the helix is proposed to be unformed when the β-strands start to fold (Kim *et al.*, 1998). Similarly, in Protein G folding, one hairpin was partially ordered in the unfolded form, however, in Protein G it is the 2nd β hairpin which forms first (McCallister *et al.*, 2000). This folding information may allow the design of new Protein L conformations with new functions.

Thermal-denaturation studies carried out during this project and by Beckingham, (1997) have shown that the mutation F39W causes no change in affinity of the protein for κ-chain but does reduce the stability of the protein. The Tm for WT PpL being 72.4°C and that of F39W being 59.8°C. Significantly Y64W was found to have a Tm of 73.8°C almost identical to that of WT PpL supporting the stability results given above.

Chapter 5

Equilibrium binding studies.

CHAPTER 5

EQUILIBRIUM BINDING STUDIES

5. Introduction

The interaction of two proteins with each other such as the binding of the single Ig-binding domain (PpL) to a single κ-chain to form the PpL.κ-chain complex is a simple second order reaction; the two proteins binding stoichiometrically to form a complex. Such interactions are described by the following equation ;

$$\text{PpL} + \kappa \underset{k_{-1}}{\overset{k_1}{\rightleftharpoons}} \text{PpL}.\kappa$$

The dissociation constant at equilibrium (K_d) is given by the comparison of the concentrations of reactants and complex at equilibrium

$$K_d = \frac{[PpL][\kappa]}{[PpL.\kappa]}$$

The examination of the K_d of the complexes formed between variants of PpL and κ-chain by equilibrium methods gives valuable information about how the mutation has affected the reaction.

The experiments described in this chapter have therefore been carried out using techniques able to determine the K_ds at equilibrium for complexes formed between mutant PpL domains and κ-chain using the available biological activity and / or the physical and spectral properties of the proteins involved which vary according to the mutant being studied.

5.1 Fluorescence spectroscopy

As previously described (Chapter 4, section 4.2 and Table 4.1), the fluorescence properties of proteins are determined by the amino acid residues tryptophan, tyrosine and phenylalanine and the micro-environments in which these residues are located. The microenvironments can change greatly on binding to another protein, either due to conformational changes or merely the proximity of the 'partner protein' in a complex. Thus the spectral properties of the reporter groups can change and these can be used to determine the K_d of the complexes formed.

Fluorescence spectra of 3μM WT PpL, 3μM κ-chain and the WT PpL.κ-chain complex formed between them are shown in Fig 5.1a together with the mathematically summated spectra of WT PpL and κ-chain. Comparison of the spectra shows that there is approximately a 36% quench in fluorescence intensity at 302nm when the spectrum of the complex is compared to the summated spectra of WT PpL and κ-chain. From these fluorescence techniques alone it is not possible to determine which of the three tyrosine residues the signal change is due to, although from previous site-directed mutagenesis studies the fluorescence change has been attributed to Y53 (J. Beckingham, 1997).

κ-chains contain a single tryptophan residue which, in the native state, is highly quenched with an emission maximum of 335nm. However, on binding to the mutant Y53F PpL (lacking Tyr53) there is no change in emission intensity. Thus the only contribution to fluorescence changes on complex formation arises from Y53, if present, or tryptophan residues incorporated into mutant PpL.

The substitution of single tryptophans into the domain have been shown to dramatically increase the intensity of fluorescence at wavelengths around 320 – 360nm and facilitate fluorescence spectroscopic studies

Figure 5.1 Fluorescence spectra of PpL and κ-chain.

The fluorescence spectra of PpL mutants and κ-chain were studied by individually measuring spectra for 3μM PpL, 3μM κ-chain, premixed 3μM PpL.κ-chain complex and by adding the individual PpL and κ-chain spectra together.

Figure (a) shows the fluorescence spectra obtained for PpL (blue), κ-chain (yellow) and the PpL.κ-chain complex (red) when an excitation wavelength of 280nm is applied. It also shows the mathematical summation of the spectra of PpL and κ-chain spectra (green) to determine whether a signal change occurs on binding.

(b) Shows the fluorescence spectra for N26,76D (blue), κ-chain (yellow), the N26,76D.κ-chain complex (red) and the mathematical summation of the spectra of N26,76D and κ-chain (green).

(c) Shows the fluorescence spectra for Y53H,F39W (blue), κ-chain (yellow), the Y53H,F39W.κ-chain complex (green) and the mathematical summation of the spectra of Y53H,F39W and κ-chain (red).

(d) Shows the fluorescence spectra for N26,76D,F39W (blue), κ-chain (yellow), the N26,76D,F39W.κ-chain complex (red) and the mathematical summation of the spectra of N26,76D,F39W and κ-chain (green).

(a)

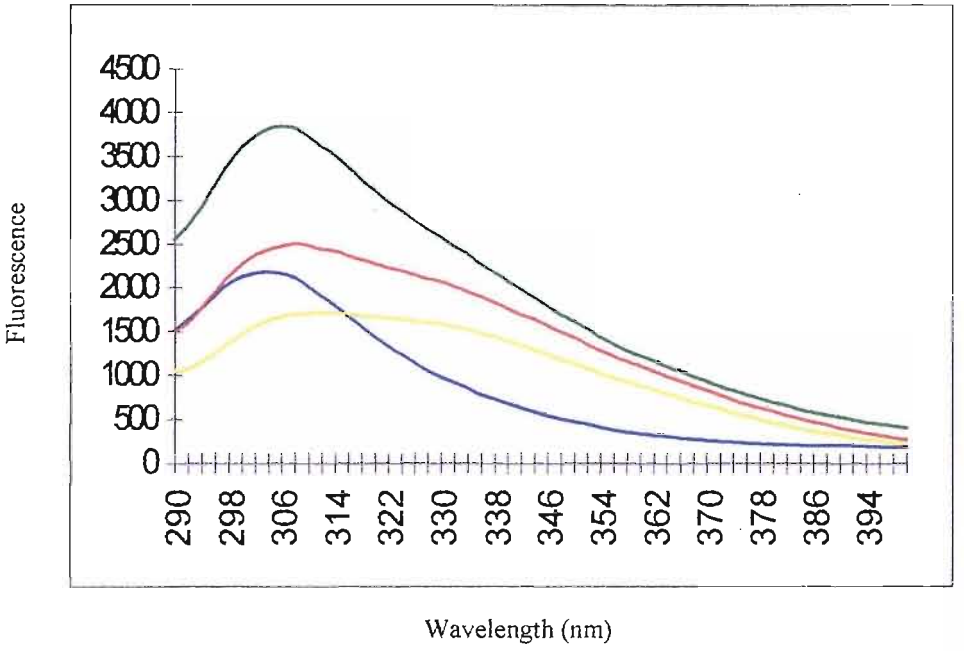
Fluorescence
4500
4000
3500
3000
2500
2000
1500
1000
500
0
290
298
306
314
322
330
338
346
354
362
370
378
386
394
Wavelength (nm)

(b)

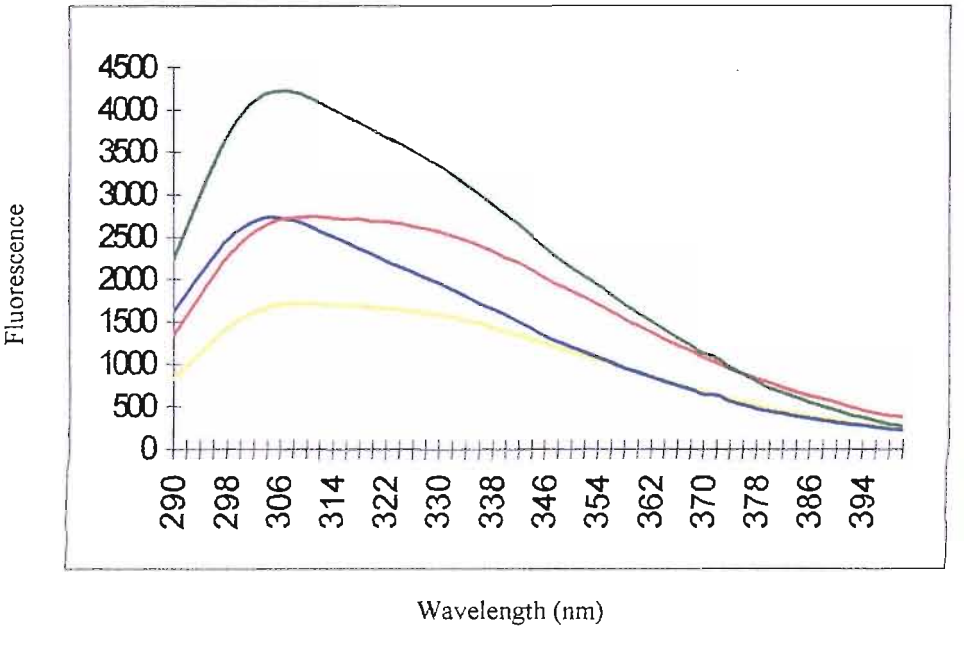
Fluorescence
4500
4000
3500
3000
2500
2000
1500
1000
500
0
290
298
306
314
322
330
338
346
354
362
370
378
386
394
Wavelength (nm)

(c)

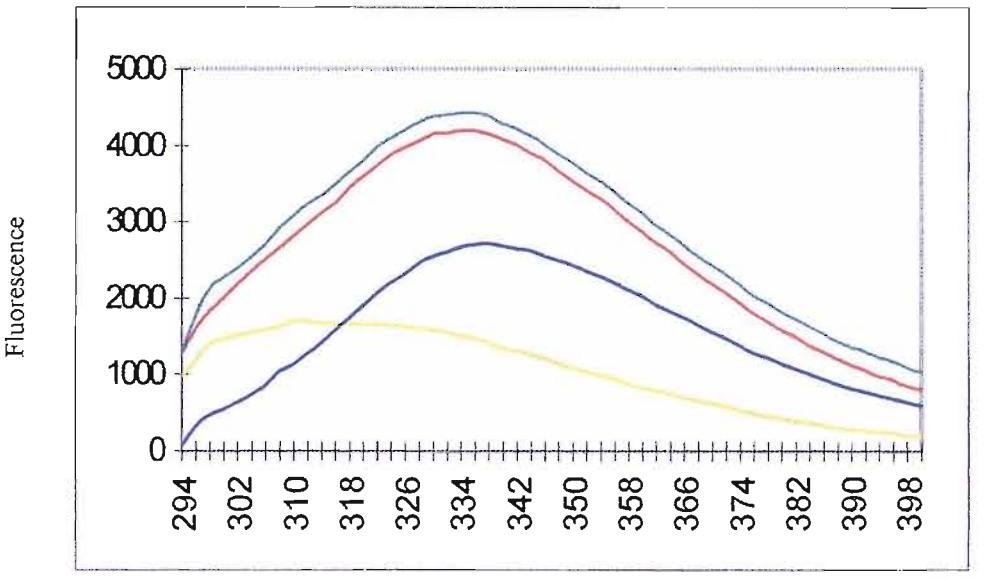
Fluorescence
5000
4000
3000
2000
1000
0
294
302
310
318
326
334
342
350
358
366
374
382
390
398
Wavelength (nm)

(d)

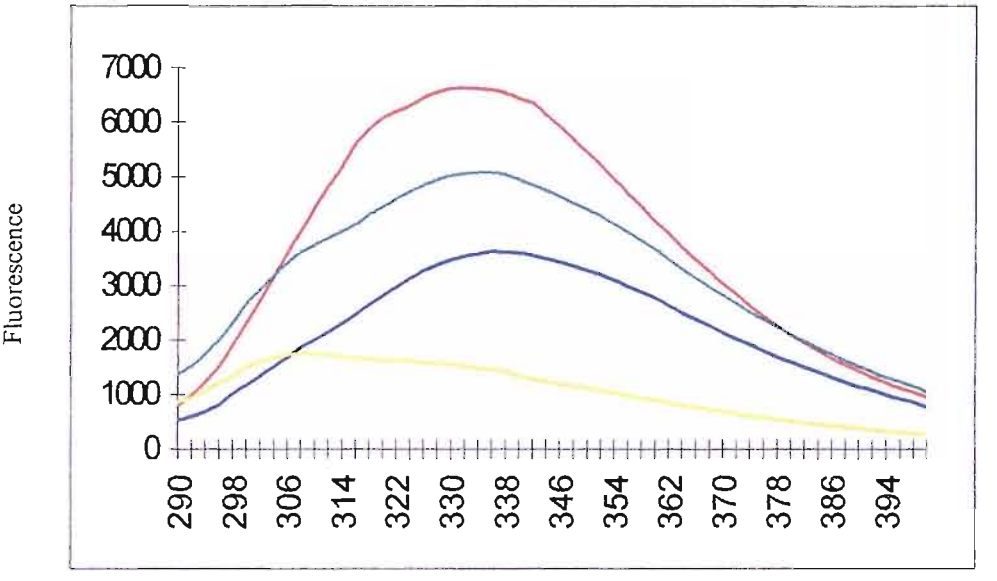
Fluorescence
7000
6000
5000
4000
3000
2000
1000
0
290
298
306
314
322
330
338
346
354
362
370
378
386
394
Wavelength (nm)

(Beckingham *et al.,* 1999). Therefore, in these studies most of the domains studied carry a unique tryptophan residue replacing Y64 or F39. It has been shown that only domains bearing F39W show a net increase in fluorescence intensity at 335nm when the domain interacts with κ-chain (Beckingham, 1997). An initial increase on forming the encounter complex with κ-chain is further increased for domains bearing F39W replacements during a proposed sequential structural change (see Chapter 6). Although the fluorescence of domains containing Y64 increase transiently when they bind to κ-chains to form initial encounter complexes, this increase is then lost and the overall fluorescence intensity is decreased by approximately 15% after the proposed post-binding structural change (Beckingham, 1997). Therefore, although the Y64W reporter group is useful for stopped flow studies, it cannot be easily used for equilibrium studies.

The N26,76D domain, like the WT PpL domain, was shown to lose approximately 36% of its fluorescence intensity at 302nm (Fig. 5.1b) due to the quenching of fluorescence arising from Y53 (as in the case of the WT PpL). This large signal change allowed fluorescence titration experiments of the domain into κ-chain to be carried out.

Figures 5.1c and 5.1d show similar spectra obtained for the Y53H,F39W and N26,76D,F39W domains, respectively, free in solution and in complexes with excess κ-chain. The spectra show that there is little change in fluorescence intensity at 335nm when the Y53H,F39W domain is mixed with κ-chain and a 30% increase for the N26,76D,F39W domain when bound to κ-chain. Some of these changes in fluorescence intensity are large enough signal changes to allow fluorescence titrations to be carried out on these proteins to determine the K_ds for their respective complexes with κ-chains. The change in fluorescence, however, also depends on the affinity of the mutant for κ-chain.
Although the mutant K33W was made to use this new position of a reporter group to allow fluorescence studies, in practice it was not

effective. Only a small change in fluorescence intensity was found to occur when mixed with κ-chains as was found with a mutant F29W (Beckingham, 1997) which has the substitution located on a similar part of the domain.

5.2 Fluorescence titrations

As can be seen from the fluorescence spectra shown above, a significant change in fluorescent intensity for some domains is observed on binding to κ-chains. Some of these differences are titratable and can be used to measure and derive the equilibrium K_ds of the complexes of these mutants with κ-chains.

The experiments were carried out using equipment and conditions as described in section 2.5.4, Chapter 2. The saturation curves for F39W, Y53H,F39W and N26,76D,F39W mutants and their analyses by the method of Stinson and Holbrook, (1973) are shown in Figs. 5.2a – 5.2f The K_d values obtained for the reactions are shown in Table 5.1. It can be noted that F39W mutation has little effect, relative to the WT PpL, on the stability of the complex with κ-chain, the K_ds being 0.13μM and 0.13μM respectively. Similarly, the mutation Y64W does not significantly alter the K_d (0.13μM) showing that these tryptophan residues are useful reporter groups to study the structure and function of the protein, in particular to study the effects of second mutations. Hence, the K_ds of the complexes formed between κ-chains and N26,76D,F39W (0.06μM) or Y53H,F39W (1.77μM) could be studied spectroscopically. Data taken from Beckingham, (1997) is included for comparison and to show the effects of the mutation Y53F,Y64W on the binding ability of this PpL domain. The K_d for the interaction between κ-chain and this mutant is 3.2μM, a slightly lower affinity than that given by Y53H,F39W, implying that the latter mutant retains more favourable binding contacts than the former.

Figure 5.2 Fluorescence titrations for PpL mutants.

Aliquots of a 15μM solution of F39W or N26,76D,F39W were titrated into 1.5ml of a 1.5μM solution of κ-chain and the fluorescence was measured at 340nm using an excitation wavelength of 280nm. For experiments using the Y53H,F39W mutant, aliquots were taken from a 150μM solution of the protein. The same solutions were titrated into buffer alone and the results of these titrations were deducted from those using κ-chain to construct the saturation curves shown. The saturation curves were analysed by the method of Stinson and Holbrook (1973).

(a) The saturation curve for F39W

(b) The analysis for (a) as in the method of Stinson and Holbrook (1973)

(c) The saturation curve for N26,76D,F39W

(d) The analysis for (c) as in the method of Stinson and Holbrook (1973)

(e) The saturation curve for Y53H,F39W

(f) The analysis for (e) as in the method of Stinson and Holbrook (1973)

(a)

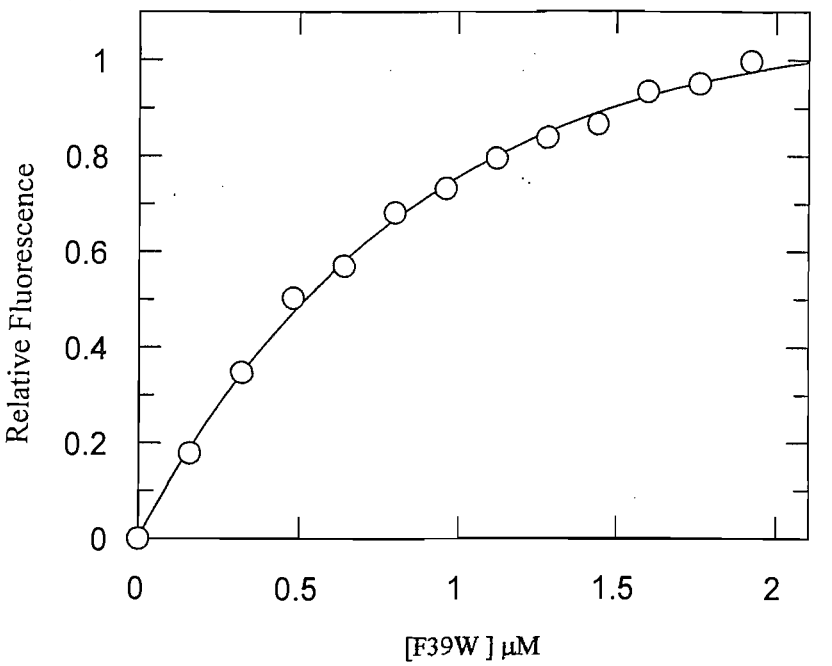
Relative Fluorescence
1
0.8
0.6
0.4
0.2
0
0
0.5
1
1.5
2
[F39W] μM

(b)

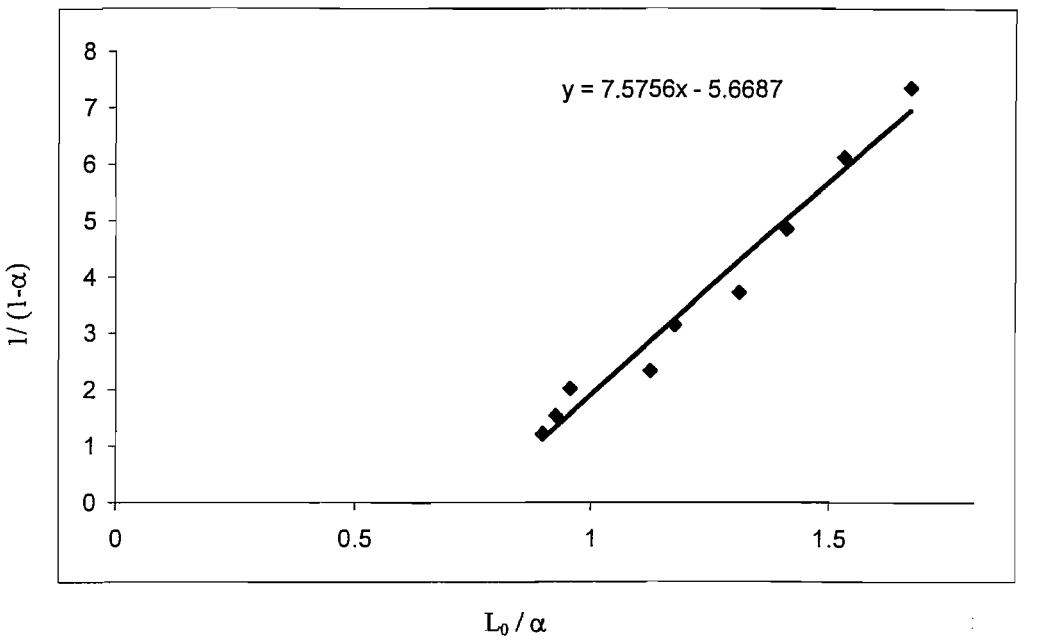
y = 7.5756x - 5.6687
1/ (1-α)
8
7
6
5
4
3
2
1
0
0
0.5
1
1.5
L0 / α

(c)

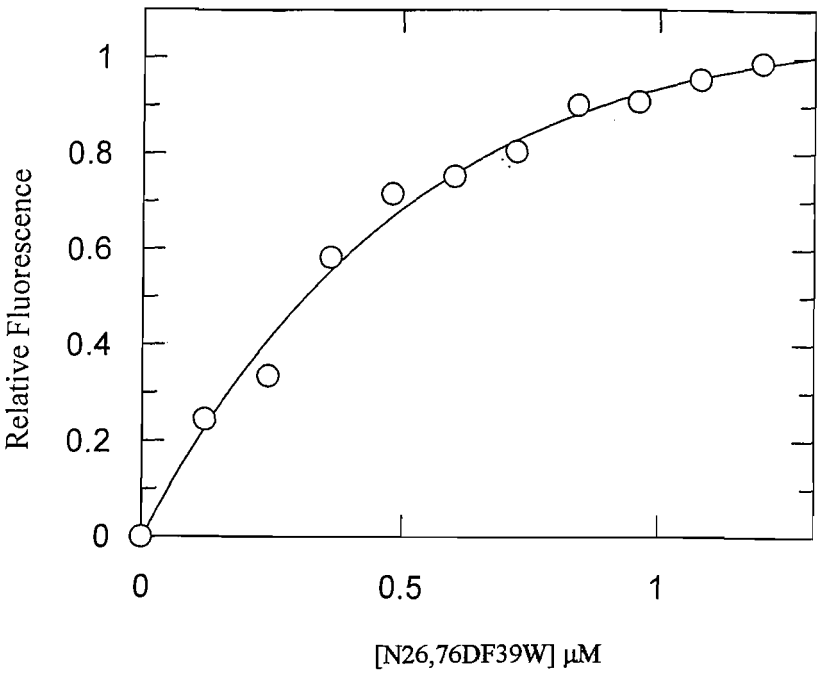
Relative Fluorescence
1
0.8
0.6
0.4
0.2
0
0
0.5
1
[N26,76DF39W] µM

(d)

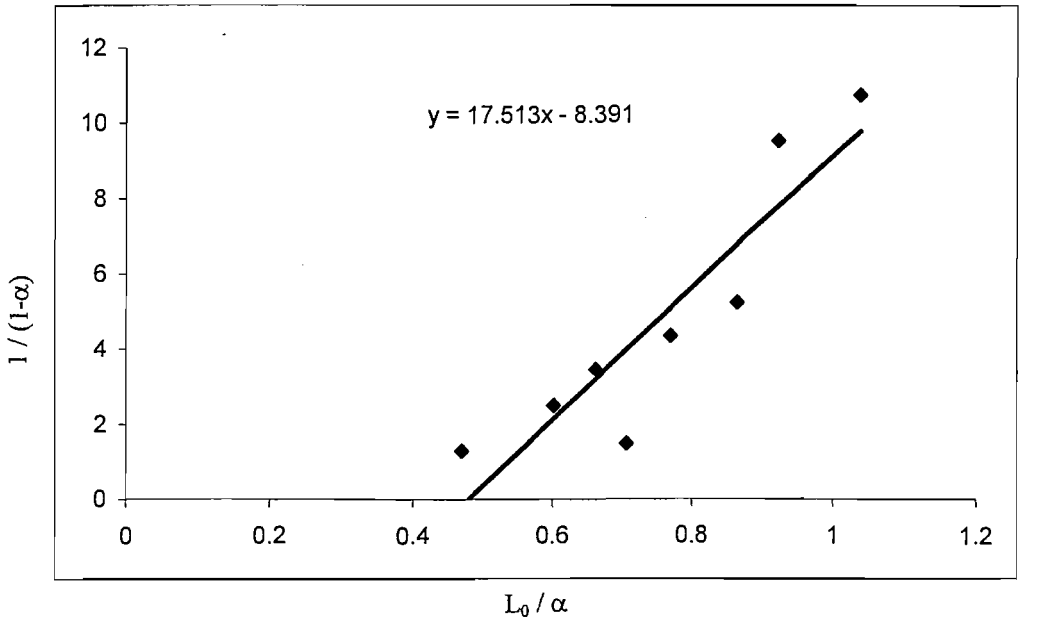
y = 17.513x - 8.391
1 / (1-α)
12
10
8
6
4
2
0
0
0.2
0.4
0.6
0.8
1
1.2
L0 / α

(e)

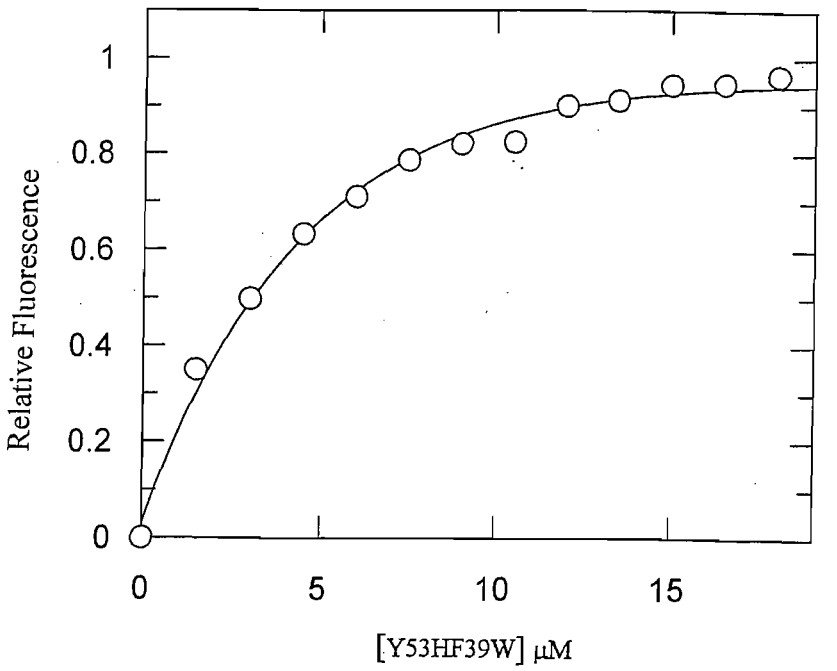
Relative Fluorescence
1
0.8
0.6
0.4
0.2
0
0
5
10
15
[Y53HF39W] μM

(f)

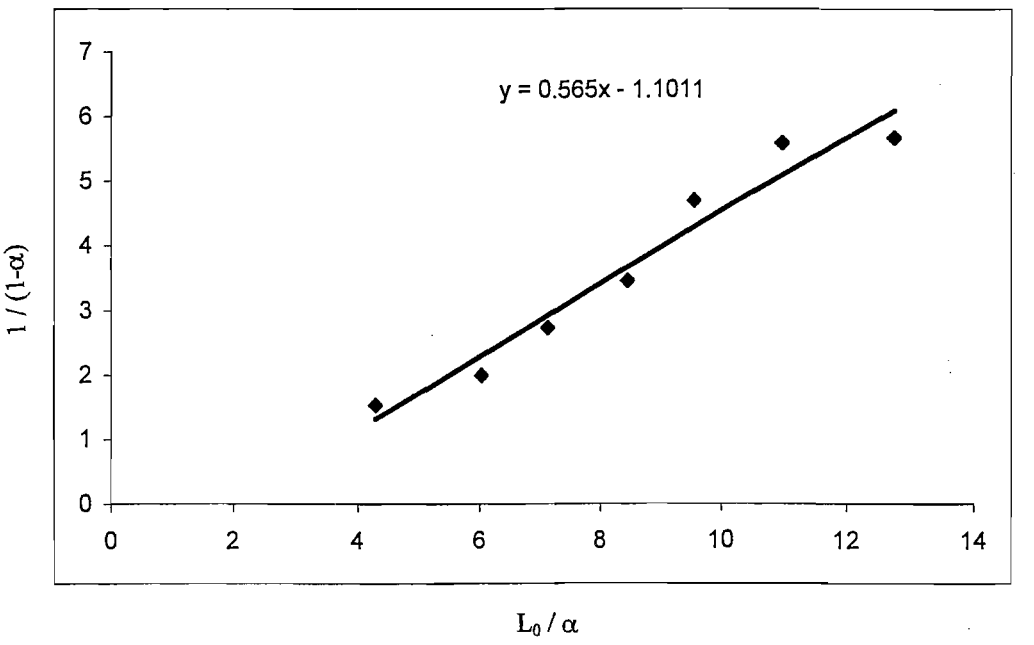
y = 0.565x - 1.1011
1 / (1-α)
7
6
5
4
3
2
1
0
0
2
4
6
8
10
12
14
L0 / α

Table 5.1 The Kd values for the complexes formed between various domains of PpL and κ-chain at pH 8.0 determined from fluorescence titrations or $^{+}$ELISA assays.

Mutant	K_d μM
Y53H,F39W	1.77 +/- 0.03
N26,76D,F39W	0.06 +/- 0.05
F39W	0.13 +/- 0.03
WT *	0.13 +/- 0.04
$^{+}$Y64W *	0.13 +/- 0.02
$^{+}$Y53F,Y64W *	3.2 +/- 0.15

* Taken from Beckingham, (1997)

5.3 ELISA (Enzyme Linked Immunosorbant Assay)

ELISAs have been the preferred method of detecting antibodies since their conception in the 1970s and make use of the bonds formed between antigen and antibody. In this case, the PpL – Ig interaction is non-antigenic in nature but still gives rise to a specific binding with a high affinity. PpL can be hydrophobically adsorbed onto the walls of the wells of a microtitre plate and after excess protein is washed off κ-chains or human IgG containing κ-chains can be added which bind to PpL. To effect a measurable colour change proportional to the amount of PpL in each well, a goat anti-κ-chain or anti-IgG-horse radish peroxidase conjugate is added to the well and binds to the PpL-Ig complex. The addition of substrates for the horse radish peroxidase leads to the development of a colour that can be quantified at 495nm. ELISA is therefore a suitable method for measuring the affinity of mutants of PpL that have no fluorescent reporter group or do not give a fluorescence signal change on binding to κ-chains or IgG containing κ-chains.

ELISA assays (for full details see section 2.5.8, Chapter 2) for K33W, F39H,Y64W, Y53H,F39W and N26,76D,F39W were carried out and in each case compared to the curves given by WT PpL which was also assayed on the same plate as the mutant under study to eliminate any differences in the level of coating between plates or reagent concentrations (see Fig. 5.3a - 5.3e). In addition, all were assessed for λ-chain and IgG-F_c binding by incubating with either λ or IgG-F_c and then using anti lambda or anti IgG-F_c HRP at the appropriate stages. However, there was no evidence that these bound to the PpL domains The results obtained with κ-chain are listed in Table 5.2.

Table 5.2. The K_d for the complexes formed between PpL and mutants of PpL with IgG containing κ-chain.

Protein	K_d ± Std. Dev. (μM) n=3
PpL	0.03 ± 0.02
K33W	0.03 ± 0.02
N26,76D	0.06 ± 0.03
N26,76D,F39W	0.13 ± 0.03
F39HY64W	0.27 ± 0.04
Y53HF39W	0.59 ± 0.06

WT PpL was found to have a K_d of 0.03 μM ± 0.02μM, in close agreement with the results of Beckingham, (1997), K33W was found to have a K_d similar to that of PpL (0.03 μM ± 0.02μM) as does N26,76D (0.06 ± 0.03 μM) and N26,76D,F39W (0.13 ± 0.03 μM). However, the table shows that the mutants F39H,Y64W (0.27μM ± 0.04 μM) and especially Y53H,F39W (0.59 ± 0.06 μM) were both shown to have substantially higher K_d values. Each of these mutants contain a histidine residue inserted into the binding region on PpL for κ-chains. These had been placed there to provide an ionisable sidechain with pKs at pHs close to neutrality so that ionisation / deionisation could be achieved by small

Figure 5.3 Standard ELISA plots for PpL and its mutants.

PpL samples were serially diluted across the plate from 0.2mg / ml and allowed to coat the wells before the excess was washed off and human IgG added. After the unbound IgG was washed off, binding was detected using a goat anti-human IgG-HRP conjugate which catalysed the oxidation of o-phenylenediamine to give a coloured product detected by its absorbance at 495nm. The plots shown are as follows ;

(a) PpL

(b) N26,76D

(c) K33W

(d) Y53H, F39W

(e) N26,76D,F39W

(f) F39H,Y64W

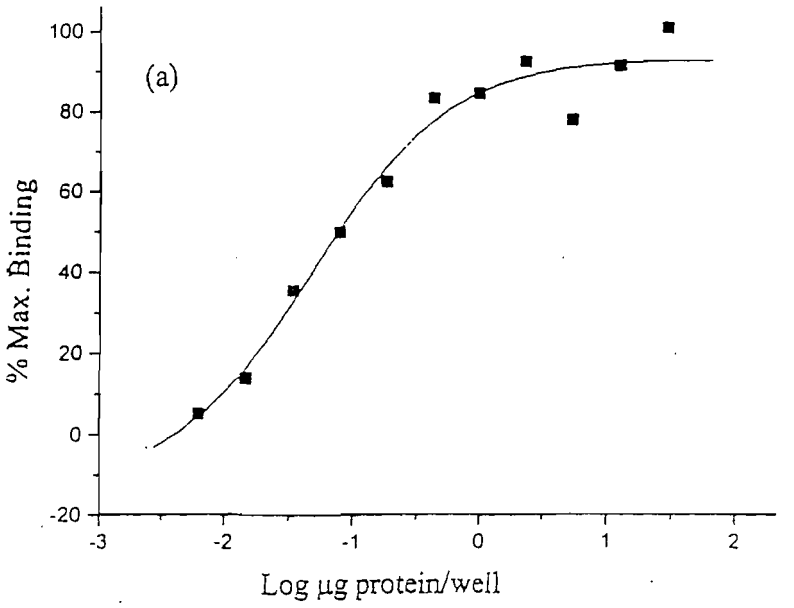
(a)
% Max. Binding
100
80
60
40
20
0
-20
-3
-2
-1
0
1
2
Log µg protein/well

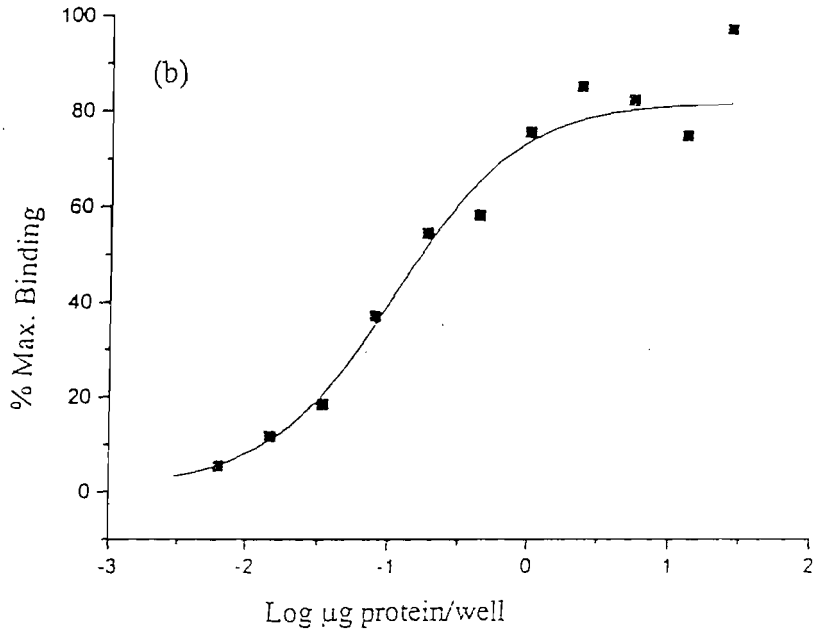
(b)
% Max. Binding
100
80
60
40
20
0
-3
-2
-1
0
1
2
Log µg protein/well

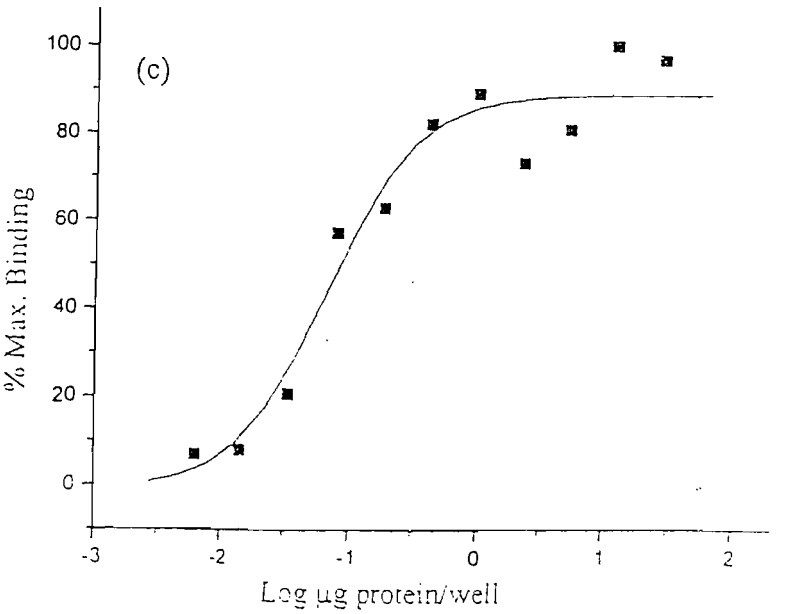
(c)
% Max. Binding
100
80
60
40
20
0
-3
-2
-1
0
1
2
Log µg protein/well

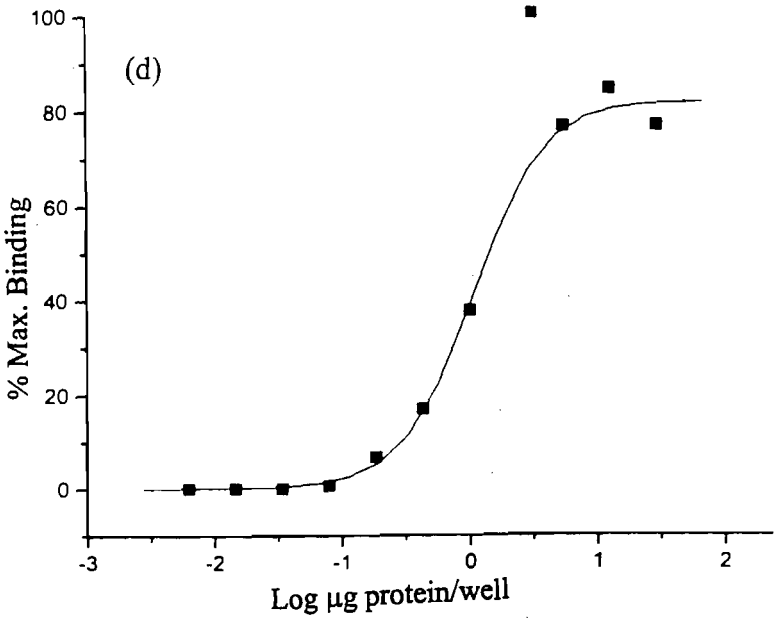
(d)
% Max. Binding
100
80
60
40
20
0
-3
-2
-1
0
1
2
Log µg protein/well

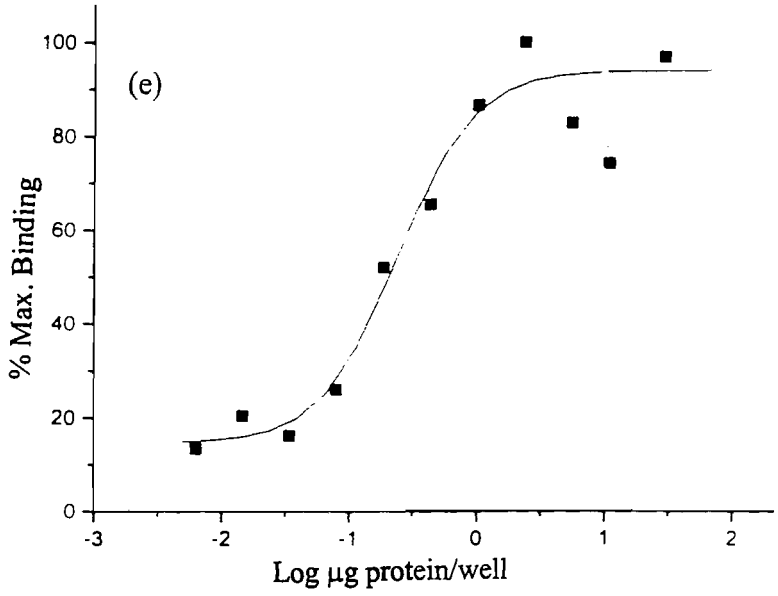
(e)
% Max. Binding
100
80
60
40
20
0
-3
-2
-1
0
1
2
Log µg protein/well

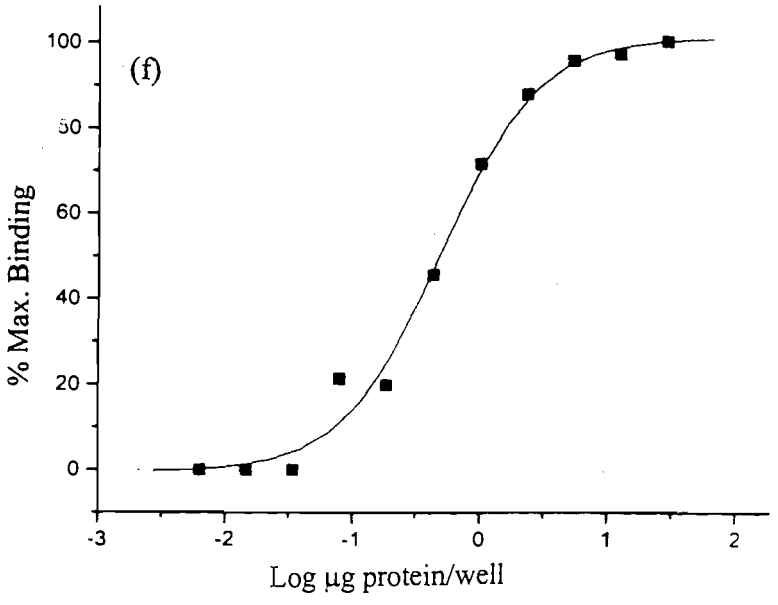
(f)
% Max. Binding
100
80
60
40
20
0
-3
-2
-1
0
1
2
Log µg protein/well

Figure 5.4 Standard ELISA plots for PpL and mutants using different pH solutions for the binding phase.

ELISAs were carried out as described in the legend to Figure 5.3 except that the human IgG used was added to the bound PpL at either pH 8.0, 7.0 or 6.0. The PpL and IgG were then incubated at this pH before the bound human IgG was detected in the usual way. The plots shown are as follows ;

(a) PpL at pH 8.0 (■) 7.0 (●) and 6.0 (▲)

(b) F39H,Y64W at pH 8.0 (■), 7.0 (●) and 6.0 (▲)

(c) Y53H, F39W at pH 8.0 (■), 7.0 (●) and 6.0 (▲)

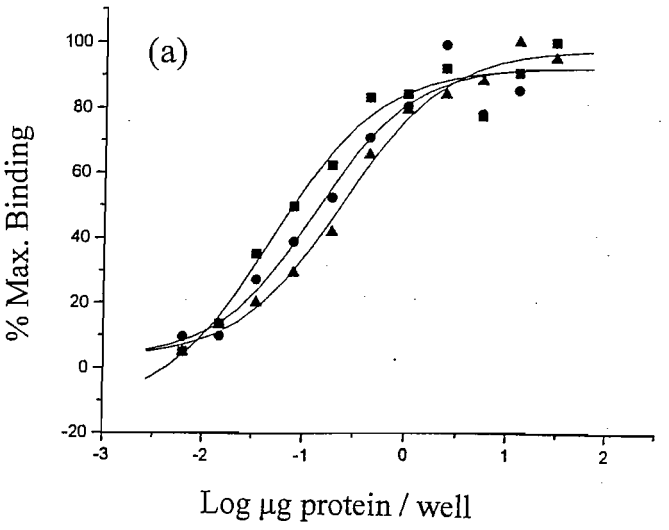
(a)
% Max. Binding
100
80
60
40
20
0
-20
-3
-2
-1
0
1
2
Log µg protein / well

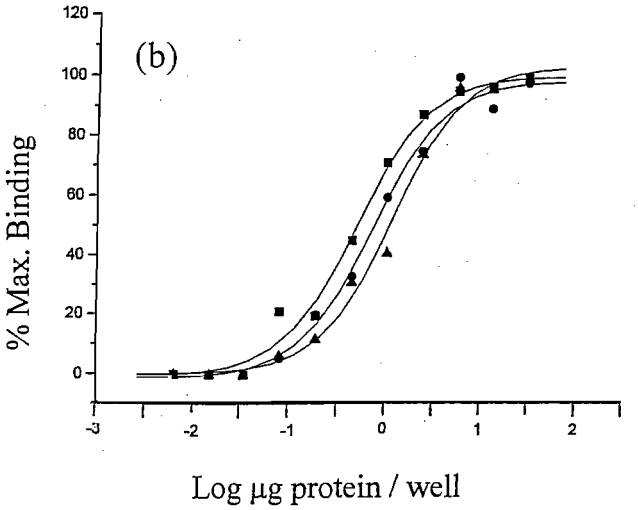
(b)
% Max. Binding
120
100
80
60
40
20
0
-3
-2
-1
0
1
2
Log µg protein / well

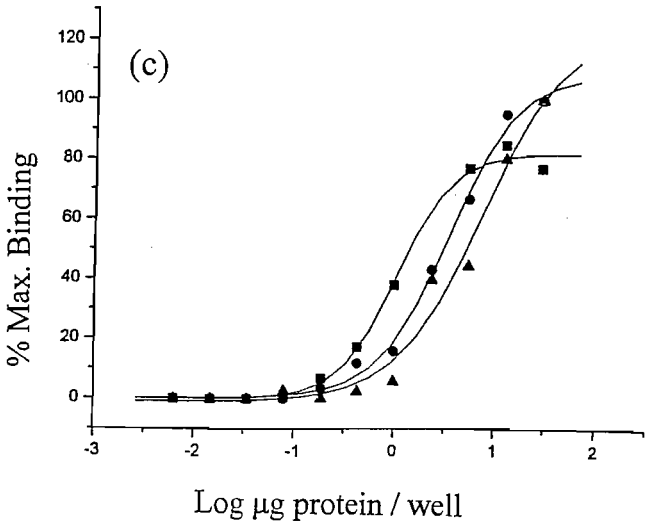
(c)
% Max. Binding
120
100
80
60
40
20
0
-3
-2
-1
0
1
2
Log µg protein / well

changes in pH without exposing the protein to highly acidic or alkaline conditions. It was anticipated that the change in charge at these positions (both neutral in the WT protein at physiological pH) might help disrupt the complexes formed between the mutants and κ-chains. Therefore the effects of pH on the Kds of the complexes with IgG containing κ-chains formed with these mutants was investigated and compared with the effects of pH on the WT-IgG.κ- chain complex. The ELISA experiments were therefore repeated as above except that IgG was added to bound PpL in buffer which had previously been adjusted to the pH at which binding was to be studied. Following washing and addition of anti IgG-HRP the substrate was then added to all wells in the same standard buffer so that the pH of the enzyme reaction was constant. The results are given in Figs 5.4a – 5.4c and Table 5.3.

Table 5.3. The effect of pH on the K_d values obtained for the complexes formed between PpL and mutated PpL and IgG containing κ-chains.

pH	K_d μM +/- Std.Dev. (n=3)	K_d μM +/- Std.Dev. (n=3)	K_d μM +/- Std.Dev. (n=3)
	WT	F39H,Y64W	Y53H,F39W
pH 8.0	0.03 ± 0.02	0.27 ± 0.04	0.59 ± 0.06
pH 7.0	0.07 ± 0.04	0.39 ± 0.06	1.94 ± 0.23
pH 6.0	0.13 ± 0.03	0.62 ± 0.10	4.14 ± 0.25

The data show that the change in K_d with pH for the WT PpL is 4.8 fold between pH 8.0 and pH 6.0 and for the F39H,Y64W and Y53H,Y64W mutants the values are 2.3 and 7 fold respectively.

5.4 Competitive ELISA

This is a more accurate way of determining the K_d of an interaction than the conventional ELISA described above where only one reactant is in free solution. In competitive ELISAs mutant proteins (in solution) compete for IgG (in solution) against immobilised WT PpL. The curve is then compared with that obtained for experiments in which WT PpL (in solution) is used to compete for IgG (in solution) against immobilised PpL. Each well of a microtitre plate is coated with a known amount of WT PpL which gives an absorbance on the linear part of the response curve relating the amount of immobilised PpL to the absorption at 495nm of the product. The full details of the methods used are given in Chapter 2, section 2.5.9. As the concentration of the competing protein is increased in a well the absorption at 495nm decreases since more of the κ-chain is bound by the PpL in solution that is eventually washed from the plate.

Table 5.4. The K_d for the complexes formed between PpL and mutants of PpL with IgG containing κ-chain determined from competitive ELISAs.

Protein	$K_d \pm$ Std. Dev. (μM)
PpL	N/A
K33W	0.14 ± 0.02
N26,76D	0.16 ± 0.02
N26,76D,F39W	0.14 ± 0.02
F39H,Y64W	1.53 ± 0.03
Y53H,F39W	4.61 ± 0.04

Figures 5.5a – 5.5f show the results of the competitive ELISA experiments and Table 5.4 shows the K_ds derived from these plots for the binding of various PpL domains to IgG bearing κ-chains. These experimental data show reasonably good agreement with those obtained

Figure 5.5 Competitive ELISA plots for PpL and its mutants.

A standard 96- well microtitre plate was used for these competitive ELISA experiments. The plate was coated with WT PpL and then human IgG was added in the presence of the competitor (free WT PpL or PpL mutants). After washing, the amount of human IgG bound to each plate was determined by the addition of a goat anti-human IgG-HRP , followed by further washing and the addition of HRP substrate. A full description of the method used is given in section 2.5.9. The percentage of maximum binding of human IgG to the well is plotted against the log of the μg of the competing PpL domain per well.

(a) WT

(b) K33W

(c) N26,76D

(d) N26,76D,F39W

(e) Y53H,F39W

(f) F39H,Y64W

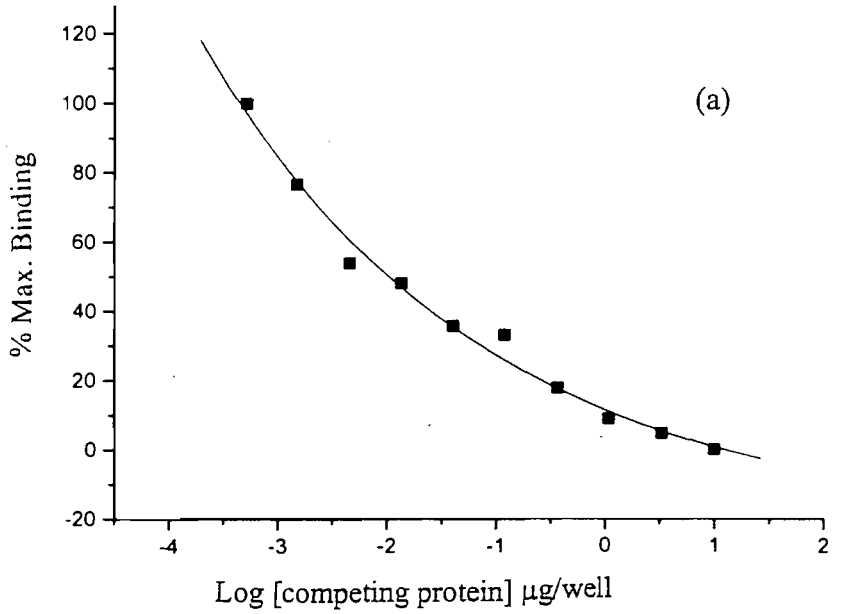
(a)
% Max. Binding
120
100
80
60
40
20
0
-20
-4
-3
-2
-1
0
1
2
Log [competing protein] µg/well

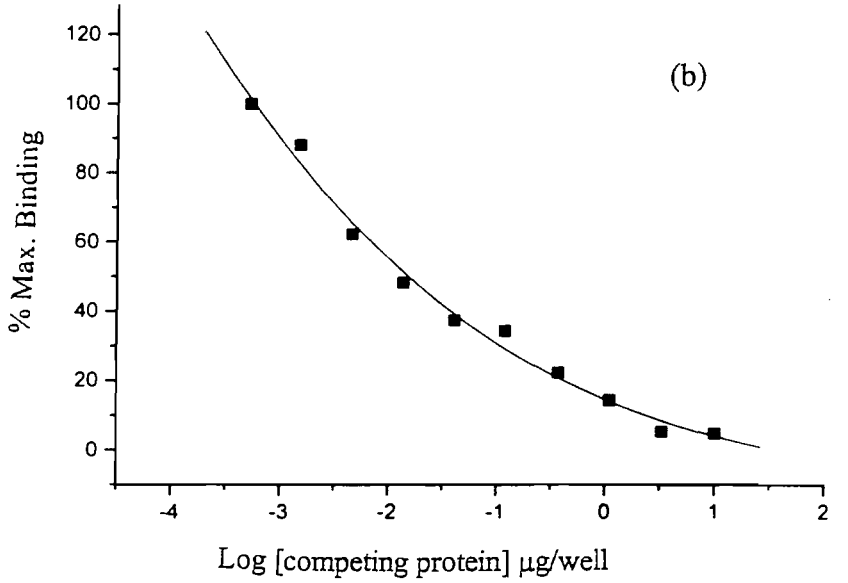
(b)
% Max. Binding
120
100
80
60
40
20
0
-4
-3
-2
-1
0
1
2
Log [competing protein] µg/well

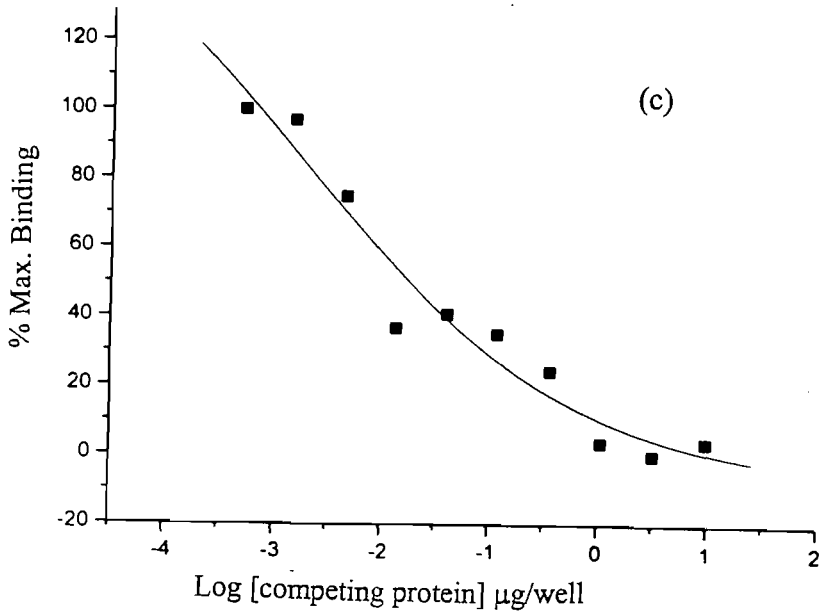
(c)
% Max. Binding
120
100
80
60
40
20
0
-20
-4
-3
-2
-1
0
1
2
Log [competing protein] µg/well

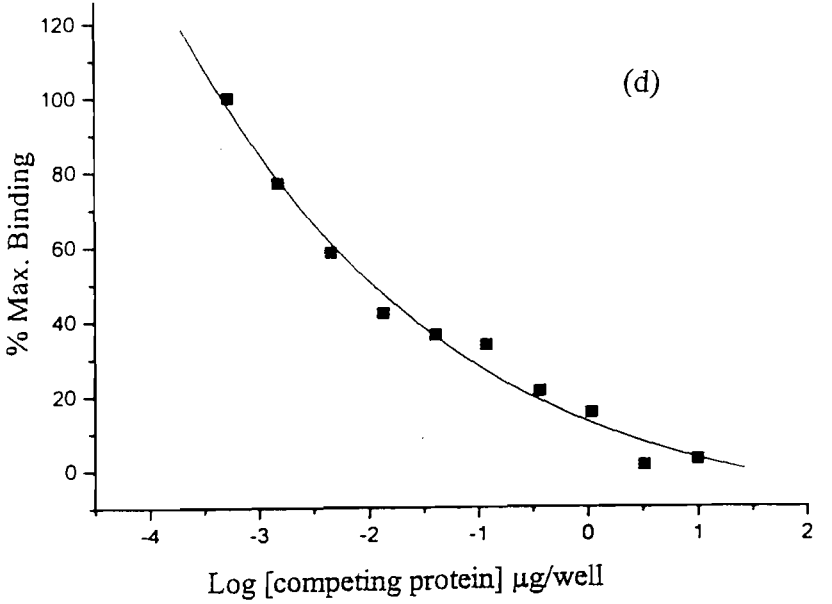
(d)
% Max. Binding
120
100
80
60
40
20
0
-4
-3
-2
-1
0
1
2
Log [competing protein] µg/well

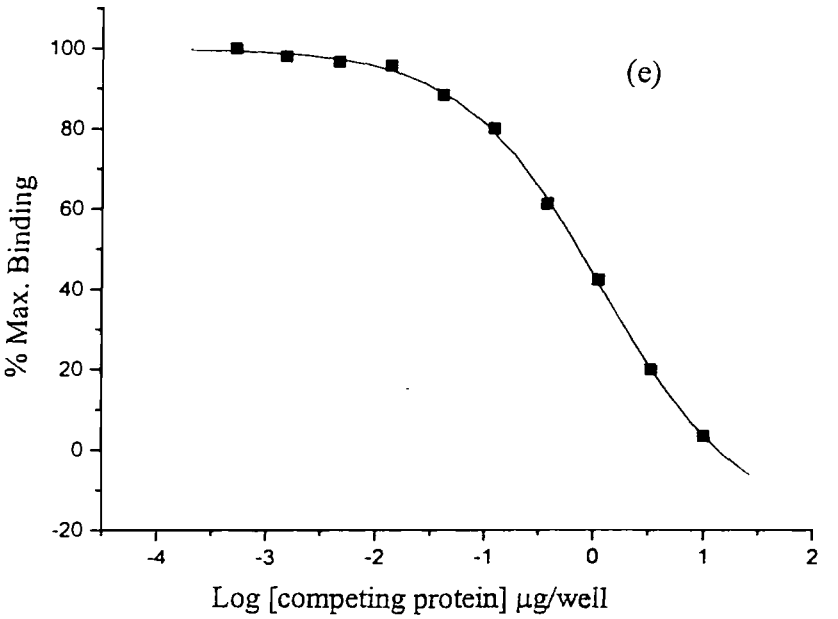
(e)
% Max. Binding
100
80
60
40
20
0
-20
-4
-3
-2
-1
0
1
2
Log [competing protein] µg/well

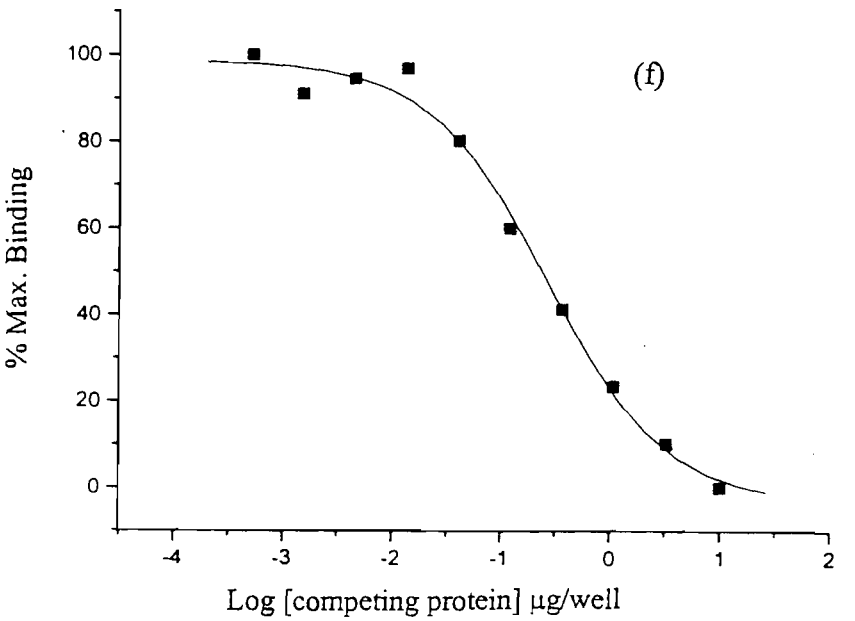
(f)
% Max. Binding
100
80
60
40
20
0
-4
-3
-2
-1
0
1
2
Log [competing protein] µg/well

from simpler ELISA experiments described in section 5.3 above. In most cases the standard errors are much smaller in the competitive ELISA experiments compared to those in the standard ELISAs probably due to the removal of the error that arises from variations in coating efficiency when using different concentrations of the coating protein.

5.5 Affinity chromatography

Affinity chromatography is a very specific separation technique which can separate proteins on the basis of biological activity i.e. the ability of a protein to recognise and bind to another protein, co-factor, metal ion etc. This ability to bind specifically to a ligand needs to be retained when the protein has been immobilised onto a polysaccharide or other insoluble matrix. Immobilisation of protein onto a polysaccharide matrix was first achieved by Axen and Ernback, (1971) by activating the matrix using cyanogen bromide. Since then, the number of available derivatised matrices has grown dramatically offering the user a wide range of insoluble supports, spacer groups and modified ligands (Affinity Chromatography Ltd, Cambridge).

Affinity chromatography is a technique which can be used to purify antibodies by immobilising an Ig-binding protein such as Protein A or G or L to a matrix then passing the solution containing antibodies down the column (Boyle and Reis, 1987). Antibodies can then be eluted by changing the pH or salt concentration. Protein A-Sepharose or Protein A-controlled pore glass columns are commercially available (Pharmacia and Bioprocessing Ltd., respectively) and are standard methods for purifying monoclonal antibodies. IgG can bind to Protein A that has been immobilised on a matrix in a column at neutral or slightly alkaline pH while other proteins pass through the column without binding. Elution of IgG is then achieved by reduction of the pH of the buffer passing through the column to pH 3.0 or below. This has many advantages over more conventional methods of purification such as gel filtration and ion

exchange chromatography that, although inexpensive, fail to provide pure antibody in a single step and therefore multiple steps are required. Multiple steps are time consuming and therefore increase cost, result in lower yield and sometimes have low capacity for the protein target.

Although a Protein A affinity column provides a high yield of pure antibody in a single step, it is more expensive than conventional methods and cannot be used for certain classes of Ig such as IgD, IgE, IgM or some subclasses of immunoglobulins. For example, IgG_3 from Caucasians cannot bind to Protein A due to a His - Arg replacement at residue 435 (Popplewell, 1991).

PpL has been used by Nilson *et al.,* (1993) to purify IgG, IgM and IgA from human and mouse serum and in addition Fab and Fv fragments derived from these antibodies. Therefore, although offering a more general Ig-binding spectrum than Protein A, it has the disadvantage of requiring harsh conditions required to elute the antibodies. PpL is able to bind Igs at pH 8.0 but to dissociate the complex and remove Igs from an affinity column a pH of 1.75 is required (Beckingham, 1997).

The aim of this part of the work was to immobilise engineered mutants of PpL with a known reduced affinity for κ-chain or IgG bearing κ- chains and find the pH at which the bound protein is eluted from the column.

In these experiments PpL mutants were bound to CNBr activated Sepharose 4B using methods described in Chapter 2, section 2.5.10. The amount of each domain coupled to the swollen gel varied slightly but was in the range of 5 – 6mg / ml. (see Table 5.5).

Table 5.5 The amount of PpL domain bound per ml of swollen Sepharose 4B.

Protein	mg / ml Sepharose 4B
N26,76D	5.5
N26,76D,F39W	5.9
K33W	6.5
Y53H,F39W	4.8
F39H,Y64W	6.3

The columns equilibrated in 20mM phosphate buffer, pH 8.0 at 20°C were loaded with 1ml of the same buffer containing 5mg of lyophilised polyclonal IgG kindly donated by Dr. D. Pepper (The Blood Transfusion Service, Edinburgh, Scotland). The column was washed with loading buffer until the absorbance at 280nm returned to the starting baseline and then a pH gradient was started and fractions collected. Full details are given in sections 2.5.10 in Chapter 2. Profiles of the IgG eluting from the columns of the mutants tested are shown in Fig.5.6a - Fig.5.6e. Since the IgG was not monoclonal and contains approximately 40% of IgG bearing lambda chains, there is a peak of the latter protein that elutes in the wash period. Once the elution gradient was started the IgG containing κ-chains was eluted.

The experiments showed that IgG bearing κ-chains is eluted from a WT PpL affinity column at pH 1.75 (Beckingham, 1997) while the mutant K33W releases IgG at a similar pH (1.9) as might be expected from the closeness of their K_d values determined from ELISA studies. Columns made from the mutants N26,76D and N26,76D,F39W release IgG at

Figure 5.6 Elution profiles for human IgG from affinity columns made from immobilized mutants of PpL.

Affinity columns were made from PpL mutants immobilized onto CNBr-activated Sepharose 4B. The columns were loaded with human IgG and washed with 20mM phosphate pH 8.0 buffer to remove unbound IgG. A pH gradient was then applied and 0.5ml fractions were collected. The eluted IgG was located by its absorbance at 280nm.

(a) The elution of IgG from a Y53H,F39W column
(b) The elution of IgG from a F39H,Y64W column
(c) The elution of IgG from a K33W column
(d) The elution of IgG from a N26,76D column
(e) The elution of IgG from a N26,76D,F39W column

The solid line shows absorbance of the solution eluted at 280nm, the dotted line shows the pH of the eluting solution.

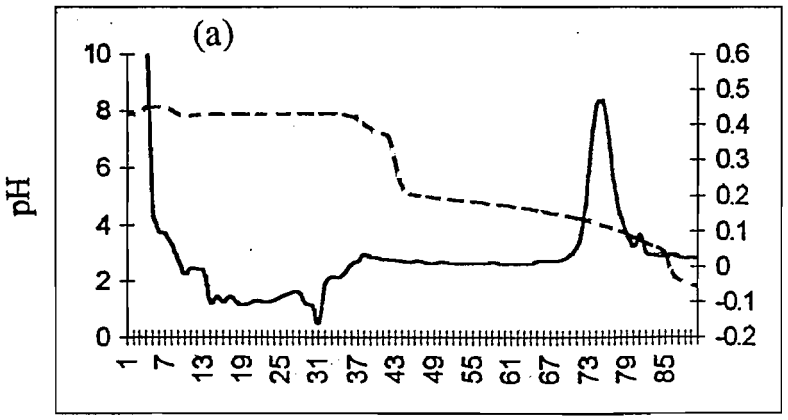
(a)
pH
Absorbance at 280nm
Fraction number

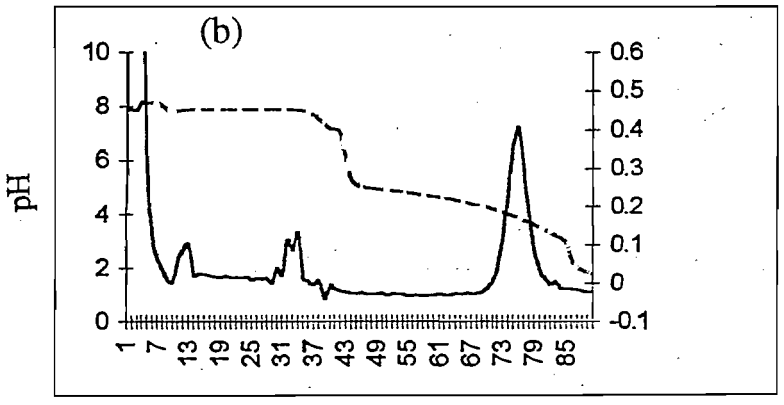
(b)
pH
Absorbance at 280nm
Fraction number

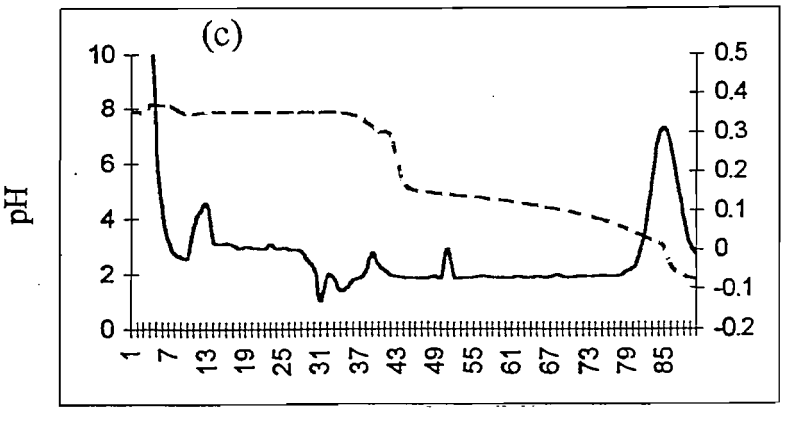
(c)
pH
Absorbance at 280nm
Fraction number

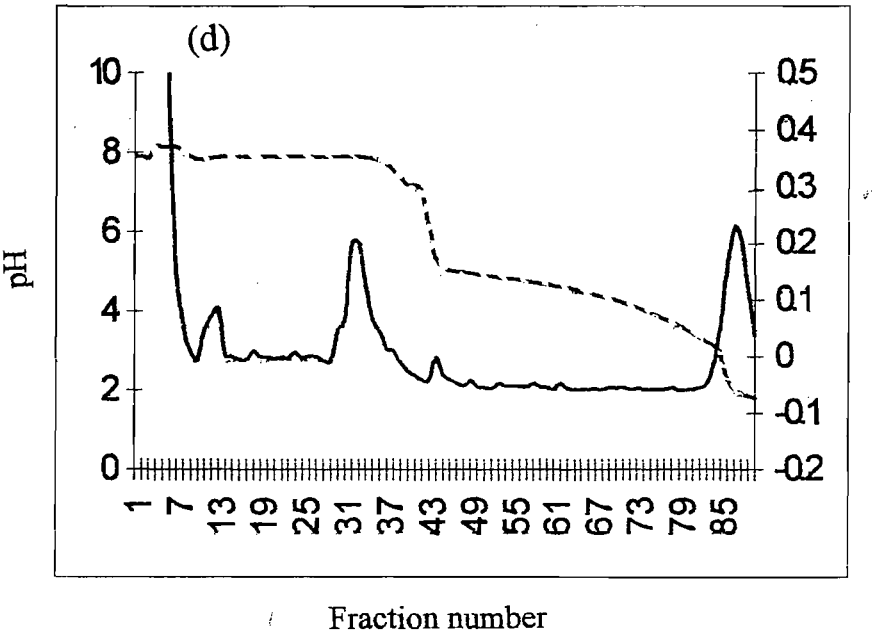
(d)
pH
Absorbance at 280nm
10
8
6
4
2
0
0.5
0.4
0.3
0.2
0.1
0
-0.1
-0.2
1 7 13 19 25 31 37 43 49 55 61 67 73 79 85
Fraction number

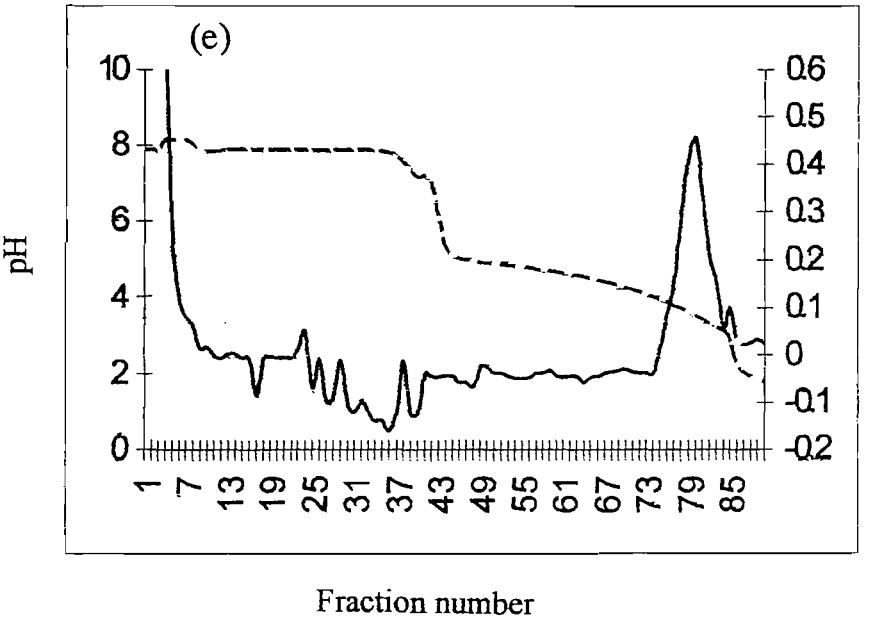
(e)
pH
Absorbance at 280nm
10
8
6
4
2
0
0.6
0.5
0.4
0.3
0.2
0.1
0
-0.1
-0.2
1 7 13 19 25 31 37 43 49 55 61 67 73 79 85
Fraction number

slightly higher pH values, pH 2.1 and 2.9, respectively. This is not a sufficient increase in pH to be useful as this is still too acidic for long term exposure of IgG and more importantly S_cFv fragments that are unstable below pH 2.5 (Dr. Ian Tomlinson, MBL, Cambridge personal communication).

However, the mutants F39H,Y64W and Y53H,F39W release IgG at pH 3.8 and pH 3.9, respectively, which are substantially better conditions for the stability of IgG and S_cFv fragments. In affinity chromatography experiments carried out by others in this laboratory using κ-chain or S_cFv as the binding ligand, the elution profiles have proved similar to those obtained with IgG.

5.6 Fluorescence labelling with an extrinsic fluorophore

5.6.1 Determination of stoichiometry of labeling of PpL with eosin-5-maleimide

This experiment was performed to determine whether labelling of cys residues with eosine-5-maleimide was occurring with a 1:1 stoichiometry, which would allow an extrinsic fluorophore to be used for binding constants for these mutants. A standard curve was prepared by measuring the fluorescence of a series of solutions containing 0-80μM of eosin-5-maleimide in 1ml 20mM phosphate buffer filtered and deionised and 1% SDS using an excitation wavelength of 524nm and measuring emission at 544nm. 1% SDS was added to a protein solution containing labelled T42C to release the fluorophore from hydrophobic pockets within the protein by unfolding it. The fluorescence was measured and the protein concentration compared to the value obtained for the label from the standard curve. The experiment showed that T42C PpL does label with approximately a 1:1 stoichiometry, and these labelled proteins can now be used to look for fluorescence changes on binding to κ-chain with a view to determining binding constants.

5.6.2 Using labeled cys mutants to determine any fluorescence change on binding to κ-chains

PpL mutants T42C, H74C and Q35C were labelled with eosin-5-maleimide as described in 5.6.1 and were mixed with κ-chain to determine whether a fluorescence change was observed which could be used in for binding constant determination by titration as previously described in section 5.1. For each of these mutants, however, no significant fluorescence change on binding occurred, so these mutants could not effectively be used for titrations with κ-chain.

5.6.3 Forster resonance energy transfer (FRET)

The fact that T42C binds to an extrinsic fluorphore with a 1:1 stoichiometry gives rise to the possibility of FRET occurring. FRET occurs when a fluorophore is excited by light and has an emission spectrum which overlaps with the excitation spectrum of a second acceptor fluorophore. A radiationless transfer occurs if the donor and acceptor fluorophores are in close enough proximity with the efficiency of transfer being dependent on the quantum yield of the donor and acceptor fluorophores. The acceptor fluorophore then emits light at its usual emission spectra which can be detected. If FRET is occurring then the fluorescence emission spectrum of the acceptor fluorophore is observed despite exciting only the donor. Tryptophan is commonly used as a donor and an acceptor is often a chemically attached group e.g. to a Cys residue. This technique is useful for determining the distances between or within proteins, and is therefore of interest in order to determine whether PpL exists as a dimer in solution.

Labelled cysteine mutants either T42C, H74C, Q35C (labelled with pyrene-5-maleimide rather than eosine due to the wavelength that pyrene

is excited at, which is close to that of Trp emission) were mixed in a 1:1 ratio with a Trp mutant either Y64W or F39W to a final concentration of $0.05 mgml^{-1}$. All combinations were tried to give maximum chance of observing FRET with the distance between the acceptor and donor fluorophores varied. This mixture was heated to 55°C for 45 minutes to break any bonds which may be allowing PpL to exist as a dimer and allowed to cool to 25°C to allow dimers to reform if indeed PpL exists as a dimer at this concentration in solution. If dimers reformed it is likely that some would form with both a domain containing Trp residue and a domain containing the extrinsic fluorphore, and these dimers may exhibit FRET.

The tryptophan residue was excited using a wavelength of 280nm. This has an emission maximum of around 338nm but should FRET be taking place the emission maxima would be that of the acceptor fluorophore (Pyrene-5-maleimide) which is around 380nm, as the excitiation wavelength for pyrene-5-maleimide (the acceptor flurophore) is 340nm. The results showed that no FRET was taking place in any of the combinations used above, suggesting that PpL does not form a dimer in solution or that dissociated monomers cannot reassociate.

5.7 Discussion

All of the methods of determining the K_d of a reaction gave similar values for each protein studied. The use of fluorescence spectroscopy to study the reaction can be a very useful and accurate method. Beckingham, (1997) showed that if Tyr53 is present then its fluorescence is quenched on forming a complex with κ-chain. Alternatively, a Trp residue in position 39 also reports binding indicating that the environment of this region of PpL changes significantly on complex formation unlike mutants with Trp in position 64. Although fluorescence titrations are of limited use for some mutants that yield small overall changes in fluorescence intensity in equilibrium studies (e.g. Y64W and mutants carrying this reporter) it does

allow examination of the pre-equilibrium kinetics of the reaction as is shown in the next chapter.

The competitive ELISAs also gave estimates of K_d with low standard deviations and could be used to study all PpL constructs. Therefore for the sake of simplicity in the following discussion the K_d values determined by this technique are quoted.

Since residues 39 and 53 are the only residues implicated by the NMR studies of Wikström *et al.,* (1996) to make contact with κ-chains in the complex it was expected that F39H,Y64W and Y53H,F39W would show the greatest change in K_d compared to that of WT PpL. The introduction of a polar and ionisable histidine residue at positions 39 and 53 was intended to disrupt hydrophobic contacts. There is an increase in K_d for both mutants F39H,Y64W (1.53μM) and Y53H,F39W (4.61μM) by approximately 12 fold and 35 fold, respectively, compared to WT PpL (0.13 μM) at pH 8.0.

It must be re-emphasised here that neither the Y64W mutation nor the F39W mutation have a significant effect on K_d (Beckingham, 1997) and therefore the changes in affinity are primarily due to the second mutation in each case i.e. F39H or Y53H. This has an important repercussion, since the studies described in Chapter 4 and the requirement of a lower temperature during the purification protocol (see Chapter 2) have shown that the inclusion of the F39W substitution makes a domain less stable both to heat and to denaturants. However, once the effect of the second mutation on the binding affinity to κ-chains has been characterised by use of the fluorescence properties of Trp39, the F39W mutation can be reversed to yield a more stable, single mutated domain.

We can use the equation

$$\Delta G^{o} = - RT\ln Keq$$

(in which ΔG^{o} is the change in free energy, R is the gas constant, T is the temperature in degrees Kelvin and Keq is the equilibrium constant) to calculate the binding energy associated with each protein binding κ-chain. Thus the change in binding energy ($\Delta\Delta G^{o}$) caused by a mutation is

$$\Delta G^{o}_{WT} - \Delta G^{o}_{Mutant} = - RTlnKeq_{WT} - [-RTlnKeq_{Mutant}]$$

and therefore

$$\Delta\Delta G^{o} = RTln(Keq_{WT} / Keq_{Mutant})$$

For the F39H,Y64W mutant the loss of binding energy is approximately 6.1 kJ / mol and for the mutant Y53H,F39W the loss is 8.8 kJ / mol compared with that of the interaction of WT PpL with IgG bearing κ-chains. Previous studies (see Table 5.1) have shown that the replacement of Y53 by F53 causes an increase in K_d to 3.2μM and that this could be due to the loss of a single hydrogen bond between the hydroxyl group of Y53 and κ-chain. If so, it suggests that the His53 replacement does not give rise to a strong compensatory hydrogen bond between the imidazole group and κ-chain. It is possible, however, that such a bond does form but that the loss of other interactions (e.g. Van der Waal, hydrophobic interactions) leads to an overall loss of binding energy. This is almost certainly the case for the mutant F39H,Y64W. This shows a smaller but still significant reduction in affinity for κ-chain; the introduction of the histidine residue to the 39 position clearly changes the characteristics of this site.

One of the aims of using a histidine substitution was to place an ionisable residue at locations that lack charged groups. It was hoped that the protonation of the imidazole group would disrupt any hydrophobic interactions and lead to a decreased stability of the complex. The ELISA experiments carried out at different pHs suggest that this does not occur to a great extent for the mutants used in these experiments. This implies that these regions of contact with κ-chain are not sensitive to the ionisation of

the imidazole ring or that the pK of the imidazole group is well below pH 6.0 and that protonation was not achieved.

One important observation is that the single domain PpL binds to κ-chains (fluorescence titration experiments) with similar affinities whether these are isolated or part of an IgG molecule (ELISA experiments). This demonstrates that there is no steric restriction to PpL binding to the Fab fragment of IgG and that the structures of the V_L domains of the κ-chains are similar whether as part of an IgG molecule or not.

The dissociation of a dimeric form of PpL occurring after the dimer has made initial contacts with κ-chain was considered as a possibility for the second stage of binding, the conformational rearrangement. This could be driven by the monomers having a higher affinity than the putative 'dimeric PpL' for κ-chains. The mutants, N26,76D and N26,76D,F39W were made to test whether the four hydrogen bonds formed between two molecules of PpL in the crystal are influential in the maintenance of a dimeric form of the protein in free solution. The results here show that no really significant differences between their affinities (0.16μM and 0.14μM respectively) and the affinity of WT PpL for κ-chain (K_d = 0.13μM) exist. The existence of four hydrogen bonds (each of approx. 4kJ/mol (Fersht, 1987) that might have to be broken for a high affinity complex to form would be expected to raise the K_d by a factor of some 600 fold.

Finally, the immobilisation of the two mutants F39H,Y64W and Y53H,F39W to Sepharose has produced two affinity columns that elute κ-chains or IgG containing κ-chains at substantially higher pHs than the WT PpL, thus achieving one of the aims of the research. The overall yields from these columns is around 1.5 – 2 mg of retained and eluted IgG per ml of gel or 5mg of PpL in close agreement with figures found for other single domain proteins (Beckingham, 1997).

Chapter 6

Stopped-flow analysis of the binding reaction between PpL and κ-chains.

CHAPTER 6

STOPPED-FLOW ANALYSIS OF THE BINDING REACTION BETWEEN PpL AND κ-CHAINS.

6. Introduction

Bimolecular reactions such as substrate or ligand binding to proteins typically occur over a time scale of 50 – 100ms and therefore require specialised instrumentation for their study. Stopped flow spectroscopy is, in principle, a simple system consisting of two syringes that hold the two reactants. The pistons of these syringes can be driven by compressed air so that a small sample of each reactant is rapidly mixed and delivered to an optical detector. Most commercial systems have a dead time (the period between the mixing of reagents and the triggering of the record of the change in optical signal) of approximately 1ms. Therefore most biochemical reactions that involve changes in spectral properties can be observed using this technique although reactions that take place very rapidly may occur during this time and not be noticed. Nevertheless, for most biological systems the stopped flow technique has proved remarkably successful. A diagram illustrating the general layout of the device used in these experiments is given in Fig. 6.1. In these studies a fluorimetric detection system was used to take advantage of the change in fluorescence that occurs when PpL bearing unique Trp residues binds to κ-chains as described in Chapter 5. The figure shows that the light is provided by a 150W Xenon lamp and the excitation light is selected by a monochromator (MC1). The fluorescence emission from the reaction cell is subsequently selected by a cut-off filter that permits light above a selected

Figure 6.1a A schematic diagram of a stopped-flow spectrophotometer.

(a) The pneumatic ram system used to drive the syringes containing reactants.
(b) The drive syringes containing reactants
(c) The mixing chamber
(d) The light source
(e) The photomultiplier
(f) The signal output
(g) The stop syringe
(h) A microswitch to trigger the data collection
(i) The optical cell viewed from the side

Figure 6.1b A view from above the optical path showing the arrangement for collecting fluorescence data.

The Xenon lamp produces light over a broad spectrum. The excitation wavelength is selected by monochromator (MCM) 1 and illuminates the flow cell. The wavelength of the emitted fluorescence is selected by MCM2 or a cut-off filter and the fluorescence is detected at right angles by photomultiplier (PMT) 2.

6.1a

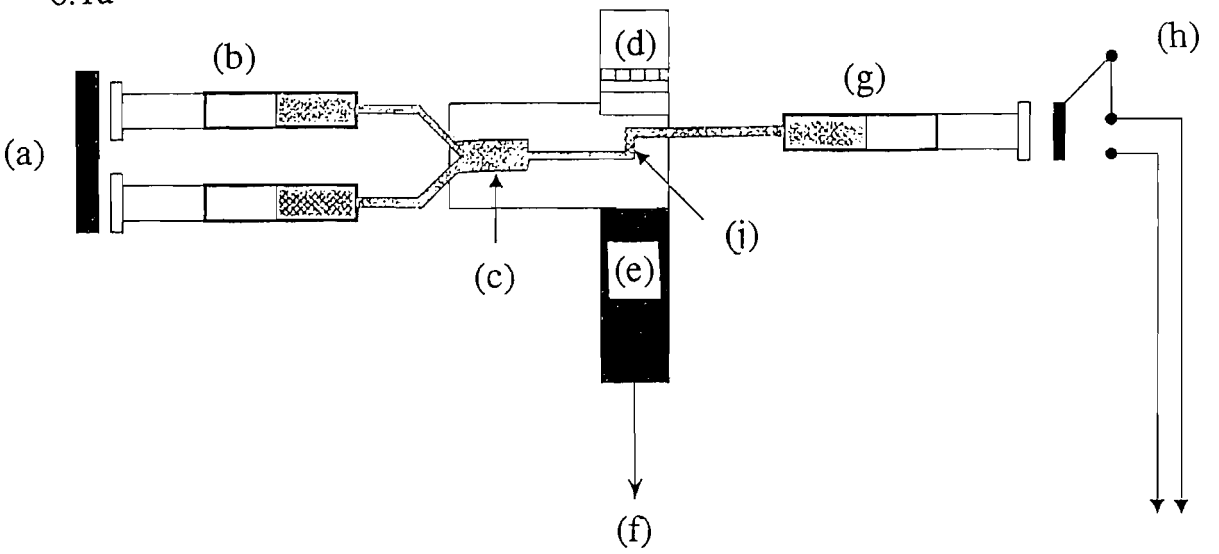
(a)
(b)
(c)
(d)
(e)
(f)
(g)
(h)
(i)

6.1b

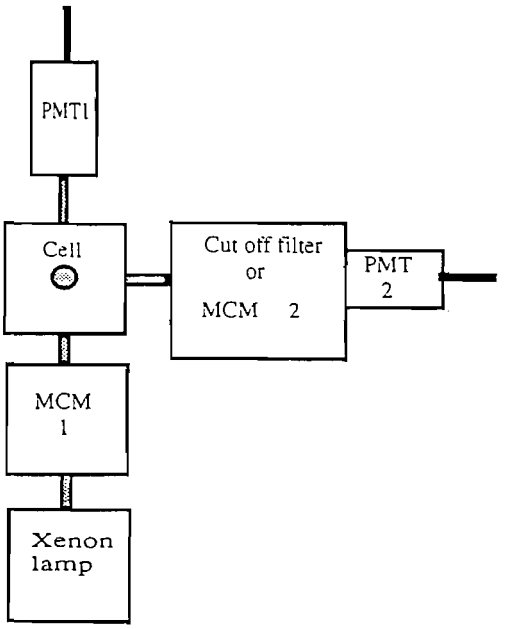
PMT1
Cell
Cut off filter
or
MCM 2
PMT
2
MCM
1
Xenon
lamp

wavelength (335nm for tryptophan emission) to pass through, but absorbs light at lower wavelengths.

6.1 Data analysis.

The reaction between PpL and κ-chain, shown below, is a second order, bimolecular reaction, the rate of which will depend upon the concentration of both reactants.

$$\text{PpL} + \kappa \underset{k_{-1}}{\overset{k_1}{\rightleftharpoons}} \text{PpL.}\kappa \qquad (1)$$

In which k_1 and k_{-1} are the rate constants for the forward (association) and reverse reactions (dissociation), respectively. The velocity of the forward direction $v_f = k_1[\text{PpL}][\kappa]$ and the velocity of the reverse direction $v_r = k_{-1}[\text{PpL.}\kappa]$. At equilibrium $v_f = v_r$ and thus

$$k_1\,[\text{PpL}][\kappa] = k_{-1}\,[\text{PpL.}\kappa] \qquad (2)$$

and

$$k_{-1}/k_1 = [\text{PpL}][\kappa] / [\text{PpL.}\kappa] = K_d \qquad (3)$$

ie. the ratio of the rate of dissociation to the rate of association of the complex = K_d, the dissociation constant for the equilibrium. For simple systems the value of K_d determined by equilibrium experiments (such as those described in Chapter 5) is normally the same as that determined by pre-equilibrium techniques.

k_1 ($M^{-1}s^{-1}$) is a second order rate constant that can be determined easily if the experiment is set up such that one reagent (in these experiments PpL) is in excess over the other. In such situations, the rate of loss of the limiting component is a pseudo-first order process which has the same rate as the rate of formation of product. However, this is not the rate of the observed reaction in the stopped-flow. The observed rate is related to k_1 and k_{-1} by the equation

$$k_{obs} = k_1[PpL] + k_{-1}. \quad (4)$$

If the dependence of the value of k_{obs} on PpL concentration is determined then the true second order rate constant k_1 can be calculated. This is achieved by reacting a fixed concentration of κ-chain with various concentrations of PpL and determining k_{obs} under each condition. A plot of $k_{obs}(s^{-1})$ against PpL concentration should give a straight line of slope equal to k_1 ($M^{-1}s^{-1}$). When the concentration of PpL = 0, then $k_1[PpL]$ also = 0 and therefore the intercept on the ordinate is equal to k_{-1} (s^{-1}). One advantage of this method for some applications is that if necessary, only the concentration of the increasing ligand concentration needs to be known accurately.

One complication of the reaction between PpL and κ-chains is that the binding process appears to take place in two stages (Beckingham, 1997). An initial fast reaction occurs, detected by a rapid increase in fluorescence intensity, and this is followed by a further change in fluorescence occurring over several seconds. The nature of the second change in fluorescence depends upon the location of the reporter group used. Fig 6.2a shows a typical reaction progress curve obtained when Y64W PpL (or mutants containing the Y64W label) is reacted with κ-chain. A rapid increase in fluorescence intensity with a half time of approximately 50ms occurs when 30μM Y64W is rapidly mixed with 2μM κ-chain (final concentrations) at pH 8.0 and 25°C. This is followed by a slow decrease in intensity with a half time of about 1.5s. It is noticeable that the final fluorescence intensity is less than the initial intensity thus giving rise to an overall quenching of fluorescence on formation of the complex as described in Chapter 5. Figure 6.2b shows a similar reaction carried out using the same concentration of F39W mutant and κ-chain. In this case there is again a rapid increase in fluorescence with a half time of about 30ms followed by a further slow increase in fluorescence intensity with a half time of about 150ms. Thus the overall increase in fluorescence shown by domains bearing a W39 on forming complexes with κ-chain (see Chapter 5) arises in two clear stages.

Figure 6.2a The reaction progress curve obtained when 30μM Y64W is reacted with 2μM κ-chain.

The plot shows the change in fluorescence intensity over a 5 second period after mixing the two reactants. The buffer was 20mM potassium phosphate, pH 8.0 at 25°C.

Figure 6.2b The reaction progress curve obtained when 30μM F39W is reacted with 2μM κ-chain.

The plot shows the change in fluorescence intensity over a 5 second period after mixing the two reactants. The buffer was 20mM potassium phosphate, pH 8.0 at 25°C.

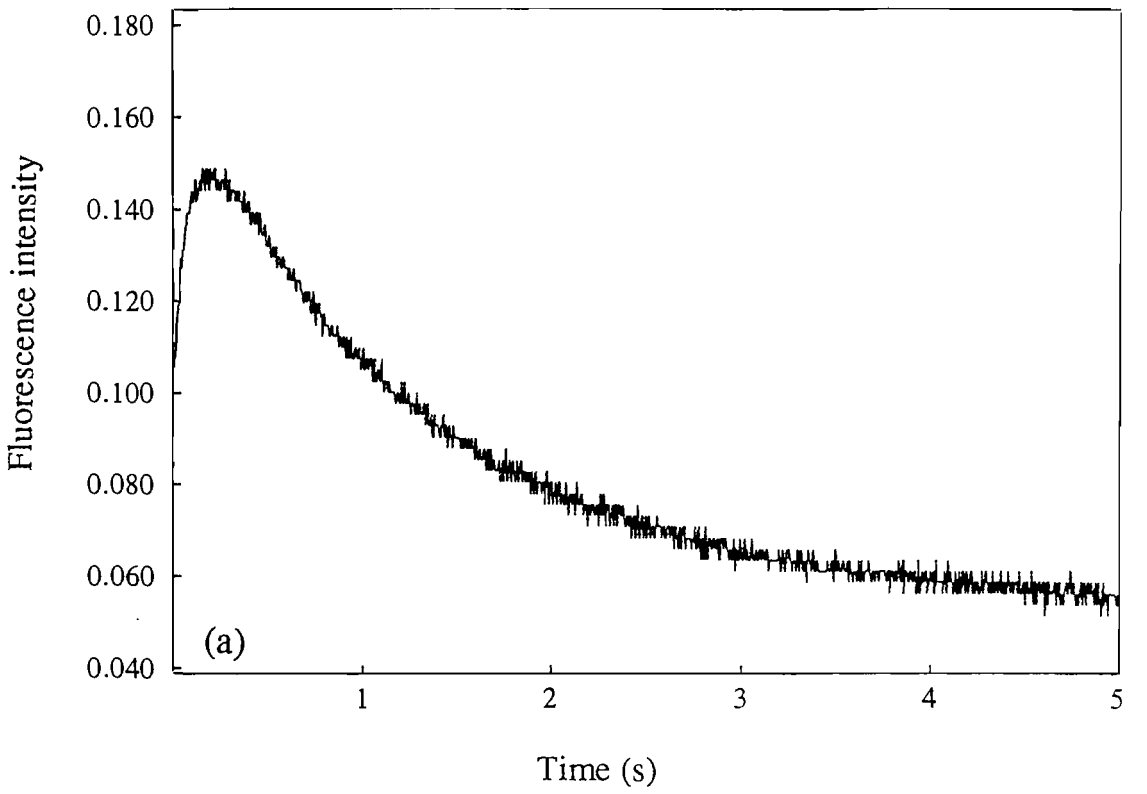
0.180
0.160
0.140
0.120
0.100
0.080
0.060
0.040
Fluorescence intensity
(a)
1
2
3
4
5
Time (s)

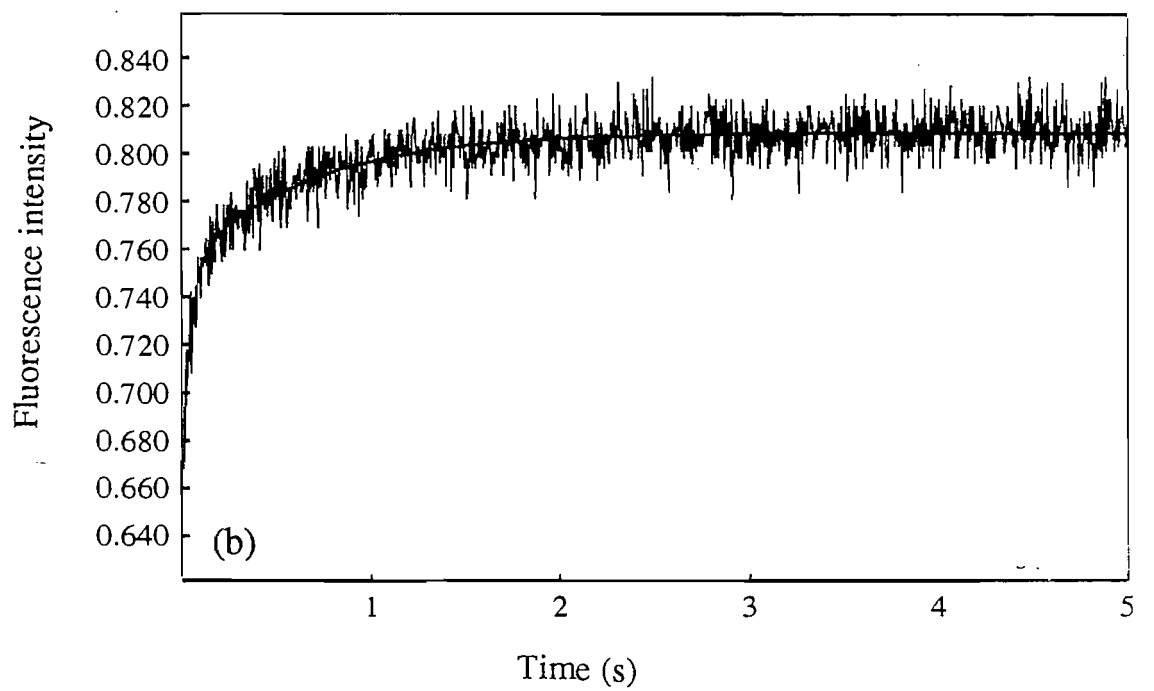
0.840
0.820
0.800
0.780
0.760
0.740
0.720
0.700
0.680
0.660
0.640
Fluorescence intensity
(b)
1
2
3
4
5
Time (s)

Figure 6.2c The dependence of k_{obs} (s^{-1}) upon the concentration of F39W.

The plot shows the increase if the observed rate of reaction with the increase in the concentration of F39W. The intercept on the ordinate, k_{-1} is $2.94s^{-1}$. The slope, k_1 is 0.546×10^6 $M^{-1}s^{-1}$.

Figure 6.2d The dependence of the observed value of k_2 on the concentration of F39W.

The line through the points shows that k_2 is $5.05s^{-1}$.

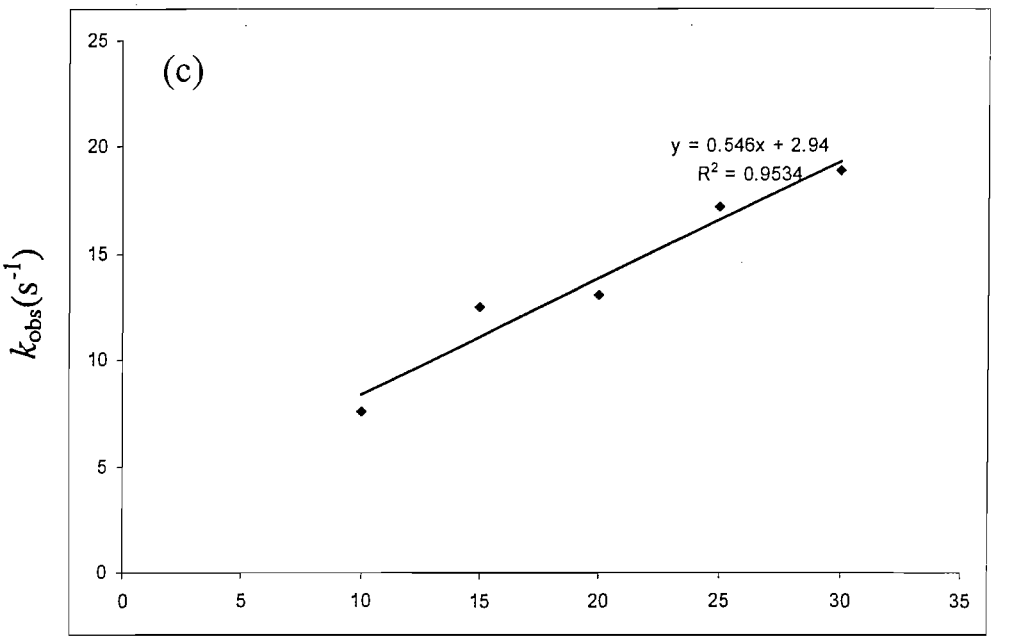
(c)
y = 0.546x + 2.94
R² = 0.9534
$k_{obs}(s^{-1})$
PpL [μM]

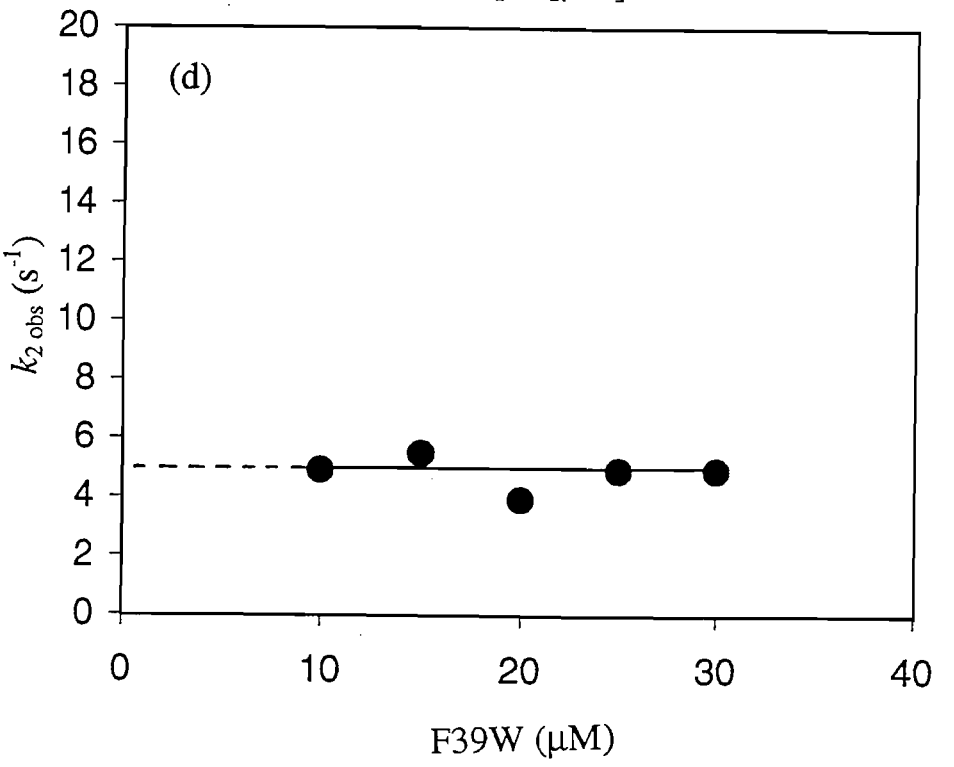
(d)
$k_{2\ obs}\ (s^{-1})$
F39W (μM)

Figure 6.2e The change in fluorescence intensity observed when a complex formed between F39W and κ-chain is rapidly mixed with 30μM WT PpL.

The curve shows the loss in fluorescence intensity at 335nm when a preformed complex made by mixing 8μM F39W and 8μM κ-chain in 20mM potassium phosphate buffer, pH 8.0 was diluted 1:1 v/v with 60μM WT PpL. The reaction shown has an observed single exponential rate of $0.46s^{-1}$.

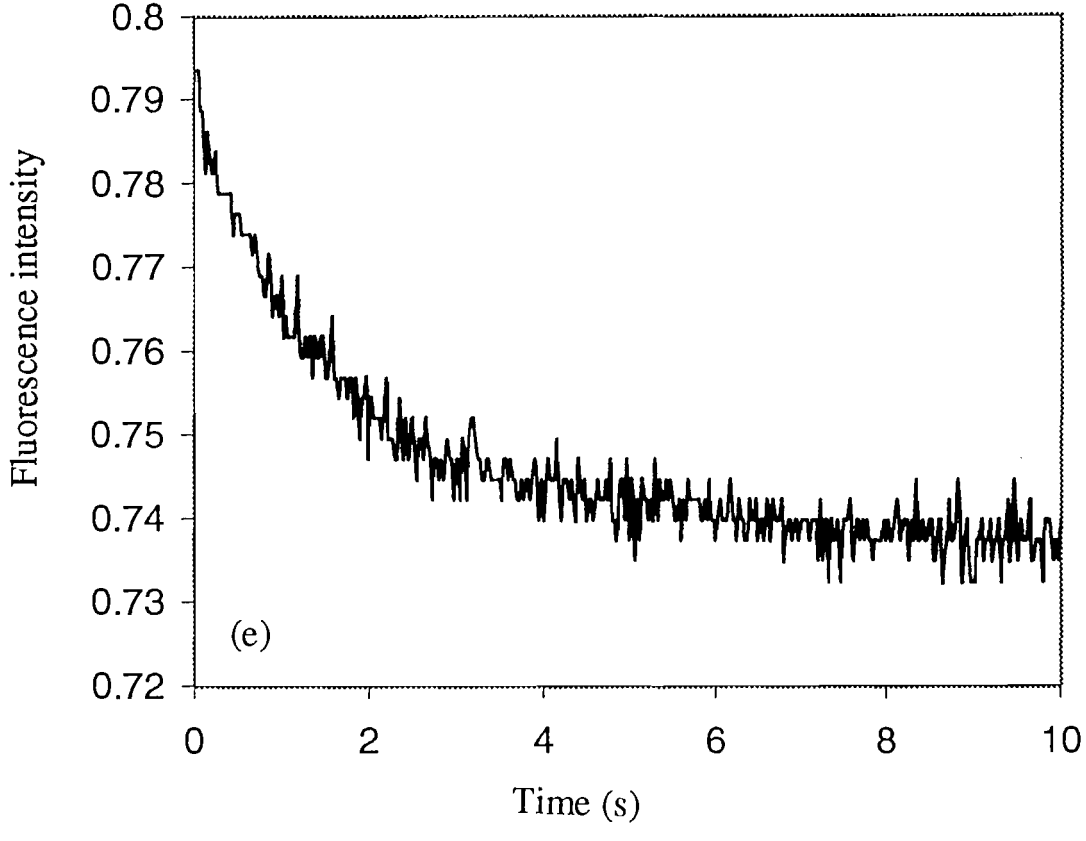
0.8
0.79
0.78
0.77
0.76
0.75
0.74
0.73
0.72
Fluorescence intensity
(e)
0
2
4
6
8
10
Time (s)

Fluorescence changes that accompany the reaction when other mutants (Y53H,F39W; F39H,Y64W or N26,76D,F39W) react with κ-chain are shown in Figures 6.3 to 6.5, respectively.

The software provided with the instrument allows both contributory parts of these curves to be analysed and thus two rates can be calculated for each reaction. For mutants bearing W39, the changes in fluorescence are both positive and therefore the double exponential curve can be fitted according to a double exponential equation as described in Chapter 2, section 2.5.5. However, for mutants bearing W64, the observed changes are, as described above, first positive and then negative. Such curves cannot be easily analysed by a double exponential algorithm without additional information, therefore these curves were analysed in two parts as shown later in Fig. 6.4a and 6.4b. Here, the first rapid increase in fluorescence can be analysed by restricting the time period selected for analysis using the 'fit-range' command on the SX17-ASVD software. This set of data was then analysed by a single exponential equation (Chapter 2, section 2.5.5). Then the signal change selected for analysis was changed to the period when the decrease in fluorescence intensity was being monitored and again the data were analysed by a single exponential equation. This method was also used for some analyses of reactions involving the W39 mutation in order to check that the two methods gave similar results.

6.2. Possible kinetic models to explain the biphasic fluorescence changes

There are several possible models that might give rise to such fluorescence changes and these are outlined below.

6.2.1. Model 1

A dimer of PpL may interact with a single molecule of κ-chain to form an intermediary complex (see Fig. 6.6(a)). This may destabilise the dimeric form of PpL and result in the dissociation of the PpL.κ-chain complex into a complex formed by one equivalent of PpL in complex with κ-chain and a free equivalent of

PpL. The liberated monomer may then bind to a κ-chain to form another complex. In this model, the rapid change in fluorescence would occur as the κ-chain binds to PpL or PpL dimer (k_1). The slow change in fluorescence might be due to the rate of binding of the second molecule of κ-chain to the free monomeric PpL (k_1) being rate-limited by the rate of dissociation of the dimer of PpL (k_2).

However, contrary to this model, single phase kinetics are not observed in conditions of excess PpL. This would be expected if PpL existed as a dimer under these conditions, unless κ-chain binds more strongly to single PpL domains than to dimers of PpL in which case biphasic kinetics would be observed provided that k_1 is larger than k_2.

Mutants, such as N26,76D,F39W, have been constructed in work described in this thesis which have all 4 possible intermolecular H-bonds between PpL domains in a putative dimer eliminated. The reaction profiles for the interaction of these proteins with κ-chain still show two phase binding kinetics, further indication that the participation of a dimeric form of PpL is unlikely.
In support of this conclusion, analytical centrifugation studies (B.Sutton, personal communication) have shown that PpL is a monomer at concentrations up to 3mg ml^{-1} and, more recently, NMR studies in this laboratory have also failed to demonstrate the existence of a dimeric form of PpL (J. Werner, personal communication). Therefore it is extremely unlikely that PpL is a dimer at the much lower protein concentrations used in the experiments in this thesis. This is also the conclusion drawn from Forster Resonance Energy Transfer experiments described in Chapter 5. Therefore this mechanism has now been eliminated.

6.2.2. Model 2

A second possible mechanism that would give rise to biphasic fluorescence changes is one in which an initial complex formed by the reaction between a monomeric PpL domain and κ-chain is followed by a slow rearrangement of

the complex that may involve structural changes in either or both of the participants in the reaction (see Fig. 6.6). The two versions of this model again involve two sequential steps. The first step being the formation of an initial encounter complex, the second step being some form of structural rearrangement. In model 2(a) the structural rearrangement involves a conformational change in one or both of the components of the encounter complex, whereas model 2(b) may be a rearrangement of the complex without, for example, any conformational changes. However, in model 2(b) the stoichiometry of the final complex would be 2 κ-chains bound per domain of PpL. This has never been observed in solution conditions but has been more recently identified under crystallisation conditions (Graille *et al.*, 2001).

Model 2(a) fitted all of the available data available at the time of these studies i.e. only monomeric PpL has been observed , 1:1 stoichiometries for the PpL:κ-chain complexes were observed by NMR (Wikström *et al.*, 1995) and PpL was shown not to form an immuno-precipitate with IgG suggesting only one binding site for Fab per domain. This model was therefore adopted for the analysis of the binding reaction.

$$\text{PpL} + \kappa \underset{k_{-1}}{\overset{k_1}{\rightleftharpoons}} \text{PpL.}\kappa \underset{k_{-2}}{\overset{k_2}{\rightleftharpoons}} [\text{PpL.}\kappa]^* \qquad (5)$$

In this model a rapid increase in fluorescence occurs on the formation of the 'encounter' binary complex PpL.κ and that the slow change in fluorescence occurs as PpL.κ rearranges to $[\text{PpL.}\kappa]^*$. This model has been proposed for a number of other protein – ligand systems (Chaiyen *et al.*, 1997; Wallis *et al.*, 1995). Here, k_1 ($M^{-1}s^{-1}$) is the second order rate constant for the formation of the binary complex and k_{-1} (s^{-1}) is the first order rate of dissociation of the complex. The rate of the fast change of fluorescence intensity is proportional to PpL concentration and represents the rate of formation of PpL.κ. Therefore, providing that the rate of formation of the encounter complex [PpL.κ] is rapid compared to the structural rearrangement the two parts of the process can be considered as two separate reactions, k_1 and k_{-1} may be derived from the slope and intercept, respectively, of a

plot of k_{obs} against the final concentration of PpL and the K_d for the encounter complex is given by k_{-1} / k_1.

The observed forward rate for the structural rearrangement is = $k_2 + k_{-2}$ ie. the sum of the forward and reverse rates of the structural rearrangement between PpL.κ and [PpL.κ]*. It is not possible to say whether the change occurs in either or both proteins in the complex. To obtain k_{obs}, k_2 must be multiplied by the fraction of the κ in the first complex PpL.κ. This is readily calculated by considering the initial part of the reaction ie.

$$\mathrm{PpL} + \kappa \underset{k_{-1}}{\overset{k_1}{\rightleftharpoons}} \mathrm{PpL}.\kappa.$$

$$K_d = \frac{[\mathrm{PpL}][\kappa]}{[\mathrm{PpL}.\kappa]} = \frac{k_{-1}}{k_1} \qquad (6)$$

In which [PpL], [κ], and [PpL.κ] are the concentrations of these components at equilibrium. This can be rearranged to give

$$[\mathrm{PpL}.\kappa] = \frac{[\mathrm{PpL}][\kappa]}{K_d} \qquad (7)$$

and the fraction of κ present in the complex will therefore be

$$= \frac{[\mathrm{PpL}.\kappa]}{[\kappa] + [\mathrm{PpL}.\kappa]} \qquad (8)$$

Substituting [PpL.κ] in the above equation by [PpL][κ] / K_d and simplifying we get the fraction of κ in the form PpL.κ

$$= \frac{[\mathrm{PpL}]}{[\mathrm{PpL}] + K_d} \qquad (9)$$

$$\text{Thus} \qquad k_{obs} = k_{-2} + \frac{k_2[\text{PpL}]}{[\text{PpL}] + \text{K}_\text{d}} \qquad (10)$$

If K_d is very low then $k_{obs} = k_{-2} + k_2$ and little correction to k_2 is required. This is the case for the wild-type PpL and mutants of PpL when [PpL] is 30μM and K_d is up to 3μM, the correction being approximately 10%.

In the reaction between PpL and κ-chain, k_{-2} can be measured directly by 'displacement' techniques. In these, preformed complexes of e.g. F39W labelled mutant PpL and κ-chain are diluted by a large excess of wild-type PpL (which lacks Trp residues and therefore gives no change in fluorescence intensity at 335nm on binding to κ-chain). Thus the decrease in fluorescence noted from the reaction of wild-type PpL with the F39W derivative mutant complex is due to the dissociation of the F39W mutant from its binary complex with κ-chain. The observed rates for these reactions are equal to k_{-2} direct, since in these experiments, the reaction in the forward direction (k_2) involving mutant proteins is competitively inhibited by a large excess of the wild-type PpL that lacks Trp residues. By subtracting the value of k_{-2} from the value of k_{obs} for the forward conformational change it is possible to calculate the value of k_2.

For this model, the K_d for the encounter complex is k_{-1} / k_1 and at equilibrium the overall K_d is dependent upon all four rate constants and is described by;

$$K_d = \frac{k_{-1}}{k_1} \times \frac{1}{1 + k_2 / k_{-2}} \qquad (11)$$

(Wallis *et al.*, 1995)

If k_2, the forward rate of the conformational change, is very large compared to k_{-2}, the rate of the reversal of the conformational change, then this simplifies to

$$K_d = \frac{k_{-1}}{k_1} \cdot \frac{k_{-2}}{k_2} \qquad (12)$$

Thus by determining the value of each of these rate constants the effect of mutations on the pre-equilibrium or equilibrium K_d can be deduced.

6.3 Results

Stopped flow fluorescence studies were carried out on PpL domains bearing unique Trp residues. In particular, the F39W PpL (in order to obtain kinetic data on this 'standard protein' under the conditions used in these experiments), on the potentially useful Y53H,F39W PpL and F39H,Y64W proteins (to determine how the mutations have led to an increase in K_d at equilibrium) and on N26,76D,F39W (to observe whether these mutations have affected the rate of any structural rearrangement).

6.3.1 F39W

Figure 6.2b shows a reaction progress curve obtained when 30μM F39W was rapidly mixed with 2μM κ-chain (final concentrations) in 20mM phosphate buffer at pH 8.0, 25°C. The trace shows a double exponential increase increase in fluorescence as expected. The experiment was completed by mixing a series of concentrations of F39W with κ-chain and determining the k_{obs} of each reaction. In practice, between 3 and 5 reaction profiles were averaged for each experiment and data were collected over various time periods so that the both the fast and slow phase on the reaction could be viewed as the dominant part of the reaction. The data are given in Table 6.1.

Table 6.1. The effect of varying the concentration of F39W on the observed rates of reaction with 2μM κ-chain (final concentrations). $k_{1\ obs}$ (s^{-1}) is the observed rate of formation of the initial complex and $k_{2\ obs}$ (s^{-1}) is the observed rate of the proposed structural rearrangement.

Concentration of F39W (μM)	$k_{1\ obs}$ (s^{-1})	$k_{2\ obs}$ (s^{-1})	k_2 (s^{-1})
10	7.6	4.3	5.1
15	12.5	4.9	5.3
20	13.1	4.1	4.1
25	17.2	4.7	4.8
30	18.9	4.9	4.9

Figure 6.2c is a plot of $k_{1\ obs}$ (s^{-1}) against the concentration of PpL F39W in the reaction. The intercept shows that k_{-1} (s^{-1}) is 2.94 (s^{-1}) and k_1 is 0.546 x 10^6 $M^{-1}s^{-1}$ which indicate a K_d for the pre-equilibrium complex of 5.39μM, close to that published by Beckingham *et al.*, (1999)

The values of $k_{2\ obs}$ (s^{-1}) were incorporated into equation (10) above to determine the corrected values of k_2 which were then plotted against the concentration of F39W used for the reaction. The results (see Fig. 6.2d) show that the calculated rate of k_2, (5.05s^{-1}) does not change with the concentration of F39W supporting the proposal that this change in signal is not due to a second order binding reaction but could be due to a structural rearrangement occurring in one (or both) proteins.

Finally, Fig.6.2e shows the decrease in fluorescence when a complex, preformed by mixing 8μM κ-chain with 8μM F39W is rapidly diluted 1:1 v/v by 60μM WT PpL. The plot shows that the decrease in fluorescence has a half time of approximately 1.5s and a rate of 0.46 s^{-1} under the conditions used.

Substituting this information into equation (11) we can estimate the K_d at equilibrium to be = 5.39μM x 1 / (1 + (5.05 / 0.46)), thus K_d = 0.45μM.

6.3.2 Y53H,F39W

Figures 6.3 a – b describe parallel experiments to the above but using the mutant Y53H,F39W. This protein carries the F39W reporter group and was therefore expected to give a double exponential increase in fluorescence intensity as it reacted with κ-chain. However, as Fig. 6.3a shows the reaction progress curve could be satisfactorily analysed by a single exponential equation since the 'residuals plot' shown beneath the reaction curve shows no significant deviation from a straight line over the whole time course of the reaction. This does not necessarily mean that no post-binding structural rearrangement is taking place, but that fluorescence spectroscopy may not report the change. Additionally, it is possible that the forward rate of the proposed structural rearrangement is so fast that it is rate limited by the binding phase. Calculation of k_1 (0.70×10^6 $M^{-1}s^{-1}$) and k_{-1} ($4.7s^{-1}$) from Fig. 6.3b suggests that the pre-equilibrium K_d = 6.71μM, similar to that obtained with F39W. Therefore it appears that this mutation has not significantly altered the K_d due to changes in the initial bimolecular contacts between the two reacting proteins. Competitive ELISA studies in Chapter 5 indicated that this mutant has an equilibrium K_d for the complex with κ-chain approximately 13 fold higher than that of WT PpL. Therefore, in this model whereas the F39W domain (equivalent to WT PpL) achieves its high affinity at equilibrium for κ-chain by the complex undergoing a structural rearrangement in which the forward rate k_2 is much higher than rate k_{-2}, it is possible that the Y53H,F39W mutant does not. This would explain the lack of a slow fluorescence change after the initial complex has formed. If this is correct then the equilibrium K_d will remain at 6.71μM and thus give the mutant a lower affinity for κ-chain than F39W. A K_d of 6.71μM is, however, slightly higher than that obtained by competitive ELISA experiments (4.6μM). The difference may of course be due to the different experimental techniques or due to the failure to detect any slow

Figure 6.3a The change in fluorescence intensity at 335nm when 10μM Y53H,F39W is reacted with 2μM κ-chain.

The increase in fluorescence intensity was fitted to a single exponential equation. The residuals to the fit can be seen in the figure below. The conditions used are described in chapter 2.

Figure 6.3b A plot of the observed rate of reaction against concentration of Y53H,F39W.

The slope indicates k_1 and has a value of 0.702 x 10^6 $M^{-1}s^{-1}$ and the intercept on the ordinate shows that k_{-1} is 4.72s^{-1}.

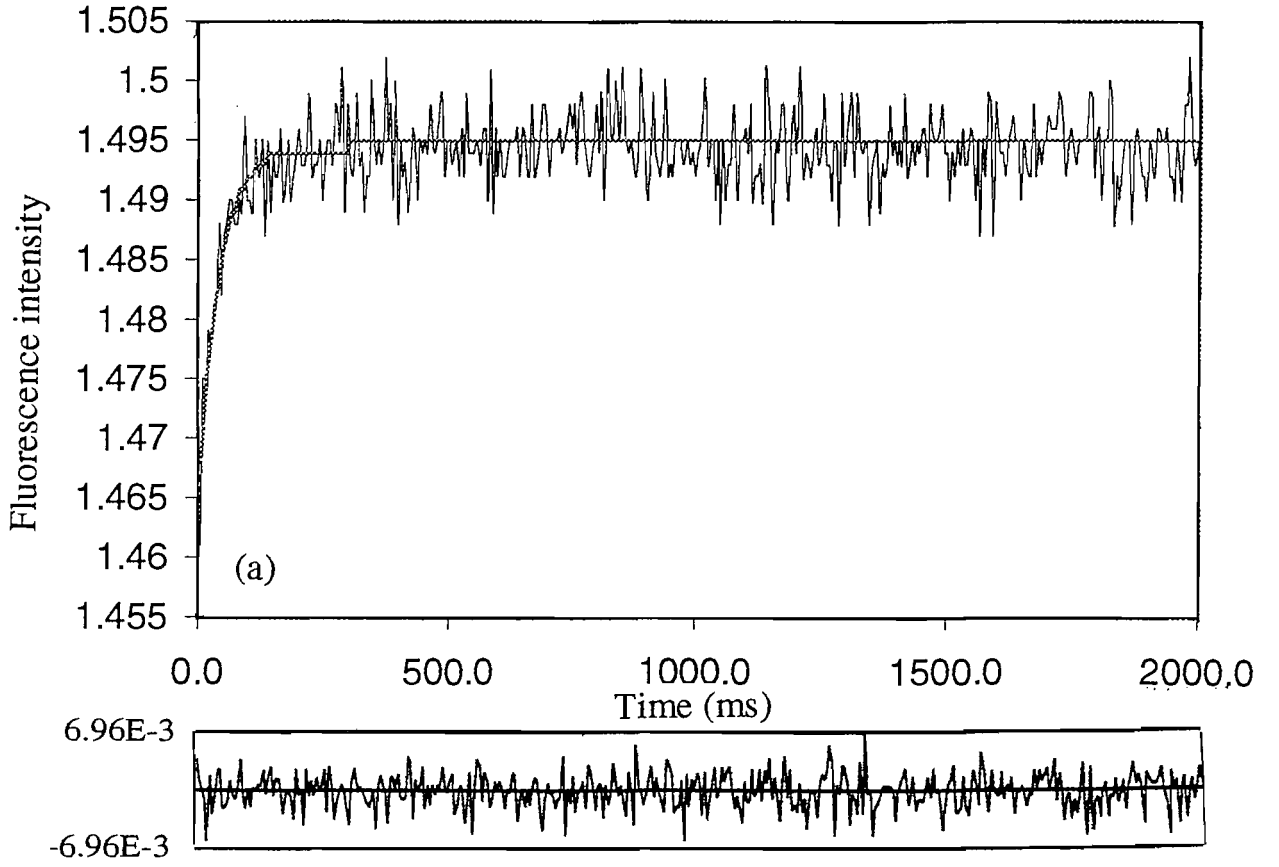
1.505
1.5
1.495
1.49
1.485
1.48
1.475
1.47
1.465
1.46
1.455
Fluorescence intensity
(a)
0.0
500.0
1000.0
1500.0
2000.0
Time (ms)
6.96E-3
-6.96E-3

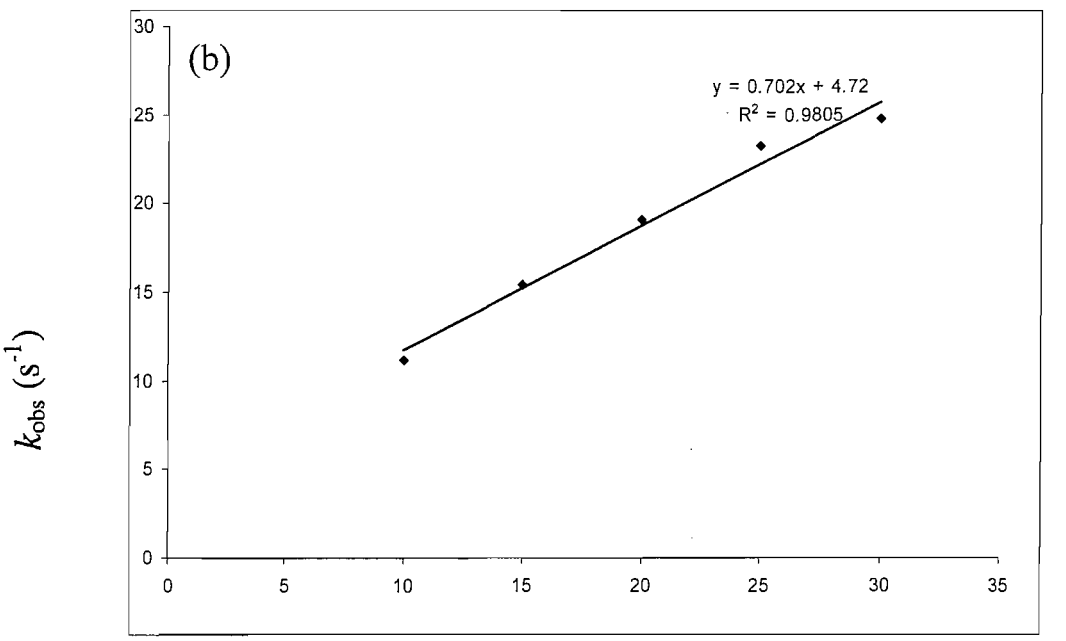
(b)
y = 0.702x + 4.72
R² = 0.9805
30
25
20
15
10
5
0
0
5
10
15
20
25
30
35
k_{obs} (s^{-1})
PpL [μM]

conformational change occurring in its complex with κ-chain. The closeness of the calculated K_d obtained by the above by kinetic analysis to that obtained by equilibrium techniques makes the possibility of a structural rearrangement being rate limited by the binding reaction improbable.

6.3.3 F39H,Y64W

Experiments with this mutant showed that two distinct processes were occurring during its reaction with κ-chain. Figure 6.4a and b show the same reaction progress curve obtained when 30μM F39H,Y64W was mixed with 2μM κ-chain (final concentration). Figure 6.4a shows the fit to the initial part of the curve and Fig. 6.4b shows the fit to the second phase of the change in fluorescence intensity. An initial increase in fluorescence intensity occurs with an observed rate of approximately $15.4s^{-1}$ followed by a slow decrease in fluorescence (as expected for a domain carrying the Y64W mutation) with an observed rate of approximately $1s^{-1}$.

Figure 6.4c shows a series of typical reactions using this mutant between 10μM (bottom trace), 15μM, 20μM, 25μM and 30μM (top trace) and Fig. 6.4d shows the plot of $k_{1\ obs}$ (s^{-1}) against total protein concentration (μM). From this plot the value of k_1 was found to be $0.72x10^6M^{-1}s^{-1}$ and k_{-1} was found to be $5.4s^{-1}$. These yield a value of 7.5μM for the pre-equilibrium K_d. The observed value of k_2 was found to be $1.04s^{-1}$ using 20μM F39H,Y64W in reactions with 2μM κ-chain and k_{-2} was found to be $0.7s^{-1}$ (Fig. 6.4e). Using this in equation (10) the true value of k_2 was found to be $0.36s^{-1}$.

Therefore under these conditions the F39H,Y64W mutant has an equilibrium K_d of 4.95μM, slightly higher than the value of 1.53μM gained by competitive ELISA experiments.

Figure 6.4 The change in fluorescence intensity at 335nm observed when 30μM F39H,Y64W is reacted with 2μM κ-chain.

The change in fluorescence was resolved into the two phases ;

Figure 6.4a shows the rapid increase in fluorescence occurring over the first 200ms.

Figure 6.4b shows the slower decrease in fluorescence observed over the time period 200ms to 2s.

Each phase was fitted to a single exponential equation. The observed rate of the fast phase is $16.4s^{-1}$ and that of the slow phase is approximately $1s^{-1}$.

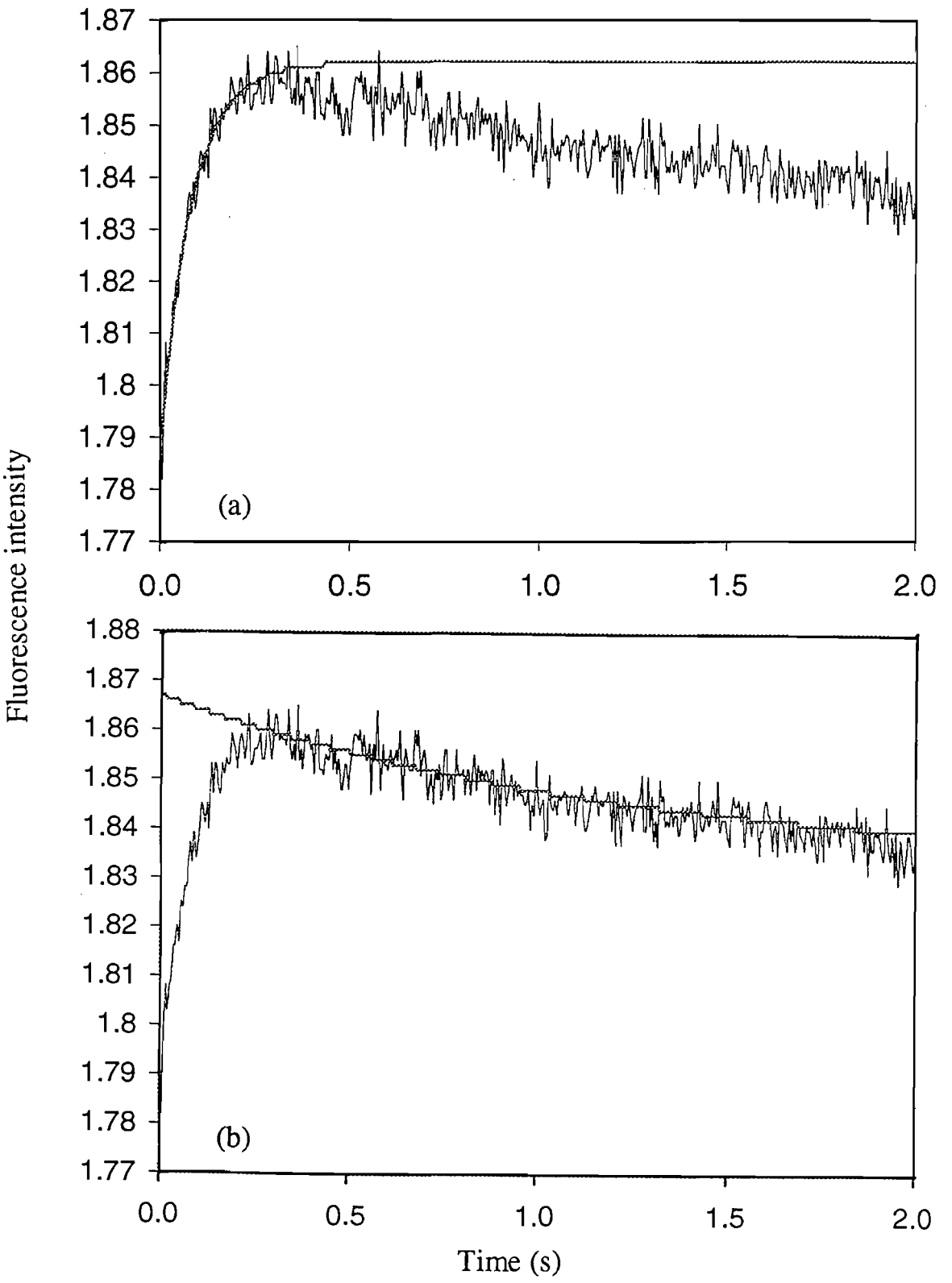
Fluorescence intensity
1.87
1.86
1.85
1.84
1.83
1.82
1.81
1.8
1.79
1.78
1.77
(a)
0.0
0.5
1.0
1.5
2.0
1.88
1.87
1.86
1.85
1.84
1.83
1.82
1.81
1.8
1.79
1.78
1.77
(b)
0.0
0.5
1.0
1.5
2.0
Time (s)

Figure 6.4c Typical reaction progress curves obtained when 2μM κ-chain is reacted with different concentrations of F39H,Y64W.

The traces recorded show the reactions of 2μM κ-chain with (from bottom to top) 10μM, 15μM, 20μM 25μM and 30μM F39H,Y64W under standard conditions (see chapter 2).
The figure illustrates how the total fluorescence intensity of the reaction mixture increases with increasing F39H,Y64W concentration. The figure also gives a visual indication of the virtual independence of k_{2obs} on the concentration of PpL.

Figure 6.4d A plot of k_{1obs} (s^{-1}) against concentration of F39H,Y64W.

From this plot the value of k_1 was found to be 0.72 x 10^6 $M^{-1}s^{-1}$ and k_{-1} was found to be 5.4s^{-1}.

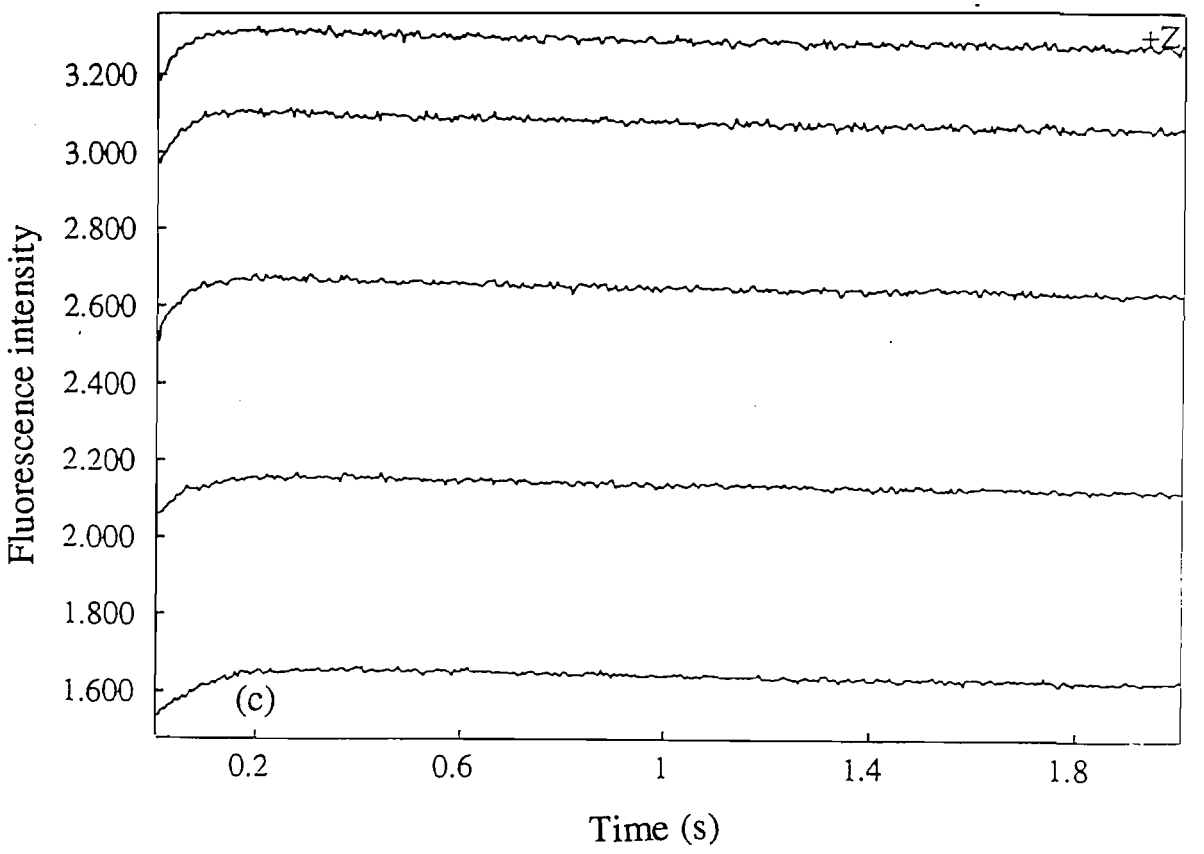
+Z
3.200
3.000
2.800
2.600
2.400
2.200
2.000
1.800
1.600
Fluorescence intensity
(c)
0.2
0.6
1
1.4
1.8
Time (s)

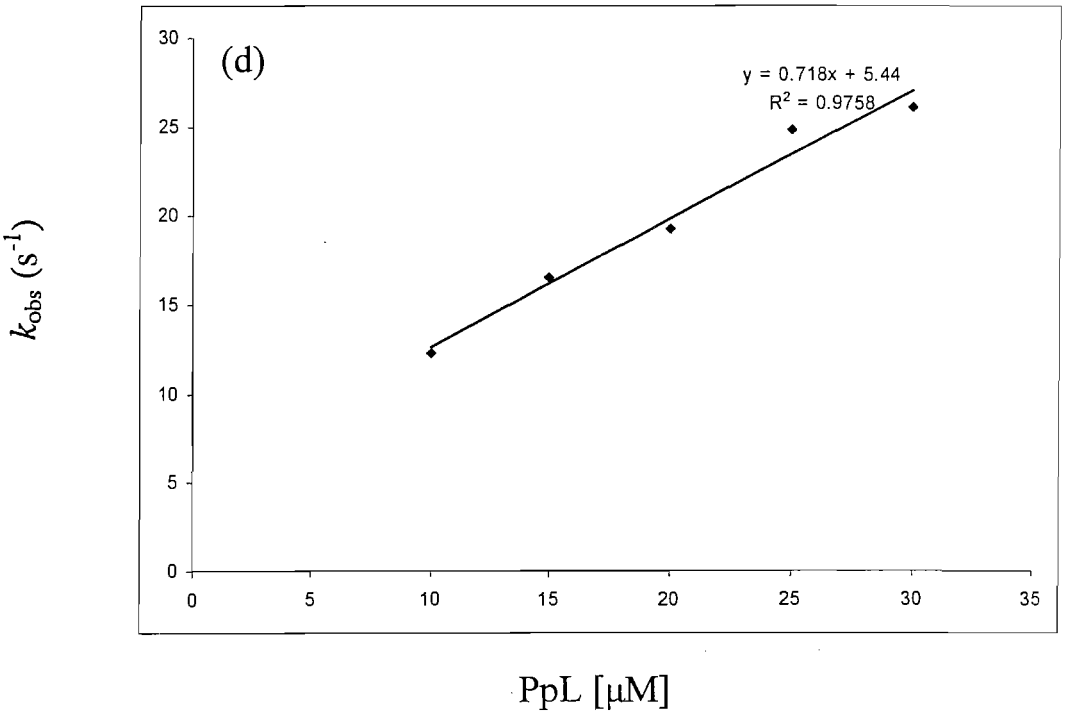
(d)
y = 0.718x + 5.44
R² = 0.9758
30
25
20
15
10
5
0
0
5
10
15
20
25
30
35
kobs (s-1)
PpL [μM]

Figure 6.4e The change in fluorescence intensity observed when a complex formed between F39H,Y64W and κ-chain is rapidly mixed with 30μM WT PpL.

The curve shows the loss in fluorescence intensity at 335nm when a preformed complex made by mixing 8μM F39H,Y64W and 8μM κ-chain in 20mM phosphate buffer, pH 8.0 was diluted 1:1 v/v with 60μM WT PpL. The reaction shown has an observed single exponential rate of $0.7s^{-1}$.

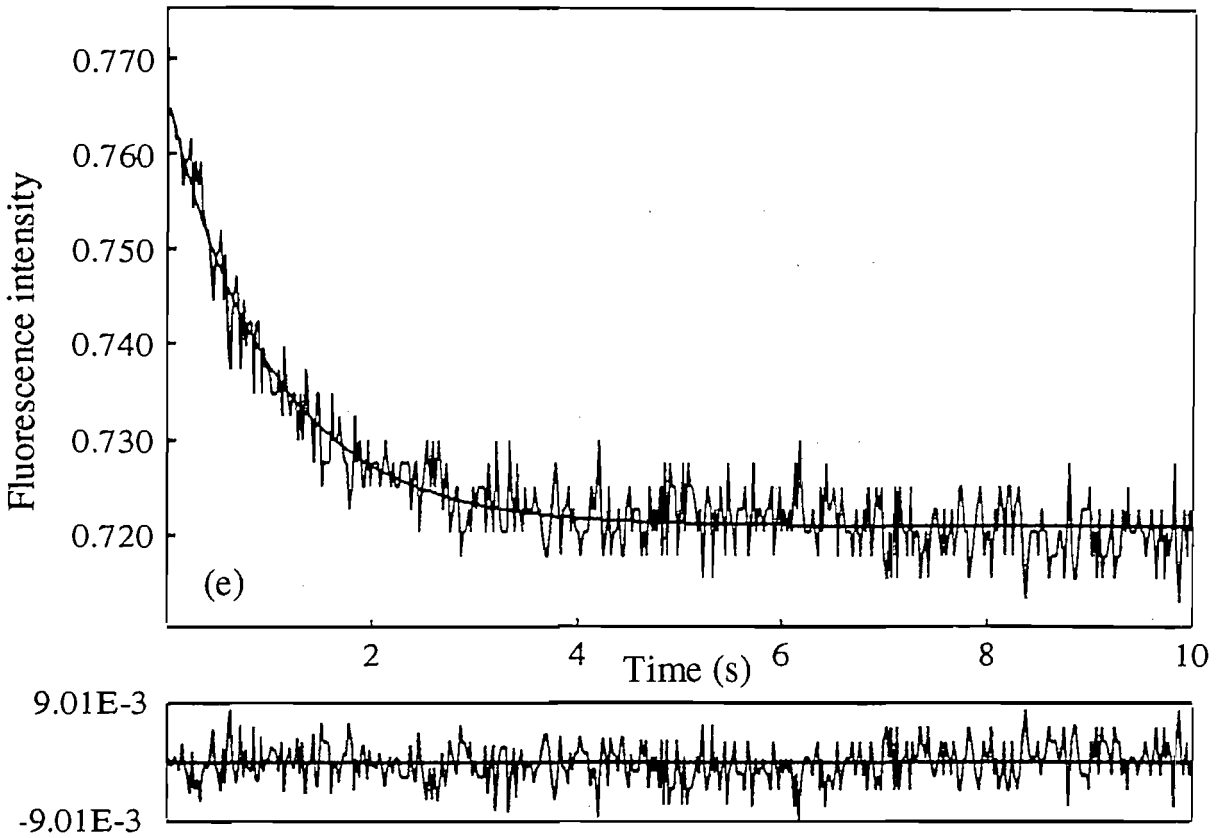
0.770
0.760
0.750
0.740
0.730
0.720
Fluorescence intensity
(e)
2
4
6
8
10
Time (s)
9.01E-3
-9.01E-3

However, whereas the Y64W mutant shows a large change in fluorescence intensity as the proposed conformational change takes place, the change in fluorescence intensity of the F39H,Y64W mutant after the initial contact with κ-chain is made is restricted to a 35% decrease. This may be due to one or a combination of phenomena. Firstly, the change in quantum yield from the Y64W reporter as the structural rearrangement takes place may not be the same in different domains in which it is placed. Secondly, the smaller decrease in fluorescence seen here may be due to the equilibrium between PpL.κ and $[PpL.\kappa]^*$ not moving over to the right (see equation 5) due to a change in relative affinities of the two species for κ-chain i.e. different ratios of k_2 to k_{-2} in Y64W and F39H,Y64W. Thus a smaller change in fluorescence decrease would be seen. If we compare the ratio of k_2 to k_{-2} in Y64W (37:1, Beckingham, 1997) to that in F39H,Y64W (1:1.94) then it is clear that the equilibrium position for the second phase of the reaction will favour PpL.κ and not $[PpL.\kappa]^*$. The expected decrease in fluorescence intensity (assuming the change in quantum yield from the reporter group is the same as in Y64W) will be about 34% (i.e. 1 / 2.94) close to the experimentally observed change.

6.3.4 N26,76D,F39W

Experiments using the mutant N26,76D,F39W were carried out to determine whether the second phase of fluorescence change seen with WT and mutated PpL domains is due to a dissociation event taking place after a dimeric form of the protein has formed an encounter complex with κ-chain. It was considered that a dissociation of two domains with bound κ-chain may well allow initial weak complexes to relax and enable high affinity complexes to form. The mutations N26,76D remove the H atoms thus breaking the proposed H bonds. The F39W mutation is also present to provide a spectral reporter group.

Figure 6.5a shows a typical reaction progress curve when 10μM domain was mixed with 2μM κ-chain (final concentrations) in buffer conditions as described above. A full analysis of the experiments showed that k_1 is 0.50 x 10^6 $M^{-1}s^{-1}$, k_{-1} is 1.97 s^{-1}, k_2 is 2.43 s^{-1} and k_{-2} is 0.14 s^{-1}. Thus the calculated pre-equilibrium K_d is

Figure 6.5a The change in fluorescence intensity at 335nm observed when 10μM N26,76D,F39W was reacted with 2μM κ-chain.

The increase in fluorescence intensity was fitted to a double exponential equation as detailed in the text. The residuals to the fit are shown in the figure below the reaction progress curve.

Figure 6.5b A plot of the observed rate of reaction against the concentration of N26,76D,F39W.

The slope indicates k_1 and has a value of 0.49 x 10^6 $M^{-1}s^{-1}$ and the intercept on the ordinate shows that k_{-1} is 1.97s^{-1}.

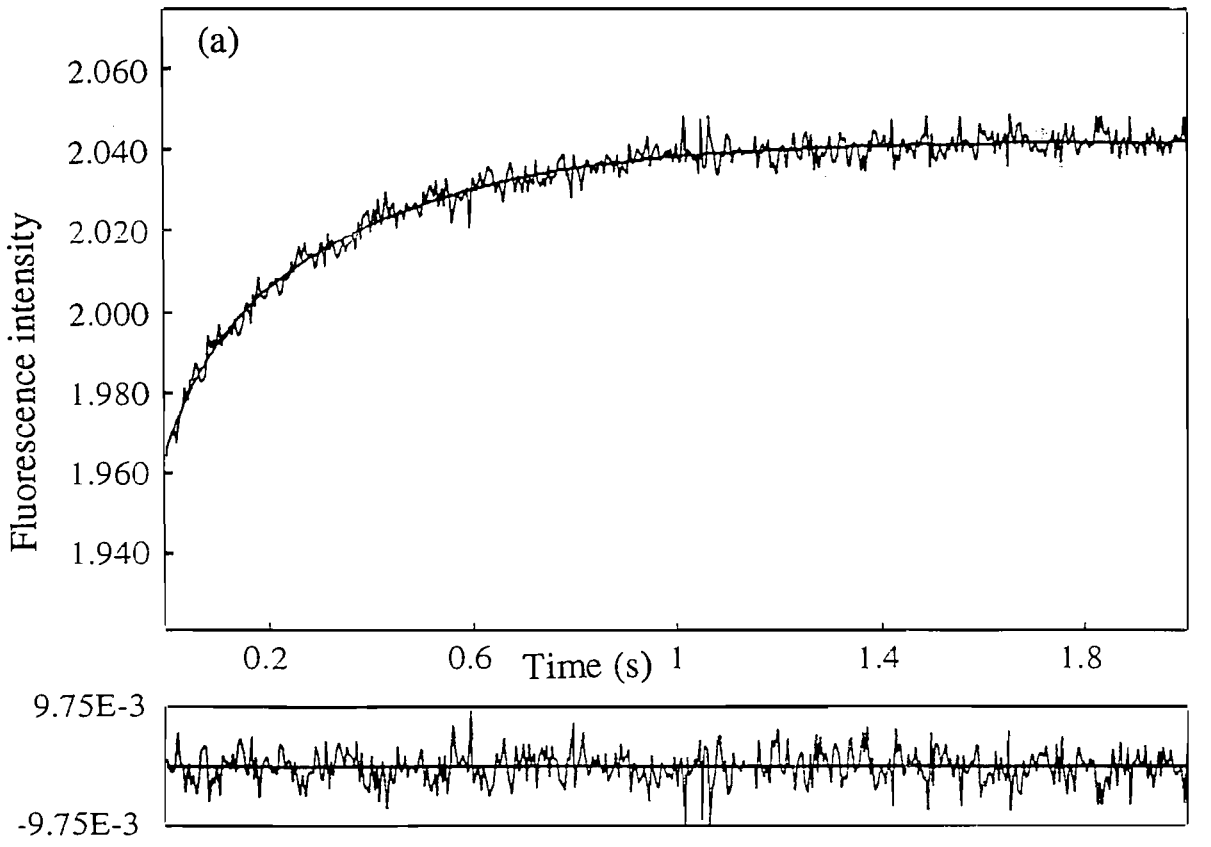
(a)
2.060
2.040
2.020
2.000
1.980
1.960
1.940
Fluorescence intensity
0.2
0.6
Time (s)
1
1.4
1.8
9.75E-3
-9.75E-3

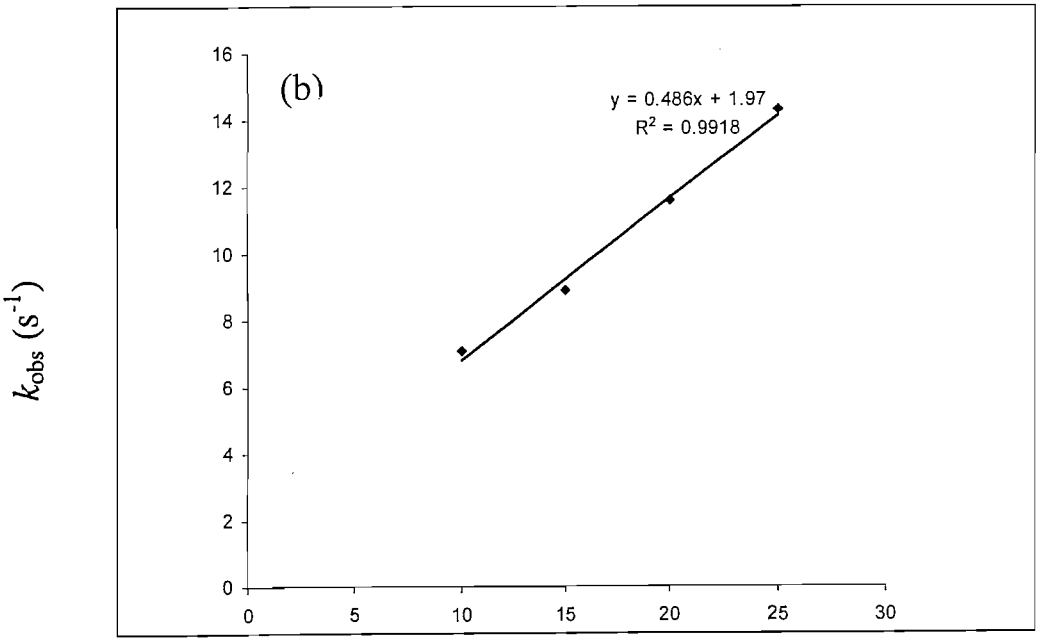
(b)
y = 0.486x + 1.97
R² = 0.9918
16
14
12
10
8
6
4
2
0
0
5
10
15
20
25
30
kobs (s-1)
PpL [μM]

Figure 6.5c The change in fluorescence intensity observed when a complex formed between N26,76D,F39W and κ-chain is rapidly mixed with 30μM WT PpL.

The curve shows the loss in fluorescence intensity at 335nm when a preformed complex made by mixing 8μM N26,76D,F39W and 8μM κ-chain in 20mM phosphate buffer, pH 8.0 was diluted 1:1 v/v with 60μM WT PpL. The reaction shown has an observed single exponential rate of $0.14s^{-1}$.

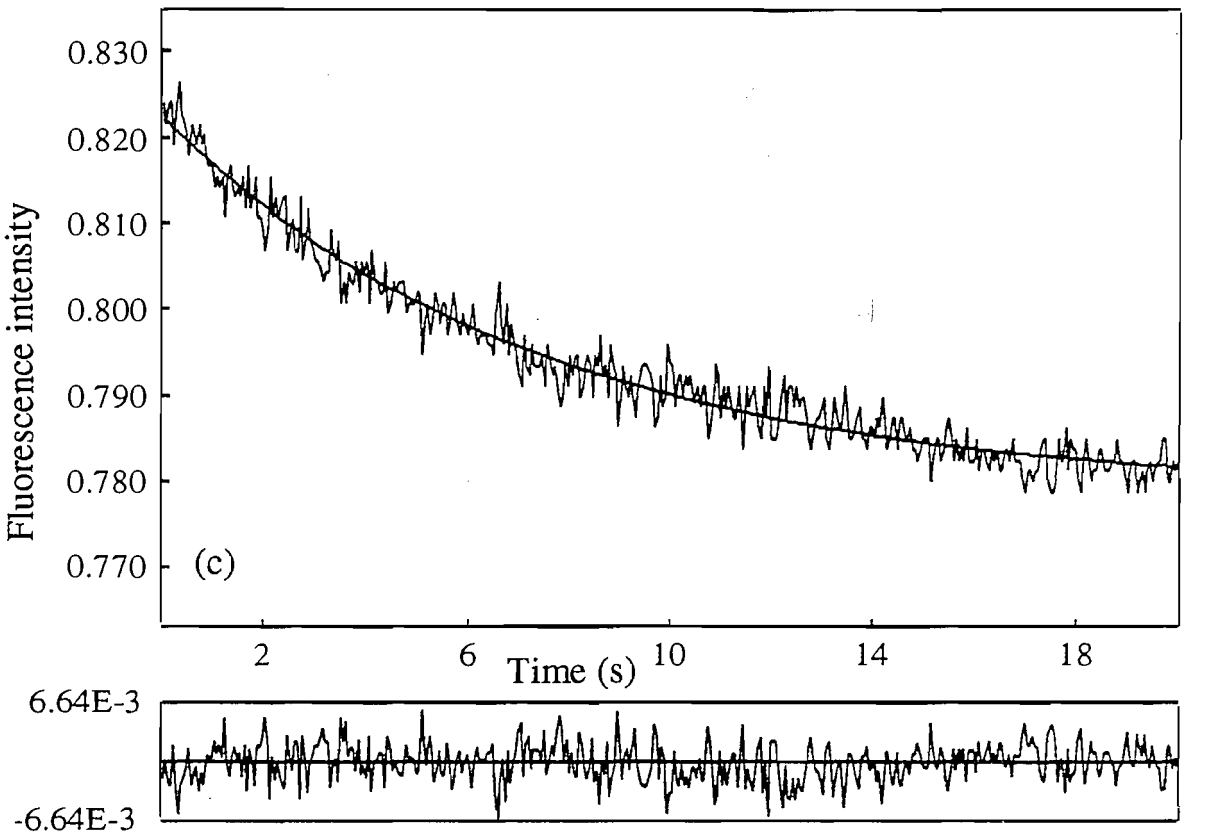
0.830
0.820
0.810
0.800
0.790
0.780
0.770
Fluorescence intensity
(c)
2
6
10
14
18
Time (s)
6.64E-3
-6.64E-3

3.94μM and the equilibrium K_d is 0.21μM, in agreement with the value determined by competitive ELISA experiments (0.14 μM).

However, perhaps the most important observation is that there actually is a second slow phase to the change in fluorescence on formation of a complex. In fact this change is approximately two fold slower than that shown by the F39W binding reaction. Thus the possible loss of four hydrogen bonds between domains in a dimeric structure has not facilitated the change to a high affinity complex as might be expected if the two domains dissociated easier without their presence (see 6.3.1).

6.4 Conclusions

Table 6.2 shows the K_d values at pre-equilibrium and at equilibrium for the reactions involving the mutants described here.

Table 6.2. The values of the K_ds obtained under pre-equilibrium and equilibrium conditions at 25°C.

Protein	K_d (pre-equilibrium) μM	K_d (equilibrium) μM
F39W	5.39	0.45
Y53H,F39W	6.71	6.71
F39H,Y64W	7.50	4.95
N26,76D,F39W	3.94	0.21

The stopped flow experiments have shown that the affinity of N26,76D,F39W for κ-chain is similar to that of F39W and WT PpL in agreement with other methods for determining their respective K_d values. These observations, together with recent results from sedimentation studies that failed to detect any dimeric species of PpL in solution (Dr. Brian Sutton, King's college, London, personal

communication) has led to the conclusion that a dissociation process is not the cause of the structural rearrangement seen in these binding studies.

The studies have suggested that the mutant Y53H,F39W may have an increased K_d for κ- chain because the mutation has dramatically reduced the forward rate of the proposed structural rearrangement that occurs after initial contacts with κ-chain. This is in agreement with studies on the mutant Y53F,Y64W (Beckingham, 1997) that show similar reaction progress curves that completely lack a noticeable second phase. Furthermore, the K_d at equilibrium for that mutant was also lower than the pre-equilibrium K_d suggesting that a structural rearrangement may well be taking place but is not reported by a fluorescence change. The mutant F39H,Y64W also has a decreased affinity for κ-chain primarily due to a low value of k_2, the rate of the forward structural rearrangement. This may be significant since the mutation F39W has been shown to markedly affect the stability of the domain (see Chapter 4) and may have reduced the intra or intermolecular interactions that are necessary for any possible structural rearrangement to take place.

The difference in binding energy between the proposed pre equilibrium and equilibrium states of PpL and κ-chain is approximately the energy of one H-bond (Beckingham *et al.*, 1999), suggesting that any structural rearrangement on binding is very small. A possible mechanism could be a simple docking followed by a re-alignment without any significant structural change.

$$\text{PpL} + \kappa \underset{k_{-1}}{\overset{k_1}{\rightleftharpoons}} \text{PpL.}\kappa \underset{k_{-2}}{\overset{k_2}{\rightleftharpoons}} \text{PpL.}\kappa^*$$

Where k_1 is the rate of initial docking, k_2 is the rate of structural rearrangement and k_{-1} and k_{-2} are the reverse rates for these processes, respectively. PpL.κ is a pre-equilibrium complex where the κ-chain has bound but structural rearrangement has not yet taken place and PpL.κ* is the final conformation after initial complex formation followed by any rearrangement. Such a model gives a plausible explanation for the lower affinity exhibited by the Y53 mutants. In the reaction between Y53F PpL and

κ-chain there is only a rapid, mono-phasic reaction progress curve, there is no slow change in fluorescence intensity. This was postulated to be due to the loss of a H-bond between the hydroxyl group of the Tyr sidechain and a peptide group of κ-chain. The difference in K_d for the complex between WT PpL and κ-chain and that between Y53F PpL and κ-chain is approximately 30 fold and the difference in binding energy is equivalent to that of a single H bond (Beckingham *et al.*, 1999). Thus the structural rearrangement may be quite small.

Although this model initially explained all the available data, it has now been shown by X-ray crystallography studies (Graille *et al.*, 2001) that the secondary structures of PpL and κ-chain after formation of a complex are not significantly different to those of the free proteins. Some disturbance of side chain orientation occurs although these changes would normally be expected to occur rapidly (J. Werner, University of Southampton, personal communication). However, crystals were found that contained complexes between PpL and two equivalents of Fab demonstrating that PpL has more than on binding site for light chains. The relative affinity of site 1and site 2 for the Fabs was estimated at approximately 50-100 fold. Thus the newly observed second site does not contribute greatly to the equilibrium concentration of bound light chain unless the latter is at a very high concentration. However, the existence of the second site allows another model (3) to be proposed and may well explain the biphasic fluorescence changes seen in the binding reaction.

6.5 Model 3

Graille *et al.*, (2001) published a crystal structure with PpL bound simultaneously to two Fab domains at two separate sites. Site 1, termed by them as the "classical site" is that described by all of the previously published data. Site 2, however, was novel, uncharacterised and was shown by site directed mutagenesis and analytical centrifugation studies (Graille *et al.*, 2001) to have an affinity for Fab approximately 50 – 100 fold weaker

than site 1. The comparatively weak binding of this site is one of the reasons it has not been detected previously by binding experiments. It was detected because despite it having a low affinity for Fab / κ-chain some of the crystals formed between PpL and the Fab were of a different form, large and were therefore selected for analysis.

The following model in which it is postulated that PpL has two binding sites for κ-chain, one high affinity and one of low affinity, is able to explain all the fluorescence changes occurring on κ-chain binding to PpL and to mutants which have been created, and is compatible with PpL being a monomer in solution. In addition, recent NMR studies (Graille *et al.*, 2002) have identified small chemical shifts for those residues located in the postulated second binding site when bound to κ-chain, clearly indicating the presence of this second site. This model fits the structural data now available. This new model is summarized in scheme 6.1 below.

Scheme 6.1. Taken from Housden *et al.*, 2004

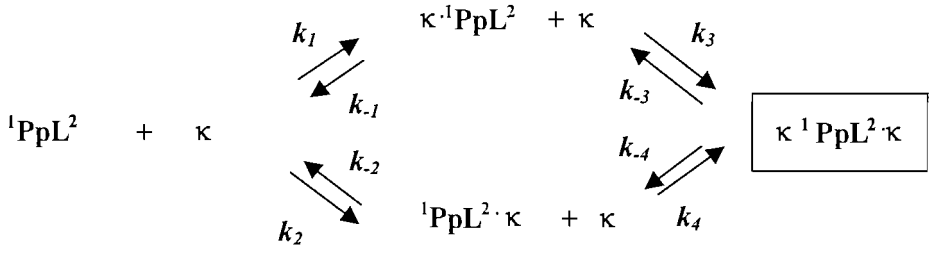

The scheme shows the rates of association and dissociation for each site. Rates k_1 and k_4 are the rates of association to site 1 and k_2 and k_3 are the rates of association of κ-chain to site 2. This assumes that the rates of association to the two binding sites are not affected by the occupation by κ-chain of the other site. A similar assumption is made for the rates of dissociation for the corresponding reactions. Both sites are only likely to be fully occupied in the presence of a high concentration of κ-chain.

Figure 6.6 Possible models for PpL binding to κ-chain.

Model 1

A dimer of PpL may interact with a single molecule of κ-chain to form an intermediary complex. This may destabilise the dimeric form of PpL and result in the dissociation of the PpL.κ-chain complex into a complex formed by one equivalent of PpL in complex with κ-chain and a free equivalent of PpL. The liberated monomer may then bind to a κ-chain to form another complex.

Model 2

A second possible mechanism that would give rise to biphasic fluorescence changes is one in which an initial complex formed by the reaction between a monomeric PpL domain and κ-chain is followed by a slow rearrangement of the complex that may involve structural changes in either or both of the participants in the reaction.
In model 2(a) the structural rearrangement involves a conformational change in one or both of the components of the encounter complex, whereas model 2(b) may be a rearrangement of the complex without, for example, any conformational changes. However, in model 2(b) the stoichiometry of the final complex would be 2 κ-chains bound per domain of PpL.

Model 3

In this model it is postulated that PpL has two binding sites for κ-chain, one high affinity and one of low affinity, is able to explain all the fluorescence changes occurring on κ-chain binding to PpL and to mutants which have been created, and is compatible with PpL being a monomer in solution.

Model 1

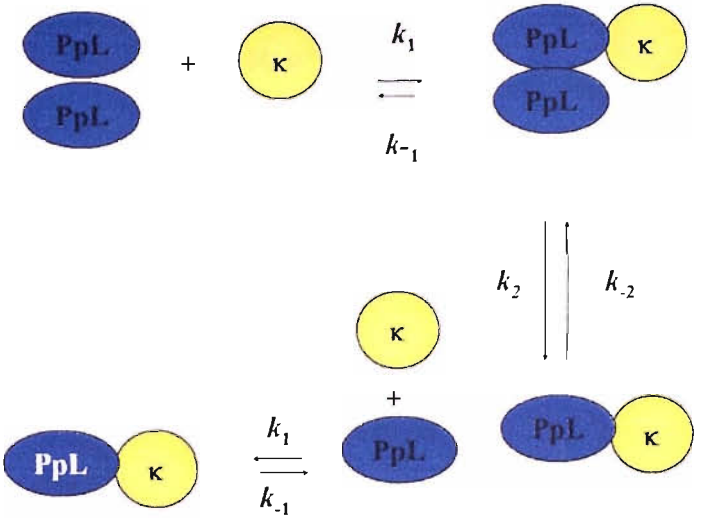

Model 2(a)

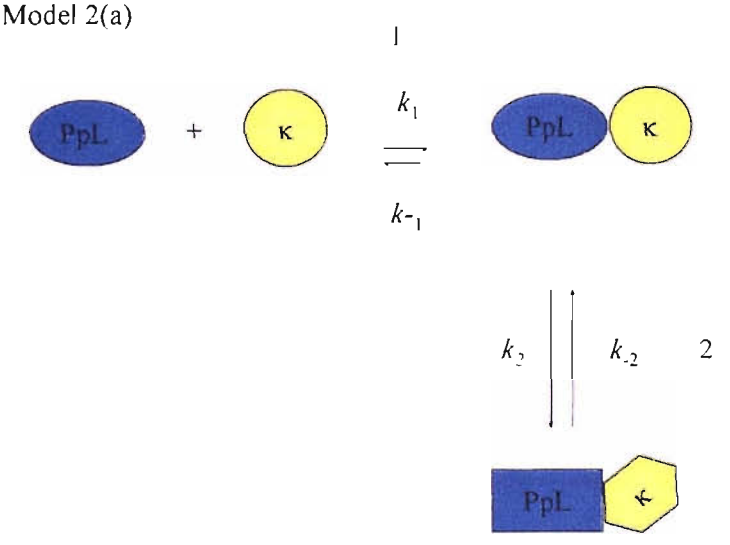

Model 2(b)

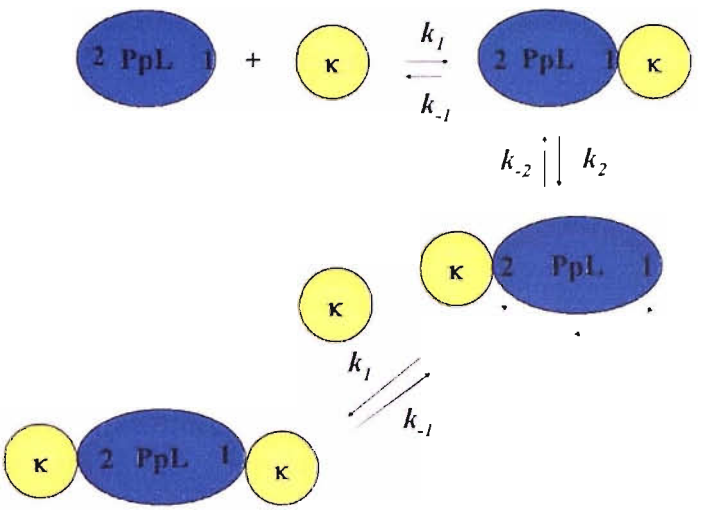

Model 3

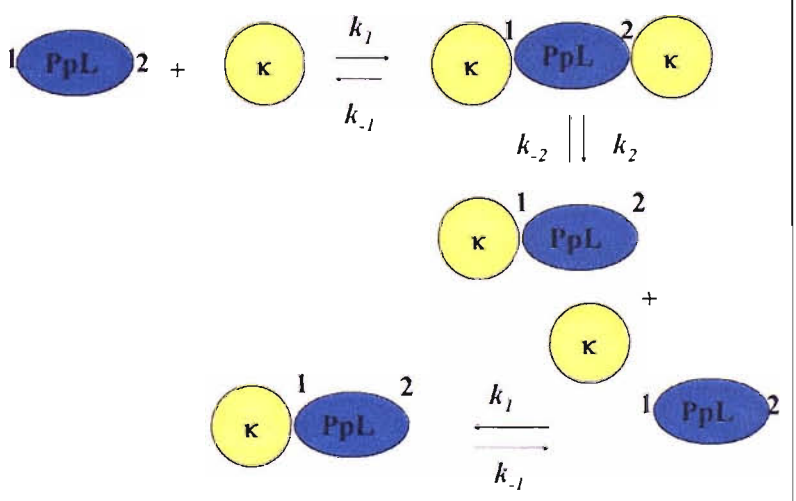

One complexity of the system is that the rates of association (k_{ass}) to each site have been found to be similar, k_{ass} for site 1 being 2 x 10^5 $M^{-1}s^{-1}$ and that for site 2 being 1.5 x 10^5 $M^{-1}s^{-1}$ (Housden *et al.*, 2004). Had these rates been very different then the existence of two sites might have been suspected earlier. However, it appeared that wherever the reporter group was placed in the domain the same reaction was being observed. Small differences such as the 25% noted above in k_{ass} could be attributed to minor structural changes due to the position of the Trp reporter group used.

6.6 The new model applied to the mutants studied in this thesis.

6.6.1 New model applied to Y64W

In this mutant, no replacements have been made in site 1 and the Y64W reporter group is located within the recently identified site 2. In pre equilibrium studies (Figure 6.2a), the initial increase in fluorescence is due to the binding of κ-chain to site 2, thus reducing the solvent accessibility of the Y64W reporter. However, because the rates of dissociation (k_{diss}) from the two sites are very different (k_{diss} for site 1 is 0.008s^{-1} and that for site 2 is 0.56 s^{-1} (Housden *et al.*, 2004)) the equilibrium shifts in favour of κ-chain binding to the higher affinity site 1 and thus a slow decrease in fluorescence is observed reflecting κ-chain leaving site 2. For Y64W, greater than 95% of κ-chain is bound to site 1 at equilibrium under the conditions used (excess PpL) and this is reflected in the small (approximately 2-5%) net increase in fluorescence from W64 at equilibrium when excited by light at 295nm (not shown). However, when excited by light at 280nm the fluorescence intensity at equilibrium is lower than the initial fluorescence intensity from the PpL + κ-chain (see Fig. 6.2a). Thus, under conditions in which there is an excess of PpL over κ-chain, the residual fluorescence intensity from W64 reflects the relative affinities of sites 1 and 2 for the κ-chain. The lower the fluorescence intensity at equilibrium the lower the affinity of site 2 relative to that of site 1. However, a very large excess of κ-chain would show a single fluorescence increase (composed of two similar rates) as both sites become saturated.

6.6.2 New model applied to F39H,Y64W

In this mutant, the F39H substitution has been made close to binding site 1 and the fluorescent reporter (Y64W) group has been placed in site 2. Figure 6.4 shows that reaction between this mutant and κ-chain is accompanied by a biphasic change in fluorescence in which a fast increase in fluorescence is followed by a slow decrease in fluorescence intensity. The latter indicates that the affinity of site 1 for the κ-chain is higher than that of site 2 despite the mutation of residue 39. However, the residual fluorescence intensity at equilibrium is much higher than that shown for the same reaction involving the Y64W mutant and therefore the relative affinity of κ-chain for site1 compared with that of site 2 has decreased ie. more κ-chain remains bound to site 2 due to a decrease in affinity of site 1.

6.6.3 New model applied to F39W

In this mutant, no substitutions have been made in site 2 and the F39W reporter group is located close to site 1. The profile (Figure 6.2b) of the reaction of F39W with κ-chain shows an initial fast increase in fluorescence due to binding of free κ -chain to site 1 followed by a slower further increase. The latter is due to κ -chain which had initially bound to the weaker site 2 being released and now being available to bind to site 1. Once again, the final fluorescence intensity from the reporter group is a reflection of the relative affinities of site 1 and site 2. However, in this case, the fluorescence intensity at equilibrium reflects the occupation of site 1. The higher the fluorescence the more κ-chain is bound at site 1 relative to site 2. Rates for the two phases of the reaction profile s are summarized in Table 6.1. The observation that the slow phase of the reaction is a positive increase in fluorescence intensity is a clear demonstration that the affinity of site 1 for the κ-chain is higher than that of site 2.

6.6.4 New model applied to N26,76D,F39W

This mutant species has three substitutions, N26D is in β-strand 2, N76D is located in β-strand 4, (both remote from the binding sites) and F39W is close to site 1. Positive biphasic fluorescence changes also occur when the N26,76D,F39W mutant reacts with κ-chain (Figure 6.5a), with a fast increase in fluorescence followed by a further, slower increase. At equilibrium there is a large increase in fluorescence intensity when κ-chain is bound reflecting saturation of site 1 where the reporter is located. Once again, the slow increase in fluorescence intensity is a clear demonstration that the affinity of site 1 is higher than that of site 2 for the κ-chain.

6.6.5 New model applied to Y53H,F39W

This mutant has a key substitution is site 1 (Y53H) and a reporter group close to site 1 (F39W). The reaction profile for Y53H, F39W (see Figure 6.3a), shows an initial fast fluorescence increase but not the further slower increase associated with the F39W mutant. It can be inferred from this result that the relative affinities of sites 1 and 2 for κ-chain are approximately the same or that binding at site 1 has been completely eliminated.

If binding at site 1 was weaker than that at site 2 then the initial rapid rise in fluorescence intensity would be followed by a slow decrease in fluorescence as κ-chain bound at site 1 dissociates to bind at the stronger site 2. Therefore it can be concluded that either κ-chain is unable to bind at all to site 1 or that κ-chains can bind to either of the sites with a similar affinity thus eliminating the slow change in fluorescence associated with dissociation of κ-chain from one or the other site.. This correlates very well with other studies (Beckingham, 1997) which showed similar reaction curves for the reaction between κ-chain and the Y53F mutant. This has been found to have an approximately 65 fold decrease (68nM to 4400nM) in affinity of site 1 for κ-

chain making it approximately the same as the affinity of κ-chain for site 2 (Housden *et al.*, 2004).

6.7 The determination of the K_d for site 1 and site 2

Recent work has been carried out to determine the K_d for site 1 and site 2 directly (Housden *et al.*, 2004). These studies have been able to take advantage of the three dimensional structure of the complex formed between PpL and human Fabs (Graille *et al.*, 2001) to make mutations that eliminate κ-chain binding at site 1 or site 2 so that one site can be studied in isolation from the other. The mutations made were Y53F,L57H to eliminate binding at site 1 and A66W to eliminate the binding at site 2. Once again Trp residues were placed close to the binding sites to facilitate fluorescence studies. The profile for I34W PpL binding to κ-chain shows a two step process, a fast decrease in fluorescence followed by a slower further decrease. However, the reaction profile for I34W,Y53F (I34W reporter in site 1) with κ-chain shows a single phase with a decreased amplitude compared to I34W. This is similar to the situation noted above and is due to Y53F reducing the affinity of site 1 to that of site 2. I34W, Y53F, L57H shows no fluorescence change when mixed with κ-chain showing that no binding of κ-chain is occurring at site 1 and that the double mutation Y53F,L57H eliminates binding at site 1. Therefore, for the mutant Y53F,L57H all κ-chain is bound to site 2, so that the mutant Y64W,Y53F,L57H (bearing a Trp reporter group in site 2) shows the largest fluorescence increase at equilibrium after binding κ-chain (Housden *et al.*, 2004).

Such studies have allowed the K_d of each of the two sites for κ-chain to be determined separately. From these, and from associated isothermal titration calorimetry experiments, site 1 was found to have a K_d of approximately 50 - 68nM, depending upon the technique used, and site 2 to have a K_d of approximately 4μM at 15°C by stopped flow fluorescence spectroscopy. The K_d value for the binding at site 1 changes very little with increasing

temperature whereas the K_d for binding at site 2 increases approximately 1.45 fold between 15°C and 25°C (Harrison, S.L.,Housden, N.G. and Gore, M.G., unpublished). Therefore the K_ds for the complexes at site 1 and 2 are approximately 50 – 68nM and 5.8μM at 25°C. These values are very close to those given in Table 6.2 which were calculated according to model 2a. The reaction between Y53H,F39W PpL and κ-chain was calculated to have a K_d of 6.71μM, very close to the value of 5.8μM shown above. This is significant, both mutations are located in site 1, the data suggest that the structure of the PpL domain and therefore binding at site 2 is unaffected confirming the CD studies shown in Chapter 4.

In the stopped flow studies described in this thesis the mutant F39H,Y64W was calculated to have a K_d of 4.95μM at 25°C. This is below the value of 5.8μM that describes the interaction at site 2 and must reflect slightly stronger binding at site 1. This is supported by the reaction progress curve seen for the reaction between κ-chain and this mutant that shows only a small, slow decrease in fluorescence after the initial rapid increase. This small decrease indicates that some, not all of the κ-chain originally bound to site 2, is re-locating to bind to site 1.

In model 3, the slow dissociation of κ-chains from site 2 of PpL to occupy available sites 1 on other molecules of PpL is the structural rearrangement that limits the rate of the secondary change in fluorescence intensity. It should be noted that the difference between models 2(b) and 3 is that in model 2(b) the initially bound κ-chain at one site is not released from the PpL as it migrates to the second, higher affinity site, whereas in model 3 it is released into free solution. It is surprising that analysis according to both models 2a and 3 give such close results.

The presence of two sites with widely differing affinities in the micromolar range explains why the second binding site was not previously detected in spectroscopic titration experiments since unacceptably high concentrations of Fab protein (which aggregates readily at high concentrations)

would be required to get saturation of the weaker site. Furthermore, high concentrations of protein, and thus high absorbance at 280nm results in unacceptably high corrections to fluorescence intensity which severely limits the use of this technique for the determination of the K_d of a weak ligand.. Clearly techniques like ELISA will reflect contribution of both sites giving an apparent K_d . Although the K_d determined will mainly reflect the contribution from the high affinity site in any mutant with a native site 1 which has an affinity approximately 50 – 100 fold higher than that of the lower affinity site.

In vivo the two sites might give the protein a wider range of binding activity for different classes of κ-chains or the ability to bind κ-chains from a broader range of species.

The reactions between κ-chain and site 1 or site 2 of PpL can be regarded as two separate equilibria as the structure of the complex between two human Fabs and PpL suggest that each site behaves independently of the other (Graille *et al.*, 2001). Furthermore, amino acid substitutions in one site have little or no effect on the affinity of the other site for κ-chain.

If the concentration of PpL is much higher than that of κ-chain then the concentration of available PpL, and therefore the concentration of available site 1 and site 2, is unchanged at equilibrium.

$K_d1 = \frac{[S1][\kappa]}{[S1.\kappa]}$ and therefore $K_d1 \times [S1.\kappa] = [S1][\kappa]$ in which S1 is the concentration of unoccupied PpL site 1 and $[S1.\kappa]$ is the concentration of the complex between κ -chain and PpL site 1 at equilibrium. K_d1 is the dissociation constant for the complex at site 1. Similar equations can be written for the equilibrium between κ-chain and PpL site 2.

i.e.

$K_d2 = \frac{[S2][\kappa]}{[S2.\kappa]}$ and $K_d2 \times [S2.\kappa] = [S2][\kappa]$

Since S1 = S2

then [S1][κ] = [S2][κ] and therefore K_d1 x [S1.κ] = K_d2 x [S2.κ]

and hence $\frac{K_d1}{K_d2} = \frac{[S2.\kappa]}{[S1.\kappa]}$ or $\frac{K_a2}{K_a1} = \frac{[S2.\kappa]}{[S1.\kappa]}$

i.e. the occupation of the two sites by κ-chain is proportional to their affinity constants (K_a1 and K_a2). Therefore estimation of the fractional occupancy of each site from the fluorescence intensities of the reporter groups at equilibrium will allow the relative K_ds to be calculated. Since the values of K_d at site 1 and site 2 are known from the use of site-deletion mutants given in Housden *et al.*, (2004), these can be used as control values for the un-mutated site of the mutants used in these studies.

The rates of association of κ-chain to sites 1 and 2 are very similar (18 - 20 x 10^4 Mol^{-1} s^{-1} and 15 x 10^4 Mol^{-1} s^{-1}, respectively. Thus the κ-chain initially binds equally to both sites. For the mutants bearing a F39W reporter group (site 1) the amplitude of the fast increase in fluorescence represents the occupation of site 1. If site 2 has no mutation then this also represents occupancy of site 2 initially. The amplitude of the slower increase in fluorescence is due to κ-chain, originally bound at site 2 moving to bind to site 1. Therefore this amplitude, subtracted from that of the fast increase, represents the amount of κ-chain still at site 2 at equilibrium and, when added to that of the fast increase, represents the amount of κ-chain at site 1 at equilibrium.

CHAPTER 7

DISCUSSION

The aim of this project was to create mutants of PpL that could be used as affinity ligands for the purification of Igs or fragments of Igs such as S_cFvs, Fab or κ-chains. It was desirable that these new affinity ligands would release the bound Igs at milder pH values than those required to elute them from a column of immobilised WT PpL which is approximately pH 1.75 (Beckingham, 1997). Dr. J. Pearson (Affinity Chromatography Ltd., Cambridge, private communication) suggests that a Kd of 2-3 μM is an appropriate Kd for an affinity ligand and with these requirements in mind a series of mutagenesis experiments were then planned. These were based upon structural knowledge of free PpL gained from NMR (Wikström *et al.*, 1996) and X-ray crystallographic techniques (in collaboration with Dr. Brian Sutton, King's College, London) and a knowledge of how a single domain from Protein G (which is structurally similar to PpL) interacts with Fab (Derrick and Wigley, 1994).

Mutants were selected by changing the charge on residues at sites which had been identified as having involvement in binding by NMR studies by Wikström *et al.*, (1996). Mutants F39H,Y64W ; Y53H,F39W ; E38Q ; Q35H,Y64W and Q35H,F39W were created to attempt to reduce the affinity of PpL for κ- chains. Unfortunately, E38Q; Q35H,Y64W and Q35H,F39W domains were unable to be expressed. This lack of expression was confirmed by the Swedish group of Professor Lars Björck and Dr. Ulf Sjöbring (Lund University) who found that residues located at the `corners' of the domain were very important for the stability of the domain (private communication). Binding characteristics of mutants were studied using ELISA, competitive ELISA and equilibrium and stopped-flow fluorescence techniques using engineered W64 or W39 residues as reporter groups. It had previously been

shown that the mutations F39W and Y64W have little effect on κ-chain binding (Beckingham, 1997). These studies all suggested that F39H,Y64W and Y53H,F39W both have significantly reduced affinities for κ-chains and are therefore good potential affinity chromatography ligands.

The effect of the mutagenesis on the elution profiles of IgG bearing κ-chains from columns of the immobilised mutant PpL domains was studied by affinity chromatography. The columns were loaded with human IgG at pH 8.0 and then subjected to a pH gradient. Two mutants, Y53H,F39W and F39H,Y64W were found to offer advantageous properties for their use in the purification of Ig and fragments of Ig containing V_L domains of κ-chains. Columns made from the mutant Y53H,F39W release Ig at pH 3.9 and those made from F39H,Y64W release Ig at pH 3.8. Both of these pH values are substantially less acidic than that required for the release of Ig from columns of WT PpL making the recovery of biologically active Ig or Ig fragments more likely. Other members of the research group at Southampton have shown that S_cFv fragments are unstable at pH values below 2.5 and that they can be eluted at the same pH as whole Ig from columns of immobilised mutant PpL. Thus the two mutants developed here will be useful for the purification of these important proteins that show considerable advantages for clinical therapy owing to their small size, increased cellular penetration and lower antigenicity.

The stability of the mutated proteins was investigated using fluorescence and CD spectroscopy. It was found that Y64W was approximately as stable as PpL with a $\Delta G°_{H20}$ of 16.93 $kJmol^{-1}$ or 18.57 $kJmol^{-1}$ (intercept / calculated , respectively) while F39W, K33W, N26,76D and F39H,Y64W proteins showed reduced conformational stabilities. These domains, however, could still be purified by the inclusion of a 30 min, 65°C heat step and refolded from high concentrations of GdnHC1. The latter is a useful characteristic as columns of immobilised protein ligands can sometimes, after an extensive

period of use, be regenerated by the application and subsequent removal of such denaturants. The Y53H,F39W mutant was, however, much less stable ($\Delta G°_{H20}$ of 4.17 / 6.02 kJmol^{-1} intercept/ calculated, respectively) as was the N26,76D,F39W mutant with a $\Delta G°_{H20}$ of 8.97 / 7.87 kJmol^{-1} intercept/ calculated, respectively. It is clear that the substitution F39W is deleterious to the stability of PpL, however, the mutation is of no value other than allowing fluorescence studies to be carried out. Therefore, the mutation can be eliminated from the Y53H,F39W mutant and this will almost certainly make the domain much more stable.

The stopped flow experiments have confirmed the importance of kinetic analysis of a binding reaction. If the binding process follows that of model 2 (a) (6.2.2) then the two process binding reaction means that the overall binding affinity of the PpL domains for κ-chains can be influenced by varying one or more of the four rate constants that define the K_d at equilibrium, for this model the on and off rates for the formation of the encounter complex and on and off rates for the proposed conformational change. The values of k_1 for the reaction between F39W PpL and the mutant N26,76D,F39W were almost identical (0.55 x $10^6 M^{-1}s^{-1}$ and 0.49 x $10^6 M^{-1}s^{-1}$, respectively indicating that the two N to D mutations per domain had not affected the rate of formation of the encounter complex. This was expected as the latter mutations are not close to the proposed binding site for κ-chains. The value of k_1 for the mutants Y53H,F39W and F39H,Y64W are 0.70 x $10^6 M^{-1}s^{-1}$and 0.72 x $10^6 M^{-1}s^{-1}$ respectively. These are not sufficiently different to those above to account for the large difference in K_d values. These mutants have altered equilibrium K_d values primarily due to a very slow forward rate for the post-binding conformation change compared to that of the WT; in fact the Y53H,F39W mutant has no detectable conformational change at all. This agrees with data obtained for the mutant Y53F,Y64W (Beckingham, 1997).

If as now looks most likely the binding follows model 3 (See 6.5) the overall K_d for κ-chain binding can be manipulated by constructing mutants that alter one or more of the four rate constants i.e. the on and off rates for κ-chain binding to site 1 and site 2.

This model is now able to explain all current data and reaction progress curves of all mutants. Analytical centrifugation studies and site directed mutagenesis (Graille *et al.,* 2001) have now identified the presence of the second site and NMR studies (Graille *et al.*, 2002) have identified small chemical shifts for residues located in the second site. All fluorescence changes are now explained. For W64 (reporter in site 2) the initial increase in fluorescence is thought to be due to the binding of κ-chain to site 2. The slow decrease is then the shift in equilibrium to the higher affinity site 2 (6.6.1). For the W39 (reporter in site 1) shows an initial increase in fluorescence due to the binding of κ-chain to site 1 followed by a slow decrease whereby κ-chain which had initially bound to the weaker site 2 is released and is now available to bind site 1 (6.6.3). As expected Y53H,F39W shows no second fluorescence change as both site 1 and 2 are now of a similar affinity due to the considerable weakening of site 1 by the Y53H mutation.

The data indicate that site 2 is approximately 50 times weaker than site 1. Although the presence of the 2^{nd} site is not suprising considering the symmetry in terms of tertiary structure and similarity in terms of amino acid residues comprising the two sites, a mutant which has similar affinity for Ig at both sites could be useful for immunoprecipitation as it can cross link Ig by binding two Ig proteins at the same time. A PpL mutant with binding at site 1 or 2 eliminated could also provide a monovalent ligand of either high (site 2 eliminated) or low (site 1 eliminated) affinity. The high affinity ligand could be useful in affinity columns where removal of as much Ig as possible is more important than intact recovery of Ig e.g. in removing Ig from blood for use in transplant surgery. The lower affinity ligand could be of use in an affinity

column where the recovery of Ig and retaining its biological activity is important. This lower affinity ligand would allow less damaging elution conditions to be used. In either case having a single site will give a sharper elution profile which is useful as it will allow the Ig to be eluted in a smaller volume than the broad peak of the bivalent PpL.

Now that there is information about the structure of the complex formed between a domain and a κ-chain it is possible to plan new mutants more strategically. It may also be possible to combine the effects of known mutations in the same domain to create a protein with a pre-determined K_d for κ-chains. This has already been achieved in similar studies carried out on a single domain of Protein A (Brown, 1995). Combining two mutations in a single domain should result in the overall K_d for the double mutant being different from that of the WT PpL by the product of the effects of the individual mutations on K_d.

One attractive possibility is to genetically fuse a gene encoding a single domain of PpL with the gene encoding a single domain of Protein G or Protein A or even to both. In this way the binding capabilities of all components can be used to form a `universal binder' for Igs. The PpL domain to bind to κ-chains, the Protein A domain to bind to the Fc region of IgG and to V_HIII class Igs and Protein G to bind to the Fc region and to the C_H1 domain of the Fab fragment. One possible problem for the use of such a hybrid protein as an affinity ligand would be that all of the component domains might require different conditions to effect the release of bound Ig. However, previous research projects carried out at Southampton have identified mutations in Protein A and G domains that affect the pH required to separate them from Ig. Thus the hybrid could be constructed from engineered single domains of each protein so that each component has a similar affinity for its target site on Igs and thus a single, symmetrical elution profile from an affinity column could be achieved. It would be useful to combine binding

domains from different proteins to provide a diverse spectrum of binding characteristics.

One requirement that has become obvious from the studies in this thesis and studies of others (Beckingham, 1997; Housden, personal communication; Actinova Ltd., private communication) is that the method of immobilising a single domain to Sepharose requires improvement. Although 5 – 6 mg of PpL can be coupled up to lml of CNBr activated Sepharose, its binding capacity for human Ig is very low. In theory, a 1:1 complex formed between PpL and Ig bearing κ-chains should allow 75mg of the Ig to be bound to 5mg of immobilised PpL. If one Ig binds to two PpL domains (since the Fab fragment contains two κ-chains) then approximately 37mg of Ig should be bound. In practice only 1.5 – 1.8mg of Ig was bound per ml to the columns used here. One problem is that although there are seven Lys residues in the domain, three of these have been implicated by the NMR studies of Wikström *et al.*, (1996) to be important for κ-chain binding. Thus coupling reactions with these residues will block the binding activity of the bound protein. One possible way to improve the yield of the coupling chemistry will be to place a Cys at one end of the domain. In the studies described in this thesis a Cys residue in position 74, close to the carboxyl terminus has been constructed. Specific ready activated matrices (thio-propyl derivatives of Sepharose) are available (Sigma Chem. Co.) to couple up proteins with available Cys residues.
An additional consideration is the relatively small size of the domain. If the coupling chemistry targets residues on some surfaces of PpL then there will be physical restrictions imposed by the matrix to the approach of Igs. This may be circumvented by engineering reactive residues into the 15 residue `leader' sequence at the amino terminal end of PpL. Alternatively a construct with two sequential domains of PpL may offer some advantages if only one domain is coupled to the matrix and acts as a spacer group for the second domain.

Finally, the development or isolation of bacterial proteins that can bind to λ-

chains would enable all Ig classes and subclasses to be isolated by a hybrid formed between it and PpL. The possibility of converting PpL to a λ-binder by mutagenesis seems remote as there are substantial differences between λ and κ-chain primary, secondary and tertiary structures. Phage library display techniques in which random mutations are generated in genes inserted into the DNA that encodes coat proteins of M13 phage may prove useful. Any phage containing a coat protein embodying a peptide that binds to λ-chains can be identified by screening the phage particles using beads containing immobilised λ- chains. Subsequent sequencing of the phage DNA will reveal the favourable mutations. However, because approximately 63% (Kihlberg *et al.*, 1992) of human Ig contain κ-chains, the evolutionary pressure for a bacterium to develop a similar protein to bind to λ-chains is quite high and such a protein probably already exists. Thus screening Gram positive bacteria for λ-chain binding properties may well prove worthwhile. However, with the advent of recombinant DNA technology, industrial producers of recombinant Igs usually have the ability to chose the light chain template on which there antigen binding sites are engineered (Dr. A. Popplewell, Celltech Ltd.) and therefore the urgency to develop an affinity ligand for λ-chains has been diminished.

REFERENCES

Achari, A., Hale, S.P., Howard, A.J., Clore, M., Gronenborn, A.M., Hardman, K.D. and Whitlow, M. (1992) *Biochemistry* **31**, 10449-10457.

Åkerström, B and Björck, L (1986) *J. Biol. Chem.* **261,** 10240-10247.

Åkerström, B and Björck, L (1989) *J. Biol. Chem.* **264,** 19740-19746.

Åkerström, B , Nilson, B.H.K., Hoogenboom, H.R. and Björck, L. (1994) *J. Immunol. Meth.* **177**, 151-163.

Åkesson, P., Cooney, J., Kishimoto, F. and Björck, L (1990) *J. Immunol.* **27**, 523-531.

Alber, T. and Wozniak, J. (1985) *Proc. Natl. Acad. Sci. U.S.A.* **82**, 747-50.

Alexander, P., Fahnestock, S., Lee, T., Orban, J. and Bryan, P. (1992) *Biochemistry* **31**, 3597-3603.

Anfinsen, C.B., (1972) *Biochem. J.* **128**, 737 – 739.

Axen, R. and Ernback, S. (1971) *Eur.J.Biochem.* **34,** 351-360.

Baneyx, F., Schmidt, C. and Georgiou, G. (1990) *Enzyme Microb. Tech.* **12,** 337-342.

Barocci, S. and Nocera, A. (1993) *Transpl. Int.* **6**, 29-33.

Beckingham, J.A. (1997) Ph.D Thesis, University of Southampton.

Beckingham, J.A, Bottomley, S.P., Hinton, R., Sutton, B.J. and Gore, M.G. (1999) *Biochem. J.* **340**, 193 - 199.

Beckingham, J.A., Housden, N.G., Muir, N.M., Bottomley, S.P. and Gore, M.G. (2001) *Biochem. J.* **355,** 395-401.

Berg, A., Tymoczko, J.L. and Stryer, L. (2002) *Biochemistry,* W.H. Freeman and Co., New York.

Berge, A., Kihlberg, B.M., Sjöholm, A.G. and Björck, L. (1997) *J. Biol. Chem.* **272,** 20774-20781.

van den Beuken, T., Pieters, H., Steukers, M., van der Vaart, M., Ladner, R.C., Hoogenboom, H.R. and Hufton, S.E. (2003) *FEBS Lett.* **546**, 288 – 294.

Björck, L. and Kronvall, G. (1984) *J. Immunol.* **133**, 969-974.

Björck, L. (1988) *J.Immunol.* **140**, 1194-1197.

Bottomley, S.P., Popplewell, A. G., Scawen, M., Wan, T., Sutton, B. J. and Gore, M. G. (1994) *Prot. Eng.* **7**, 12, 1463 - 1470.

Bottomley, Beckingham, J., S. P., Murphy, J. P., Atkinson, M., Atkinson, T., Hinton, R. and Gore, M.G. (1995) *Bioseparations.* **5**, 359 – 367.

Braisted, A.C. and Wells, J.A.(1996) *Proc. Natl. Acad. Sci. U.S.A.* **93**, 5688-5692.

Brosius, J. and Holy, A. (1984) *Proc. Natl. Acad. Sci. U.S.A.* **81,** 6929-6933.

Brown, N. (1995) Ph.D Thesis, University of Southampton.

Boyle, M.D.P. and Reis, K.J. (1987) *Biotechnology* **5**, 697-703.

Chadd, H.E. and Chamow, S.M. (2001) *Curr. Opinion in Biotech.* **12,** 188 - 194.

Chen, J.M., Stevens, R.A.E., Wray, P.W., Rawlings, N.D. and Barrett, A.J. (1998) *F.E.B.S. Lett.* **435**, 16-20.

Chiayen, P., Brissette, P., Ballou, D.P. and Massey, V., (1997) *Biochemistry* **36**, 2612-2621.

Chou, P.Y. and Fasman, G.D. (1974) *Biochemistry*, **13**, 211-245.

Chou, P.Y. and Fasman, G.D. (1978) *Annu. Rev. Biochem.* **47**, 251-76.

Churchich, J. E., Pineda, T.,Thorne, M.J.and Gore, M.G. (1996) *Biochem. Biophys. Acta.* **1292**, 259 – 264.

Clark, N.S., Dodd, I., Moussakowska, E., Smith, R.A.G. and Gore, M.G. (1996) *Protein Eng.* **9,** 877-884.

Cleland, J.L., Jones, A.J.S. and Craik, C.S. (1996) Protein Engineering : Principles and Practice. Wiley-Liss.

Creighton, T.E. (1992) Protein Structure: A Practical Approach. (Creighton, T.E. Ed.) IRL Press, Oxford.

de Château, M., Nilson, B.H.K.,Erntell, M., Myhre, M., Magnusson, C.G.M., Åkerström, B. and Björck, L. (1993) *Scand. J. Immunol.* **37**, 399-405.

Cunningham, B.C., Ultsch, M., deVos, A.M., Mulkerrin, M.G., Clause, K.R. and Wells, J.A. (1991) *Science* **254**, 821-825.

Deisenhofer, J. (1981) *Biochemistry* **20**, 2361-2370.

Derrick, J.P. and Wigley, D.B. (1994) *J. Mol. Biol.* **243**, 906-918.

Drewett, V.L. (1998) Ph.D. Thesis, University of Southampton.

Eftink, M.R. (1991) *Meth. Biochem. Anal.* **35**, 127-205.

Eliasson, M., Andersson, R., Olsson, A., Wigzell, H. and Uhlèn , M. (1989) *J.immunol.* **142**, 575-581.

Engvall, E. (1980) *Meth. Enzymology.* **70**, 419-439.

Eyring, H. (1935) *Chem.Rev.* **17**, 65-77.

Ferris, W.F. (1992) Ph.D Thesis, University of Southampton.

Fersht, A.R. (1987) *Prot. Eng.* **3**, 233-238.

Foote, J. and Winter, G. (1992) *J. Mol. Biol.* **224**, 487-499.

Forsgren, A. and Grubb, A.O. (1979) *J. Immunol.* **122**, 1468-1472.

Forster, T.H. (1965) *Modern Quantum Chemistry*, Academic press N.Y. 93-137.

Freifelder, D. (1982) *Physical Biochemistry* 2nd Edition.

Frick, I., Wikström, M., Forsén, S., Drakenberg, T., Gomi, H., Sjöbring, U. and Björck, L (1992) *Proc. Natl. Acad. Sci. USA* **89**, 8532-8536.

Goward, C.R., Scawen, M.D., Murphy, J.P. and Atkinson, T. (1993) *T.I.B.S.* **18,** 136-140.

Graille, M., Stura, E.A., Corper, A.L., Sutton, B.J., Taussig, M.J., Charbonnier, J.B. and Silverman, G.J. (2000) *Proc. Natl. Acad. Sci. U.S.A.* **97**, 5399-5404.

Graille, M., Stura, E.A., Housden, N.G., Beckingham, J.A., Bottomley, S.P., Beale, D., Taussig, M.J., Sutton, B.J., Gore, M.G. and Charbonnier, J.B. (2001) *Structure* **9**, 679-687.

Graille, M., Harrison, S., Housden, N.G., Crump, M., Findlow, I.S.C., Muller, B.H., Battail-Poirot, N., Sibai, G., Taussig, M.J., Jolivet-Reynaud, C., Gore, M.G. and Stura, E.A. (2002) *J. Biol. Chem.* **277**, 47500-47506.

Greasley, P., Gore, M.G., McAllister, G. and Ragan, C.I. (1993) *Biochem. J.* **296,** 811-815.

Gronenborn, A.M., Filpula, D.R., Essig, N.Z., Achari, A., Whitlow, M., Wingfield, P.T. and Clore, G.M. (1991) *Science* **253**, 657-661.

Guss, B., Eliasson, M., Olsson, A., Uhlèn, M., Frej, A.K., Jornvall, H., Flock, J.I. and Lindberg, M. (1986) *E.M.B.O. J.* **5**, 1567-1575.

Harrison, S.L. (2003) PhD Thesis, University of Southampton.

Heden, L.O., Frithz, E. and Lindahl, G. (1991) *Eur. J. Immunol.* **21**, 1481-1490.

Hjelm, H., Hjelm, K. and Sjöquist, J. (1972) *F.E.B.S. Lett.* **28**, 73-76.

Housden, N.G., Harrison, S., Housden H.R., Thomas, K.A., Beckingham, J.A., Roberts, S.E., Bottomley, S.P., Graille, M., Stura, E. and Gore, M.G. (2004) *J. Biol. Chem.* **279**, 9370-9378.

Huston, J.S., Levinson, D., Mudgett-Hunter, M., Tai, M.S., Novotny, J., Margolies, M.N., Ridge, R.J., Bruccoleri, R.E., Haber, E. and Crea, R. (1988) *Proc. Acad. Natl. Sci. U.S.A.*. **85**, 5879-5883.

James, E.L., Whisstock, J.C., Gore, M.G. and Bottomley, S.P. (1999) *J. Biol. Chem.* **274,** 9482-9488.

Jendeberg, L., Tashiro, M., Tejero, R., Lyons, B.A., Uhlèn, M., Montelione, G.T. and Nillson, B. (1996) *Biochemistry* **35**, 22-31.

Kastern, W., Holst, E., Nielsen, E., Sjöbring, U. and Björck, L (1990) *Infect. Immun.* **58**, 1217-1222.

Kastern, W., Sjöbring, U. and Björck, L (1992) *J. Biol. Chem.* **267**, 12820-12825.

Kihlberg, B., Sjöbring, A.G., Kastern, W. and Björck, L. (1992) *J. Biol. Chem* **267,** 25583-25588.

Kihlberg, B., Sjoholm, A.G., Björck, L. and Sjöbring, U. (1996) *Eur. J. Biochem.* **240,** 556-563.

Kim, D.E., Yi, Q., Gladwin, S.T., Goldberg, J.M. and Baker, D. (1998) *J. Mol. Biol.* **284**, 807-815.

Kim, D.E., Fisher, C., Baker, D. (2000) *J. Mol. Biol.* **298**, 971-984.

Krauss, O. (1996) Ph.D Thesis, University of Southampton.

Krauss, O. and Gore, M.G. (1996) *Eur. J. Biochem.* **241**, 538 – 545.

Kristiansen, S.V., Pascual, V., Lipsky, P.E.(1994) *J. Immunol.* **153**, 2974-2982.

Kronvall, G (1973) *J. Immunol.* **111**, 1401-1406.

Kuhlman, B., O'Neil, J.W., Kim, D.E., Zhang, K.Y.J. and Baker, D. (2001) *Proc. Acad Sci. USA.* **98**, 1067-1069.

Kuhlman, B., O'Neil, J.W., Kim, D.E., Zhang, K.Y.J. and Baker, D. (2002) *J. Mol. Biol.* **315**, 471-477.

Kunkel, T.A., Roberts, J.D. and Zabour, R.A., (1987) *Methods Enz.* **154**, 367-382.

Kyte, J. and Doolittle, R.F. (1982) *J. Mol. Biol.* **157**, 105-132.

Laemlli, U.K. (1970) *Nature* **227**, 680-685.

Lakowicz, J.R. (1983) Principles in Fluorescence Spectroscopy. Plenum Press.

Langone, J. (1982) *Adv. Immunol.* **32**, 157-252.

Lesk, A.M. and Chothia, C. (1982) *J. Mol. Biol.* **160**, 325-342.

Lian, L.Y., Derrick, J.P., Sutcliffe, J., Yang, J.C. and Roberts, G.C.K. (1992) *J. Mol. Biol* **228**, 1219-1234.

Lian, L.Y., Barsukov, I.L., Derrick, J.P. and Roberts, G.C. (1994) *Nat. Stuct. Biol.* **1**, 355-357.

Lindbladh, C., Mosbock, K. and Bulow, L (1991) *J. Immunol. Meth* **137**, 199-207.

Lindbladh, C., Mosbock, K. and Bulow, L (1993) *TIBS* **18**, 279-283.

Ljungquist, C., Jansson, B., Moks, T. and Uhlèn, M. (1989) *Eur. J. Biochem.* **186**, 557-561.

Matouchek, A., Fersht, A.R., Kellis, J.T. and Serrano, L. (1989) *Nature* **340,** 122-126.

Matthews, B.W., Nicholson, H. and Becktel, W.J. (1987) *Biochemistry* **26,** 6885-6888.

McAllister, E.Z., Alm, E., and Baker, D. (2000) *Nat.Struct. Biol.* **7**, 669-673.

Messing, J., Crea, R. and Seeberg, P.H. (1981) *Nucleic Acid Res.* **9**, 309-321.

Moks, T., Abrahmsen, L., Holmgren, E., Bilich, M., Olsson, A., Uhlèn, M., Pohl, G., Sterky, C., Hultberg, H., Josephson, S., Holmgren, A., Jornvall, H. and Nilsson, B. (1987) *Biochemistry* **26**, 5239-5244.

Murphy, J.P., Duggleby, C.J., Atkinson, M.A., Trowern, A.R., Atkinson, T. and Goward, C.R. (1994) *Mol. Microbiol.* **12**, 911-920.

Musher, D.M., Verbrugh, H.A. and Verhoef, J. (1981) *J.Immunol.* **127**, 84-88.

Myhre, E.B. and Erntell, M. (1985) *Mol. Immunol.* **22**, 879-885.

Nilson, B.H.K., Solomon, A., Björck, L. and Åkerström, B. (1992) *J. Biol. Chem.* **267**, 2234-2239.

Nilson, B.H.K., Logdberg, L., Kastern, W., Björck, L. and Åkerström, B. (1993) *J. Immunol. Meth.* **164**, 33-40.

Nilson, B.H.K., Frick, I., Åkesson, P., Forsén, S., Björck, L. and Åkerström, B. (1995) *Biochemistry* **34**, 13688-13698.

Pace, C.N., Laurents, D.V. and Erickson, R.E. (1992) *Biochemistry* **31**, 2728-34.

Pace, C.N. (1986) *Meth. Enz.* **131**, 266-280.

Palmer, A., Taube, D., Welsh, K., Bewick, M., Gjorstrup, P. and Thick, M, (1989) *Lancet* **8628**, 10-12.

Pancholi, V. and Fischetti, V.A. (1988) *J. Bacteriology* **170**, 2618-2624.

Patella, V., Casolaro, V., Björck, L. and Marone, G. (1990) *J. Immunol.* **145**, 3054-3061.

Perry, L.J. and Wetzel, R. (1984) *Science* **226**, 555-557.

Popplewell, A.G. (1991) Ph.D Thesis, Southampton

Privalov, P.L. and Gill, S.J. (1988) *Adv. Protein Chem.* **39**, 191-234.

Reis, K.J., Ayoub, E.M. and Boyle M.D.P. (1984) *J. Immunol.* **132**, 3091-3097.

Roitt, I.M. (1997) *Essential Immunology* 9th Ed. Blackwall Scientific.

Sanger, F., Nicklen, S. and Coulson, A.R. (1977) *Proc. Natl. Acad. Sci. U.S.A.* **74,** 5463-5467.

Sasso, E.H., Silverman, G.J. and Mannik, M. (1991) *J. Immunol.* **147,** 1877-1885.

Sauer-Eriksson, A.E., Kleywegt, G.J., Uhlèn, M. and Jones, T.A. (1995) *Structure* **3**, 265-278.

Scalley, M.L., Yi, Q., Gu, H., McCormack, A., Yates, J.R. and Baker, D. (1997) *Biochemistry* **36,** 3373-3382.

Scalley, M.L., Nauli, S.N., Gladwin, S.T. and Baker, D. (1999) *Biochemistry* **38**, 15927-15935.

Sjöbring, U., Björck, L. and Kastern W. (1991) *J.Biol.Chem.* **266** 399-405.

Smith, E., Johnson, H.M. and Blalock, J.E. (1983) *J.Immunol.* **130**, 773-776.

Smith, P.K., Krohn, R.I., Hermanson, T.G., Mallia, A.K., Gartner., F.H., Provezano, M.D., Fujimoto, E.K., Goeke, N.M., Olson, B.J. and Klenk, D.C. (1985) *Anal. Biochem.* **150**, 76-85.

Sohi, M.K., Wan, T., Sutton, B.J., Atkinson, T., Atkinson, M.A., Murphy, J.P., Bottomley, S.P. and Gore, M.G. (1995) *Proteins: Structure, function and genetics* **23,** 610-612.

Solomon, A. (1976) *N. Engl.J.Med.* **294,** 17-23.

Sorenson, J.M. and Head-Gordon, T. (2002) *J. Comput. Biol.* **9**, 35-54.

Stalenheim, G., Gotze, O., Cooper, N.R., Sjöquist, J. and Muller-Eberhard, H.J. (1973) *Biochemistry* **10**, 501-507.

Stinson, R.A. and Holbrook, J.J. (1973) *Biochem. J.* **131**, 719-728.

Stura, E.A., Graille, M., Housden, N.G. and Gore, M.G. (2002) *Acta. Crystallogr. D. Biol. Crystallogr.* **58**, 1744-1748.

Svensson, H.G., Hoogenboom, H.R. and Sjöbring, U. (1998) *Eur. J. Biochem.* **258**, 890-896.

Tanford, C. (1968) *Adv. Protein Chem.* **23,** 121-282.

Taylor, J.W., Ott, J and Eckstein, F (1985) *Nucleic Acid Res.* **13**, 8765-8785.

Terman, D.S., Yamamoto, T., Tillquist, R., Henry, J.F., Cook, G.L., Silvers, A. and Shearer, W.T. (1980) *Science* **209**, 1257-1270.

Torigoe, H., Shimada, I., Saito, M. and Arata, Y. (1990) *Biochemistry* **29**, 8787-8774.

Uhlèn, M., Nilsson, B., Lindberg, M., Gatenbeck, S., and Philipson, L. (1983) *Gene* **23**, 369-378.

Voet, D. and Voet, J. (1990) *Biochemistry* 2nd Ed. Wiley and Sons.

deVos, A.M., Ultsch, M. and Kossiakoff, A.A. (1992) *Science* **255**, 306-312.

Wallis, R., Leung, K-Y., Pommer, A.J., Videler, H., Moore, G.R., James, R. and Kleanthous, C. (1995) *Biochemistry* **32**, 13751-13759.

Wikström, M., Sjöbring, U., Kastern, W., Björck, L., Drakenberg, T. and Forsén, S. (1993) *Biochemistry* **32**, 3381-3386.

Wikström, M., Drakenberg, T., Forsén, S., Sjöbring, U. and Björck, L. (1994) *Biochemistry* **33**, 14011-14017.

Wikström, M., Sjöbring, U., Drakenberg, T., Forsén, S. and Björck, L. (1995) *J. Mol. Biol* **250**, 128-133.

Wikström, M., Forsén, S. and Drakenberg, T (1996) *Eur J. Biochem.* **235**, 543-548.

Yang, J.T., Wu, C.S. and Martinez, H.M. (1986) *Meth. Enz*, **130**, 208-269.

Yannisch-Perron, C., Viera, J. and Messing, M. (1985) *Gene* **33**, 103-119.

Zenno, S. and Innouye, S. (1990) *Biochem. & Biophys. Res. Comm* **171**, 169-174.